IDŐJÁRÁS

QUARTERLY JOURNAL
OF THE HUNGARIAN METEOROLOGICAL SERVICE

Special issue: Climate change and adaptation

Guest Editor: Rita Pongrácz

* * * * *

Regular papers

VOL. 124 * NO. 2 * APRIL – JUNE 2020

IDŐJÁRÁS

Quarterly Journal of the Hungarian Meteorological Service

Editorial Office: Kitaibel P.u. 1, H-1024 Budapest, Hungary
P.O. Box 38, H-1525 Budapest, Hungary
E-mail: journal.idojaras@met.hu
Fax: (36-1) 346-4669

Indexed and abstracted in Science Citation Index Expanded™ and Journal Citation Reports/Science Edition
Covered in the abstract and citation database SCOPUS®
Included in EBSCO's databases

Subscription by mail:
IDŐJÁRÁS, P.O. Box 38, H-1525 Budapest, Hungary
E-mail: journal.idojaras@met.hu

Editorial

Special Issue: Climate change and adaptation

The most prestigious scientific meeting of the meteorology community of Hungary, the so-called Meteorological Scientific Days, has been organized since 1975. The 44th Meteorological Scientific Days of this series were organized by the Climatology subcommittee of the Meteorological Scientific Committee of the Hungarian Academy of Sciences in November 2018, and focused on one of the major challenges of the 21st century, namely, climate change issues. The importance of this topic is emphasized by the fact that climate change related research was revisited after the previous (36th) meeting in 2010.

Altogether 21 oral presentations and 11 posters represented the various research results accomplished in Hungary. They covered the detection of climate change signals on the basis of measurements, the climate modeling efforts using different regional and mesoscale models, and the climate change related impacts in various sectors, e.g., agriculture, hydrology and water management, urban environment, human health issues, tourism, energy production. This special issue includes scientific papers from all these major subtopics. First, *Lakatos et al.* analyze the precipitation measurements on sub-daily scale. Since extreme conditions especially affect the different socio-economic sectors, they focus on the 60-minute extreme rainfall in Hungary, and discuss the results received for the various return periods using fitted General Extreme Value distribution. Their results are the most relevant in the planning and operating demands of drainage and sewerage systems. Then, the study of *Kis et al.* evaluates regional climate model simulations from the EURO-CORDEX database. They analyze temperature and precipitation projections for the plain areas of Serbia and Hungary for the 21st century using three different RCP scenarios: a very optimistic (RCP2.6), a moderately optimistic (RCP4.5), and a pessimistic (RCP8.5) scenario. The multi-model comparison clearly concludes that warmer conditions tend to occur if greater radiative forcing change is assumed. The obtained results for precipitation suggest similar changes in the cases of the different RCP scenarios, namely, a clear decreasing trend for July, and overall wetter conditions for the rest of the year.

The third paper was written by *Zsebeházi* and *Szépszó*, they selected one specific regional climate model, i.e., ALADIN-Climate, being run at the Hungarian Meteorological Service, and downscaled the simulations for mesoscale resolution (using the SURFEX model) in order to evaluate urban climatic effects for Budapest. The simulation results for 2001–2010 show that

SURFEX simulation overestimates the air temperature (at the standard 2 m measuring height) throughout the year in spite of the too cold driving ALADIN-Climate simulation. The evaluation concludes that the strength of the urban heat island effect is slightly underestimated in summer and overestimated in the rest of the year.

Finally, the last publication of the Special Issue focuses on one of the impact studies related to climate change. More specfically, *Pokovai et al.* present a deterministic biogeochemical model to estimate the possible effects of climate change on agro-ecosystems. This study concludes that regional climate change in Hungary is likely to negatively affect the spring sown crops; and even though the predicted yield losses may be prevented if irrigation is properly organized or sowing is shifted earlier, the role of winter crops is likely to become more important in Hungary in the future.

The organizing committee of the 44th Meteorological Scientific Days appreciates the valuable scientific work of all the authors of this Special Issue; and thanks the Journal IDŐJÁRÁS for the opportunity to publish the results in this Special Issue and the anonymous reviewers for their efforts and suggestions to improve the published papers.

Rita Pongrácz
Guest Editor

DOI:10.28974/idojaras.2020.2.1

IDŐJÁRÁS

Quarterly Journal of the Hungarian Meteorological Service
Vol. 124, No. 2, April – June, 2020, pp. 143–156

Return values of 60-minute extreme rainfall for Hungary

Mónika Lakatos*, **Beatrix Izsák**, **Olivér Szentes**, **Lilla Hoffmann**, **Andrea Kircsi**, and **Zita Bihari**

Hungarian Meteorological Service
Kitabel P. s 1, H-1024, Budapest, Hungary

**Corresponding Author e-mail: lakatos.m@met.hu*

(Manuscript received in final form February 27, 2020)

Abstract— The rainfall intensity for various return periods are commonly used for hydrological design. In this study, we focus on rare, short-term, 60-minute precipitation extremes and related return values which are one of the relevant durations in the planning and operating demands of drainage and sewerage systems in Hungary. Time series of 60-minute yearly maxima were analyzed at 96 meteorological stations. To estimate the return values for a given return period, the General Extreme Value (GEV) distribution was fit to the yearly maxima. The GEV fit and also the Gumbel fit (GEV Type I.) were tested. According to the goodness of fit test results, both GEV and Gumbel distributions, are adequate choices. The return values for 2, 4, 5, 10, 20, and 50 year return periods are illustrated on maps, and together with their 95% confidence intervals, are listed in tables for selected stations. The maps of return values demonstrate that the spatial patterns of the return values are similar, although the enhancing effect of orography can be explored in the Transdanubia region and in the North Hungarian Range. As the return period is increasing, so the range of the confidence are widening as it is expected.

Key-words: extreme precipitation, rainfall intensity, GEV, return level

1. Introduction

In recent decades, an increasing number of studies have reported about the presence of significant positive trends in precipitation extremes in Europe (e.g., *Alexander et al*., 2006; *Klein Tank* and *Konnen*, 2003; *Moberg et al*., 2006; *Zolina et al*., 2009). The observed more frequent heavy precipitation events are also consistent with increasing amounts of water vapor in the atmosphere due to global warming (*Allen* and *Ingram*, 2002; *Willett et al.,* 2008). The warming climate induces increasing frequency of extreme precipitation in some region. Significant trends in precipitation extremes over Europe have been found since the middle of the 20th

century in earlier regional studies for Northern Europe (*Groisman et al.,* 2005), the UK (*Fowler* and *Kilsby*, 2003), the Mediterranean region (*Pujol et al*., 2007), and western and eastern parts of the Czech Republic (*Kysely,* 2009) and Poland (*Łupikasza et al.,* 2010). E.J.M. van den Besselaar and co-authors (*Besselaar et al*, 2013) showed that despite the considerable decadal variability, 5-, 10-, and 20-year events of 1-day and 5-day precipitation amounts for the first 20 years in the period 1951-2010 became more common in the analyzed 60 years for the daily precipitation series from the European Climate Assessment and Dataset (ECA&D, http://www.ecad.eu) project *(Klein Tank et al.,* 2002; *Klok* and *Klein Tank*, 2008).

Considering the precipitation changes in Hungary, the decrease of the yearly precipitation sum is not remarkable, it is 3% from 1901 to 2019. From the beginning of the 1990s, precipitation has been increasing both on annual and seasonal scales, however, this rise is not significant. Recent years have been dominated by extremes. The magnitude of the change in precipitation intensity (mm/day) is about 1.3 mm/day in the countrywide average. The number of days with daily sum above 20 mm increased by 1 day in the period 1901-2019.

Estimation of precipitation extremes are essential for the planning of important infrastructure, such as water control systems, reservoirs, dams, and urban runoff. The rainfall intensity for various return periods are commonly used for hydrological design (*Hailegeorgis, et al*., 2013). The Hungarian Meteorological Service provides climate services on return periods of short-term precipitation (10 min, 20 min, 30 min, 60 min, 180 min) to the authorities responsible for roads, railways, hydrological and urban planning. The return period is the average time between the occurrences of extremes of a specified size. The return period of extremely high values of short-term rainfall has shortened in recent years in Hungary, as it is shown in a case study for the Pécs-Pogány meteorological station (*Lakatos* and *Hoffmann*, 2019). *Lakatos* and *Hoffmann* (2019) also published the intensity-duration-frequency (IDF) curves for the Pécs-Pogány station. The IDF curves are commonly used in planning to describe the return period associated with a given rainfall event. Earlier studies of the short-term precipitation intensity covered the period 1967–1990, when the rainfall was registered by ombrographs (*Váradi* and *Nemes*, 1992). The return values (or design values) for different return period were estimated by Váradi and Nemes for 26 stations in Hungary. *Gayer* and *Ligetvári* (2006) refer to results of Váradi and Nemes as an exemplary work in the municipal water management planning in Hungary. High intensity, short-term showers, typically 1 hour or less, occasionally up to 3 hours has the greatest impact on the urban environment (*Gayer* and *Ligetvári*, 2006). Due to the recent and projected climate change, existing design criteria for infrastructure should be revised as it is pointed out in *Varga et al.,* 2016.

In this study, we focus on rare, short-term, hourly, namely 60-minute precipitation extremes and related return values which are relevant in the planning and operating demands of drainage and sewerage systems in Hungary.

2. Data

The focus area is Hungary. Automatic weather stations replaced the ombrographs in many places in Hungary, particularly from the late 1990s. As a result of automatization, 22-year-long 10 minutes data series are available to analyze the behavior of the sub-daily precipitation for Hungary from 1998. The 10-minute sums of precipitation are stored in the digital meteorological database of the Hungarian Meteorological Service. The 10-minute data was used to derive all the 60-minute rainfall sums which are used in this study. Then the yearly maxima of the 60-minute rainfall were computed for each station to apply extreme value analysis. Time series of yearly maxima were analyzed at 96 meteorological stations in this paper (*Fig. 1)*. The analysis performed here covers almost the complete automatic weather station network in Hungary. Stations with lot of missing data and with shorter time series were excluded from this study. Time series of the yearly maxima have been quality controlled, and their temporal homogeneity were checked using the MASH (*Szentimrey,* 1999) method before applying extreme value analysis. The MASH method is an internationally well-known homogenization procedure, one of the best performing methods according to the benchmarking test executed in the COST (European Cooperation in Science and Technology) Action ES060: advances in homogenization methods of climate series: an integrated approach (HOME) (*Venema et al.,* 2012). Erroneous data and inhomogeneities may severely affect the extremes. Therefore, great care must be taken during the decision making on inclusion or exclusion of the erroneous data, as sometimes it is difficult to distinguish the extremes and outliers.

Fig. 1. Automatic weather stations used in this study. Additional statistics are shown for the labeled stations.

3. Methods

The objective of our analyses is to estimate the amount of rainfall falling at a given point for a fixed duration (60 minutes in our case) and a given return period. To estimate the return values for a given return period, the extreme value theory and relating statistical methods have to be applied. Extremes can be found in the tails of the probability distribution. An introduction to extreme value theory can be found in many publications, for example in *Coles* (2001) and *Katz* (2002).

In recent years, two statistical approaches are frequently used in modeling extreme rainfall events: the model of annual maxima (block maxima) and the peaks over threshold (POT) model (*Coles,* 2001). The most common approach in modeling extremes involves fitting a statistical model to the annual extremes in a time series of data. The classical POT model defines a threshold and considers all events with intensity higher than this threshold. The block maxima are usually modeled by a Gumbel or a generalized extreme value (GEV) distribution (*Katz et al.,* 2002), while the POT is modeled by the generalized Pareto distribution (*Katz et al.*, 2002; *Coles*, 2001). Despite its advantages, the POT model is much less applied in the analysis of hydrological extremes (*Madsen et al*., 1997). The World Meteorological Organization (WMO) report entitled "Statistical Distributions for Flood Frequency Analysis" (*Cunnane*, 1989) provides a review of probability distributions of extreme values and methods for estimation of their parameters. Other WMO source in this topic is the "Guidelines on Analysis of extremes in a changing climate in support of informed decisions for adaptation" (*Klein Tank*, 2009).

The GEV distribution was introduced by Jenkinson (*Jenkinson,* 1955). It describes the three types of extreme value distributions for block maxima of any variable (*Coles*, 2001). The distribution of the block maxima converges to a GEV distribution *G(x)* while the record length approaches infinity. The three-parameter GEV distribution can be defined in the form

$$G(x;\mu,\sigma,\xi) = exp\left\{-\left[1+\xi\left(\frac{x-\mu}{\sigma}\right)\right]^{-1/\xi}\right\}, \quad (1)$$

where μ is the location, σ is the scale, and ξ is the shape parameter. Note that σ and $1 + \xi(x-\mu)/\sigma$ must be greater than zero. Depending on ξ, the *G(x)* converges to one of three types: Type I (Gumbel) ($\xi = 0$), Type II (Fréchet) ($\xi > 0$), and Type III (Weibull) ($\xi < 0$). Thereby the shape parameter determines whether the fitted distribution will have a finite lower bound, a finite upper bound, or no bound. In the unbounded case, the shape parameter has value zero, and the GEV distribution becomes the well-known Gumbel distribution (*Gumbel*, 1958), which have been used extensively in hydrology, meteorology, and engineering. The Gumbel/Type 1 distribution have been applied in hydrology to model floods

and extreme rainfalls (*Chow et al.,* 1988; *Stedinger et al.,* 1993). According to several studies, extreme 24-hour precipitations follow Type II distribution (heavy upper tail; $\xi > 0$) (*Wilks,* 1993; *Koutsoyiannis* and *Baloutsos,* 2000; *Katz et al*. 2002; *Coles* and *Pericchi*, 2003; *Coles et al*., 2003; *Koutsoyiannis*, 2004). Fréchet distribution represents the lowest risk for technological architecture, as design values are higher than for Type I (Gumbel) and Type III (Weibull).

From the fitted extreme value distribution, we can estimate the return value which is defined as a value that is expected to be equaled or exceeded on average once in every time interval T (return period), with a probability of $p= 1/T$. Therefore, the return values (z) can be calculated from the Eq.(1) by inverting the GEV distribution in the case of a stationary climate (*Matyasovszky*, 2002):

$$\begin{aligned} z_{Type\ I.} &= -\sigma \ln(-lnp) + \mu \\ z_{Type\ II.} &= \sigma(-lnp^{-\xi} + \mu) \\ z_{Type\ III.} &= -\sigma(-lnp)^{-\xi} + \mu. \end{aligned} \tag{2}$$

The POT method was applied by *Lakatos* and *Matyasovszky* for 10-minute precipitations measured at Baja meteorological station. Pareto distribution was fitted to 10-minute sums of rainfalls above a specified threshold to estimate the distribution of extreme values (*Lakatos* and *Matyasovszky*, 2004).

In accordance with the recent practice of the Hungarian Meteorological Service, the GEV distribution is fitted to the time series of annual maxima/minima. The data are stored in the digital meteorological database, and functions to estimate the different return values are implemented and operated within the digital database. These functions are based on the procedure that was published by Tibor Faragó (*Faragó*, 1989; *Faragó et al.,* 1989; *Faragó* and *Katz*, 1990). The return values pertaining to predefined return periods (2, 4, 5, 10, 20, 50, 100, and 200 years) are computed and displayed for various meteorological elements, e.g., for the short-term precipitation sum (10-, 20-, 30-, 60-, and 180-minute).

In this paper GEV distribution was fit to yearly maximum series of 60-minute rainfall measured at 96 automatic weather stations (AWS) in the period of 1998–2019 first. Moreover, the Gumbel fit was tested. The second step was the computation of the return values for 2, 4, 5, 10, 20, 50 years together with their 95% confidence intervals. Maximum-likelihood method was used to estimate μ location, σ scale, and ξ shape parameters of the GEV distribution (*Prescott* and *Walden*, 1980). The distribution fit and the computation of the return values and the 95% confidence intervals were executed by applying the R statistical software (*R Core Team*, 2012). The return values are illustrated on maps. The results of the distribution fit and the bounds of the confidence intervals are presented in tables for 10 selected meteorological stations.

4. Results and discussion

Return value can be interpreted as the value that is expected to be equal or exceeded on average once in every return period (T), or with probability $p=1/T$ in any given year. The T= 2, 4, 5, 10, 20, and 50-year return values of the 60 minutes rainfall can be seen on the maps in *Figs. 2-7* for Hungary. The GEV distribution were fitted to the 60-minute yearly maxima at the 96 measuring sites, and the return values were then derived. Return values calculated for return periods frequently used in engineering practice are ccalculated on the maps. For instance, the intensity of a 60-minute event which would be exceeded once every 2 years, on average, is shown in *Fig. 2.* The maps of return values demonstrate that the longer the return period the greater the pertaining return value. The spatial patterns of the return values are similar on each map. The enhancing effect of orography can be explored in the Transdanubia region and in the North Hungarian Range, although it is not pronounced. It often occurs that hills and mountains enhance the moving air masses, and the largest intensity can be experienced afterwards under the mountains. On the maps greater values appear also in plain regions, typically in the southeast. The reason for this pattern is that short-duration high-intensity rainfalls happen mainly through local convective cells, which have similar physical properties less respective of geographical location. Occasionally, intensive rainstorms evolve during fast moving cold fronts, and sometimes the storms structured in squall-line and cause extreme rainfall in a very short time interval.

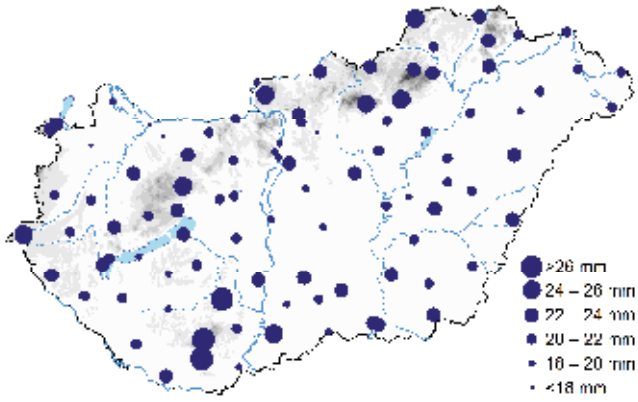

Fig. 2. 2-year return values of the 60-minute rainfall.

Fig. 3. 4-year return values of the 60-minute rainfall.

Fig. 4. 5-year return values of the 60-minute rainfall.

Fig. 5. 10-year return values of the 60-minute rainfall.

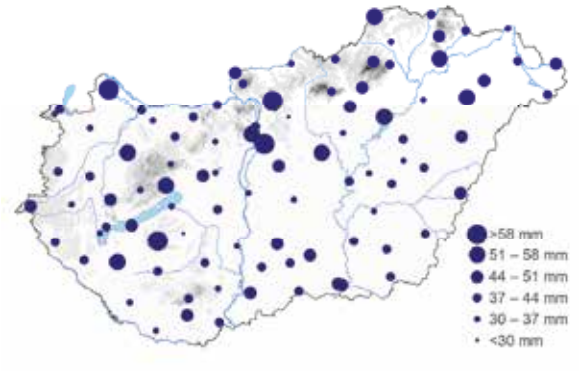

Fig. 6. 20-year return values of the 60-minute rainfall.

Fig. 7. 50-year return values of the 60-minute rainfall.

Over the years, the GEV distribution has become a widely used model in extreme value analysis. Although it is essential to draw attention to the fact that the GEV distribution is simply a model, our observational series and associated statistics do not precisely follow the theory. The GEV fit procedure resulted in the μ (location), σ (scale), and ξ (shape) parameters of the asymptotic probability distribution function. Depending on the value of the ξ parameter, the extremes will converge to the Gumbel (ξ=0), Fréchet ($\xi > 0$), or Weibull ($\xi < 0$) types. According to our analysis, the ξ parameter is under -0.1, at about one fourth (27%) of the stations resulting the upper bound, and ξ is above 0.1 at 42 % of the stations resulting the lower bound in the extreme value distribution. *Table 1* contains these three parameters (μ, σ, ξ) for 10 selected stations from the 96 in total, equally covering the territory of Hungary. Possibly the ξ parameter varies according to the dominating precipitation systems and orographic effects. The

larger positive ξ values appear at stations located chiefly in the western and southern part of Hungary which is under the influence of the Atlantic and Mediterranean climate respectively. The largest ξ value appears at observation stations operating in rural areas of the capital.

Table 1. The μ (location), σ (scale), and ξ (shape) parameters of the GEV distribution and the p-values that are the outputs of the goodness of fit tests for GEV (p value KS) and Gumbel (p_value_C and p_value_A) distribution for selected stations

	μ	σ	ξ	p_value_KS	p_value_C	p_value_A
Szombathely	18.44	5.67	0.15	0.934	0.458	0.322
Nagykanizsa	19.29	4.08	0.28	0.988	0.272	0.198
Győr-Likócs	16.56	3.02	0.53	0.998	0.270	0.207
Siófok	20.33	6.60	-0.21	0.890	0.804	0.695
Paks	21.08	6.77	-0.37	0.934	0.717	0.524
Budapest-Lőrinc	19.12	8.00	0.44	0.944	0.237	0.166
Baja	21.13	8.53	0.02	0.756	0.169	0.146
Miskolc	20.04	7.01	0.06	0.861	0.754	0.645
Szeged	19.69	9.28	-0.06	0.931	0.836	0.718
Debrecen	20.22	6.67	0.14	0.871	0.697	0.704

It is necessary to check if the GEV model fits to the series. Various tests can be used for this purpose. We applied the Kolmogorov–Smirnov test which is a nonparametric test to compare our samples with the GEV probability distribution (*Stephens*, 1970). The Gumbel distribution is frequently used in hydrological applications to estimate the extremes. Therefore, the Type I. (Gumbel) distribution has been checked too. The Cramer-von Mises and Anderson-Darling tests for Gumbel distribution function proposed by *Chen* and *Balakrishnan* (1995) was applied to check the Gumbel fit (*Anderson* and *Darling*, 1954;. *Stephens*, 1986; *Marsaglia,* 2004). The null hypothesis is that the GEV is an appropriate model in the case of Kolmogorov-Smirnov test, and the Gumbel model is appropriate in the case of Cramer-von Mises and Anderson-Darling tests. We reject the null hypothesis at level α if the p-value is smaller than α (usually 0.05 or 0.01), otherwise we fail to reject the null hypothesis at level α. The p-values resulted in the goodness of fit tests are listed in *Table 1.* for 10 selected stations. The higher p-values represents greater strength of evidence in support of the null hypothesis. The p_value_KS (Kolmogorov-Smirnov test) describes the measure of the evidence of the GEV fit, while the p_value_C (Cramer-von Mises test) and the p_value_A (Anderson-Darling test) describe the evidence of the Gumbel fit.

Although smaller sizes of data record may hide the appropriateness of GEV distribution, in our case it fits adequately to the 22-year-long records for each station. The Gumbel model was considered suitable for all station at all reasonable significance level using Cramer-von Mises and Anderson-Darling tests.

Having the parameters of the GEV distribution, the return values and related 95% confidence intervals were computed. The 2-year, 5-year, 10-year, 20-year, and 50-year return levels together with the lower bound and upper bound of the interval where the return level lies in with p=0.95 probability can be found in *Table 2*. As the time interval is increasing, the range of the confidence are widening. For the 5-year return period (which is the usual time interval for designing the sewerage system in urban environment) the estimated return values are between 23.5 mm and 36.1 mm, but the lowest upper bound of the 95% confidence intervals is 28.7 mm (*Table 2*). In the case of the 50-year return period, the largest return values turned out to be at Győr-Likócs and Budapest-Lőrinc stations, where the ξ is a large positive value (see *Table 1.*). The confidence interval is extremely expanded in the case of the 50-year return level at Budapest-Lőrinc, whicht is a rural station in the capital. The return levels for very long return periods tends to enlarge the error due to inaccurate estimates of the shape parameters which describe the tails of a distribution. Generally, the confidence of the return levels decreases rapidly, when the return period is about two times longer than the length of the data series (*Klein Tank et al*., 2009).

Table 2. The return values of the 60-minute rainfall with the lower bound and the upper bound of the 95% confidence interval (mm)

	2-year			**5-year**			**10-year**			**20-year**			**50-year**		
Szombathely	17.5	20.6	23.7	22.6	28.0	33.4	25.3	33.7	42.2	26.6	39.8	53.0	26.1	48.8	71.6
Nagykanizsa	18.5	20.9	23.2	22.2	26.9	31.7	24.0	32.2	40.4	24.5	38.3	52.2	22.4	48.5	74.5
Győr-Likócs	15.7	17.8	19.8	18.3	23.5	28.7	18.1	29.7	41.2	13.9	38.4	62.9	3.2	59.3	115.4
Siófok	19.3	22.7	26.1	25.1	28.8	32.5	27.8	32.1	36.4	29.2	34.9	40.6	29.3	37.8	46.3
Paks	19.7	23.4	27.1	25.7	28.9	32.1	28.4	31.5	34.5	29.3	33.3	37.4	28.8	35.1	41.5
Budapest-Lőrinc	17.1	22.3	27.5	24.2	36.1	48.0	25.4	49.8	74.3	19.6	68.1	116.5	6.5	108.5	210.6
Baja	19.8	24.3	28.7	27.5	34.1	40.7	31.4	40.8	50.1	33.7	47.2	60.7	34.4	55.7	77.0
Miskolc	18.5	22.6	26.8	25.2	31.1	37.0	28.0	37.0	45.9	28.4	42.9	57.4	25.2	51.0	76.8
Szeged	17.8	23.0	28.2	26.5	33.0	39.4	30.3	39.2	48.0	31.5	44.8	58.2	29.6	51.8	73.9
Debrecen	18.7	22.7	26.8	25.1	31.3	37.6	27.6	37.8	48.0	27.4	44.7	61.9	22.6	54.6	86.7

The return levels, or design values are often expressed in terms of rainfall intensity (mm/h) rather than rainfall depth (mm) over a certain duration in construction engineering. The latter has been chosen here, because this is what is actually measured at the meteorological stations.

5. Conclusion

This study focused on the short-term precipitation that is essential for hydrological planning. Hourly, namely 60-minute maximum precipitation series were analyzed from 96 stations operated by the Hungarian Metrological Service. The return values are widely used parameters in planning, for example in construction of drainage systems. The return value can be determined as a value that is expected to occur on average once during the return period. To give an estimation for return values, the general extreme value distribution fitting is an adequate procedure. The 60-minute yearly maxima follow the GEV distribution and also the Gumbel fit suits to the sample series from all 96 stations. The spatial patterns of the return values for 2, 4, 5, 10, 20, 50 years coming from the GEV fit are similar. The influence of the orographic effect turns up in the Transdanubia region and in the territory of the North Hungarian Range, although greater values appear also in the plain regions in the southeastern part of Hungary. The 95% confidence intervals were computed to illustrate the uncertainty of the rainfall estimates to various return periods. Naturally, as the return period is increasing the range of the confidence are widening.

The methodology introduced here can be applied in the future for the renewing of the existing design criteria for infrastructure. The uncertainty can be decreased with using longer data series for estimation of the parameters of the GEV distribution. The series of automatic measurements can be lengthened for about a dozen of stations by the measurements rescued from the ombrograph registering papers after eliminating the inhomogeneity caused by the different sampling. Estimation of areal precipitation return levels by applying regional GEV distribution (*Stedinger et al.,* 1993) is one of the possible directions of the continuation of our examinations. The methodology for estimating extreme areal precipitation by shifting the station-based precipitation to areal precipitation from the grid-based (*Dyrrdal* et al., 2016) also an option to consider.

References

Alexander, L., Zhang, X., Peterson, T., Caesar, J., Gleason, B., Klein Tank, A., Haylock, M., Collins, D., Trewin, B., Rahimzadeh, F., Tagipour, A., Ambenje, P., Rupa Kumar, K., Revadekar, J., and *Griffiths, G.*, 2006: Global observed changes in daily climate extremes of temperature and precipitation. *J. Geophys. Res. 111: D05*,109. https://doi.org/10.1029/2005JD006290

Allen, M. and *Ingram, W.*, 2002: Constraints on future changes in climate and the hydrologic cycle. *Nature 419*, 224–232. https://doi.org/10.1038/nature01092

Anderson, T.W. and *Darling, D.A.*, 1954: A test of goodness of fit. *J. Amer. Statistic. Assoc. 49*, 765–769. https://doi.org/10.1080/01621459.1954.10501232

Besselaar, E.J.M. van den, Klein Tank, A.M.G., and *Buishand, T.A.,* 2013: Trends in European precipitation extremes over 1951-2010. *Int. J. Climatol. 33*, 2682–2689.

Coles, S., 2001: An introduction to statistical modeling of extreme values. Springer Series in Statistics. London: Springer-Verlag, 45–57. https://doi.org/10.1007/978-1-4471-3675-0_3

Coles, S. and *Pericchi, L.*, 2003: Anticipating catastrophes through extreme value modelling. *Appl. Statistics 52*, 405–416. https://doi.org/10.1111/1467-9876.00413

Coles, S., Pericchi, L.R., and *Sisson, S.,* 2003: A fully probabilistic approach to extreme rainfall modeling. *J. Hydrol. 273*, 35–50. https://doi.org/10.1016/S0022-1694(02)00353-0

Chow, V.T., Maidment, D.R., and *Mays, L.W.,* 1988: Applied Hydrology. McGraw-Hill. New York.

Chen, G. and *Balakrishnan, N.,* 1995: A General Purpose Approximate Goodness-of-Fit Test. Journal of Quality Technology 27, 154–161. https://doi.org/10.1080/00224065.1995.11979578

Cunnane, C., 1989: Statistical Distributions for Flood Frequency Analysis, WMO-report no. 781 (Operational Hydrology Report no. 33), 73 pp. + 42 pp. appendix

Dyrrdal., A.V., Skaugen, T., Stordal, F. and *Førland, E.J.*, 2016: Estimating extreme areal precipitation in Norway from a gridded dataset. *Hydrol. Sci. J. 61*, 483–494 https://doi.org/10.1080/02626667.2014.947289

Faragó, T., 1989: Extreme value analysis and some problems of applications in meteorology. Meteorological Studies 64, Hungarian Meteorological Service. Budapest.

Faragó, T., Dobi, I., Katz, R. W. and *Matyasovszky I.*, 1989: Meteorological application of extreme value theory: Problems of finite, dependent and non-homogeneous samples. *Időjárás 93*, 261–274.

Faragó, T. and *Katz, R.W.,* 1990: Extremes and design values in climatology. WMO, TD-No. 386, Geneva.

Fowler, H. and *Kilsby, C.,* 2003: A regional frequency analysis of United Kingdom extreme rainfall from 1961 to 2000. *Int. J. Climatology 23*, 1313–1334. https://doi.org/10.1002/joc.943

Gayer, J. and *Ligetvári, F.*, 2006: Települési vízgazdálkodás csapadékvíz elhelyezés, VITUKI, Budapest, 76–90. (in Hungarian)

Groisman, P., Knight, R., Easterling, D., Karl, T., Hegerl, G., and *Razuvaev, V.*, 2005: Trends in intense precipitation in the climate record. *J. Climate 18*, 1326–1350. https://doi.org/10.1175/JCLI3339.1

Gumbel, E.J., 1958: Statistics of Extremes, Columbia University Press. https://doi.org/10.1175/JCLI3339.1

Hailegeorgis, T.T., Thorolfsson, S.T., and *Alfredsen, K.*, 2013: Regional frequency analysis of extreme precipitation with consideration of uncertainties to update IDF curves for the city of Trondheim. *J. Hydrol. 498*, 305–318. https://doi.org/10.1175/JCLI3339.1

Jenkinson, A.F., 1955: The frequency distribution of the annual maximum (or minimum) values of meteorological events. *Quart. J. Roy. Meteorol. Soc. 81*, 158–172. https://doi.org/10.1002/qj.49708134804

Katz, R.W., Parlange, M.B., and *Naveau, P.,* 2002: Statistics of extremes in hydrology. *Adv.Water Res.* 25, 1287–1304. https://doi.org/10.1016/S0309-1708(02)00056-8

Kysely, J., 2009: Trends in heavy precipitation in the Czech Republic over 1961–2005. *Int. J. Climatol. 29,* 1745–1758. https://doi.org/10.1002/joc.1784

Klein Tank, A.M.G., Zwiers, F.W. and *Zhang, X.,* 2009: Guidelines on Analysis of extremes in a changing climate in support of informed decisions for adaptation. Climate Data and Monitoring WCDMP-No. 72, WMO-TD No. 1500, 56pp.

Klein Tank, A.M.G. and *Konnen, G.*, 2003: Trends in indices of daily temperature and precipitation extremes in Europe, 1946–99. *J. Climate 16*, 3665–3680 https://doi.org/10.1175/1520-0442(2003)016<3665:TIIODT>2.0.CO;2

Klein Tank, A.M.G., Wijngaard, J., Konnen, G., Bohm, R., Demarree, G., Gocheva, A., Mileta, M., Pashiardis, S., Hejkrlik, L., Kern-Hansen, C., Heino, R., Bessemoulin, P., Muller-Westermeier, G., Tzanakou, M., Szalai, S., Palsdottir, T., Fitzgerald, D., Rubin, S., Capaldo, M., Maugeri, M., Leitass, A., Bukantis, A., Aberfeld, R., van Engelen, A., Forland, E., Mietus, M., Coelho, F., Mares, C., Razuvaev, V., Nieplova, E., Cegnar, T., Antonio Lopez. J., Dahlstrom. B., Moberg, A., Kirchhofer, W., Ceylan, A., Pachaliuk, O., Alexander, L., and *Petrovic, P.,* 2002: Daily

dataset of 20th-century surface air temperature and precipitation series for the European Climate Assessment. *Int. J. Climatology 22*, 1441–1453. https://doi.org/10.1002/joc.773

Klok, E. and *Klein Tank, A.M.G.*, 2008: Updated and extended European dataset of daily climate observations. *Int. J. Climatology 29*, 1182–1191. https://doi.org/10.1002/joc.1779

Koutsoyiannis, D. and *Baloutsos, G.*, 2000: Analysis of a long record of annual maximum rainfall in Athens, Greece, and design rainfall inferences. *Nat. Hazards 22*, 29–48. https://doi.org/10.1023/A:1008001312219

Koutsoyiannis, D., 2004: Statistics of extremes and estimation of extreme rainfall: I. Theoretical investigation. *Hydrol. Sci. J. 49*, 575–590. https://doi.org/10.1623/hysj.49.4.575.54430

Lakatos, M. and *Matyasovszky, I.*, 2004: Analysis of the extremity of precipitation intensity using the POT method. *Időjárás108*, 163–171.

Lakatos, M. és *Hoffmann, L.*, 2019: Növekvő csapadékintenzitás, magasabb mértékadó csapadékok a változó klímában. In (ed. *Bíró, T.*) Országos Települési Csapadékvíz-gazdálkodási Konferencia tanulmányai. 8-16. ISBN 978-615-5845-22-2 (in Hungarian) https://vtk.uni-nke.hu/document/vtk-uni-nke-hu/K%C3%A9zik%C3%B6nyv_csapad%C3%A9k.pdf

Łupikasza, E., Hansel, S., and *Matschullat, J.,* 2010: Regional and seasonal variability of extreme precipitation trends in southern Poland and central-eastern Germany 1951–2006. *Int. J. Climatol. 31*. 2249–2271. https://doi.org/10.1002/joc.2229

Madsen, H., Pearson, C.P. and *Rosbjerg, D.,* 1997: Comparison of annual maximum series and partial duration series methods for modeling extreme hydrologic events 2. Regional modeling. *Water Resour. Res. 33*, 759769. https://doi.org/10.1029/96WR03849

Marsaglia, G., 2004: Evaluating the Anderson-Darling Distribution. *J. Statistic. Software 9*, 730–737. https://doi.org/10.18637/jss.v009.i02

Matyasovszky I., 2002: Statisztikus klimatológia. ELTE Eötvös Kiadó, Budapest. (In Hungarian)

Moberg, A., Jones, P., Lister, D., Walther, A., Brunet, M., Jacobeit, J., Alexander, L., Della-Marta, P., Luterbacher, J., Yiou, P., Chen, D., Klein Tank, A., Saladie, O., Sigro, J., Aguilar, E., Alexandersson, H., Almarza, C., Auer, I., Barriendos, M., Begert, M., Bergstrom, H., Bohm, R., Butler, C.J., Caesar, J., Drebs, A., Founda, D., Gerstengarbe, F., Micela, G., Maugeri, M., Osterle, H., Pandzic, K., Petrakis, M., Srnec, L., Tolasz, R., Tuomenvirta, H., Werner, P., Linderholm, H., Philipp, A., Wanner, H. and *Xoplaki, E.*, 2006: Indices for daily temperature and precipitation extremes in Europe analyzed for the period 1901–2000. *J. Geophys. Res. 111*, https://doi.org/10.1029/2006JD007103

Prescott, P. and *Walden, A.T.*, 1980: Maximum likelihood estimation of the parameters of the generalized extreme value distribution. *Biometrika 67*, 723–724. https://doi.org/10.1093/biomet/67.3.723

Pujol, N., Neppel, L., and *Sabatier, R.*, 2007: Regional tests for trend detection in maximum precipitation series in the French Mediterranean region. *Hydrol. Sci. J. 52,* 956–973. https://doi.org/10.1623/hysj.52.5.956

R Core Team, 2012: R: A language and environment for statistical computing. R Foundation for Statistical Computing, Vienna, Austria. ISBN 3-900051-07-0, URL http://www.R-project.org/

Stedinger, J. R., Vogel, R. M., and *Foufoula-Georgiu, E.*, 1993: Frequency analysis of extreme events, In: D. R. Maidment (ed.), Handbook of Hydrology, McGraw-Hill, New York, 18.1–18.66.

Stephens, M.A., 1986: Tests Based on EDF Statistics. In (eds. *D'Agostino, R.B.; Stephens, M.A.*) Goodness-of-Fit Techniques. New York: Marcel Dekker. ISBN 0-8247-7487-6.

Stephens, M.A., 1970: Use of the Kolmogorov-Smirnov, Cramer-von Mises and related statistics without extensive tables. *J. Roy. Statistic. Soc., Series B*, 32, 115-122. https://doi.org/10.1111/j.2517-6161.1970.tb00821.x

Szentimrey, T., 1999: Multiple Analysis of Series for Homogenization (MASH). Proceedings of the Second Seminar for Homogenization of Surface Climatological Data, Budapest, Hungary; WMO, WCDMP-No. 41, 27–46.

Varga, L., Buzás, K. és *Honti, M.*, 2016: Új csapadékmaximum-függvények. *Hidrológiai Közlöny 96*, 64–69. (in Hungarian)

Váradi, F. and *Nemes, Cs.*, 1992: Rövid időtartamú csapadékmaximumok gyakorisága Magyarországon. *Légkör XXXVII. 3*, 8–13. (In Hungarian)

Venema, V., Mestre, O., Aguilar, E., Auer, I., Guijarro, J.A., Domonkos, P., Vertacnik, G., Szentimrey, T., Štěpánek, P., Zahradnicek, P., Viarre, J., Müller-Westermeier, G., Lakatos, M., Williams, C.N., Menne, M., Lindau, R., Rasol, D., Rustemeier, E., Kolokythas, K., Marinova, T., Andresen, L., Acquaotta, F., Fratianni, S., Cheval, S., Klancar, M., Brunetti, M., Gruber, C., Duran, M.P., Likso, T., Esteban, P. and *Brandsma,T.,* 2012: Benchmarking monthly homogenization algorithms. *Climate Past 8*, 89–115. https://doi.org/10.5194/cp-8-89-2012

Wilks, D.S., 1993: Comparison of three-parameter probability distributions for representing annual extreme and partial duration precipitation series. *Water Resour. Res. 29*, 3543–3549. https://doi.org/10.1029/93WR01710

Willett, K., Jones, P., Gillett, N., and *Thorne, P*., 2008: Recent changes in surface humidity: development of the HadCRUH dataset. *J. Climate 21*, 5364–5383. https://doi.org/10.1175/2008JCLI2274.1

Zolina, O., Simmer, C., Belyaev, K., Kapala, A., and *Gulev, S*., 2009: Improving estimates of heavy and extreme precipitation using daily records from European rain gauges. *J. Hydrometeorol. 10,* 701–716. https://doi.org/10.1175/2008JHM1055.1

DOI:10.28974/idojaras.2020.2.2

IDŐJÁRÁS

Quarterly Journal of the Hungarian Meteorological Service
Vol. 124, No. 2, April – June, 2020, pp. 157–190

Multi-scenario and multi-model ensemble of regional climate change projections for the plain areas of the Pannonian Basin

Anna Kis*[,1,2], **Rita Pongrácz**[1,2], **Judit Bartholy**[1,2], **Milan Gocic**[3], **Mladen Milanovic**[3], and **Slavisa Trajkovic**[3]

[1] *Department of Meteorology, Eötvös Loránd University*
Pázmány Péter st. 1/A, H-1117, Budapest, Hungary

[2] *Faculty of Science, Excellence Center*
Eötvös Loránd University
Brunszvik u. 2., H-2462, Martonvásár, Hungary

[3] *Faculty of Civil Engineering and Architecture*
University of Nis
Univerzitetski trg 2, Niš 18000, Serbia

**Corresponding Author e-mail: kisanna@nimbus.elte.hu*

(Manuscript received in final form February 27, 2020)

Abstract— This study is focusing on the projected temperature and precipitation changes in the plain areas of Serbia and Hungary. The simulated changes are calculated for two future time periods (namely, 2021–2050 and 2069–2098) on a monthly scale, and they are compared to the 1971–2000 reference period. In order to estimate the uncertainties deriving from different sources, 10 RCM simulations driven by different GCMs, and three RCP scenarios (RCP2.6, RCP4.5, and RCP8.5) were taken into account. According to the obtained results, higher temperature values are likely to occur in the future, and warmer conditions tend to occur if greater radiative forcing change is assumed. In the case of precipitation, larger variability emerges, but for July, a clear decreasing trend is projected, especially in the case of RCP8.5; while from October to June an increase is projected by most of the RCM simulations. Rainfall variability index shows that the number of dry years will be 5–20 from 30-year time series in the mid-century, and slightly less in the late-century. Extreme dry conditions will tend to occur in 2–12 years overall during 30-year future time periods in the northern plain subregions, and somewhat more frequently in the southern subregions (i.e., in Serbia). The obtained results do not show substantial differences depending on the RCP scenarios, since the scenario plays a less important role in the overall uncertainty of climatic projections compared to the model physics and parameterizations or the internal climatic variability.

Key-words: precipitation, temperature, RVI, Hungary, Serbia, lowland, EURO-CORDEX

1. Introduction

The present study contributes to the Pannon Basin Experiment (PannEx), which is an international initiative, under the umbrella of the Global Energy and Water Exchanges project (GEWEX), which is a part of the World Climate Research Programme (WRCP). PannEx aims to better understand the components of the Earth climate system, the regional climate conditions in the Pannonian Basin, their driving forces, and interactions and feedbacks between the surface and the atmosphere (*Ceglar et al.,* 2018). Researchers, who are interested in the PannEx initiative, cover a wide range of scientific expertise, including climatology, meteorology, urban geography, agronomy, air quality, sustainable development, water management, and education in general. The most important issues related to these topics were summarized by *Lakatos et al.* (2018). Particularly, we are focusing on the projections of climatic conditions in the plain areas of the Pannonian Basin within the framework of a bilateral project between Serbia and Hungary. The bilateral projects are especially encouraged by the PannEx, because they facilitate the cooperation between researchers from different scientific areas and different countries of the Pannonian region. Therefore, the effects of climate change and anthropogenic activities on the environment can be investigated by applying an integrated and multi-disciplinary approach. For example, in order to estimate the surface energy budget components of the Pannonian Basin above different surfaces, micrometeorological measurements were completed in typical vineyards around Zagreb and Keszthely in the framework of a bilateral Croatian-Hungarian project (*Weidinger et al.,* 2019). The area around Zagreb was also investigated by *Prtenjak et al.* (2018) who applied the Weather Research and Forecasting (WRF) high-resolution numerical model (*Skamarock et al.,* 2008) on a meso-scale to analyze the downslope wind induced fog events in the region. Another subregion within the Pannonian Basin, namely, the Budapest agglomeration area, and more specifically the urban heat island effect of Budapest was addressed by using WRF simulations by *Göndöcs et al.* (2017).

Here, we focus on the projected climate conditions in Serbia and Hungary, especially in the plain areas, using up-to-date regional climate model (RCM) simulations embedded in global climate model (GCM) simulations for the new Representative Concentration Pathways (RCP) scenarios, namely, RCP2.6, RCP4.5, and RCP8.5 (*Moss et al.,* 2010; *van Vuuren et al.,* 2011). One of our goals is to evaluate the differences between the scenarios, so we selected the above-mentioned three available RCPs, as they cover quite a wide range considering the radiative forcing change relative to the pre-industrial era. RCP2.6 represents the mitigation scenario aiming to limit the global temperature increase to 2 °C. RCP4.5 assumes a decrease in overall energy demands and especially in fossil fuel use, but an increase in renewable and nuclear energy use. The most pessimistic scenario is RCP8.5 with high greenhouse gas

emissions, high population, and modest technological change. The ultimate goal of this study is to compare the regional temperature and precipitation projections for these different scenarios, in addition, we also aim to evaluate the uncertainties of projections due to the different possible sources, i.e., applied models, internal climatic variability, and scenarios.

Jacob et al. (2014) analyzed the projected mean changes of temperature and precipitation on a European scale. They concluded that a significant warming of 1–4.5 °C (RCP4.5) or 2.5–5.5 °C (RCP8.5) is likely to occur with regional differences. Considering precipitation conditions, dry spells were projected to become longer in Central Europe, contrary to this, a decrease in the length of extended dry spells is likely to occur in some parts of Scandinavia. Nevertheless, heavy precipitation was generally projected to increase throughout the European continent with the exception of Southern Europe in summer.

Because of the projected warming trend, several consequences are likely to emerge, e.g., less snowfall is projected in the future. Specifically, *Frei et al.* (2018) investigated the occurrence of snowfall in the Alps, using a 14-member ensemble of simulations applying different combinations of GCMs and RCMs. They found that the projected mean decrease of snowfall between September and May is 25% in the case of RCP4.5 based on the multi-model ensemble, or even 45% in the case of RCP8.5. Furthermore, even less snowfall (by at least 80%) will occur in the low-elevated regions.

We aim to specify the future warming trends on a finer scale focusing on the Pannonian region within the European continent using 10 RCM simulations driven by different GCMs. *Pieczka et al.* (2018) also focused on the future climate of the Pannonian Basin, but they used only a specific RCM, namely the RegCM4 model (*Elguindi et al.,* 2011), whereas we use other RCMs as well. Validation results showed that RegCM4 simulations overestimated summer temperature by 2.9 °C on average, while the bias did not exceed 1 °C in the rest of the year (*Pieczka et al.,* 2019).

In order to assess uncertainty due to the different physical parameterizations, it is advisable to analyze as many model simulations as possible (this is limited by the availability of simulations), especially in the case of impact studies or in the case of decision-making support studies. However, in order to reduce the required computing time, impact modelers prefer to use one single climate simulation that represents the robust changes projected by an ensemble of climate simulations. Therefore, as a compromise, *Dalelane et al.* (2018) investigated simulations provided by EURO-CORDEX (*Giorgi et al.*, 2009) to reduce the number of the ensemble members and found that a reduction from 15 to 7 members leads to a $> 90\%$ remaining spread of the climatic variables. Such reduction is important, as on the one hand, it helps to keep the ensemble manageable for impact modeling; and on the other hand, the reduced ensemble still covers almost the entire range of climate change uncertainty.

First, data and methods used in the current study are presented in the next section, then, the validation results are shown. After that, the projected temperature and precipitation changes are discussed in details, focusing on the uncertainty due to the RCM simulations and the applied RCP scenarios. Finally, the conclusions are drawn.

2. Data and methods

In the case of climate change studies, the first step is validation when the reliability of RCM simulations is evaluated for the present/historical period. For this purpose, it is important to define a reference dataset, to which the present/historical simulations can be compared. In our study, the CARPATCLIM database (*Szalai et al.,* 2013) was chosen as a reference, since it covers the area of our interest (44°–50° N; 17°–27° E), and it is publicly available. CARPATCLIM contains homogenized (by using the MASH software; *Szentimrey*, 2007; *Bihari* and *Szentimrey,* 2013) meteorological variables and indices for 1961–2010, interpolated (by using the MISH software; *Szentimrey* and *Bihari,* 2006; *Bihari* and *Szentimrey,* 2013) to a 0.1° horizontal grid.

After validation, future climatic conditions are compared to the present/historical period on the basis of RCM simulations. In the present study, 10 RCM experiments were selected (*Table 1*); all of them were carried out in the framework of the CORDEX initiative (*Giorgi et al.,* 2009) of the WCRP. CORDEX defined 14 domains, from which the entire European continent is covered by EURO-CORDEX (*Jacob et al.,* 2014). Altogether 23 different RCMs and 12 GCMs were used in EURO-CORDEX simulations with different resolutions (http://is-enes-data.github.io/CORDEX_status.html). To choose the RCM simulations for this study, our selection criteria are as follows: (i) the RCM domain covers Hungary and Serbia with 0.11° horizontal resolution, (ii) the RCM simulation encompasses at least the 1970–2098 time period, (iii) historical and three different future (i.e. for RCP2.6, RCP4.5, and RCP8.5 scenarios (*Moss et al.,* 2010; *van Vuuren et al.,* 2011)) simulations are available.

Table 1. List of the RCM simulations and their driving GCMs used in the present study

GCM ↓ / RCM →	**RCA4**	**RACMO22E**	**REMO2009**	**CCLM4-8-17**	**ALARO-0**
ICHEC-EC-EARTH	X	X		X	
CNRM-CERFACS-CNRM-CM5		X			X
MPI-M-MPI-ESM-LR	X		X (versions r1 and r2)		
MOHC-HadGEM2-ES	X	X			

Considering the selected simulations for this study, four different GCMs provided the necessary initial and boundary conditions. The main components of the GCMs are summarized in *Table 2*, and their main characteristics can be briefly summarized as follows:

- The ICHEC-EC-EARTH model (http://www.ec-earth.org/) is developed as a part of a European consortium. This model is based on the seasonal forecasting system of ECMWF. It can be used as a classical climate model and as an Earth System Model also (by adding atmospheric chemistry, aerosols, ocean bio-geo-chemistry, dynamic vegetation, and Greenland ice sheet).
- CNRM-CERFACS-CNRM-CM5 is an Earth System Model (*Voldoire et al.,* 2013), which is based on the coupling of several models. It is a developed version of the CNRM-CM3, which can reproduce well the large-scale circulation, the Asian monsoon, and the Arctic sea ice cover. However, it also has some deficiencies, e.g., underestimation of the tropical sea surface temperature, overestimation of precipitation, or weak southern ocean circulation. The model's horizontal resolution is 1.4° in the atmosphere and 1° in the ocean.
- MPI-M-MPI-ESM-LR (*Giorgetta et al.,* 2013) is based on the coupled GCMs, namely, the ECHAM6 atmospheric submodel and the MPIOM ocean submodel. Other subsystem models (for land and vegetation as well as marine geochemistry) are also included in MPI-M-MPI-ESM-LR.
- HadGEM2-ES is an Earth System Model (*Collins et al.,* 2011), developed from the HadGEM1. The atmospheric component has 38 vertical layers, and it has a horizontal resolution of 1.25° × 1.875° in latitude and longitude, respectively. A large-scale hydrology module has also been introduced into HadGEM2. Considering aerosols, eight species are available in HadGEM2, from which nitrate (only if tropospheric chemistry is used), fossil-fuel organic carbon, and biogenic aerosols are new.

Table 2. The applied submodels in the GCMs used in this study

	ICHEC-EC-EARTH	**CNRM-CERFACS-CNRM-CM5**	**MPI-M-MPI-ESM-LR**	**MOHC-HadGEM2-ES**
Atmospheric circulation model	ECMWF's atmospheric circulation model IFS (https://www.ecmwf.int/en/publications/ifs-documentation), cycle 36r4, including the land surface model H-Tessel (*Balsamo et al.,* 2009)	ARPEGE-Climate (*Déque et al.,* 1994)	ECHAM6 (*Roeckner et al.,* 2006)	HadAM3 (*Pope et al.,* 2000)
Ocean model	NEMO3.6, including the Louvain-la-Neuve Sea Ice Model (LIM3) (*Rousset et al.,* 2015)	NEMO (*Gurvan et al.,* 2017)	MPIOM (*Jungclaus et al.,* 2013)	NEMO (*Gurvan et al.,* 2017)
Ocean bio-geo-chemistry component	PISCES v2 (*Aumont et al.,* 2015)		HAMOCC5 (*Maier-Reimer et al.,* 2005)	diat-HadOCC (*Totterdell,* 2019)
Dynamical vegetation model	LPJ-GUESS v4 (*Smith et al.,* 2001; *Lindeskog et al.,* 2013)		JSBACH (*Raddatz et al.,* 2007)	TRIFFID (*Cox,* 2001)
Atmosphere composition and aerosol model	TM5 (*Huijnen et al.,* 2010)			UKCA (*Morgenstein et al.,* 2009)
Ice sheet model	PISM 0.7 (*Winkelmann et al.,* 2011)	GELATO (*Salas-Mélia,* 2002)		
Ocean-atmospheric fluxes		SURFEX (*Masson et al.,* 2013)		
River routing and water discharge from rivers to the ocean		TRIP (*Oki & Sud,* 1998; *Oki et al.,* 1999)		TRIP (*Oki & Sud,* 1998; *Oki et al.,* 1999)
Land-surface		ISBA (*Noilhan* and *Mahfouf,* 1996)		MOSES II (*Essery et al.,* 2001)

For the current study, the following five RCMs were selected from the 23 different RCMs used in EURO-CORDEX. In the next lines we give a short overview about them.

- The RCA4 model (*Kupiainen et al.,* 2014) was developed from RCA3 (*Samuelsson et al.,* 2011). One of the main important developments is that the former overestimation of soil-heat transfer was reduced by the inclusion of soil carbon. Furthermore, the Kain-Fritsch convection scheme (*Kain*, 2004) has been updated, so the model distinguishes the shallow and deep convection processes.
- The RACMO22E model is built on the ECMWF physics package merging into the dynamical kernel of HIRLAM (*Undén et al.,* 2002). The model takes into account more soil layers, and it includes a surface runoff scheme. The leaf area index (LAI) also plays an important role, especially in the surface energy budget. The model applies parametric formulations to treat the ice surfaces (*van Meijgaard et al.,* 2008).
- The REMO model was developed from the Europa-Model (EM) numerical weather prognostic model by adding dynamical core and physics. It uses a terrain-following hybrid coordinate system. The vertical structure encompasses 20 levels, as in the case of EM model. The vertical fluxes are treated implicitly (*Jacob* and *Podzun,* 1997).
- The CCLM4-8-17 model is based on the non-hydrostatic Local Model (LM) developed by the German Meteorological Service. The model uses direct coupled components, such as TERRA (surface and soil model) or Flake (fresh-water lake model); whereas ART modul is used for representing chemistry and aerosols (*Schättler et al.*, 2019).
- The ALADIN limited area model was developed from the ARPEGE GCM and the ECMWF Integrated Forecasting System (IFS). The ALARO physics parameterization package, which is suitable to run at convection-permitting fine resolution, was coupled to the ALADIN model (www.euro-cordex.be/meteo/view/en/29038078-ALARO-0+model.html). ALARO uses the Modular Multiscale Microphysics and Transport (MMMT) microphysics scheme that improves the representation of convective precipitation for Europe as validation analysis showed (*Giot et al.,* 2016).

Our study primarily focuses on the plain areas in Hungary and Serbia. Hence, we defined five subregions within the analyzed domain (*Fig. 1*). Three of them (NHU, CHU, SHU) are located mainly in Hungary, representing the north-central-south regions; the other two (NSR, SSR) are in the northern parts of Serbia (*Table 3*). Each subregion contains 70 grid cells, covering about ~7800 km^2.

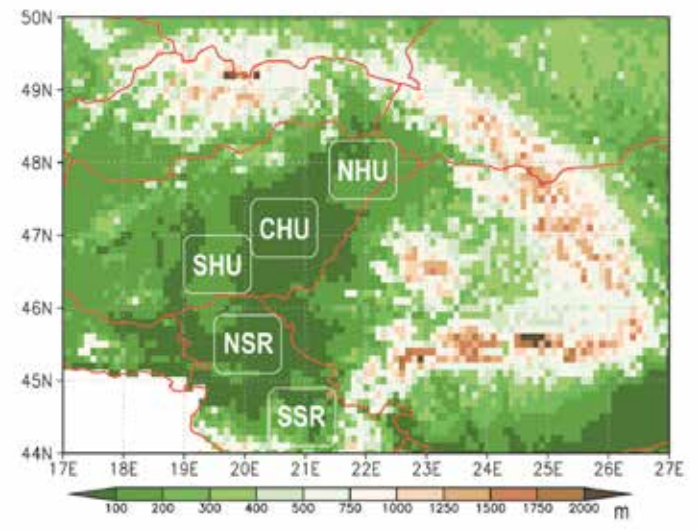

Fig. 1. Topography map of the target area. The selected subregions are indicated by boxes and their abbreviations.

Table 3. List of the five subregions, which are analyzed in the present study, indicating their abbreviations and geographical coordinates

Region	***Northern latitude***	***Eastern longitude***
NHU (Northern Hungarian Plain)	47.6°–48.2°	21.5°–22.4°
CHU (Central Hungarian Plain)	46.8°–47.4°	20.2°–21.1°
SHU (Southern Hungarian Plain)	46.3°–46.9°	19.1°–20.0°
NSR (Northern Serbian Plain)	45.2°–45.8°	19.6°–20.5°
SSR (Southern Serbian Plain)	44.2°–44.8°	20.5°–21.4°

Two meteorological variables, namely, daily mean temperature and daily precipitation total are investigated in this study. The analysis focuses on three time periods: the historical time period (1971–2000), the middle of the 21st century (2021–2050), and the end of the 21st century (2069–2098, since some of the RCM simulations do not include the last two years, 2099 and 2100, due to the lack of driving GCM data; however, this selected period can be considered as representing 2071–2100 since a couple of years' shift does not change the climate change signal on a century scale). The projected changes are calculated

for these three 30-year time slices, for all the five subregions in the case of all RCP scenarios using all RCM simulations selected for this study, hence, a comprehensive comparison analysis is completed.

From the agricultural point of view, the projection of drought conditions is especially important in the plain areas. Therefore, the rainfall variability index (RVI; *Gocic* and *Trajkovic,* 2013) is also calculated in this study beside the changes of monthly mean temperature values and the relative changes of monthly precipitation totals. RVI is calculated by the following formula:

$$RVI = \frac{P_i - P_a}{s},$$

where i is the index of the year, P is the annual precipitation total, P_a is the average annual precipitation total, and s is the standard deviation of annual precipitation totals in the 1971–2000 reference period.

3. Results and discussion

3.1. Validation (historical experiments versus reference data)

First of all, validation results are analyzed using Taylor-diagrams (*Taylor,* 2001), for which monthly mean precipitation totals and monthly mean temperature values were calculated for the five subregions, based on the CARPATCLIM datasets as well as all the 10 historical RCM simulations individually. Thus, the reproduction of the mean annual cycle in the RCM simulations can be evaluated against the CARPATCLIM data for the time period 1971–2000.

In the case of temperature, no substantial differences can be recognized between the subregions, so only one example is presented here, namely, the CHU subregion (*Fig. 2*). We can conclude that all the RCM simulations perform well, as the correlation coefficient is above 0.95 in every case, and all the symbols, indicating the individual RCM simulations, are close to the reference black point, which represents CARPATCLIM data. A small difference occurs in relation with the driving GCM: the two least well-performing RCM simulations were both driven by the CNRM-CERFACS-CNRM-CM5 (indicated by triangles in *Fig. 2*). It can also be seen that the driving GCM of the best overall performing RCM simulations was the MPI-M-MPI-ESM-LR (indicated by diamonds in *Fig. 2*).

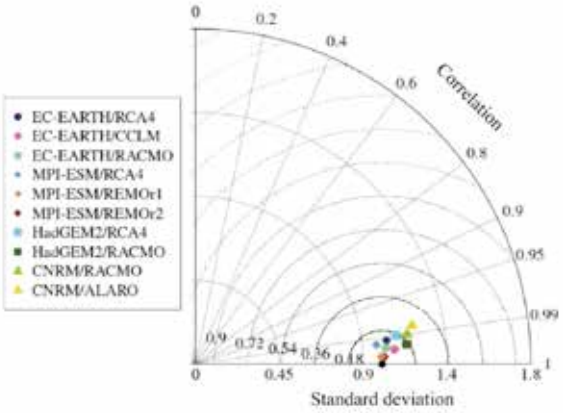

Fig. 2. Taylor-diagram for the CHU subregion, based on temperature data (1971–2000). Different driving GCMs are marked with different symbols; each simulation is indicated by a unique color. The black point indicates the reference (CARPATCLIM).

Considering precipitation, validation results show a less successful reproduction of the mean annual cycle compared to temperature. Results are somewhat better in the Hungarian subregions than in the Serbian subregions, where correlation coefficients are generally closer to zero or even negative (*Fig. 3*) implying very different simulated annual cycle compared to the reference. In spite of that, the CNRM-CERFACS-CNRM-CM5 driven RCM simulations are the least successful in reproducing the reference temperature cycle, this GCM provides the necessary initial and boundary conditions to the overall best performing RCM simulation (CNRM/RACMO) in the case of precipitation. This validation result supports the finding that one cannot choose solely a specific model, which can be considered as the best model from all possible aspects (e.g., *Jacob et al.,* 2007; *Torma,* 2019). For example, one model is good in the simulation of temperature values, while another model performs more reliably the annual cycle of precipitation, and a third one is capable to simulate extreme values better. In the present case, the effects of different GCMs cannot be separated clearly, as their performances are different considering the different subregions.

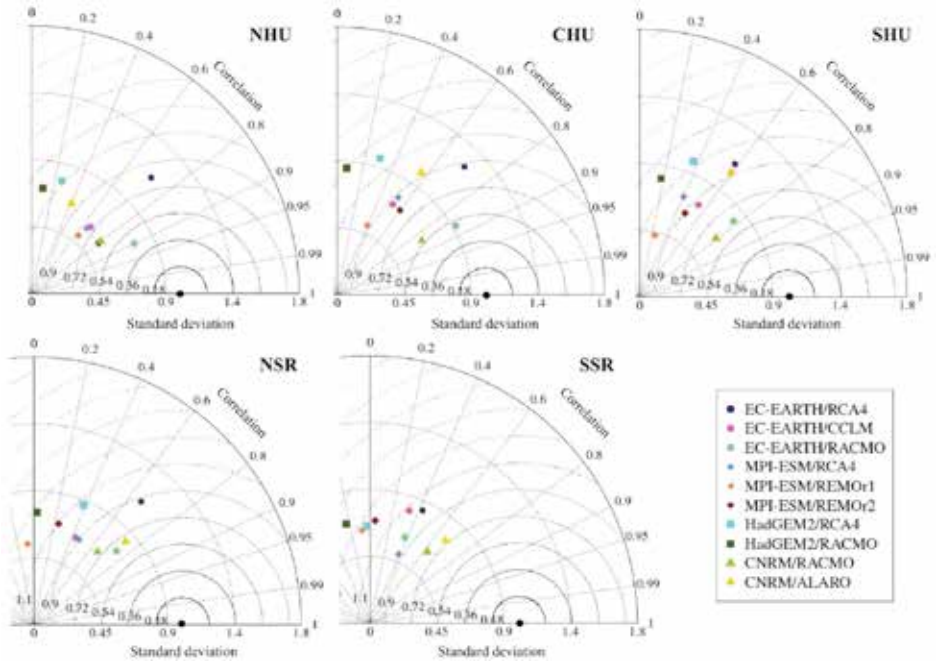

Fig. 3. Taylor-diagrams for the five subregions (NHU, CHU, SHU, NSR, SSR) based on precipitation data (1971–2000). Different driving GCMs are marked with different symbols; each simulation is indicated by a unique color. The black point indicates the reference (CARPATCLIM).

Kotlarski et al. (2014) discussed a validation analysis of the CORDEX simulations (*Giorgi et al.,* 2009) with the ERA-Interim driving data using the E-OBS database (*Haylock et al.,* 2008) as a reference. Overall temperature biases were found to be smaller than 1.5 °C for the European continent, but in the case of precipitation, larger (~ 40%) over- and underestimations can be seen. *Torma* (2019) validated the EURO-CORDEX and MED-CORDEX projections for the 1989–2008 time period using altogether nine ERA-Interim driven RCM simulations. This study found that temperature bias is between –3 °C and +3 °C in the Pannonian region. In the case of precipitation, the RCM-ensemble could reproduce the annual cycle quite well in general, but with a more dominant maximum in June.

For the validation of RVI, the CARPATCLIM database served as a reference. The best agreement can be found in the SSR subregion, where there were 15 dry years according to the CARPATCLIM, and all the RCMs simulated the number of dry years between 13 and 17 (i.e., ±2 years compared to the reference). The least agreement can be found in the NHU and SHU subregions, where four RCMs simulated more or less dry years by at least 3 years compared to the reference.

3.2. The projected temperature and precipitation changes

Since the two most important climatic variables are temperature and precipitation in terms of the agricultural activities being dominantly present in the target regions, we continue the analysis with the projected monthly mean temperature and precipitation changes for the five subregions taking into account the three different RCP scenarios. The climatic variables were analyzed together by evaluating the two-dimensional or bi-variate changes of the spatial averages of the subregions (temperature changes are represented horizontally, whereas precipitation changes appear vertically). In *Fig. 4*, two selected months are shown, namely, January and July (because in the present climate, these are the coldest and the warmest months of the year, respectively). The diagrams summarize the predicted changes by the end of the 21st century on the basis of the 10 individual RCM simulations. Results showing average bi-variate changes reflect the uncertainty of projections due to the model physics. It can be clearly seen that higher temperature values are very likely to occur in the future. January (and overall the winter half year) will be wetter, especially in the northern subregions, whereas July (and August) will tend to become drier, especially in the case of RCP8.5. The projected temperature changes for RCP2.6 and RCP4.5 are closer to each other, while RCP8.5 induces the greatest regional warming. This can be explained by the definition of the RCP scenarios themselves: i.e., RCP8.5 indicates a radiative forcing change of 8.5 W/m^2 by the end of the 21st century compared to the pre-industrial era (whereas RCP2.6 and RCP4.5 assumes only a change of 2.6 W/m^2 and 4.5 W/m^2, respectively). Since temperature is highly correlated with radiation, the conclusion is straightforward: the largest increase is projected in the case of RCP8.5. The smaller overall difference between the other two scenarios can be expected, because the difference between the assumed radiative forcing changes is smaller between RCP2.6 and RCP4.5 than either between RCP2.6 and RCP8.5, or between RCP4.5 and RCP8.5.

In the case of RCP2.6, the smallest multi-model average temperature increase in January (1.88 °C) is projected for SHU (where the entire range from all the 10 RCM simulations is 0.82–3.41 °C), and the largest average warming (1.92 °C) is only slightly greater than the smallest, and is predicted for the neighboring subregions: NSR (where the entire range considering all the 10 RCM simulations is 0.80–3.41 °C, quite similar to SHU) and CHU (where the entire range considering all the 10 RCM simulations is 0.91–3.68 °C, shifted slightly by 0.1–0.2 °C relative to NSR and SHU). Smaller overall warming is projected for July, the projected temperature change is ~ 1 °C; the entire range considering all the 10 RCM simulations and the five subregions is 0.07–1.74 °C implying a smaller variability of simulation results compared to January. Partially due to the small variability and average values, the difference between the subregions is quite small.

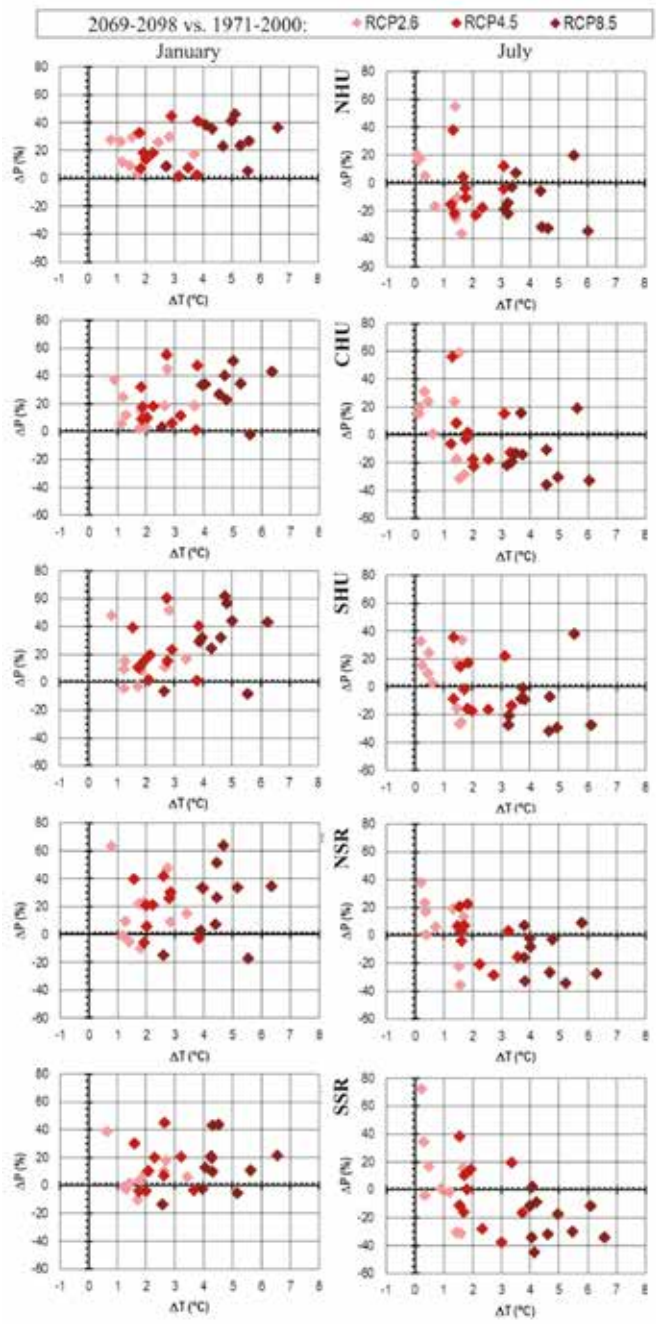

Fig. 4. Projected changes of precipitation (y-axis) and temperature (x-axis) in the five subregions according to the three RCP scenarios (represented by different colors) for the 2069–2098 time period in January (left column) and July (right column) based on the 10 RCM simulations. The reference period is 1971–2000.

Taking into account the RCP4.5 scenario, the projected change based on the multi-model mean for January is more than +2.5 °C in all the five subregions; the greatest change on average (2.71 °C) is likely to occur in the northernmost subregion, NHU (where the entire range considering all the 10 RCM simulations is 1.79–3.82 °C). For July, an increase by ~ 2 °C on average is projected, with the largest change on average (2.28 °C) for the southernmost subregion, SSR (where the entire range considering all the 10 RCM simulations is 1.55–3.74 °C). According to the RCP8.5 scenario, temperature values in January will be higher on average by at least 4.5 °C (in NHU it is 4.9 °C on average and the entire range considering all the 10 RCM simulations is 2.73–6.61 °C) compared to the historical time period. In the case of July, the smallest change on average (4.15 °C) is projected for the northernmost subregion, NHU (where the entire range considering all the 10 RCM simulations is 3.11–6.03 °C) and the greatest on average (4.83 °C) for the southernmost subregion, SSR (where the entire range considering all the 10 RCM simulations is 4.00–6.59 °C). The projected monthly mean warming for the mid- and late-century is compared in *Fig. 5* (since the differences between the subregions are small in projected temperature changes, diagrams show the overall spatial averages), thus the different regional warming trends of the three scenarios can be evaluated for all months. RCP8.5 induces continuous warming in all months; most RCM simulations (at least 7 RCMs from the 10 RCMs in each month) project even accelerating regional warming in the plain areas of Hungary and Serbia. All the 10 RCM simulations predict such an increasing rate of warming in May, July, August, and September. Contrary to this, the projected monthly mean regional warming tends to slow down during the second half of the 21st century in the case of the RCP4.5 scenario; all the 10 RCM simulations project less warming between the middle and late 21st century in January, July, and August than the estimated warming between the end of the 20th century and the middle of the 21st century. However, an accelerating temperature increase is projected for April, May, and November by at least half of the RCM simulations. Moreover, many RCM simulations projects temperature decrease during the second half of the 21st century in the case of the RCP2.6 scenario; more specifically, at least half of the RCM simulations predicts such changes for May, July, August, October, and November (the number of RCM simulations with projected cooling during this coming 50 years is 7, 8, 5, 6, and 6, respectively).

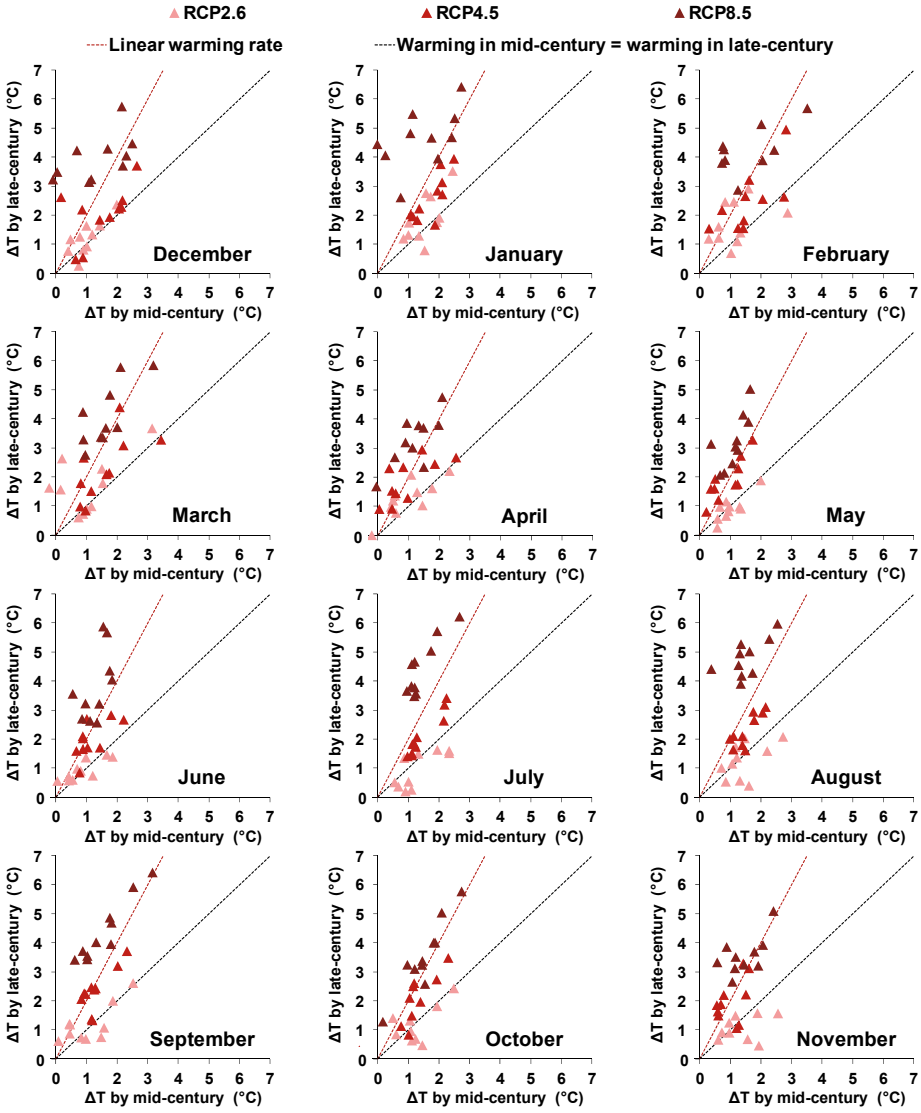

Fig. 5. Projected monthly mean temperature changes averaged for the 5 subregions (ΔT) using the three RCP scenarios (represented by different colors) for the 2069–2098 and 2021–2050 time periods based on the 10 RCM simulations. The reference period is 1971–2000.

The projected mean precipitation changes show substantially higher variability than temperature projections. January (which is currently one of the driest months in the region) is very likely to become wetter, especially in the northern subregions (i.e., NHU and CHU), where all of the 10 RCM simulations

project increased precipitation by the end of the 21st century compared to the reference period. However, some simulations project decreasing precipitation monthly totals in the southern subregions, especially when the RCP8.5 scenario is taken into account (e.g., the projected mean change in January is 22% on average in NSR, and the entire range is between –17% and 64%). On the contrary, a general decreasing trend is likely to occur in July according to the most RCM simulations (except for the case of RCP2.6), but the uncertainty of projections is quite high due to different parameterizations in RCMs. More specifically, RACMO simulations (driven by either the HadGEM2, CNRM, or EC-EARTH models) predict opposite, greater positive changes in July precipitation for RCP4.5 and RCP2.6, whereas the projections of precipitation for RCP8.5 imply either much less, or even negative changes by the end of the 21st century. Overall, we can conclude that the greater the assumed radiative forcing change and the more southern the subregion is located, the more pronounced the drying trend will be in July. So the greatest multi-model mean monthly precipitation decrease (–22%) is projected in the case of RCP8.5 for SSR (where the entire range considering all the 10 RCM simulations is between –45% and 2%).

Fig. 6 shows the projected multi-model mean temperature and precipitation changes by 2069–2098 for all the 12 months for the five subregions, taking into account the three RCP scenarios. As we already mentioned above, the differences between RCP2.6 (indicated by diamonds) and RCP4.5 (indicated by circles) is relatively small, about 1 °C, while RCP8.5 (indicated by squares) can be distinguished more clearly from the other two scenarios (the difference between RCP4.5 and RCP8.5 is about 2–3 °C). Considering temperature, solely increasing trend occurs for all the monthly averages. The greatest increase, 5.16 °C, is projected for August in SSR – this is the only case when the projected multi-model mean change exceeds 5 °C. Furthermore, the projected regional warming exceeds 4 °C in January, February, July, August, and September in all the five subregions in the case of RCP8.5. Similarly, greater warming can be expected in mid- and late-summer, early-autumn, and mid- and late-winter in the case of RCP4.5, while in the case of RCP2.6, the intra-annual variation of the monthly mean projected warming values is substantially smaller.

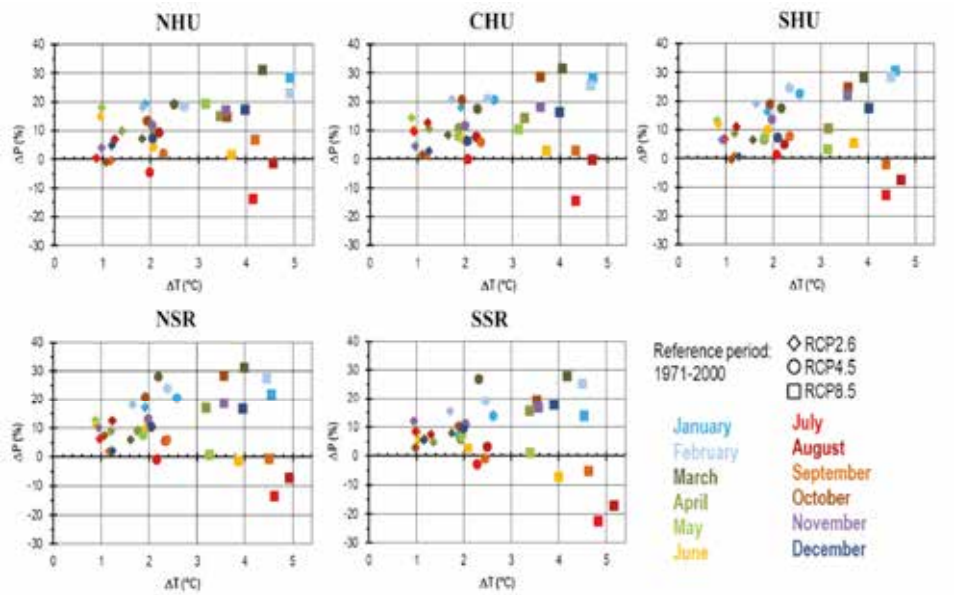

Fig. 6. Projected changes of precipitation (y-axis) and temperature (x-axis) in the five subregions according to the three RCP scenarios (represented by different symbols) for the 2069–2098 time period in the 12 months (different colors) based on the multi-model mean of 10 RCM simulations. The reference period is 1971–2000.

Considering precipitation, *Fig. 6* shows that most of the months will likely become wetter by the end of the 21st century compared to the reference period according to the multi-model average of the 10 RCM simulations. The greatest increase (> 20%) is projected for January, February, and March in all the 5 subregions in the case of all the RCP scenarios. Also, quite high increase (> 15%) is projected in the subregions for December, November, October, and April (except for SHU). Overall, the greatest multi-model mean precipitation change (+32%) is projected for CHU for March, in the case of RCP8.5. Drier conditions are projected only for summer and early autumn, however, different scenarios imply different overall results. A clear drying trend can be seen in July (between –13 and –22%) and August (up to –17% in SSR) in the case of RCP8.5, i.e., assuming high radiative forcing change. Drier conditions are likely to occur in the southern regions even in June (the projected precipitation change is –1% in NSR and –7% in SSR) and in September (the projected precipitation change is –2% in SHU, –1% in NSR, and –5% in SSR). If RCP4.5 scenario is taken into account the multi-model mean precipitation is projected to decrease only in July in most subregions, the greatest change is projected for NHU (–4%)

and SSR (–3%); however, the predicted mean drying trend is substantially less than in the case of RCP8.5 due to the smaller projected decreases of the individual RCM simulations for RCP4.5. In the case of the RCP2.6 scenario, none of the months can be expected to become substantially drier in the future.

The spatial distribution of the multi-model mean projected temperature changes by the end of the 21st century is presented in *Fig. 7* for January and July for the three RCP scenarios. As it can already be seen from the results of *Figs. 4–6*, the greater radiative forcing change results in higher temperature-increase regionally as well as globally (*IPCC*, 2013), which is quite evident from the definition of the RCP scenarios. The patterns of the projected changes reflect dominantly the topography of the domain in January, while a clear zonal structure can be seen in the maps of multi-model mean warming for July, especially for RCP4.5 and RCP8.5. In January, somewhat smaller temperature increase (< 3 °C) is projected for the Carpathian Mountains compared to the plain areas in the case of RCP4.5, while it is the opposite in the case of RCP8.5, namely, the highest projected increase (> 5 °C) appears in the mountainous regions. In July, an east-west difference will emerge in the case of RCP2.6, with slightly higher values in the western parts of the domain. The patterns are different in the case of RCP4.5 and RCP8.5, namely, a north-south gradient appears with greater mean increase (> 2 °C and > 4.5 °C, respectively) in the southern regions. The zonal gradient is the highest for RCP8.5 when the overall warming is also greater.

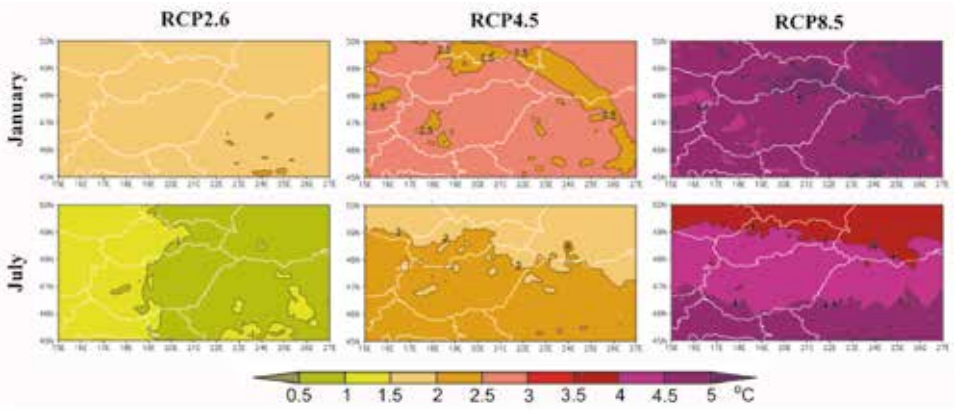

Fig. 7. Projected changes of temperature according to the three RCP scenarios for 2069–2098 relative to 1971–2000 in January and July based on the multi-model mean of 10 RCM simulations.

As a consequence of these projected monthly mean temperature increases, temperature-related extremes are expected to change. Specifically, warm extremes (e.g., tropical nights with daily minimum temperature exceeding 20 °C) will occur more frequently and with a longer duration in the future, whereas cold extremes (e.g., frost days with daily minimum temperature below 0 °C) are very likely to decrease by the late-century. The Pannonian Basin is analyzed from this aspect by *Pieczka et al.* (2018), using one specific RCM taking into account RCP4.5 and RCP8.5.

Considering the spatial distribution of precipitation in January and July for the late-century, we can conclude that the greatest changes are projected in the case of RCP8.5, and the differences between RCP2.6 and RCP4.5 are smaller (*Fig. 8*). In January, multi-model mean precipitation increase exceeding 20% is projected only for the western and northern parts of the domain in the case of RCP2.6. The overall pattern is different from this in the case of RCP4.5, since at least 20% increase is estimated for almost the whole territory of Hungary and the eastern Carpathians. Finally, when taking into account the RCP8.5 scenario, an increasing trend by 20–30% is likely to occur over most parts of the domain (except the northeastern and southern Carpathians); the projected change is positive according to at least seven RCM simulations in almost the entire domain. Contrary to this, a precipitation decrease is projected for July; this drying trend is more pronounced in the southern part of the domain (i.e., the predicted decrease can exceed 20%). The uncertainty originating from the different RCM simulations is higher, which is indicated by the hatched areas covering overall less part of the domain in July than in January. The multi-model mean of July precipitation change is much smaller for either RCP2.6 or RCP4.5 than for RCP8.5, which is due to the fact that RCM simulations result in increasing and decreasing precipitation trends more diversely, thus they eliminate each other.

Since the greatest temperature and precipitation changes are projected by the end of the 21st century for the RCP8.5 scenario, a more detailed analysis based on the multi-model mean of the 10 RCM simulations is presented in *Figs. 9–12* for each month grouped by season. In the case of temperature, all the RCMs simulate a clear increasing trend, i.e., only positive changes by the late-century compared to the reference period. However, precipitation projections show higher variability within the ensemble of RCM simulations, including even different signs of changes (therefore, hatching on the precipitation maps indicates where at least seven model-simulations agree in the sign of the projected change with the change exceeding ±10%).

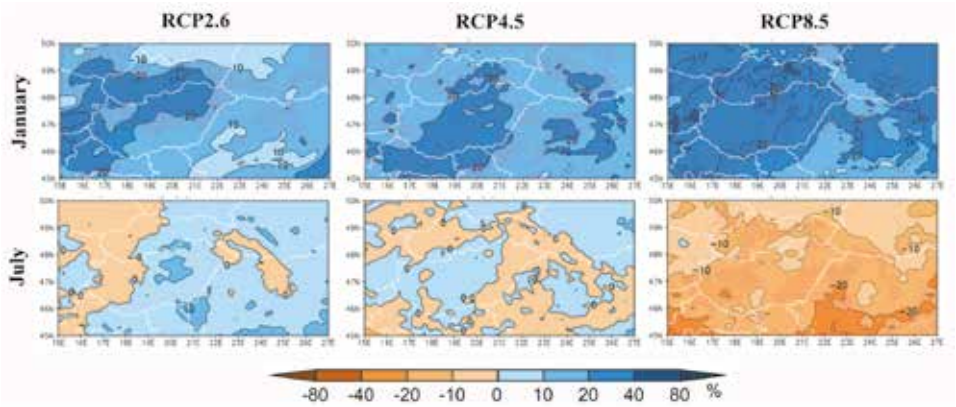

Fig. 8. Projected changes of precipitation according to the three RCP scenarios for 2069–2098 relative to 1971–2000 in January and July based on the multi-model mean of 10 RCM simulations. Hatched areas show where at least seven simulations indicated the same direction of change, and the projected change was at least ±10%.

In summer, the multi-model mean warming is the most pronounced in August, when the projected change can exceed 5 °C in the southern parts of the domain (*Fig. 9*). Similar zonal pattern appears in July, the difference between August and July is about 0.5 °C. The overall smallest temperature increase is predicted for June, but a mean change of at least 3 °C is predicted even in the northwesternmost parts of the domain (where the smallest increase appears). Considering precipitation, *Fig. 8* already shows the multi-model mean decreasing trend projected for July, which can be larger than –20% in the southern parts of the domain. August is projected to become also drier, however, the multi-model mean change is closer to zero compared to July, and the precipitation decrease is more robust in the southeastern part of the domain. Contrary to these, a clear north-south difference can be recognized in June, i.e., there is an increasing trend in Austria, Slovakia, Ukraine, and Hungary, whereas decreasing trend in Slovenia, Croatia, Serbia, and the most parts of Romania; note that the uncertainty is quite high, as the multi-model mean precipitation change is within the range of (–10%; 10%) with very few hatched areas (only outside the Pannonian Basin in the plain areas south and east from the Carpathian mountain ranges).

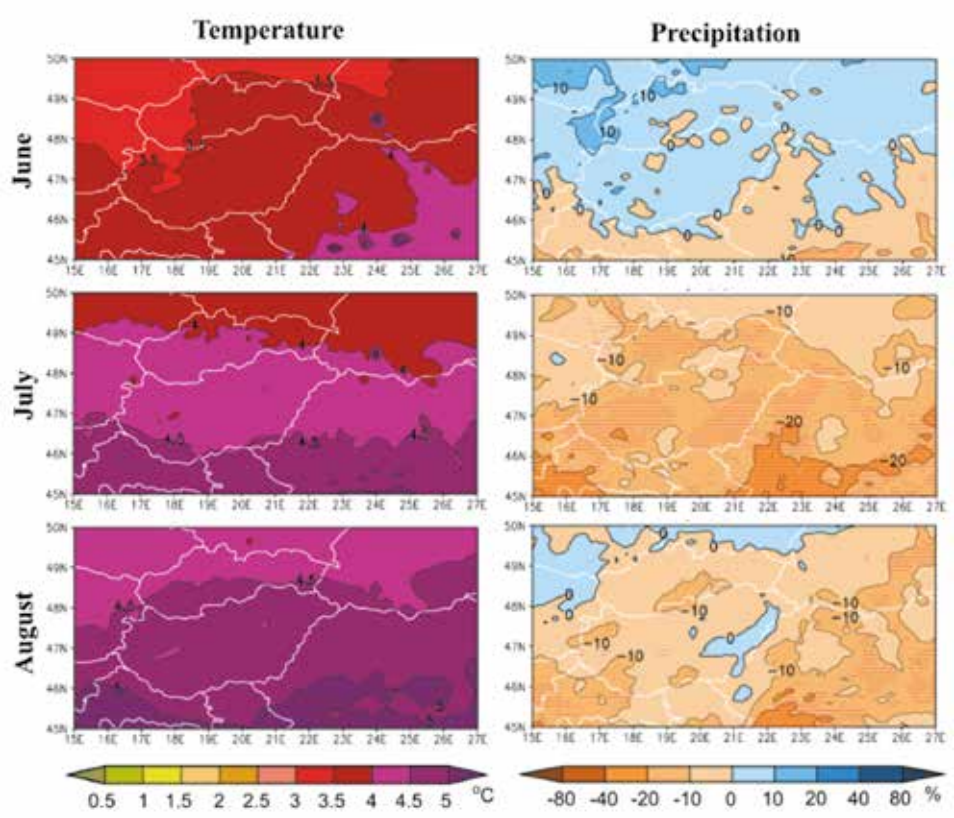

Fig. 9. Projected changes of temperature and precipitation according to the RCP8.5 scenario for 2069–2098 relative to 1971–2000 in the summer months based on the multi-model mean of 10 RCM simulations. In the case of precipitation, hatched areas show where at least seven models indicated the same direction of change, and the projected change was at least ±10%.

Topography-dependent warming is projected in winter (especially in January and February), the projected multi-model mean temperature change by the end of the 21st century is 4–5.5 °C (3.5–4.5 °C in December) compared to the reference period (*Fig. 10*). The greatest increase (> 5 °C) is projected in the Carpathians, except for December, when somewhat smaller (> 4 °C) increase is projected for the eastern parts of Hungary and Transylvania. In the case of winter precipitation, the projected multi-model mean monthly changes imply wetter conditions, moreover, most of the RCM simulations agree on the sign of the predicted change in all the three winter months. The smallest change is projected for December; in January and February the simulated change is at least 20% almost in the entire domain. Considering both meteorological variables simultaneously, one can

conclude that more precipitation is likely to occur in the future in winter, but the rate of snow will be less due to the projected temperature-rise resulting in important consequences from hydrological point of view (e.g., *Kis et al.,* 2017b).

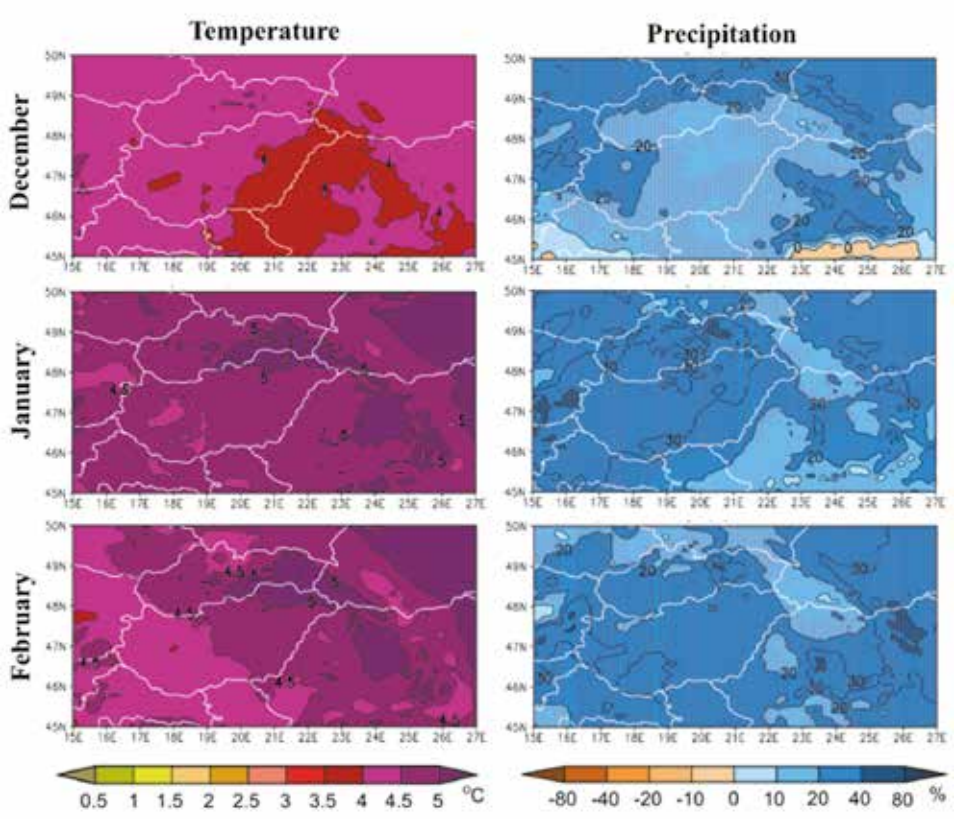

Fig. 10. Projected changes of temperature and precipitation according to the RCP8.5 scenario for 2069–2098 relative to 1971–2000 in the winter months based on the multi-model mean of 10 RCM simulations. In the case of precipitation, hatched areas show where at least seven models indicated the same direction of change, and the projected change was at least ±10%.

September is similar to the summer months: the multi-model mean temperature increase shows a zonal pattern (with a warming of 3.5–4.5 °C) together with an overall drying trend projected over the southern and mountainous parts of the domain (*Fig. 11*). The simulated changes for October and November are more

similar to the projected changes for winter, as an overall 10–30% precipitation increase is likely to occur (somewhat smaller change is projected for November than for October), the estimated temperature increase is somewhat smaller (< 4 °C) than for winter. Furthermore, the spatial variability within the domain is much smaller than in the winter months.

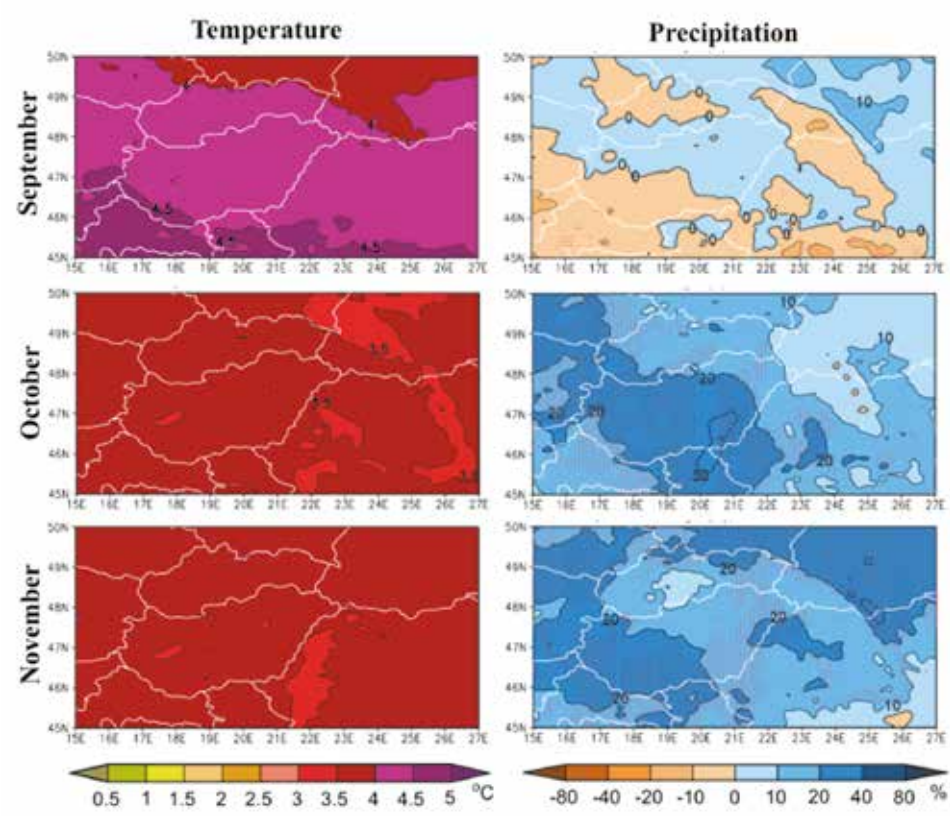

Fig. 11. Projected changes of temperature and precipitation according to the RCP8.5 scenario for 2069–2098 relative to 1971–2000 in the autumn months based on the multi-model mean of 10 RCM simulations. In the case of precipitation, hatched areas show where at least seven models indicated the same direction of change, and the projected change was at least ±10%.

The projected multi-model mean temperature changes for March, April, and May are similar to January and February considering the spatial pattern (i.e., reflecting the topography of the domain), but the predicted values of spring warming are not so high as in winter (*Fig. 12*). Precipitation is likely to increase

in spring, especially in March (by ~ 30%±10%) with a high agreement in the sign of projected changes. Positive changes are projected by fewer RCM simulations in April, and even fewer in May, thus the multi-model projected change of monthly mean precipitation is smaller in April, and even smaller in May compared to March. The multi-model mean precipitation change even shows a slight decrease in May at the southern border of the domain, since some RCM simulations project drier conditions for the late-century compared to the reference period, especially in the southern part of the domain.

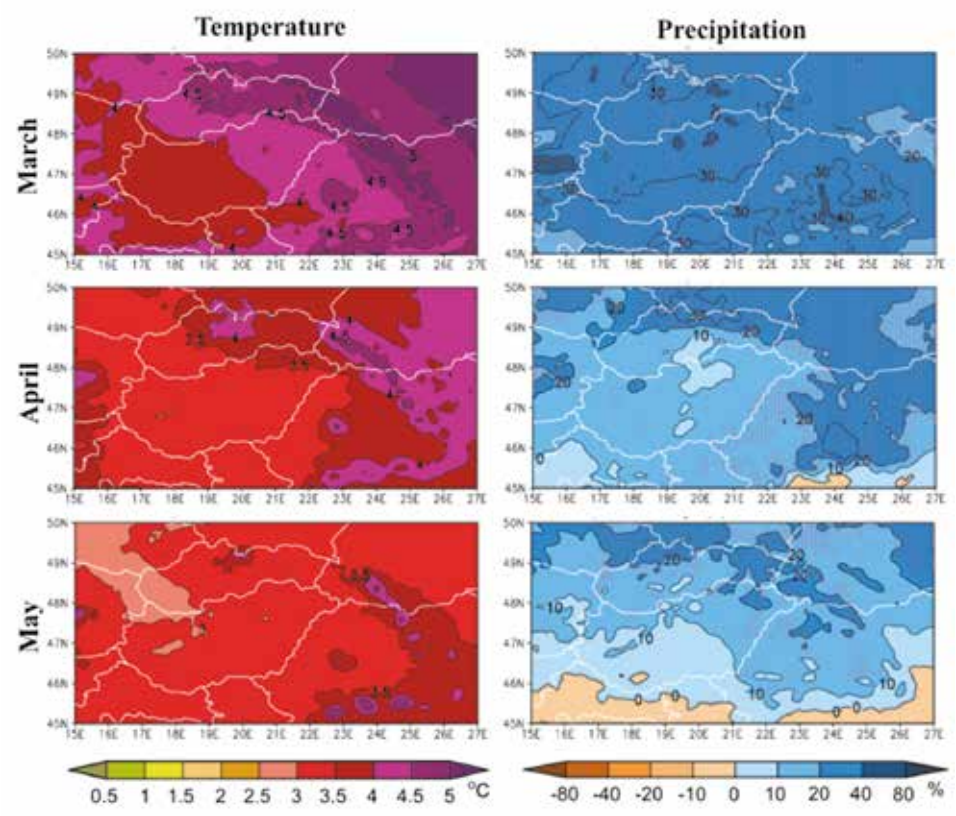

Fig. 12. Projected changes of temperature and precipitation according to the RCP8.5 scenario for 2069–2098 relative to 1971–2000 in the spring months based on the multi-model mean of 10 RCM simulations. In the case of precipitation, hatched areas show where at least seven models indicated the same direction of change, and the projected change was at least ±10%.

On the basis of maps with multi-model mean changes, similar changes are projected for the mid-century as for the late-century, but the temperature increase is more moderate (1–2 °C) and more homogeneous in space. In the case of precipitation, an increase is projected for 2021–2050, except for July and August, when decreasing trend is likely to occur, but with greater uncertainty and smaller overall changes compared to the changes simulated for the 2069–2098 time period.

In order to analyze the variability of precipitation changes in more details, *Fig. 13* shows each simulated monthly precipitation total in January and July during the 30-year period at the end of the 21st century compared to the average monthly total in the 1971–2000 reference period. Results for the five investigated subregions are quite similar to each other. Therefore, we only present one example here, namely, the SHU subregion (located in the middle among the five subregions regarding the north-south extension). In order to illustrate uncertainty not only due to the climatic variability but also due to the model physics and parameterizations, all the 10 RCM simulations are presented (x-axis) in the diagrams taking into account the three different RCP scenarios (indicated by different colors). The differences between the RCP scenarios are not substantial, which can be explained by the fact that in the case of precipitation, the role of the scenario is relatively low within the full uncertainty range of simulations compared to the choice of the model or to the internal variability (*Hawkins* and *Sutton,* 2011). Overall, it can be concluded that greater inter-annual differences occur between the individual monthly anomalies in July in some RCM simulations (e.g., the spread is especially wide in the case of RCM simulations where EC-EARTH or HadGEM2 provide driving inputs to the regional scale), because extremely high precipitation is simulated in a few years. In the case of RCP8.5, according to four RCM simulations, more than 20 years out of 30 will be drier in July compared to the reference period. In SSR, which is the southernmost subregions among the five analyzed subregions, the same conclusion can be made, but the number of these RCM simulations is six, implying higher confidence in expecting drier Julies in the future. Three RCMs simulated drier July conditions relative to the reference period for all the five subregions at least 20 years out of 30 in the case of RCP8.5 (whereas only one RCM simulated similarly for RCP2.6). When taking into account RCP4.5, none of the RCM simulations resulted in drier Julies with such dominance in all the five subregions, however, unlike other simulations, one RCM simulation (i.e., CNRM_RACMO) projects that at least 20 years out of 30 will be wetter in the future in NHU and CHU (in general, wetter July conditions do not exceed the half of all the 30 years in neither scenario or subregions).

Contrary to July, mainly wetter conditions are simulated for January compared to the reference period; two RCM simulations project more monthly precipitation totals in all the five subregions in at least 20 years out of 30, namely, HadGEM2_RCA4 in the case of RCP4.5 and MPI-ESM_REMOr2 in

the case of RCP8.5. Drier Januaries also occur in the simulations, but less frequently compared to the wetter conditions relative to the reference period in any of the subregions.

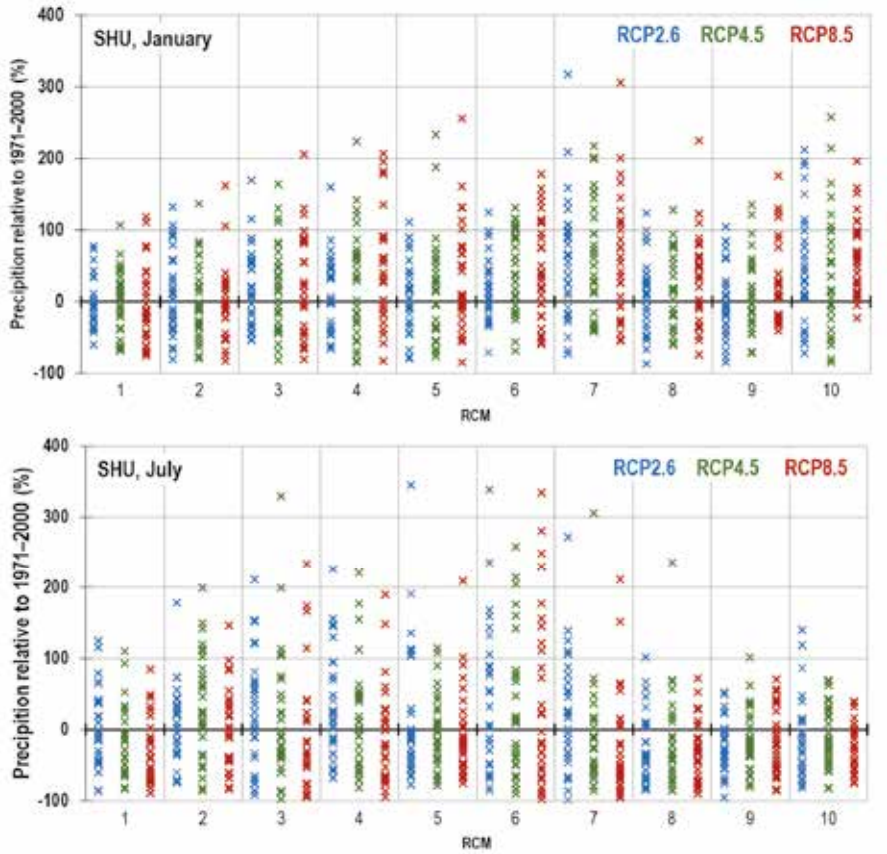

Fig. 13. Projected changes of monthly precipitation in January (top) and July (bottom) according to the three RCP scenarios (indicated by different colors) for each year in 2069–2098 (indicated by crosses) relative to the 1971–2000 reference period based on the 10 individual RCM simulations (x-axis). Spatial averages for the SHU subregion are shown. The RCM simulations are as follows: (1) CNRM_ALARO, (2) CNRM_RACMO, (3) EC-EARTH_CCLM, (4) EC-EARTH_RACMO, (5) EC-EARTH_RCA4, (6) HadGEM2_RACMO, (7) HadGEM2_RCA4, (8) MPI-ESM_RCA4, (9) MPI-ESM_REMOr1, (10) MPI-ESM_REMOr2.

Finally, RVI is analyzed as a precipitation-related feature for the entire year, it is calculated for the five subregions. If the RVI value is smaller than zero for a given year that year is considered as a dry year; if the RVI value is less than –2, it is considered as an extreme dry year. The projected RVI values for the 2021–2050 (x-axis) and 2069–2098 (y-axis) time periods are shown in *Fig. 14* based on the 10 RCM simulations, taking into account the three RCP scenarios (indicated by different colors). In order to facilitate the analysis, two lines are drawn in the diagrams at 15 years indicating the half of the entire simulation period. It can be clearly seen that in the future wetter years are likely to occur. This is a quite straightforward consequence of the monthly changes analyzed above, namely, decreasing trend is projected only for July and August, whereas precipitation is likely to increase in the rest and most parts of the year, so overall the annual average total will also increase. The difference between the RCP scenarios is not so remarkable; it may be explained by the role of different sources of uncertainty in the case of precipitation (as the choice of the scenario is not the most important factor discussed by *Hawkins* and *Sutton* (2011)).

The number of extreme dry years is obviously smaller than the number of dry years, and their distributions show a closer pattern in the diagrams. In the case of the number of dry years, higher variability can be seen: in some RCM simulations the number of years is close to 15 (which is the half of the investigated time period), while in others, only 5 dry years out of 30 are projected to occur in the future. Extreme dry conditions will tend to occur in 2–12 years overall during 30-year future time periods in the northern plain subregions (NHU, CHU, SHU), whereas more frequent extreme dry years are likely to occur in the southern subregions (i.e., NSR, SSR). The RVI results for the mid- and late-century are not substantially different implying only very slight changes between these future periods.

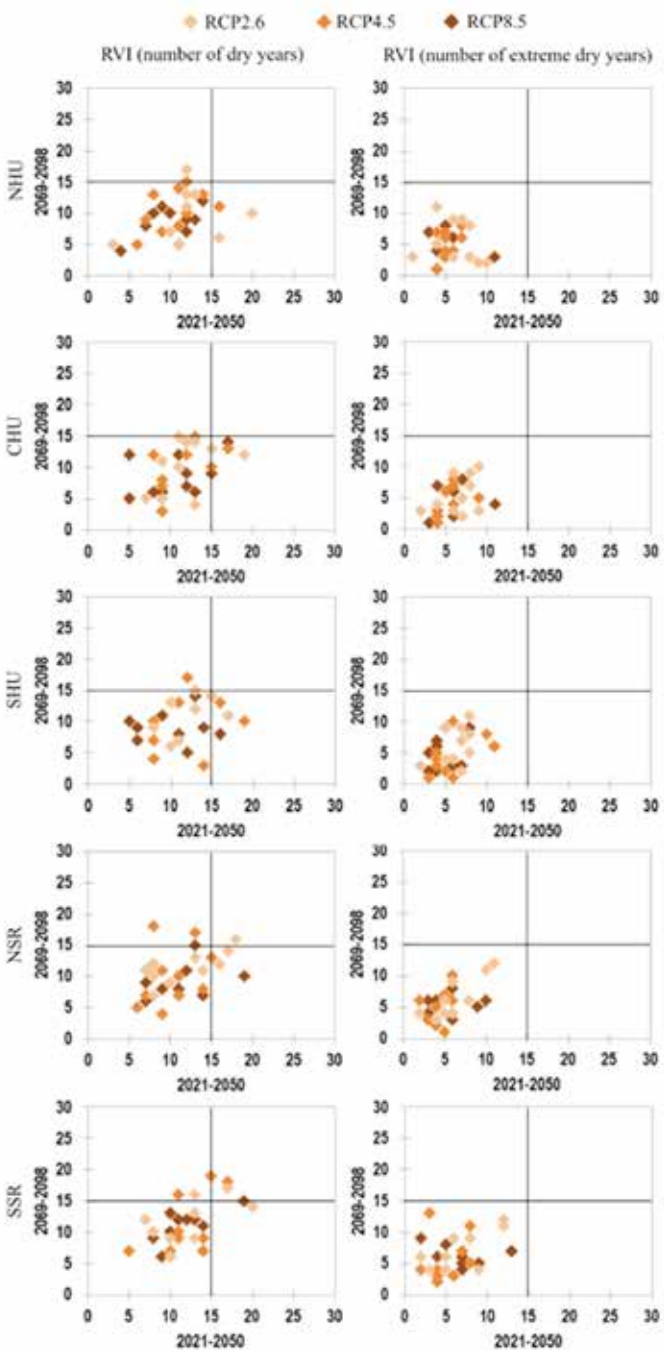

Fig. 14. Projected number of dry and extreme dry years based on RVI 2021–2050 (x-axis) and 2069–2098 (y-axis) in the five subregions according to the three RCP scenarios (indicated by different colors) based on the 10 RCM simulations (indicated by diamonds).

4. Conclusions

The projected temperature and precipitation changes are analyzed for the Pannonian Basin, focusing on five subregions: the plain areas of Serbia and Hungary in a north-south sequence. For the investigation, 10 RCM simulations are used considering three different RCP scenarios, namely, the RCP2.6, RCP4.5 and RCP8.5. Three time periods were analyzed, one historical (1971–2000) and two future time periods (2021–2050, 2069–2098). Since the greater changes are likely to occur by the end of the 21st century, this time period is presented and discussed in more details in this paper.

On the basis of the results shown here, it can be concluded that higher temperature values can be expected in the plain areas of Serbia and Hungary (and in the whole Pannonian Basin) in the future. The projected change by the end of the 21st century is at least 3 °C in every month. Considering the spatial pattern, zonal structure can be clearly recognized in summer, with greater increase (> 4.5 °C) in the southern parts of the domain; while topography plays the key role in winter, with higher values in the mountainous areas. The higher the assumed radiative change in the scenario, the higher the simulated temperature change, which is due to the strong relationship between the radiative forcing and temperature.

Considering precipitation, a decrease is likely to occur in July and in August; and also in June and in September in the southern subregions. In the rest of the year, wetter conditions are projected for the end of the 21st century compared to the end of the 20th century; the projected increase of precipitation is ~ 20% when taking into account the RCP8.5 scenario.

To conclude, in general, warmer and wetter climatic conditions are likely to occur in the plain areas of Serbia and Hungary in the future, but the amplitudes of the projected changes depend on the applied RCP scenario. In the case of temperature, the presented results are in good agreement with former analyzes (e.g., *Bartholy et al.,* 2007), however, in the case of precipitation, some differences can be seen, i.e. summer drying in not so evident, as former simulations showed (*Bartholy et al.,* 2007; *Pongrácz et al.,* 2014; *Kis et al.,* 2017a).

The obtained results can serve as key input in further impact studies (e.g., *Pokovai et al.,* 2020) for the Pannonian region, thus, appropriate adaptation strategies can be developed to cope with the future regional climatic changes. Agriculture, water management and energy sector should take into account these projected changes in long-term planning at regional and national scales.

It is important to note that the projection results for the different RCP scenarios can be clearly distinguished in the case of temperature – as the correlation between the radiative forcing (its change serves as the definition of RCP scenarios) and temperature is quite high –, while in the case of precipitation the differences among RCM results are often greater than those among RCPs. This result is fostered by the conclusion of *Hawkins* and *Sutton*

(2011), namely, the selected RCM plays a higher role in the uncertainty of the projected precipitation change compared to the applied emission scenario, furthermore, internal variability also shows greater effect generally than in the case of temperature (*von Trentini et al.,* 2019). Therefore, it is advisable to take into account more RCM simulations for those studies, which aim to help decision making, to cover the entire range of uncertainty. All in all, the further improvements of both GCMs and RCMs are still a key issue in order to use as reliable simulations as possible for getting relevant results in impact studies. For this purpose non-hydrostatic approach (e.g. *Sasaki et al.,* 2008; *Lyra et al.,* 2018) will probably provide a better reproduction of precipitation conditions. Nevertheless, the main challenge due to the high internal variability of precipitation still remains.

Acknowledgements: Research leading to this paper has been supported by the following sources: the Széchenyi 2020 programme, the European Regional Development Fund and the Hungarian Government via the AgroMo project (grant number: GINOP-2.3.2-15-2016-00028), the Hungarian National Research, Development and Innovation Fund under grants K-129162 and K-120605, the Hungarian Ministry of Human Capacities under the ELTE Excellence Program (grant number: 783-3/2018/FEKUTSRAT), the Ministry of Education, Science and Technological Development, Republic of Serbia (Grant No. TR37003), and the Bilateral science and technological cooperation program between Serbia and Hungary (Grant No. 451-03-02294/2015-09/10 and TÉT_16-1-2016-0135). This study is a contribution to the PannEx Regional Hydroclimate Project of the World Climate Research Programme (WCRP) Global Energy and Water Exchanges (GEWEX) Project. Furthermore, we acknowledge the CARPATCLIM Database compiled with the support of the European Commission in JRC in 2013.

References

Aumont, O., Ethé, C., Tagliabue, A., Bopp, L., and *Gehlen, M.,* 2015: PISCES-v2: an ocean biogeochemical model for carbon and ecosystem studies. *Geosci. Model Dev. 8,* 2465–2513. https://doi.org/10.5194/gmd-8-2465-2015

Balsamo, G., Viterbo, P., Beljaars, A., van den Hurk, B., Hirschi, M., Betts, A.K. and *Scipal, K.,* 2009: A revised hydrology for the ECMWF model: Verification from field site to terrestrial water storage and impact in the Integrated Forecast System. *J. Hydrometeorol. 10,* 623–643. https://doi.org/10.1175/2008JHM1068.1

Bartholy, J., Pongrácz, R., and *Gelybó, Gy.,* 2007: Regional climate change expected in Hungary for 2071-2100. *Appl. Ecol. Environ. Res. 5,* 1–17. https://doi.org/10.15666/aeer/0501_001017

Bihari, Z., and *Szentimrey, T.,* 2013: CARPATCLIM Deliverable D2.10. Annex 3 – Description of MASH and MISH algorithms. 100p.

Ceglar, A., Croitoru, A-E., Cuxart, J., Djurdjevic, V., Güttler, I., Ivancan-Picek, B., Jug, D., Lakatos, M., and *Weidinger, T.*, 2018: PannEx: The Pannonian Basin Experiment. Climate Serv. 11, 78–85. https://doi.org/10.1016/j.cliser.2018.05.002

Collins, W.J., Bellouin, N., Doutriaux-Boucher, M., Gedney, N., Halloran, P., Hinton, T., Hughes, J., Jones, C.D., Joshi, M., Liddicoat, S., Martin, G., O'Connor, F., Rae, J., Senior, C., Sitch, S., Totterdell, I., Wiltshire, A., and *Woodward, S.*, 2011: Development and evaluation of an Earth-system model – HadGEM2. *Geosci. Model Develop. Discus. 4*, 997–1062. https://doi.org/10.5194/gmdd-4-997-2011

Cox, P., 2001: Description of the „TRIFFID" Dynamic Global Vegetation Model. Hadley Centre technical note 24.

Dalelane, C., Früh, B., Steger, C., and *Walter, A.,* 2018: A Pragmatic Approach to Build a Reduced Regional Climate Projection Ensembles for Germany Using the EURO-CORDEX 8.5 Ensemble. *J. Appl. Meteorol. Climatol. 57,* 477–491. https://doi.org/10.1175/JAMC-D-17-0141.1

Déqué, M., Dreveton, C., Braun, A., and *Cariolle, D.,* 1994: The ARPEGE-IFS atmosphere model: a contribution to the French community climate modelling. *Climate Dynamics 10,* 249–266. https://doi.org/10.1007/BF00208992

Elguindi, N., Bi, X., Giorgi, F., Nagarajan, B., Pal, J., Solmon, F., Rauscher, S., Zakey, A., and *Giuliani, G.*, 2011: Regional climatic model RegCM – User manual. Version 4.3. ICTP, Trieste, Italy. 32p.

Essery, R., Best, M., and *Cox, P.,* 2001: MOSES 2.2 Technical Documentation. Hadley Centre technical note 30.

Frei, P., Kotlarski, S., Liniger, M.A., and *Schar, C.,* 2018: Future snowfall in the Alps: projections based on the EURO-CORDEX regional climate models. *The Cryosphere 12,* 1–24. https://doi.org/10.5194/tc-12-1-2018

Giorgetta, M.A., Jungclaus, J., Reick, C.H., Legutke, S., Bader, J., Bo ̈ttinger, M., Brovkin, V., Crueger, T., Esch, M., Fieg, K., Glushak, K., Gayler, V., Haak, H., Hollweg, H-D., Ilyina, T., Kinne, S., Kornblueh, L., Matei, D., Mauritsen, T., Mikolajewicz, U., Mueller, W., Notz, D., Pithan, F., Raddatz, T., Rast, S., Redler, R., Roeckner, E., Schmidt, H., Schnur, R., Segschneider, J., Six, K.D., Stockhause, M., Timmreck, C., Wegner, J., Widmann, H., Wieners, K-H., Claussen, M., Marotzke, J., and *Stevens, B.*, 2013: Climate and carbon cycle changes from 1850 to 2100 in MPI-ESM simulations for the Coupled Model Intercomparison Project phase. *J. Adv. Model. Earth Syst. 5*, 572–597. https://doi.org/10.1002/jame.20038

Giorgi, F., Jones, C., and *Asrar, G.R.,* 2009: Addressing climate information needs at the regional level: the CORDEX framework. *WMO Bull. 58,* 175–183.

Giot, O., Termonia, P., Degrauwe, D., De Troch, R., Caluwaerts, S., Smet, G., Berckmass, J., Deckmyn, A., De Cruz, L., De Meutter, P., Duerinckx, A., Gerard, L., Hamdi, R., Van den Bergh, J., Van Ginderachter, M., and *Van Schaeybroeck, B.*, 2016: Validation of the ALARO-0 model within the EURO-CORDEX framework. Geosci. Model Dev. 9, 1143–1152. https://doi.org/10.5194/gmd-9-1143-2016

Gocic, M., and *Trajkovic, S.,* 2013: Analysis of precipitation and drought data in Serbia over the period 1980–2010. *J. Hydrol. 494,* 32–42. http://dx.doi.org/10.1016/j.jhydrol.2013.04.044

Göndöcs J., Breuer H., Pongrácz R., and *Bartholy J.,* 2017: Urban heat island mesoscale modelling study for the Budapest agglomeration area using the WRF model. *Urban Climate 21,* 66–86. https://doi.org/10.1016/j.uclim.2017.05.005

Gurvan, M., Bourdallé-Badie, R., Bouttier, P-A., Bricaud, C., Bruciaferri, D., Calvert, D., and *Vancoppenolle, M.,* 2017: NEMO ocean engine (Version v3.6-patch). Notes Du Pôle De Modélisation De L'institut Pierre-simon Laplace (IPSL). http://doi.org/10.5281/zenodo.3248739

Hawkins, E., and *Sutton, R.,* 2011: The potential to narrow uncertainty in regional climate predictions. *Clim Dyn 37,* 407–418. https://doi.org/10.1007/s00382-010-0810-6

Haylock, M.R., Hofstra, N., Klein Tank, A.M.G., Klok, E.J., Jones, P.D., and *New, M.,* 2008: A European daily high-resolution gridded dataset of surface temperature and precipitation for 1950–2006. *J. Geophys. Res. 113(D20),* 27. https://doi.org/10.1029/2008JD010201

Huijnen, V., Williams, J., van Weele, M., van Noije, T., Krol, M., Dentener, F., Segers, A., Houweling, S., Peters, W., de Laat, J., Boersma, F., Bergamaschi, P., van Velthoven,, P., Le Sager, P., Eskes, H., Alkemade, F., Scheele, R., Nédélec, P., and *Patz, H-W.*, 2010: The global chemistry transport model TM5: description and evaluation of the tropospheric chemistry version 3.0. *Geosci. Model Dev. 3*, 445–473. https://doi.org/10.1029/2008JD010201

IPCC, 2013: *Climate Change 2013*: The Physical Science Basis. Contribution of Working Group I to the Fifth Assessment Report of the Intergovernmental Panel on Climate Change (*Eds. Stocker, T.F., Qin, D., Plattner, G.-K., Tignor, M., Allen, S.K., Boschung, J., Nauels, A., Xia, Y., Bex, V., Midgley, P.M.*). Cambridge University Press, Cambridge, United Kingdom and New York, NY, USA.

Jacob, D., and *Podzun, R.,* 1997: Sensitivity studies with the regional climate model REMO. *Meteorol. Atmosph. Phys. 63,* 119–129. https://doi.org/10.1007/BF01025368

Jacob, D., Barring, L., Christensen, O.B., Christensen, J.H., de Castro, M., Déqué, M., Giorgi, F., Hagemann, S., Hirschi, M., Jones, R., Kjellström, E., Lenderink, G., Rockel, B., Sánchez, E., Schar, C., Seneviratne, S.I., Somot, S., van Ulden, A., and *van den Hurk, B.*, 2007: An inter-comparison of regional climate models for Europe: model performance in present-day climate. *Climatic Change 81(Suppl 1*), 31–52. https://doi.org/10.1007/s10584-006-9213-4

Jacob, D., Petersen, J., Eggert, B., Alias, A., Christensen, O.B., Bouwer, L.M., Braun, A., Colette, A., Déqué, M., Georgievski, G., Georgopoulou, E., Gobiet, A., Menut, L., Nikulin, G., Haensler, A., Hempelmann, N., Jones, C., Keuler, K., Kovats, S., Kröner, N., Kotlarski, S., Kriegsmann, A., Martin, E., van Meijgaard, E., Moseley, C., Pfeifer, S., Preuschmann, S., Radermacher, C., Radtke, K., Rechid, D., Rounsevell, M., Samuelsson, P., Somot, S., Soussana, J.-F., Teichmann, C., Valentini, R., Vautard, R., Weber, B., and *Yiou, P.*, 2014: EURO-CORDEX: New high-resolution climate change projections for European impact research. Reg. Environ. Change 14, 563–578. https://doi.org/10.1007/s10113-013-0499-2

Jungclaus, J.H., Fischer, N., Haak, H., Lohmann, K., Marotzke, J., Matei, D., Mikolajewicz, U., Notz, D., and *von Storch, J.S.,* 2013: Characteristics of the ocean simulations in the Max Planck Institute Ocean Model (MPIOM) the ocean component of the MPI-Erth system model. *J. Adv. Model. Earth Syst. 5,* 422–446. https://doi.org/10.1002/jame.20023

Kain, J.S., 2004: The Kain–Fritsch convective parameterization: An update. *J. Appl. Meteor. 43,* 170–181. https://doi.org/10.1175/1520-0450(2004)043<0170:TKCPAU>2.0.CO;2

Kis, A., Pongrácz, R., and *Bartholy, J.,* 2017a: Multi-model analysis of regional dry and wet conditions for the Carpathian Region. *Int. J. Climatol. 37,* 4543–4560. https://doi.org/10.1002/joc.5104

Kis, A., Pongrácz, R., Bartholy, J., and *Szabó, J.A.,* 2017b: Application of RCM results to hydrological analysis. *Időjárás 121,* 437–452.

Kotlarski, S., Keuler, K., Christensen, O. B., Colette, A., Déqué, M., Gobiet, A., Goergen, K., Jacob, D., Lüthi, D., van Meijgaard, E., Nikulin, G., Schär, C., Teichmann, C., Vautard, R., Warrach-Sagi, K., and *Wulfmeyer, V.,* 2014: Regional climate modeling on European scales: a joint standard evaluation of the EURO-CORDEX RCM ensemble. Geosci. Model Dev. 7, 1297–1333.https://doi.org/10.5194/gmd-7-1297-2014

Kupiainen, M., Jansson, C., Samuelsson, P., Jones, C., Willén, U., Hansson, U., Ullerstig, A., Wang, S., and *Döscher, R*., 2014: Rossby Centre regional atmospheric model, RCA4. Rossby Center Newsletter, Rossby Centre regional atmospheric model, RCA4. Last updated Aug 11, 2015.

Lakatos, M., Guettler, I., Jug, D., Weidinger, T., Djurdjevic, V., Croitoru, A., Ivancan-Picek, B., and *Couxart, J.,* eds., 2018: Regional hydro-climate project (RHP) over the Pannonian basin (PannEx). White Book. Budapest. 120p. https://sites.google.com/site/projectpannex/

Lindeskog, M., Arneth, A., Bondeau, A., Waha, K., Seaquist, J., Olin, S., and *Smith, B.,* 2013: Implications of accounting for land use in simulations of ecosystem services and carbon cycling in Africa. *Earth Syst. Dynam. 4,* 385–407. https://doi.org/10.5194/esd-4-385-2013

Lyra, A., Tavares, P., Chou, S.C., Sueiro, G., Dereczynski, C., Sondermann, M., Silva, A., Marengo, J., and *Giarolla, A.,* 2018: Climate change projections over three metropolitan regions in Southeast Brazil using the non-hydrostatic Eta regional climate model at 5-km resolution. *Theor. Appl. Climatol. 132*, 663–682. https://doi.org/10.1007/s00704-017-2067-z

Maier-Reimer, E., Kriest, I., Segschneider, J., and *Wetzel, P.*, 2005: The HAMburg Ocean Carbon Cycle Model HAMOCC5.1 – Technical Description Release 1.1. *Ber. zur Erdsystemforsc.* 14.

Masson, V., Le Moigne, P., Martin, E., Faroux, S., Alias, A., Alkama, R., Belamari, S., Barbu, A., Boone, A., Bouyssel, F., Brousseau, P., Brun, E., Calvet, J.C., Carrer, D., Decharme, B., Delire, C., Donier, S., Essaouini, K., Gibelin, A-L., Giordani, H., Habets, F., Jidane, M., Kerdraon, G., Kourzeneva, E., Lafaysse, M., Lafont, S., Lebeaupin Brossier, C., Lemonsu, A., Mahfouf, J-F., Marguinaud, P., Mokhtarti, M., Morin, S., Pigeon, G., Salgado, R., Seity, Y., Taillefer, F., Tanguy, G., Tulet, P., Vincedon, B., Vionnet, V., and *Voldoire, A.,* 2013: The SURFEXv7.2 land and ocean surface platform for coupled or offline simulation of earth surface variables and fluxes. Geosci. Model Dev. 6, 929–960. https://doi.org/10.5194/gmd-6-929-2013

van Meijgaard, E., van Ulft, L.H., van de Berg, W.J., Bosveld, F.C., van den Hurk, B.J.J.M., Lenderink, G., and *Siebesma, A.P.*, 2008: The KNMI regional atmospheric climate model RACMO version 2.1. Technical Report302, 50p.

Morgenstern, O., Braesicke, P., O'Connor, F.M.O., Bushell, A.C., Johnson, C.E., Osprey, S.M., and *Pyle, J.A.,* 2009: Evaluation of the new UKCA climate-composition model – Part 1: The stratosphere. *Geosci. Model Dev. 2*, 43–57. https://doi.org/10.5194/gmd-2-43-2009

Moss, R.H., Edmonds, J.A., Hibbard, K.A., Manning, M.R., Rose, S.K., van Vuuren, D.P., Carter, T.E., Emori, S., Kainuma, M., Kram, T., Meehl, G.A., Mitchell, J.F.B., Nakicenovic, N., Riahi, K.,

Smith, S.J., Stouffer, R.J., Thomson, A.M., Weyant, J.P., and *Wilbanks, T.J.*, 2010: The next generation of scenarios for climate change research and assessment. Nature 463, 747–756. https://doi.org/10.1038/nature08823

Noilhan, J., and *Mahfouf, J-F.,* 1996: The ISBA land surface parameterisation scheme. *Glob. Planet. Change 13,* 145–159. https://doi.org/10.1016/0921-8181(95)00043-7

Oki, T., and *Sud, Y.C.,* 1998: Design of Total Runo Integrating Pathways (TRIP)-a global river channel network. *Earth Interact. 2,* https://doi.org/10.1175/1087-3562(1998)002<0001:DoTRIP>2.0.CO;2

Oki, T., Nishimura, T., and *Dirmeyer, P.A.,* 1999: Assessment of annual runo from land surface models using Total Runo Integrating Pathways (TRIP). *J. Meteorol. Soc. Jpn. 77,* 135–255. https://doi.org/10.2151/jmsj1965.77.1B_235

Pieczka, I., Pongrácz, R., Bartholy, J., and *André, K.,* 2018: Future temperature projections for Hungary based on RegCM4.3 simulations using new Representative Concentration Pathways scenarios. *Int. J. Glob. Warming 15,* 277–292. https://doi.org/10.1504/IJGW.2018.093121

Pieczka, I., Bartholy, J., Pongrácz, R., and *André, K.,* 2019: Validation of RegCM regional and HadGEM global climate models using mean and extreme climatic variables. *Időjárás 123,* 409–433. https://doi.org/10.28974/idojaras.2019.4.1

Pokovai K., Hollós R., Bottyán E., Kis A., Marton T., Pongrácz R., Pásztor L., Hidy D., Barcza Z., and *Fodor N.*, 2020: Estimation of agro-ecosystem services using biogeochemical models. *Időjárás 124*, 209-225. https://doi.org/10.28974/idojaras.2020.2.4

Pongrácz, R., Bartholy, J., and *Kis, A.,* 2014: Estimation of future precipitation conditions for Hungary with special focus on dry periods. *Időjárás 118,* 305–321.

Pope, V.D., Gallani, M.L., Rowntree, P.R., and *Stratton, R.A.,* 2000: The impact of new physical parametrizations in the Hadley Centre climate model - HadAM3. *Climate Dynamics 16,* 123–146. https://doi.org/10.1007/s003820050009

Prtenjak, M.J., Klaić, M., Jeričević, A., and *Cuxart, J.,* 2018: The interaction of the downslope winds and fog formation over the Zagreb area. *Atmos. Res. 214,* 213–227. https://doi.org/10.1016/j.atmosres.2018.08.001

Raddatz, T.J., Reick, C.H., Knorr, W., Kattge, J., Roeckner, E., Schnur, R., Schnitzler, K.G., Wetzel, P., and *Jungclaus, J.*, 2007: Willthe tropical land biosphere dominate the climate-carbon cycle feed-back during the twenty-first century. *Clim. Dyn. 29*, 565–574. https://doi.org/10.1007/s00382-007-0247-8

Roeckner, E, Brokopf, R, Esch, M, Giorgetta, M, Hagemann, S, Kornblueh, L., Manzini, E., Schlese, U., and *Schulzweida, U.,* 2006: Sensitivity ofsimulated climate to horizontal and vertical resolution in the ECHAM5 atmosphere model. *J. Climate 19*, 3771–3791. https://doi.org/10.1175/JCLI3824.1

Rousset, C., Vancoppenolle, M., Madec, G., Fichefet, T., Flavoni, S., Barthélemy, A., Benshila, R., Chanut, J., Levy, C., Masson, S., and *Vivier, F.*, 2015: The Louvain-La-Neuve sea ice model LIM3.6: global and regional capabilities. Geosci. Model Dev. 8, 2991–3005. https://doi.org/10.5194/gmd-8-2991-2015

Salas-Mélia, D., 2002: A global coupled sea ice-ocean model. *Ocean Modelling 4,* 137–172. https://doi.org/10.1016/S1463-5003(01)00015-4

Samuelsson, P., Jones, C., Willen, U., Ullerstig, A., Gollvik, S., Hansson, U., Jansson, C., Kjellström, E., Nikulin, G., and *Wyser, K.*, 2011: The Rossby Centre Regional Climate model RCAS3:model description and performance. *Tellus 63 A*, 4–23. https://doi.org/10.1111/j.1600-0870.2010.00478.x

Sasaki, H., Kurihara, K., Takayabu, I., Uchiyama, T., 2008: Preliminary experiments of reproducing the present climate using the non-hydrostatic regional climate model. *SOLA 4*, 25–28. https://doi.org/10.2151/sola.2008-007

Schättler, U., Doms, G., and *Schraff, C.,* 2019: A Description of the Nonhydrostatic Regional COSMO-Model. Part VII :User's Guide. COSMO 5.06a, Deutscher Wetterdienst, Offenbach. 187p. Available online at http://www.cosmo-model.org/content/model/documentation/core/cosmo_userguide_5.06a.pdf

Skamarock, W.C., Klemp, J.B., Dudhia, J., Gill, D.O., Barker, D.M., Duda, M.G., Huang, X.-Y., Wang, W., and *Powers, J.G.,* 2008: A Description of the Advanced Research WRF Version 3. NCAR Tech. Note NCAR/TN-475+STR. http://dx.doi.org/10.5065/D68S4MVH

Smith, B., Prentice, I.C., and *Sykes, M.T.*, 2001: Representation of vegetation dynamics in the modelling of terrestrial ecosystems: comparing two contrasting approaches within European climate space. *Glob. Ecol. Biogeograp. 10,* 621–637. https://doi.org/10.1046/j.1466-822X.2001.00256.x

Szalai, S., Auer, I., Hiebl, J., Milkovich, J., Radim, T.. Stepanek, P., Zahradnicek, P., Bihari, Z., Lakatos, M., Szentimrey, T., Limanowka, D., Kilar, P., Cheval, S., Deak, Gy., Mihic, D., Antolovic, I., Mihajlovic, V., Nejedlik, P., Stastny, P., Mikulova, K., Nabyvanets, I., Skyryk, O., Krakovskaya, S.,Vogt, J., Antofie, T., and *Spinoni, J.*, 2013: Climate of the Greater Carpathian Region. Final 740 Technical Report. http://www.carpatclim-eu.org.

Szentimrey, T., and *Bihari, Z.,* 2006: MISH (Meteorological Interpolation based on Surface Homogenized Data Basis). In (Eds: *O.E.Tveito, M.Wegehenkel, F. van der Wel* and *H. Dobesch*) COST Action 719 Final Report, The use of GIS in climatology and meteorology, 54–56.

Szentimrey, T., 2007: Manual of homogenization software MASHv3.02. Hungarian Meteorological Service, Budapest. 65p.

Taylor, K.E., 2001: Summarizing multiple aspects of model performance in a single diagram. *J. Geophys. Res. 106(D7),* 7183–7192. https://doi.org/10.1029/2000JD900719

Torma, Cs.Zs., 2019: Detailed validation og EURO-CORDEX and Med-CORDEX regional climate model ensembles over the Carpathian Region. *Időjárás 123,* 217–240. https://doi.org/10.28974/idojaras.2019.2.6

Totterdell, I. J., 2019: Description and evaluation of the Diat-HadOCC model v1.0: the ocean biogeochemical component of HadGEM2-ES. *Geosci. Model Dev. 12,* 4497–4549. https://doi.org/10.5194/gmd-12-4497-2019

Undén, P., Rontu, L., Jarvinen, H., Lynch, P., Calvo, J., Cats, G., Cuxart, J., Eerola, K., Fortelius, C., Garcia-Moya, J.A., Jones, C., Lenderlink, G., McDonald, A., McGrath, R., Navascues, B., Nielsen, N.W., Odegaard, V., Rodriguez, E., Rummukainen, M., Room, R., Sattler, K., Sass, B.H., Savijarvi, H., Schreur, B.W., Sigg, R., The, H., and *Tijm, A*., 2002: HIRLAM-5 Scientific Documentation, 144 pp. Available from SMHI, S-601 76 Norrköping, Sweden.

Voldoire, A., Sanchez-Gomez, E., Salas y Mélia, D., Decharme, B., Cassou, C., Sénési, S., Valcke, S., Beau, I., Alias, A., Chevallier, M., Déqué, M., Deshayes, J., Douville, H., Fernandez, E., Madec, G., Maisonnave, E., Moine, M.-P., Planton, S., Saint-Martin, D., Szopa, S., Tyteca, S., Alkama, R., Belamari, S., Braun, A., Coquart, L., and *Chauvin, F*., 2013: The CNRM-CM5.1 global climate model: description and basic evaluation. *Climate Dynam. 40*, 2091–2121. https://doi.org/10.1007/s00382-011-1259-y

van Vuuren, D.P., Edmonds, J., Kainuma, M., Riahi, K., Thomson, A., Hibbard, K., Hurtt, G.C., Kram, T., Krey, V., Lamarque, J-F.,Masui, T., Meinshausen, M., Nekicenovic, N., Smith, S.J., and *Rose, S.K.,* 2011: The representative concentration pathways: an overview. *Climatic Change 109*, 5–31.https://doi.org/10.1007/s10584-011-0148-z

von Trentini, Fabian, Leduc, M., and *Ludwig, R.,* 2019: Assessing natural variability in RCM signals: comparison of a multi model EURO-CORDEX ensemble with a 50-member single model large ensemble. *Climate Dynam. 53*, 1963–1979. https://doi.org/10.1007/s00382-019-04755-8

Weidinger, T., Vecenaj, Z., Krámer, T., Lázár, I., Gyöngyösi A.Z., Pticar, D., Torma, P., Rehák, A., Szilágyi, M., Breuer, H., Tordai Á., Bordás, Á., and *Grisogono, B*., 2019: Joint Croatian-Hungarian micrometeorological experiments in Zagreb vineyards (2016-2018) and on Lake Balaton (2018): instrumentations, data-sets, and modelling work. Book of Abstracts. 5th PannEx Workshop, Novi Sad, Serbia. Eds.: Jug, D. and Güttler, I. Published by Facutly of Agrobiotechnical Sciences Osijek. 58p. ISBN 978-953-7871-85-7, http://www.fazos.unios.hr/upload/documents/5th%20PannEx%20workshop_Book%20of%20Abstracts_2019.pdf

Winkelmann, R., Martin, M. A., Haseloff, M., Albrecht, T., Bueler, E., Khroulev, C., and *Levermann, A.,* 2011: The Potsdam Parallel Ice Sheet Model (PISM-PIK) – Part 1: Model description. *The Cryosphere 5,* 715–726. https://doi.org/10.5194/tc-5-715-2011

DOI:10.28974/idojaras.2020.2.3

IDŐJÁRÁS

Quarterly Journal of the Hungarian Meteorological Service
Vol. 124, No. 2, April – June, 2020, pp. 191–207

Modeling the urban climate of Budapest using the SURFEX land surface model driven by the ALADIN-Climate regional climate model results

Gabriella Zsebeházi * and **Gabriella Szépszó**

Hungarian Meteorological Service
P.O. Box 38, H-1525 Budapest, Hungary

* *Corresponding author E-mail: zsebehazi.g@met.hu*

(Manuscript received in final form March 11, 2020)

Abstract— Urbanized areas modify the local climate due to the physical properties and morphology of surface objects. The urban impacts on local scale interact with the regional climate resulting in an amplification of certain climate aspects in the cities (e.g., higher maximum air temperature), which may be further enhanced with climate change. Regional climate models provide adequate tool for assessing the regional characteristics of global changes, however, they are incapable for describing the local impacts, e.g., in cities, due to their relatively low resolution (usually 10–25 km horizontally) and due to the lack of detailed description of relevant physical processes. To investigate the future climate change in cities, surface models provide a scientifically sound and cutting-edge solution for the previous problem. In this study, the behavior of SURFEX externalized land surface model including the TEB urban canopy scheme and coupled to the ALADIN-Climate regional climate model in offline mode is investigated. A 10-year-long simulation for 2001–2010 was achieved on 1 km resolution for Budapest. The main goals of our investigation are i) to assess how the biases of the regional climate model inherited and modified by SURFEX, ii) what is the added value of SURFEX to ALADIN-Climate, and iii) what are the capabilities of SURFEX in terms of describing urban and suburban seasonal temperature cycle and daily urban heat island (UHI) evolution in Budapest. Quantified validation is conducted using the measurements of two stations located in the city center and in the suburban area. It was found that SURFEX overestimates the 2 m temperature in both locations throughout the year, in spite of the too cold ALADIN forcings. The strength of nocturnal UHI is overestimated from autumn till spring, while it is slightly too weak in summer. Moreover, the evolution and collapse of daily UHI is imperfectly simulated, namely some delay and slower daily dynamics occur, which might be caused by the method applied for deriving the atmospheric forcings.

Key-words: urban climate change, urban heat island, land surface modelling, SURFEX, TEB, ALADIN-Climate, validation

1. Introduction

More than half of the world's population lives in cities nowadays, and this rate is projected to increase to 66% by 2050 (*UN*, 2014). The growing number of cities' inhabitants has been detected also in Hungary in the past decades, which currently counts 70% of total population (*KSH*, 2013). The air of cities is warmer, drier, and more polluted than of natural areas due to the specific surface characteristics (i.e., impervious surfaces, narrow streets, high buildings, large heat capacity of buildings) and anthropogenic activity (e.g., internal heating and transportation; *Oke*, 1987). All these cause that cities are especially exposed to the impacts of climate change.

To tackle these challenges, proper adaptation and mitigation strategies – supported by targeted vulnerability studies – are needed. Different methodologies with different complexity exist to quantitatively estimate the impact of climate change in cities. *Wilby* (2003) developed a *multivariate statistical model*, in which a relationship was set up between the atmospheric variables (e.g., near surface wind speed, relative humidity, vorticity) and the nocturnal urban heat island (UHI) for London. They used the statistical model to project the future changes. Although this method does not require large computing capacity, its greatest drawback is that it lacks the physical relationship between the atmospheric and land surface processes, which might alter the statistical relations as time goes by. *Large-eddy simulation (LES) models* take place on the other end of complexity, they partially resolve turbulence and are able to investigate atmospheric processes in cities on meter-scale with an appropriate urban surface module, such as the PALM-USM (Parallelized Large-Eddy Simulation Model – Urban Surface Model) model (*Resler et al*., 2017). Their very high resolution and elaboration require extremely large computation capacity; therefore, they are used for short periods, but it is almost impossible to apply them for a whole city for several decades in transient mode. *Urban canopy surface balance models* (*Masson,* 2006) simulate surface energy balance components and energy transfer in the Prandtl-layer on the neighborhood scale, i.e., individual building characteristics (e.g., geometry, material) are averaged, streets are considered as a unit. These simplifications enable to apply them on long timescale (decades) with km-scale resolution. For example, *Hamdi et al.* (2015) examined the urban climate change in Brussels and Paris in the mid-21st century using SURFEX (Surface Externalisé) driven by[1] the ALARO[2] model. *McCarthy et al.* (2010) simulated the global response of cities to doubling CO_2 by inline coupling the MOSES (Met Office Surface Exchange Scheme) land surface model to the HadAM3 (Hadley Centre

[1] SURFEX can be coupled to its driving model in two ways. Offline coupling refers to standalone mode, when SURFEX has no feedback to its driving model. Inline coupling means two-way coupling, in which case SURFEX outputs influence the driving model as well.

[2] ALARO stands for ALADIN-AROME, and it is a development of ALADIN mesoscale model with a physics parameterization package designed specifically for convection-permitting resolutions.

Atmospheric Model version 3) global climate model. *Lemonsu et al.* (2015) assessed the impact of different urban expansion scenarios under heat waves in Paris using the TEB (Town Energy Balance) urban scheme driven by the Meso-NH (Mesoscale Non-hydrostatic Model) numerical model.

At the Hungarian Meteorological Service, the SURFEX (*Le Moigne*, 2009) surface model coupled to the ALADIN-Climate (climate version of the ALADIN[3] numerical weather prediction model; hereinafter ALADIN) is applied for urban climate investigations. A detailed validation procedure has been started, in order to familiarize the model behavior and reveal its capabilities from the aspect of our needs. *Vértesi* (2011) analyzed 2 m temperature and 10 m horizontal wind field of a 10-year (1961–1970) SURFEX simulation over Budapest. The study compared grid point model data against urban and suburban station measurements. It was concluded that SURFEX adds extra heat to the ALADIN fields principally over the city, catching the urban heat island phenomenon (especially in spring and autumn). On the other hand, the study revealed that the simulated diurnal summer temperature in the urban point is colder than in the suburban point. *Krüzselyi et al.* (2016) performed similar investigation for the period of 1991–2000 and compared the results to those of 1961–1970. They examined i) whether the temperature biases in the two gridpoints change with time, and ii) whether using the land cover dataset based on recent surface information in SURFEX simulations explains the relatively warmer temperature of the suburb of Budapest in the 60s (note that these areas were greener at that time). They found that the investigated gridcells are characterized with the same type (temperate suburban) in the land cover dataset, which explains the lack of urban heat island emergence in SURFEX, contrary to measurements. Therefore, other grid point – which is described as urban point in the database – has to be selected to study the UHI. It implies also to choose a more recent validation period, since new measurement stations inside the city have been installed only from the 2000s.

In this paper, the applicability of SURFEX land surface model was investigated from the aspect of describing the urban climate of Budapest. Validation results of SURFEX and its driving model, ALADIN are presented for Budapest for the period of 2001–2010. We explore more in detail the impact of ALADIN results on SURFEX daily and sub-daily temperature and UHI results in a newly selected urban gridpoint, where the land cover database performs better. The paper is organized as follows: the overview of the model and experimental design is presented in Section 2, in Section 3, the performance of ALADIN over Budapest is assessed and temperature results of SURFEX and its added value to the regional climate model (RCM) are investigated. Finally, the conclusions of our results and future plans are given in Section 4.

[3] ALADIN stands for Air Limitée Adaptation Dynamique Dévéloppement International.

2. Models and methods

2.1. The SURFEX land surface model

SURFEX simulates energy, momentum, and moisture fluxes between the surface and the surface boundary layer (SBL; lower 10% of the planetary boundary layer). In order to bridge the gap between the model resolution (typically 1 km) and the heterogeneity of land cover, the model applies the tiling method, i.e., a grid cell may be composed of four different surface types (nature, sea, inland water, and town). For each tile, different parameterization scheme computes the relevant fluxes, which are then area weighted aggregated over the grid cell. Advection is not taken into account in SURFEX, meaning there is no interaction between neighboring grid points.

From the aspect of urban climate investigation, in Hungary two surface types, the urban and natural surfaces are in focus. Over urban surfaces the Town Energy Balance (TEB) scheme (*Masson,* 2000) is applied, which approximates the complex geometry of cities with the canyon concept. It means that streets are represented by roads with homogenous, uniform buildings on their two sides. Real orientation of roads is not taken into account it is integrated over all directions instead. Town characteristics are described by three main parameters: building height, building aspect ratio (rate of building height and roof width), and canyon aspect ratio (rate of building height and canyon width). TEB computes moisture budget for roof and road and energy budget for roof, wall, and road separately. Heat conduction is parameterized with considering several layers in urban surfaces. Heating, traffic, and industrial sourced anthropogenic energy and moisture fluxes are also taken into account.

Physical processes of natural surfaces are computed by the ISBA (Interaction Soil Biosphere Atmosphere) scheme (*Noilhan* and *Mahfouf*, 1996), which applies the force-restore method (*Noilhan and Planton*, 1989) to determine surface temperature and water content evolution. Ground is divided into three layers (*Boone et al.,* 1999) for describing heat and moisture conduction.

Atmospheric forcings for the model are short and longwave downward radiation, temperature, wind speed and wind direction, specific humidity, surface pressure and precipitation which are prescribed on a few tenth of meter above surface. These forcings can be supplied either by measurements or available atmospheric model results.

In the model, surface boundary layer is resolved by the Surface Boundary Layer scheme (*Masson* and *Seity*, 2009; *Hamdi* and *Masson*, 2008) that introduce several model levels between the surface and the forcing level, and computes temperature, humidity (e.g., on 2-m height), wind speed (e.g., on 10-m height), and turbulent fluxes in prognostic equations.

2.2. The ALADIN-Climate model

Atmospheric forcings for SURFEX were provided by the ALADIN-Climate version 5.2 regional climate model (*Colin et al.,* 2010). ALADIN-Climate was developed at the Météo-France by combining the dynamical core of the ALADIN hydrostatic weather prediction model (*Termonia et al.,* 2018) and the physical parameterization package of the ARPEGE-Climat (climate version of ARPEGE; Action de Recherche Petite Echelle Grande Echelle; *Déqué et al.,* 1994) general circulation model. The land surface model of ALADIN is SURFEX, in which ISBA computes the fluxes over natural tiles, and urban covers are not taken into account.

2.3. Experimental setup

In order to investigate how the model describes the urban climate features, a 10-year-long simulation was conducted for 2001–2010 with the 5.1 version of SURFEX over Budapest. The 1 km resolution domain consists of 72x72 gridpoints (*Fig. 1*). The 10-km horizontal resolution ALADIN was driven by the ERA-Interim re-analysis (*Dee et al.,* 2011), which fields on 30 m above surface were interpolated to 1 km horizontal resolution over the SURFEX domain using the EE927 configuration (*Fig. 1*). This configuration is for horizontal and vertical interpolation of the ALADIN outputs to prepare lateral boundary conditions for a nested model simulation. Its main advantage is that it takes into account the topography as well. These forcings were provided 3 hourly for SURFEX, which linearly interpolates them to its own timestep, i.e., 5 minutes. Land cover information was obtained from the 1 km resolution ECOCLIMAP-I database (*Masson et al.,* 2003), which combines satellite data, climate maps, and other existing land cover maps and provide parameters for 255 different cover types. Over our domain it distinguishes eight different urban types, amongst them the most important ones are dense urban, temperate suburban, industries and commercial areas, and urban parks. These differ in fraction of urban and nature tiles, canyon parameters (e.g., building height, canyon width, roughness length), vegetation parameters (e.g., leaf area index), etc. *Table 1* summarizes the main features of the SURFEX setup and the achieved simulation.

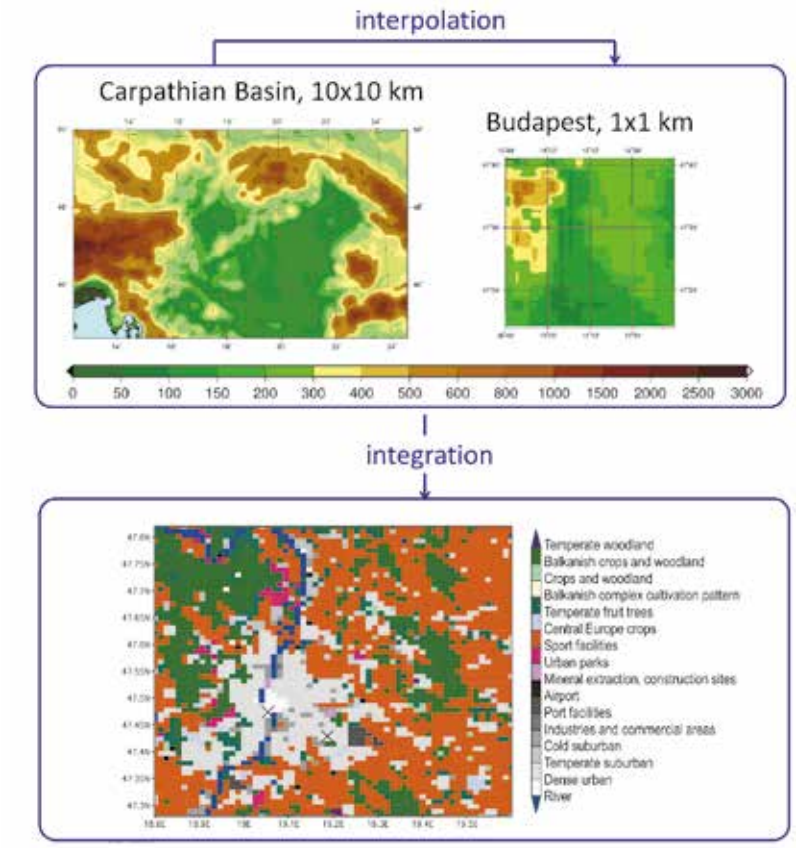

Fig. 1. Flow chart about the use of SURFEX. Top left: domain and topography of the 10 km resolution ALADIN-Climate; top right: ALADIN model fields interpolated to a 1 km resolution domain over Budapest. Bottom: land cover type of grid cells according to the ECOCLIMAP database for Budapest. The two validation gridpoints are marked with x.

Table 1. Main parameters of SURFEX setup

Atmospheric forcings	3-hour outputs of ERA-Interim driven ALADIN-Climate v5.2
Height of forcing coupling	30 m
Resolution	1 km
Scheme for urban tiles	TEB
Scheme for nature tiles	ISBA
Land cover	ECOCLIMAP
Domain	Budapest
Integration period	2001–2010

First we briefly validated the 10 km resolution ALADIN fields against the 10 km resolution CarpatClim gridded dataset based on observations (*Szalai et al.*, 2013) over the Budapest domain. Then urban climate characteristics simulated by SURFEX were studied investigating the spatial pattern and temporal evolution of 2 m temperature. In Budapest, the number of operational SYNOP (Surface Synoptic Observations) stations are quite scarce compared to the 1 km model resolution, hence quantitative validation is possible only in a few gridpoints. Based on location and data availability, 2 m temperature time series of two stations were used to validate SURFEX (*Fig. 2*): one in the city center (Lágymányos; 19°3'43"E, 47°28'29"N) and one in the suburban area (Pestszentlőrinc; 19°10'56"E, 47°25'45"N). From SURFEX, the corresponding nearest gridpoints were chosen. In ECOCLIMAP, these two gridpoints are associated with dense urban and temperate suburban cover types, respectively (*Fig. 1*). *Table 2* shows their main parameters.

Fig. 2. Two validation points: meteorological stations located in the city center (Lágymányos) and in the southern part of Budapest (Pestszentlőrinc).

Table 2. Urban parameters in the selected gridpoints according to ECOCLIMAP

Land cover type	Dense urban	Temperate suburban
Fraction of urban tile	0.9	0.6
Fraction of nature tile	0.1	0.4
Building height	30 m	10 m
Building aspect ratio	1	0.5
Canyon aspect ratio	1	0.5

3. Results and discussion

3.1. Validation of ALADIN-Climate

The performance of regional climate model providing atmospheric forcings has a great influence on the behavior of the land surface model, therefore, we briefly evaluate the ALADIN near surface fields (2 m temperature and relative humidity, 10 m windspeed and precipitation) over Budapest for 2001–2010. The validation domain consists of 70 grid points data of which were compared to the CarpatClim data. It has to be noted that the spatial and temporal representations of the compared fields differ to some extent. While an ALADIN gridpoint represents the mean value of the corresponding gridbox, CarpatClim consists of pointwise data, although the interpolation technique ensures that they are spatially representative. Daily mean of instantaneous variables (temperature, windspeed, and relative humidity) was computed from 3-hourly ALADIN outputs, while in CarpatClim, only 3–4 data measured in the main standard synoptic hours were considered, except mean temperature, which was derived as the average of daily minimum and maximum temperature values. Nevertheless, we believe that these discrepancies lessen as applying multiyear monthly and seasonal means.

The 2 m temperature is underestimated with -1.0 – (-1.5) °C in all seasons except summer, as can be seen on the left panel of *Fig. 3,* in *Fig. 4* and *Table 3*. However, probably due to the insufficient representation of the hilly area on the northwestern-western part of the domain (i.e., the elevation is lower than in the reality), higher temperatures compared to reference occur in the related gridpoints. The temperature interpolated with ALADIN EE927 (recall that the applied method considers elevation) and aggregated to 10 km reveal some improvement over these areas (right panel of *Fig. 3*).

The 2 m relative humidity is overestimated by ALADIN on average throughout the year, except summer, when the model nearly perfectly simulates the observed values (*Fig. 4*). However, in this season 37% more precipitation falls in ALADIN (*Table 3*), which, together with the positive temperature bias, is a well-known attribute of the model over Hungary (*Illy et al*., 2015). It may be supposed that the too warm near-surface air layer contains more moisture as well (since relative humidity is unbiased), therefore precipitation overestimation may be related to the enhanced convective activity. *Krüzselyi* (2013) also found that ALADIN produces too much convective precipitation in summer compared to the ERA-Interim re-analysis. Concurrent to *Illy* (2017), we also identified too weak near-surface wind speed simulated by ALADIN in every season.

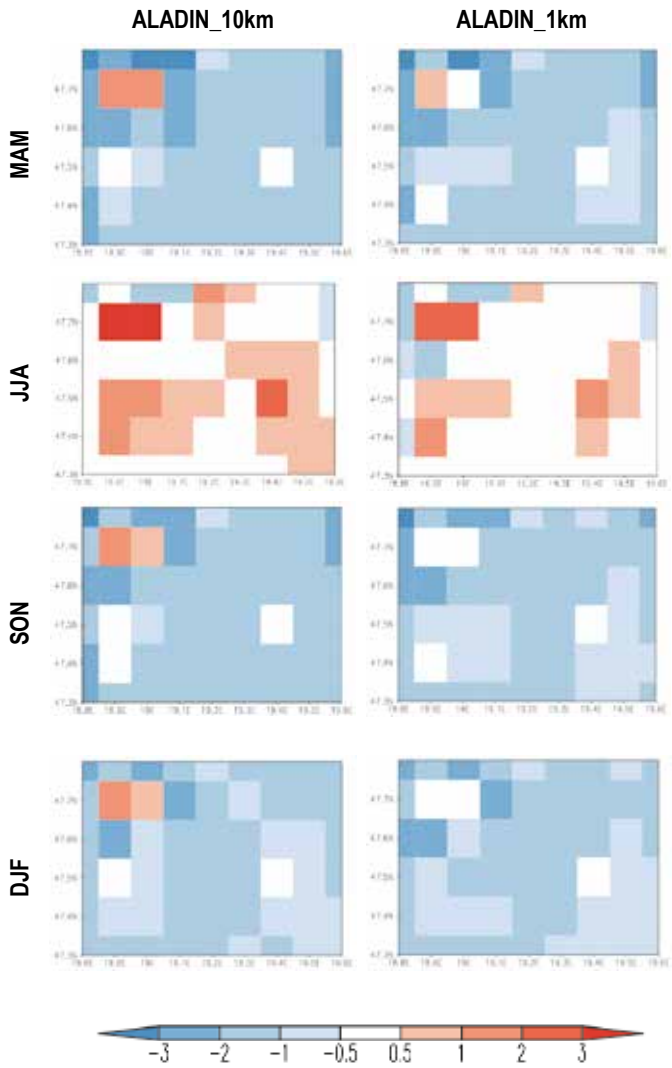

Fig. 3. 2 m temperature bias of the 10 km resolution ALADIN and 1 km resolution interpolated field aggregated to 10 km, with reference to CarpatClim for 2001–2010.

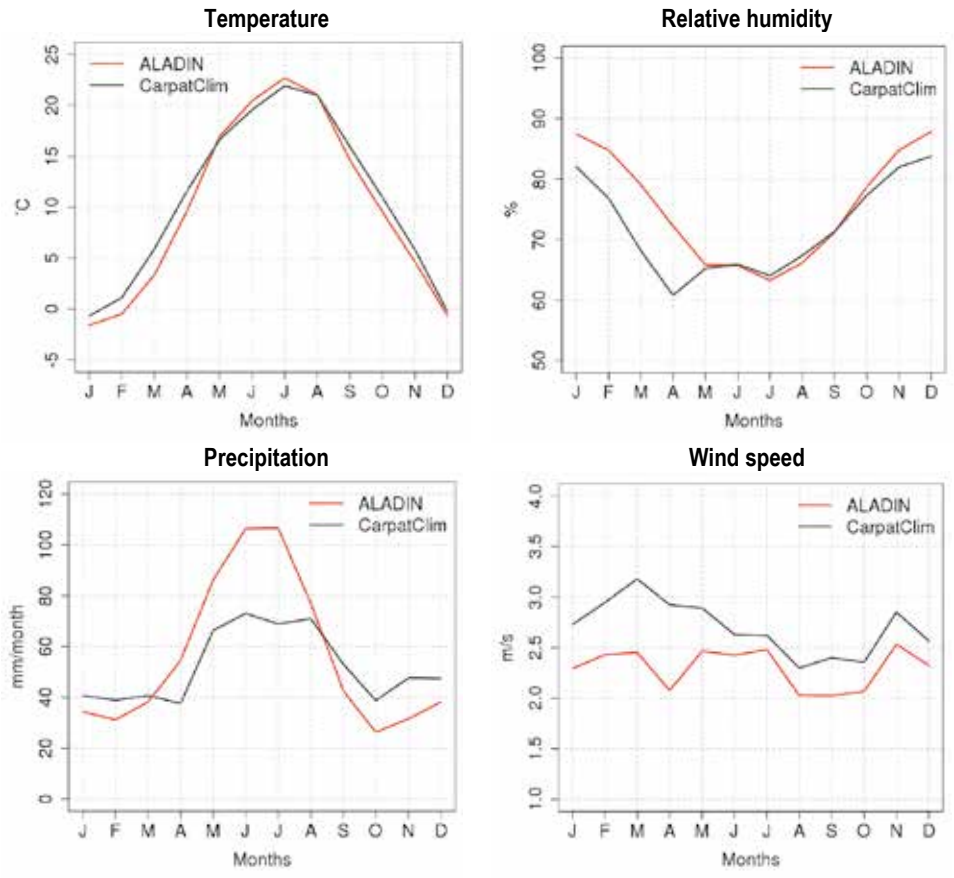

Fig. 4. Area-averaged monthly mean 2 m temperature (in °C), relative humidity (in %), precipitation (in mm/month), and 10 m wind speed (in m/s) according to ALADIN and CarpatClim for 2001–2010.

Table 3. Seasonal mean area-averaged bias of different variables of ALADIN compared to CarpatClim for 2001–2010

	Temperature [°C]	**Relative humidity [%]**	**Precipitation [%]**	**Wind speed [m/s]**
MAM	-1.5	8	25	-0.7
JJA	0.5	0	37	-0.3
SON	-1.4	2	-27	-0.4
DJF	-1.0	6	-16	-0.5

3.2. *Validation of SURFEX*

An important feature of TEB is the specific, urban relevant repartitioning of the net radiation into turbulent fluxes. *Fig. 5* illustrates the surface energy balance components over the urban and suburban reference points. It can be seen that the available net radiation slightly differ in these two locations, while in the diurnal hours the energy is transported in the form of sensible heat flux rather than latent heat flux in the urban point, thanks to the larger urban land cover fraction. Moreover, more energy is conducted and stored during the day, and slightly more energy is emitted during the night in the urban objects than in the natural surfaces, that leads to the emergence of the nocturnal heat island.

Therefore, due to the detailed representation of surface physical processes and to the fine horizontal resolution, SURFEX simulates mean seasonal 2 m temperature over Budapest and its vicinity more realistically than ALADIN does (*Fig. 6*). Urban heat island can be detected in every season and the city center is approximately 2 °C warmer than the rural areas. Moreover, the detailed orography implemented in SURFEX and the applied interpolated atmospheric forcings result in a realistic spatial distribution of 2 m temperature outside the city as well, namely the Buda, Pilis, and Visegrád Hills on the northwest-west and the Gödöllő Hills on the east stand out with cooler temperatures, among which the warmer Pest Plain is located.

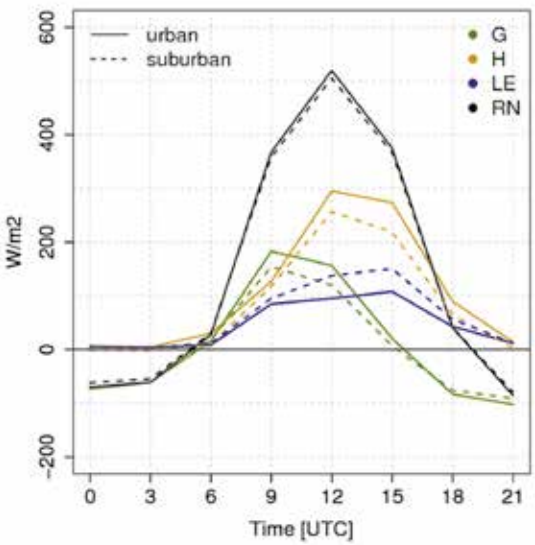

Fig. 5. Summer mean daily cycle of surface energy balance components (G: ground heat flux, H: sensible heat flux, LE: latent heat flux, RN: net radiation) in the urban and suburban reference points in 2001–2010.

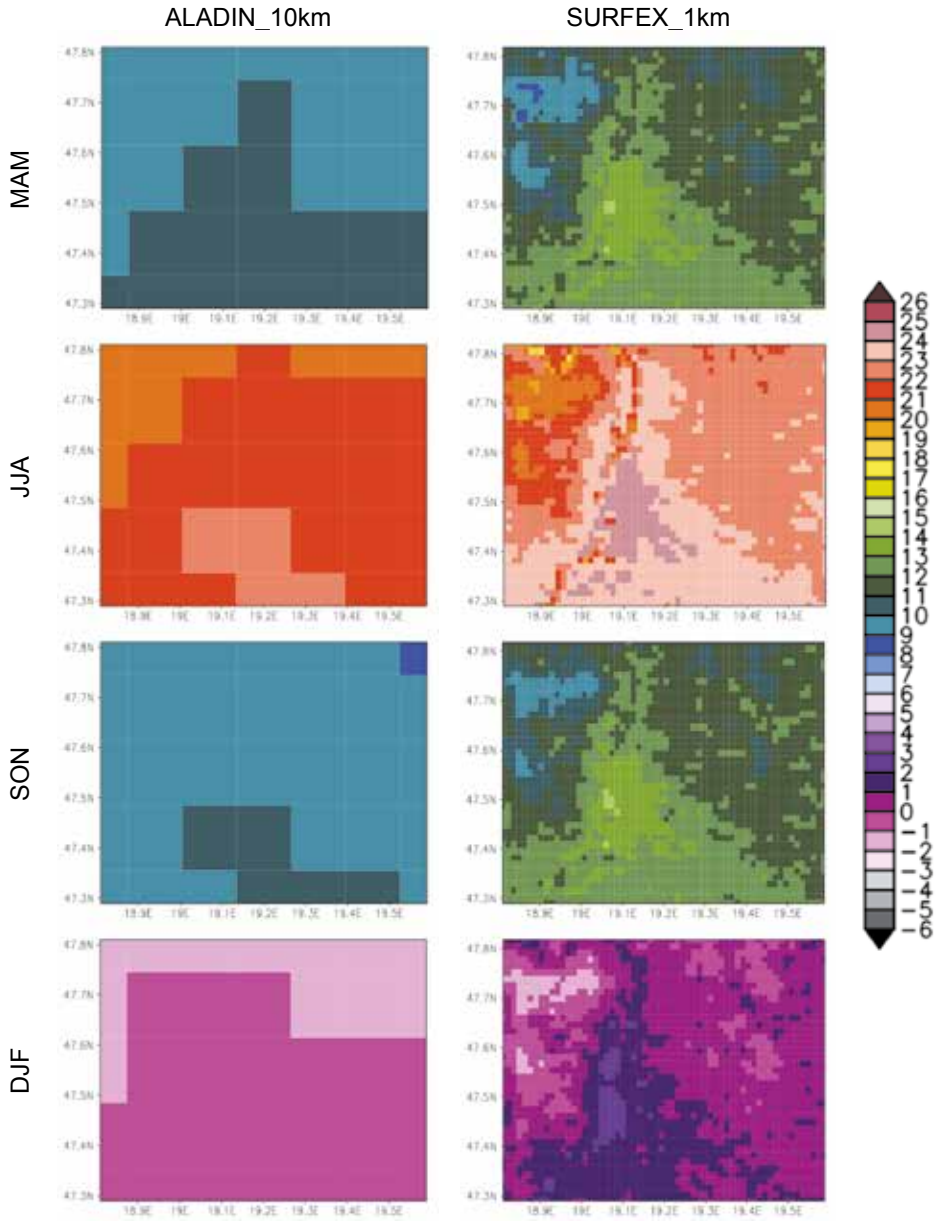

Fig. 6. Seasonal mean 2 m temperature in the 10 km resolution ALADIN (left panel) and 1 km resolution SURFEX (right panel) in 2001–2010.

It can be said that SURFEX is able to simulate the main characteristics of the climate of Budapest and the surrounding complex orography. To validate the surface model more quantitatively, the annual cycle of 2 m temperature in the reference urban and suburban gridpoints resulted by SURFEX and interpolated from ALADIN outputs is presented in *Fig. 7*. As it was already mentioned, ALADIN is too cold in almost every season, except summer, when its bias is significantly reduced. Comparing the two locations, larger underestimation appears in the urban point, that can be explained by the lack of urban representation in ALADIN. As *Fig. 6* also suggests, SURFEX adds extra heating to the ALADIN fields resulting in a 0.5–3 °C overestimation throughout the year, mostly from July to October. This warming is more intense in the urban point (thanks to TEB), therefore, the differences between the bias in the two points reduced. It results in an improved description of the urban heat island, since the systematic bias of SURFEX is eliminated when UHI is derived.

Fig. 7 shows that both minimum and maximum daily temperatures contribute to the mean temperature overestimation. Apart from summer, there is no big difference between the magnitude of daily minimum and maximum overestimation, but in summer, the model has significant shortcomings in simulating nocturnal temperatures.

We also examined the performance of SURFEX describing the diurnal cycle of UHI in each season in the reference points (*Fig. 8*). From autumn to spring too strong nocturnal urban heat island is simulated, while in summer the daily maximum values do not reach the observed ones. From May to August larger positive bias is found in the suburban point which cause weaker UHI intensity (*Fig. 7*). This relation between the biases in the two points shift in the rest of the months, which explains the nocturnal UHI overestimation. A delay in the daily UHI cycle can be detected: nocturnal UHI develops slower than observed, and it collapses later as well. A possible explanation behind this deficiency is that we introduce some error, when atmospheric forcings are prepared for SURFEX. Certain variables that are stored cumulatively in ALADIN files (such as radiation and precipitation) in 3-hourly steps are transformed to instantaneous values using linear interpolation. During sunrise and sunset, the linear interpolation method fails to determine correctly the radiation intensities from 3-hourly cumulative values. Therefore, in the morning less energy is provided to the surface that may cause slower warm-up of natural surfaces and longer lasting UHI. In contrast, during sunset larger radiation intensities are produced that delays the development of temperature difference between the urban and rural surfaces.

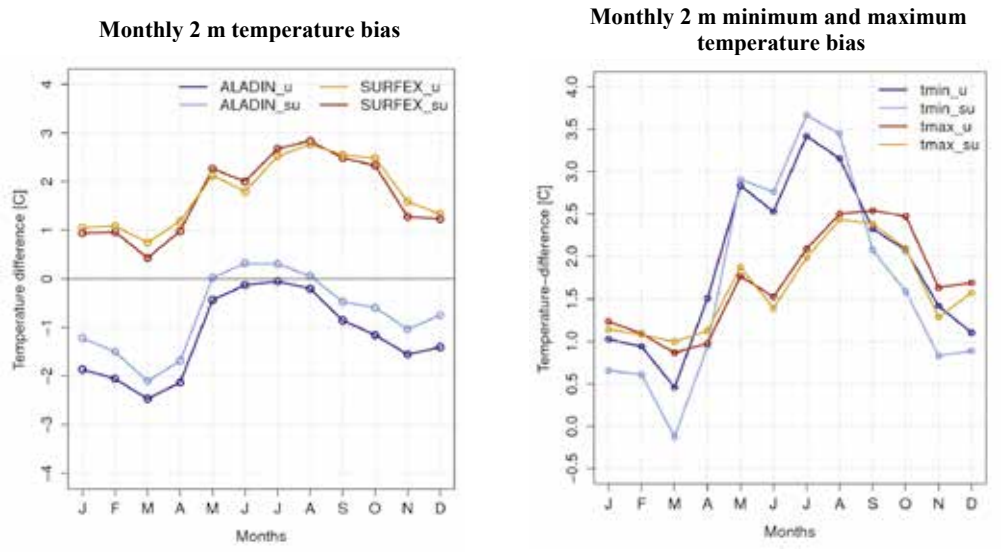

Fig. 7. Monthly 2 m temperature (left) bias of interpolated ALADIN and SURFEX and minimum and maximum temperature bias (right) of SURFEX in 2001–2010 in the urban (_u) and suburban (_su) reference points with respect to station measurements.

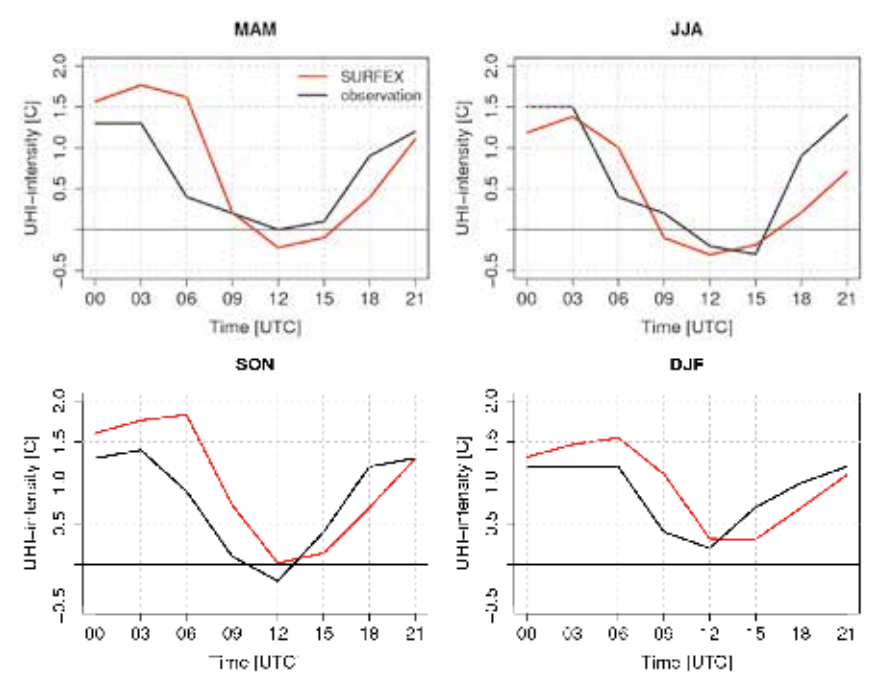

Fig. 8. Daily cycle of UHI in each season according to the SURFEX and station measurements in the reference points for 2001–2010.

4. Conclusions

In this study, the SURFEX surface model was investigated from the aspect of simulating urban climate of Budapest for the period of 2001–2010. The model was coupled in offline mode to the 10 km resolution ALADIN-Climate with 3-hourly update of atmospheric forcings. On the one hand, added value of the detailed TEB urban parameterization scheme of SURFEX was explored compared to the regional climate model results; on the other hand the simulated temperature and UHI seasonal and daily cycles were validated in an urban and a suburban grid point against station measurements. The main findings are as follows:

- ALADIN underestimates the temperature over Budapest with (-1.0) – (-1.5) °C throughout the year except summer, when a slightly positive bias, followed with a strong precipitation overestimation is observed.
- SURFEX warms the ALADIN fields but too heavily, leading to a 0.5–3 °C seasonally varying positive temperature bias.
- The abovementioned two conclusions coincide with the findings of *Vértesi* (2011) and *Krüzselyi et al.* (2016), regardless the investigated time period, gridpoints and the newer re-analysis applied in ALADIN. However, as far as UHI is concerned, a different urban gridpoint selection largely improved the pointwise validation results.
- Nocturnal UHI is overestimated from spring to autumn which can be explained by the larger overestimation in the urban point compared to the suburban one. This relation is veered in summer, therefore nocturnal UHI is weaker as well.
- A delay in the evolution and collapse of UHI is found which may be the outcome of the inadequate linear method of forcing creation.

These results suggest that with a higher forcing frequency update, better daily UHI evolution may be reached. On the other hand, due to the complex orography of Budapest, one cannot purely distinguish the impact of interpolation and the impact of urban scheme on the final results. Therefore, to better understand the behavior of SURFEX, the investigation will be continued over flat terrain, using a more simple spatial interpolation method for deriving atmospheric forcings.

References

Boone, A., Calvet, J.-C., and *Noilhan, J.,* 1999: Inclusion of a Third Soil Layer in a Land Surface Scheme Using the Force–Restore Method. *J. Appl. Meteorol. 38*, 1611–1630. https://doi.org/10.1175/1520-0450(1999)038<1611:IOATSL>2.0.CO;2

Colin, J., Déqué, M., Radu, R., and *Somot, S.,* 2010: Sensitivity study of heavy precipitations in Limited Area Model climate simulation: influence of the size of the domain and the use of the spectral nudging technique. *Tellus-A 62*, 591–604. https://doi.org/10.1111/j.1600-0870.2010.00467.x

Déqué M., Dreveton C., Braun A., and *Cariolle D.*, 1994: The ARPEGE-IFS atmosphere model: a contribution to the French community climate modelling. *Climate Dynam. 10,* 249–266. https://doi.org/10.1007/BF00208992

Dee, D.P., Uppala, S.M., Simmons, A.J., Berrisford, P., Poli, P., Kobayashi, S., Andrae, U., Balmaseda, M.A., Balsamo, G., Bauer, P., Bechtold, P., Beljaars, A.C.M., van de Berg, L., Bidlot, J., Bormann, N., Delsol, C., Dragani, R., Fuentes, M., Geer, A.J., Haimberger, L., Healy, S.B., Hersbach, H., Hólm, E.V., Isaksen, L., Kållberg, P., Köhler, M., Matricardi, M., McNally, A.P., Monge-Sanz, B.M., Morcrette, J.-J., Park, B.-K., Peubey, C., de Rosnay, P., Tavolato, C., Thépaut, J.-N., and *Vitart, F.,* 2011: The ERA-Interim reanalysis: configuration and performance of the data assimilation system. *Quart. J. Roy. Meteorol. Soc. 137,* 553–597. https://doi.org/10.1002/qj.828

Hamdi, R. and *Masson, V.,* 2008: Inclusion of a Drag Approach in the Town Energy Balance (TEB) Scheme: Offline 1D Evaluation in a Street Canyon. *J. Appl.Meteorol. Climatol. 47*, 2627–2644. https://doi.org/10.1175/2008JAMC1865.1

Hamdi, R., Giot, O., De Troch, R., Deckmyn, A., and *Termonia, P.,* 2015: Future climate of Brussels and Paris for the 2050s under the A1B scenario. *Urban Climate 12*, 160–182. https://doi.org/10.1016/j.uclim.2015.03.003

Illy T., Sábitz J., and *Szépszó G.,* 2015: Validation of the ALADIN-Climate simulation results. *Report of the RCMTéR EEA-C13-10 project,* Hungarian Meteorological Service, Budapest. 19 p.

Illy, T., 2017: Near-surface wind speed changes in the 21st century based on the results of ALADIN-Climate regional climate model. *Időjárás 121*, 161–187.

Krüzselyi, I., 2013: Evaluation of a Euro-CORDEX ALADIN-Climate experiment focusing on Hungary. Paper presented at: General Assembly of the European Geoscience Union. 11 April 2013. Vienna, Austria.

Krüzselyi, I., Zsebeházi, G., and *Kovács, M.,* 2016: Urban Climate Modelling with SURFEX/TEB at the Hungarian Meteorological Service. In (Ed. *Musco, F.*) Counteracting Urban Heat Island Effects in a Global Climate Change Scenario, pp. 14–21. Springer Nature, Switzerland. https://doi.org/10.1007/978-3-319-10425-6

KSH, 2013*: Population cencus 2011. 3. National data.* (eds.: *Bada, I. Cs., Bulik, L., Dobróka, Z., Gyulai, K., Kerner-Kecskés, B., Simonné H. G., Trybek, K., Weisz, T.*) Hungarian Central Statistical Office, Budapest, Hungary. 276p. ISBN 978-963-235-417-0 (in Hungarian)

Le Moigne, P., 2009: SURFEX Scientific Documentation. Note de centre (CNRM/GMME). Météo-France, Toulouse, France. 211p.

Lemonsu, A., Viguié, V., Daniel, M., and *Masson, V.,* 2015: Vulnerability to heat waves: Impact of urban expansion scenarios on urban heat island and heat stress in Paris (France). *Urban Climate 14,* 586–605. https://doi.org/10.1016/j.uclim.2015.10.007

Masson, V., 2000: A Physically-Based Scheme For The Urban Energy Budget In Atmospheric Models. *Bound.-Lay. Meteorol. 94*, 357–397. https://doi.org/10.1023/A:1002463829265

Masson, V., Champeaux, J.-L., Chauvin, F., Meriguet, C., and *Lacaze, R.,* 2003: A Global Database of Land Surface Parameters at 1-km Resolution in Meteorological and Climate Models. *J. Climate 16*, 1261–1282. https://doi.org/10.1017/S1350482705001519

Masson V., 2006: Urban surface modeling and the meso-scale impact of cities. *Theor. Appl. Climatol. 84*, 35–45. https://doi.org/10.1007/s00704-005-0142-3

Masson, V. and *Seity, Y.,* 2009. Including Atmospheric Layers in Vegetation and Urban Offline Surface Schemes. *J. Appl. Meteorol. Climatol. 48*, 1377–1397. https://doi.org/10.1175/2009JAMC1866.1

McCarthy, M.P., Best, M. J., and *Betts, R. A.,* 2010: Climate change in cities due to global warming and urban effects. *Geophys. Res. Lett. 37*, L09705. https://doi.org/10.1029/2010GL042845

Noilhan, J. and *Mahfouf, J.-F.,* 1996: The ISBA land surface parameterisation scheme. *Glob. Planet. Change 13*, 145–159. https://doi.org/10.1016/0921-8181(95)00043-7

Noilhan, J. and *Planton, S.,* 1989: A Simple Parameterization of Land Surface Processes for Meteorological Models. *Mon. Weather Rev. 117*, 536–549. https://doi.org/10.1175/1520-0493(1989)117<0536:ASPOLS>2.0.CO;2

Oke, T.R., 1987: Boundary Layer Climates. 2nd edition. Methuen Publishers, London, United Kingdom. 435p. ISBN 0-415-04319-0

Resler, J., Krč, P., Belda, M., Juruš, P., Benešová, N., Lopata, J., Vlček, O., Damašková, D., Eben, K., Derbek, P., Maronga, B., and *Kanani-Sühring, F.,* 2017: PALM-USM v1.0: A new urban surface model integrated into the PALM large-eddy simulation model. *Geosci. Model Dev. 10*, 3635–3659. https://doi.org/10.5194/gmd-10-3635-2017

Szalai, S., Auer, I., Hiebl, J., Milkovich, J., Radim, T. Stepanek, P., Zahradnicek, P., Bihari, Z., Lakatos, M., Szentimrey, T., Limanowka, D., Kilar, P., Cheval, S., Deak, Gy., Mihic, D., Antolovic, I., Mihajlovic, V., Nejedlik, P., Stastny, P., Mikulova, K., Nabyvanets, I., Skyryk, O., Krakovskaya, S.,Vogt, J., Antofie, T., and *Spinoni, J.* 2013: Climate of the Greater Carpathian Region. Final Technical Report.

Termonia, P., Fischer, C., Bazile, E., Bouyssel, F., Brožková, R., Bénard, P., Bochenek, B., Degrauwe, D., Derková, M., El Khatib, R., Hamdi, R., Mašek, J., Pottier, P., Pristov, N., Seity, Y., Smolíková, P., Španiel, O., Tudor, M., Wang, Y., Wittmann, C., and *Joly, A.,* 2018: The ALADIN System and its canonical model configurations AROME CY41T1 and ALARO CY40T1. *Geosci. Model Dev. 11,* 257–281. https://doi.org/10.5194/gmd-11-257-2018

UN, 2014: Concise Report on the World Population Situation in 2014. Department of Economic and Social Affairs, United Nations, New York, USA. 38p. ISBN 978-92-1-151518-3

Vértesi, Á. É., 2011: Modelling possibilities of the urban heat island effect in Budapest Master Thesis. ELTE, Budapest, Hungary. 78p. (in Hungarian)

Wilby, R., 2003: Past and projected trends in London's Urban heat island. *Weather 58*, 251–260. https://doi.org/10.1256/wea.183.02

DOI:10.28974/idojaras.2020.2.4

IDŐJÁRÁS

Quarterly Journal of the Hungarian Meteorological Service
Vol. 124, No. 2, April – June, 2020, pp. 209–225

Estimation of agro-ecosystem services using biogeochemical models

Klára Pokovai [1,*], **Roland Hollós** [2,3], **Emese Bottyán** [2,3], **Anna Kis** [2,3], **Tibor Marton** [6], **Rita Pongrácz** [2,3], **László Pásztor** [5], **Dóra Hidy** [2,3], **Zoltán Barcza** [2,3,4], and **Nándor Fodor** [6]

[1] *Department of Soil Physics and Water Management*
Institute for Soil Sciences and Agricultural Chemistry
Centre for Agricultural Research, Hungarian Academy of Sciences,
H-1022 Budapest, Herman Ottó út 15, Hungary

[2] *Department of Meteorology, Eötvös Loránd University,*
H-1117 Budapest, Pázmány P. sétány 1/A, Hungary

[3] *Excellence Center, Faculty of Science, Eötvös Loránd University,*
H-2462 Martonvásár, Brunszvik u. 2, Hungary

[4] *Faculty of Forestry and Wood Sciences*
Czech University of Life Sciences
Prague, 165 21 Prague 6, Kamýcká 129, Czech Republic

[5] *Department of Soil Mapping and Environmental Informatics*
Institute for Soil Sciences and Agricultural Chemistry
Centre for Agricultural Research, Hungarian Academy of Sciences,
H-1022 Budapest, Herman Ottó út 15, Hungary

[6] *Crop Production Department, Agricultural Institute*
Centre for Agricultural Research, Hungarian Academy of Sciences,
H-2462 Martonvásár, Brunszvik u. 2, Hungary

**Corresponding author E-mail: pokovai.klara@agrar.mta.hu*

(Manuscript received in final form July 5, 2019)

Abstract— Agro-ecosystem services are the various benefits (e.g., crop yield) that people freely obtain from the properly functioning agricultural lands. The estimated changes in climatic conditions including increasing temperature, with particular attention to the summer means, together with the expected changes in the temporal precipitation distribution pose enormous challenge to the agriculture. Currently, dynamic system models are most frequently used tools that are capable of estimating the prospective effects of climate change on agro-ecosystems. A deterministic biogeochemical model is presented that is developed by Hungarian scientists within the framework of the AgroMo project. The main goal of the AgroMo project is to develop climate-smart strategies in order to mitigate the effect of potential future hazards in the context of climate change by 1) creating a complex, state-of-the-art experimental platform; 2) producing ten new, 0.1° spatial resolution climate scenarios based on the RCP (Representative Concentration Pathway) 4.5 and RCP8.5 scenarios; 3) developing an integrated assessment and modeling framework that is capable of simulating every major land use types; 4) analyzing/simulating a great number of adaptation strategies that can be used to support decision makers. Based on the preliminary simulation results, climate change will most likely expose significant negative impact on the spring sown crops in Hungary. Although, the yield losses could be avoided with irrigation or could be mitigated with earlier sowing, the role of winter crops is likely to become more significant in Hungary in the future.

Key-words: model, simulation, climate change, crop yield, nitrate leaching, decision support

1. Introduction

Ecosystem services are the various benefits that people freely obtain from the properly functioning natural environment. Agricultural ecosystems cover nearly 40% of the terrestrial ecosystems (*FAO,* 2017). Their role is essential in human wellbeing, while food, forage, natural fibre, timber and biomass fuels, pharmaceuticals, and other biochemicals and products from floriculture are essential agro-ecosystem services as well as such non-marketed services like regulation of soil and water quality, carbon sequestration, support of biodiversity and cultural services (*Power,* 2010), pest and disease regulation as well as climate regulation (*Jarvis et al.,* 2011). Malfunctioning agro-ecosystems also can be a source of disservices, like loss of wildlife habitat, nutrient runoff, sedimentation of waterways, greenhouse gas emissions, pesticide poisoning of humans and non-targeted species (*Power,* 2010). Global food security is a major area of interest of all these agro-ecosystem services and disservices. According to relevant statistics, at present over 800 million people remain food insecure (*FAO,* 2017). Scientists repeatedly call attention on climate change that could potentially interrupt progress toward a world without hunger. Studies support the need for considerable investment in adaptation and mitigation actions toward a "climate-smart food system" that is more resilient to climate change influences on food security (*Wheeler* and *von Braun,* 2013).

Recent global climate change is thought to be caused by increasing atmospheric greenhouse gas concentration, which is in large part the consequence of human activity, mainly fossil fuel combusting, cement production, and land use change (*Stocker et al.,* 2013). The global mean surface temperature has increased since the late 19th century, and each of the past three decades has been warmer than all the previous ones (*Stocker et al.,* 2013). In Hungary, the first decade of the 21st century (2001–2010) was the warmest period since 1901. The average temperature was 0.7 °C warmer than the 30-year (1970–2000) average (*Lakatos* and *Bihari,* 2011). Precipitation measurements suggest that the overall intensity and frequency of extreme precipitation events – related to both the excess and lack of precipitation – increased in the 1901-2009 period and, at the same time, the total precipitation slightly decreased (*Bartholy* and *Pongrácz,* 2005; *Lakatos et al.,* 2011).

In order to quantitatively evaluate the future climate change, global climate models (GCMs) were applied in the framework of climate model intercomparison projects (e.g., CMIP3, CMIP5; (*Knutti* and *Sedláček,* 2012; *Meehl et al.,* 2007; *Taylor et al.,* 2011). Continuous warming is projected for Europe according to climate model simulations with an annual mean temperature of 1–5.5 °C higher in 2071–2100 than in 1971–2000. A continental warming of 1–4.5 °C and 2.5–5.5 °C is projected by the new ensemble of regional climate model (RCM) simulations from the EURO-CORDEX program for RCP4.5 and RCP8.5, respectively (*Jacob et al.,* 2014).

Pieczka et al. (2018) has provided downscaled temperature time fields for the Carpathian Basin with 10 km horizontal resolution using the RCP4.5 and RCP8.5 scenarios. Simulations for the whole 21st century using either scenario show a clear warming trend with the largest estimated changes in summer, and the smallest changes in spring. Spatial average temperature changes are 2.4 °C and 5.1 °C in the last 20 years of the 21st century compared to the 1981–2000 reference period, with 3.6 °C and 6.9 °C projected warming in the summer months. In case of temperature related extreme events, e.g., hot days (when daily Tmax > 30 °C) and tropical nights (when daily Tmin > 20 °C), significant increase is projected for the 21st century. Precipitation projections for the Carpathian Basin indicate that substantially drier climatic conditions are likely for summer (*Kis et al.,* 2017) on the basis of the results of 11 RCM simulations. In addition, the length of summer dry periods and the total number of dry days are projected to increase. The temporal precipitation distribution seems to be restructured by the end of the 21st century, namely the currently wettest season (summer) can become the driest and the currently driest season (winter) will become the wettest if greenhouse gas concentration continue to increase throughout the century (*Pongrácz et al.,* 2014).

As the Carpathian Basin is located in a transitional zone between a warmer Mediterranean (where a general drying is expected) and a colder continental climate (where overall wetter conditions are projected), the uncertainty of GCM projections are quite high (*Stocker et al.,* 2013). It means that further

investigations on finer spatial resolution are needed to get more precise information on the future climatic conditions (*Kis et al.,* 2017).

The estimated changes in climatic conditions including increasing annual mean temperature, with particular attention to the summer means, together with the expected changes in the temporal precipitation distribution pose enormous challenge to the agriculture. Currently, dynamic system models (crop models) are the most frequently used tools that are capable of estimating the prospective effects of climate change on agro-ecosystems (*Fodor et al.,* 2017). Coupling of crop models with climate change scenarios, this crop-climate modeling is essential to the development of future agricultural outlooks that can inform policy processes and/or field-level decisions (*Porter et al.,* 2014). It can be suitable for (i) deriving stakeholder-driven portfolios of options for farmers, communities, and countries; (ii) ensuring that adaptation actions are relevant to those most vulnerable to climate change; and (iii) combining adaptation and mitigation (*Campbell et al.,* 2016). Possible applications of crop modeling are understanding the drivers of yield levels under climate change and promoting adaptation planning and response to changing production risks (*Webber et al.,* 2018). In this paper, a deterministic biogeochemical model is presented that is developed by Hungarian scientists within the framework of the AgroMo project.

2. Materials and methods

Modeling is an essential tool in agricultural systems science (*Jones et al.,* 2017). Different types of models are developed and used depending on the purpose of use and spatial and temporal scales (*Fodor et al.,* 2017). Climate or environmental index-based methods determine the vulnerability of the studied agricultural area on production factors that are characterized by multidimensional scoring system (*Olesen et al.,* 2011). Statistical models use regression equations to show linkage between yield or yield components and climate variables (*Kern et al.,* 2018; *Leng* and *Huang,* 2017; *Lobell* and *Burke,* 2010). Niche-based models define the geographical distribution of a crop species and specify the concerning environmental suitability expressed on a scale (0-1) (*Estes et al.,* 2013). Process based or dynamic crop models synthesize the latest scientific understanding of biophysical processes and are currently the primary scientific tools available to assess potential impacts of climate change on crop production (*Bindi et al.,* 2015). The complexity of risks posed by climate change and possible adaptations for crop production requires integrated assessment and modeling (IAM) approaches linking biophysical, geochemical, and economic models (*Ewert et al.,* 2015). *Jones et al.* (2017) pins out that recent trends in broader collaboration across institutions, across disciplines, and between the public and private sectors suggest that the stage is set for the major advances in agricultural systems science that are needed for the next generation of models, databases, knowledge products, and

decision support systems. International model comparison projects like the Agricultural Model Intercomparison and Improvement Project (*Rosenzweig et al.,* 2013) and the Modelling European Agriculture with Climate Change for Food Security (*Bindi et al.,* 2015) show that there is a major international effort linking the climate, crop, geochemical, and economic modeling communities with cutting-edge information technology to produce improved systems models and the next generation of climate impact projections for the agricultural sector.

2.1. The AgroMo project

The main goal of the AgroMo project is to develop climate-smart strategies in order to mitigate the effect of potential future hazards in the context of climate change. The AgroMo project is carried out by a multidisciplinary group of scientist from the related research areas: meteorology, climatology, soil physics, soil chemistry, soil biology, plant physiology, plant nutrition, plant breeding, agro-economy, and informatics implementing four major tasks:

1) To create a complex experimental platform by combining multiple long-term experiments and newly established state-of-the-art experiments with the latest info-communication, remote sensing, and data mining techniques in order to produce large amount, good quality observed data for developing and calibrating deterministic simulation models.

2) To produce 10 continuous, bias-corrected, daily-step climate projections for the 2006–2100 period based on the RCP4.5 and RCP8.5 scenarios using different GCM-RCM combinations. These projections, together with the 10 already existing SRES A1B based projections (*Dobor et al.,* 2015) will be used to predict the potential impact of climate change on the agricultural sector of the Carpathian Basin.

3) To develop an integrated assessment and modeling framework (AgroMo) by combining the 4M crop simulation model (*Fodor et al.,* 2003), the Biome-BGC biogeochemical model (*Thornton,* 2000), and a simple agro-economical model in order to support decision makers at multiple scales: from plot level to country level. The AgroMo system will be capable of: (a) simulating every major land use types (arable land, pasture, forest) as well as the key soil processes including CO_2 and N_2O emissions; (b) simulating plots; (c) simulating extended areas (using a gridded database of soil and climatic data). It will work for Hungary as a default, but European and even World wide datasets can be linked in a plug&play manner; (d) carrying out inverse modeling for calibration (parameter estimation); (e) supporting ensemble runs: using many climate projections and/or using alternative routines for key processes (e.g., photosynthesis based on the Farquhar model vs Beer-Lambert Law); (f) calculating the economic consequences of

specific agromanagement changes (e.g., intensification of fertilization or starting irrigation) as well as of land use changes.

4) To analyze/simulate a great number of adaptation strategies (irrigation, earlier sowing, etc.) that can be used for supporting decision makers in promoting sustainable and climate-smart agricultural activities.

2.2. The AgroMo experimental platform

Beside installing a great number of environmental monitoring sensors (soil respiration, soil moisture content, soil temperature, NDVI, etc.) in several long-term field experiments, the project is supported by a newly launched experimental infrastructure comprising a 3-ring FACE experiment, two eddy-covariance stations, and a 12-column lysimeter station.

Free-air carbon dioxide enrichment (FACE) is a climate manipulation technique performed in open field conditions (*Ainsworth* and *Long,* 2005). Using FACE technology, CO_2 concentration is increased within circular areas and is kept at a relatively stable level (typically 100–200 ppm above current atmospheric levels) for longer time intervals. Elevated CO_2 concentration is expected to affect photosynthetic activity, evapotranspiration, plant growth and many other processes that affect crop yield quantity and quality. FACE is believed to provide the most realistic measure to estimate the effect of increasing CO_2 concentration on plant processes (*Ainsworth et al.,* 2008). In the FACE rings at Martonvásár, 3 different cultivars are planted in 2 fertilizer levels, and the target CO_2 concentration is 600 ppm. This dataset will be used to benchmark the AgroMo system in terms of parameterization of the model for simulating the response of plant processes to increasing atmospheric CO_2 burden.

Eddy covariance (EC) is a micrometeorological measurement technique that is widely used to quantify the exchange of CO_2 and water vapor between terrestrial ecosystems and the atmosphere (*Baldocchi,* 2003). Eddy covariance systems use fast response gas analyzers and sonic anemometers to sample atmospheric turbulence. Based on the turbulent signal it is possible to estimate the so-called net ecosystem exchange of CO_2 (typically called NEE), which is the net CO_2 flux between the atmosphere and the plant/soil system at the field scale. Using state-of-the-art mathematical methods NEE is further processed to calculate gross primary production (GPP, which is equivalent with plant photosynthesis) and total ecosystem respiration (TER or R_{eco}, which is the sum of autotrophic and heterotrophic respiration of the ecosystem). Latent heat flux is also routinely measured by the EC towers and then is used to calculate evapotranspiration (ET). EC measurements are typically operated continuously for many years, thus they provide invaluable and rich dataset to quantify plant carbon and water balance processes. Within the framework of AgroMo, two EC towers were established close to Martonvásár (near Pettend and Kajászó) providing NEE, GPP, TER, and

ET at half hourly resolution. Long term operation of these EC towers will provide substantial information about the carbon balance of typical crop rotations in Hungary.

The AgroMo lysimeter station comprises twelve 2 m high and 1 m^2 cross-section area undisturbed soil columns. Soil temperature, soil water content, and soil water potential sensors were inserted in the columns at 10 different depths, and the columns were set on sensitive scales that are capable of detecting 1 mm of precipitation or evaporation. The drain water exiting the columns at the bottom is also collected in vessels that are also placed on sensitive scales. Measurements are taken in every minute. Data collected within a day are uploaded to the FTP server of the AgroMo project at the end of each day. The collected data will be used for testing and improving the water and heat balance related subroutines (e.g., evapotranspiration calculation) of the AgroMo model.

2.3. The AgroMo biogeochemical model

The core element in the AgroMo system is the hybrid 4M – Biome-BGCMuSo simulation model. The 4M crop simulation model (*Fodor et al.,* 2012) is a daily-step, deterministic model whose computations are determined by the numerical characteristics (defined by input parameters) of the atmosphere-soil-plant system. Besides the data that describe the physical, chemical, and biological profile of the system, it is also necessary to set its initial, boundary, and constraint conditions in the input file of the model. The parameters regulate the functions and equations of the model: the development and growth of plants and the heat, water, and nutrient balance of the soil. The initial conditions are the measured system variables at the beginning of the simulation run, e.g., the water or nutrient content of the soil. The boundary conditions are primarily the daily meteorological data, such as global radiation, temperature, and precipitation. The constraint conditions cover the numerical representation of human activities, e.g., data about planting, harvest, fertilization, or irrigation. Besides the plant development and growth, the model calculates the water, heat, and nitrogen flow as well as the nitrogen transformation processes of the soil: for example, the amount of nitrate that percolates down under the root zone and the amount of NO_x gases released from the soil due to denitrification (*Fig. 1*).

Biome-BGCMuSo was developed from the Biome-BGC family of models (*Thornton,* 2000), and in this sense it is an extension and generalization of the Forest-BGC model for the description of different vegetation types including C3 and C4 grasslands (*Running* and *Coughlan,* 1988; *Thornton,* 2000; *Trusilova et al.,* 2009). During the past years, our research group developed an updated version of Biome-BGC (called Biome-BGCMuSo – where the abbreviation refers to Multilayer Soil Module) to improve the ability of the model to simulate carbon and water cycle in managed ecosystems, with options for managed croplands, grasslands, and forests. The modifications included structural improvements of

the model (e.g., the simple, outdated, one-layer soil module was replaced by a multilayer soil module; drought related plant senescence was implemented; model phenology was improved) and also management modules were developed (e.g., to simulate mowing, grazing, fertilization, ploughing, sowing, harvesting, forest thinning, and clearcut) (*Fig. 1*). Beyond these modifications, additional modules were developed to simulate cropland management (e.g., planting, harvest, ploughing, and application of fertilizers). Forest thinning was also implemented as a possible human intervention, and dynamic (annually varying) whole plant mortality was implemented in the model to enable more realistic simulation of forest stand development. The modifications were published in detail in *Hidy et al.* (2012, 2016).

Biome-BGCMuSo uses meteorological data, site-specific data, ecophysiological data, carbon-dioxide concentration and nitrogen deposition data to simulate the biogeochemical processes of the given biome. The main simulated processes assessed are photosynthesis, allocation, litterfall, carbon, nitrogen and water dynamics in the plant, litter as well as in the soil. The most important blocks of the model are the carbon flux block, the phenological block, and the soil flux block. In the carbon flux block, gross primary production of the biome is calculated using Farquhar's photosynthesis routine (*Farquhar et al.,* 1980). Autotrophic respiration is separated into maintenance and growth respirations. Maintenance respiration is the function of the nitrogen content of living material, while growth respiration is calculated proportionally to the carbon allocated to the different plant compartments. The phenological block calculates foliage development; therefore, it affects the accumulation of carbon and nitrogen in leaf, stem, root, and litter. The soil block describes the decomposition of dead plant material and soil carbon pools (*Running* and *Gower,* 1991).

The 4M model was integrated in the Biome-BGCMuSo by reimplementing the algorithm codes of 4M in the Biome-BGCMuSo program code, and including the 4M specific input parameters in the Biome-BGCMuSo input files. The AgroMo model simulation consists of two main phases. The first is the spinup simulation (in other words self-initialization, or equilibrium run), which starts with very low initial level of soil carbon and nitrogen, and runs until a climate and soil specific steady state is reached in order to estimate the initial values of the state variables (mostly soil carbon and nitrogen pools including recalcitrant soil organic matter, the latter is being the primary source of nitrogen mineralization in the model (*Thornton,* 2000). The second phase is the normal simulation that uses the results of the spinup simulation as initial values for the carbon and nitrogen pools.

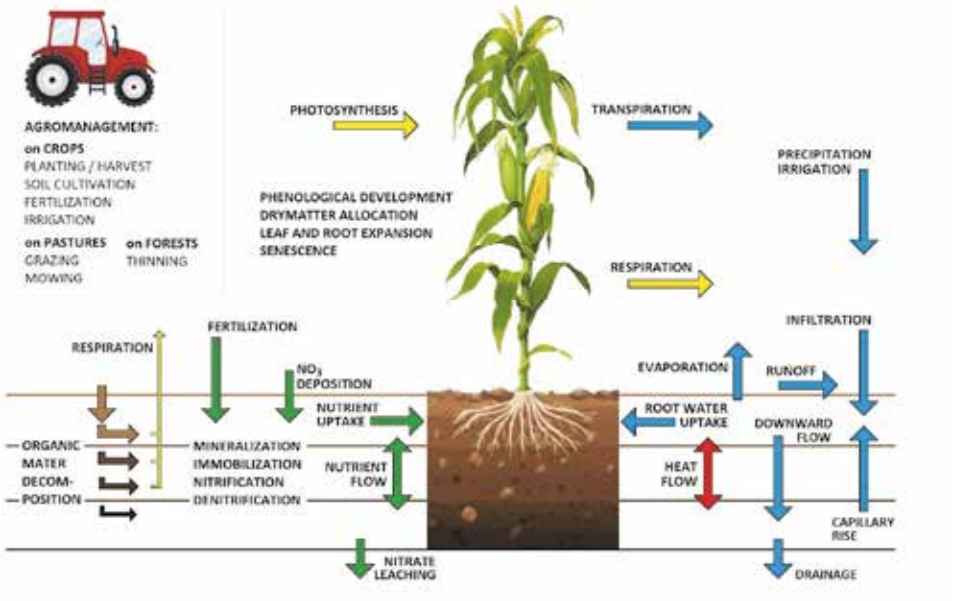

Fig. 1. Major processes simulated by the AgroMo model.

3. Results and case studies

In general, biogeochemical models could be successfully applied in the following areas: (1) Education: by promoting the system-oriented thinking, a comprehensive overview of the interrelations of the soil-plant system as well as of the environmental protection related aspects of the human activities could be presented. (2) Research: The results of observations and experiments could be extrapolated in time and space, thus, for example, the possible effects of climate change could be estimated. (3) Practice: Model calculations could be used in intelligent irrigation control and decision supporting systems as well as for providing scientific background for policy makers. AgroMo is designed to mimic the Hungarian agriculture (*Fig. 2*): the impacts of actions in the reality (R) are simulated in the virtual reality (VR). A graphical user interface (GUI) was designed for translating real life problems into modeling tasks as well as for publishing model results in easily comprehensible ways. AgroMo stores its data in a SQLite database (*SQLite,* 2019) designed to provide quick and complex queries but, it also uses data from external data sources (DS) such as Hungarian Central Statistical Office datasets.

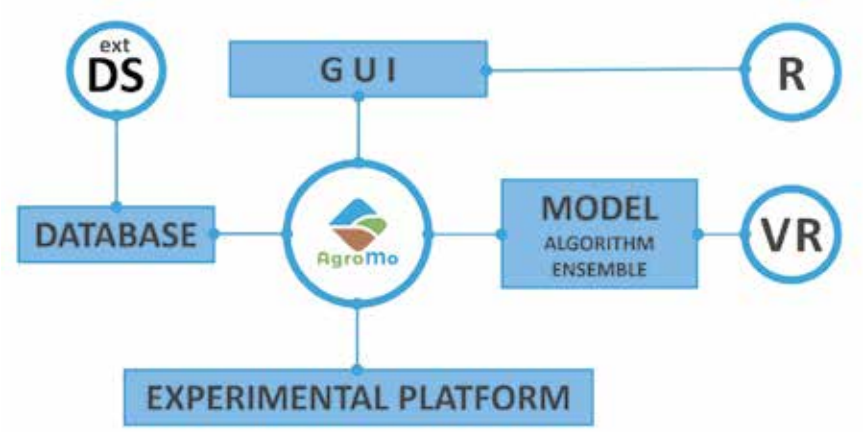

Fig. 2. Structure of the AgroMo system. DS: external data sources, DATABASE: SQLite tables, GUI: graphical user interface, R: reality, VR: virtual reality.

Undoubtedly, the most important way of using biogeochemical models is decision support. Models can even be used for resolving scientific arguments between experts. Representatives of the European Union revise the practical realization of the Nitrate Directive (91/676/EEC) in every five years (*European Comission,* 2018). Based on the collected experiences, the EU proposes amendments to the Directive for every member state in order to minimize the risk of one of the most important ecosystem disservices: the nitrate leaching of agricultural origin. One of the most recent proposed amendments is the idea of extending the spring fertilization prohibition period. At present, it is allowed to apply fertilizers starting from February 1. According to the proposal, this date would be moved to March 1. Though one can assume that it is highly unlikely that a portion of the fertilizer applied on the soil surface can go through the continuously deepening root zone without taken up by the plants, someone else can be more aware of the environment protection aspects. The Hungarian experts usually emphasize the yield safety in this matter, while EU experts tend to focus on the increasing risk of subsurface water contamination. A debate has been developed along the following questions: Does the earlier fertilization increase the risk of nitrate leaching significantly? Could the initiative to lengthen the fertilization prohibition period be substantiated scientifically? Experimentally, these questions could be answered only by time-consuming and expensive long-term field trials. Since we do not have years to find the answers by measurements, the only remaining scientific tool that is able to handle this problem is a biogeochemical model. Using the available soil (*Pásztor et al.,* 2013) and climatic

(*Spinoni et al.,* 2015) databases, 50-year-long crop rotations (maize – winter wheat, winter wheat – rapeseed, winter barley – rapeseed, silage maize – winter barley) were simulated for every major soil type (from sand to clay) in Hungary. Three fertilization scenarios were investigated for each of the rotation that differed only in the date of the first spring fertilization: I) February 1; II) February 15; III) March 1. The yields as well as the annual nitrate leaching amounts were calculated by the model, and the latter is presented in *Fig. 3*. According to the results, the amount of nitrate leaching does not increase as the date of the first spring fertilization moves from the end of February to the beginning of the month. On the other hand, if the prohibition period have been lengthened with one month, the yields of the winter crops would significantly decrease independently of the soil type due to the increased nutrient shortage in the early vegetative phase. Consequently, there is no need for extending the fertilization prohibition period by moving its end to March 1, as in fact it may cause yield loss. Leaving the prohibition period as it is today will not increase the risk of contaminating the subsurface water reservoirs due to nitrate leaching.

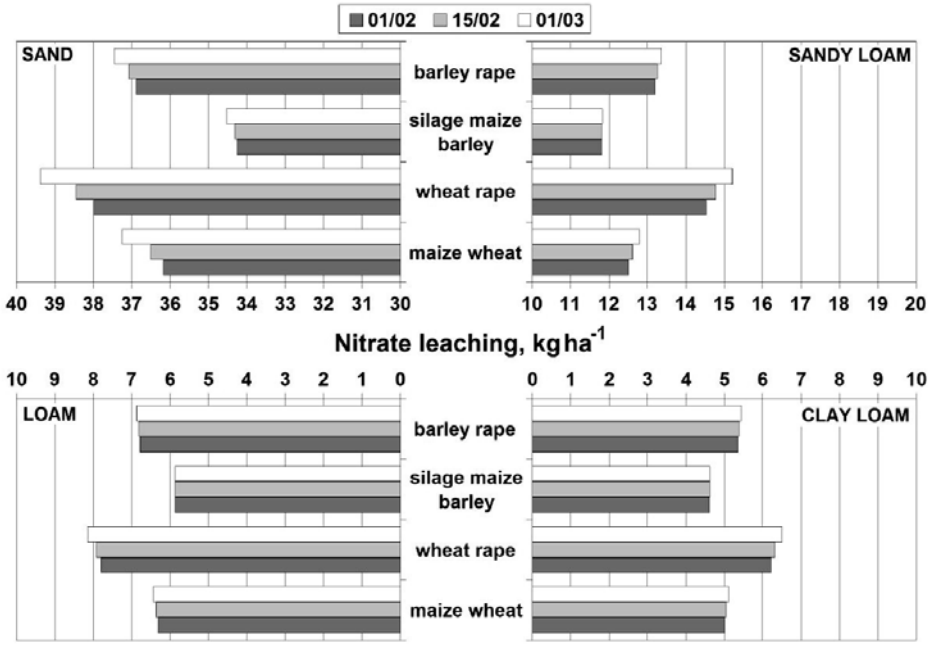

Fig. 3. Annual nitrate leaching rates as a function of the first spring fertilization date (dd/MM) of winter crops based on 50-year-long simulations (1961–2010).

Unquestionably, the most important ecosystem service of agricultural lands is the yield or production of the plants. In the context of climate change, one of the most burning questions is how the level of production will change due to the gradually changing environmental conditions. This question could also be answered by coupling biogeochemical models with regional gridded geodatabases. Within the frame of a pilot project, we analyzed the possible impacts of climate change on Hungarian crop yield. In this case, the climatic database was based on daily meteorological data measured at the weather stations of the Hungarian Meteorological Service and spatially interpolated for a cc. 10×10 km^2 resolution grid in the framework of the CarpatClim project (*Spinoni et al.,* 2015). The observation-based dataset is freely available for the 1961–2010 period. The applied data contained future climate simulations based on the IPCC SRES A1B scenario (*Nakicenovic* and *Swart,* 2000). The climate scenario was constructed based on the outputs of the ARPEGE-CLIMATE GCM (*Déqué et al.,* 1998) and ECHAM GCM (*Roeckner et al.,* 2006), which were then dynamically downscaled for Hungary with two different the regional climate models: ALADIN (*Csima* and *Horányi,* 2008) and REGCM (*Torma et al.,* 2008), respectively. These future climate projections were available for the 2021–2050 and 2071–2100 periods with the same 10×10 km^2 spatial resolution as of the observation-based data. The model simulations were run using the baseline (1981–2010) and future (2051–2070 and 2071–2100) climate time series. The difference in the yield and biomass levels simulated with the baseline and future climatic conditions was assumed to be the potential impact of climate change on crop production (*Table 1*).

Table 1. Potential impact of climate change on the major crops in Hungary. (Ensemble average of the yields (Y) and biomass (BM) obtained with all the available climate projections.)

	2051–2070		**2071–2100**	
	Y, t/ha	BM, t/ha	Y, t/ha	BM, t/ha
maize	-0.86	-0.77	-2.26	-2.61
sunflower	-0.37	-0.82	-0.92	-2.33
winter wheat	0.83	1.52	1.36	2.68
winter barley	0.72	1.34	1.23	2.46
rapeseed	0.48	1.72	0.99	3.70

Based on the simulation results, climate change will most likely expose significant negative impact on the spring sown crops primarily due to the more frequently occurring summer droughts and the heat weaves around flowering. Though the yield losses could be avoided with irrigation or could be mitigated with earlier sowing, the role of winter crops is likely to become more significant in Hungary in the future.

4. Conclusions and further developments

The objectives and the first indicative results of the AgroMo project has been presented. Preliminary simulation results show that the AgroMo integrated assessment and modeling framework could be successfully used for providing scientific background for stakeholders as well as for policy makers at various scales. Beyond the complex scientific content (model development and improvement), the most important challenge of the project is to provide a user interface that can be effectively used for communicating the simulation results. Simulations, even at the default 0.1° spatial resolution grid of Hungary (1104 grid points) produce enormous amount of data; literally billions of data records for only one single simulation. Using the services of the powerful SQLite (*SQLite,* 2019) database application, the simulation results could be presented on graphs (TimeSeries, BarChart, XYplot), in tables as well as on color coded maps. Users can use prewritten regular sentences (e.g., Average yield in the 2071–2100 period) to query the database of the results. AgroMo translates the regular sentence into an SQL query and presents the query results in the requested form (e.g., on a map). With this feature, AgroMo can support the work of any actor in the agriculture sector who does not necessarily has high level ICT skills.

Agro-economical considerations are in need to raise economic importance of sustainable development in changing biophysical conditions. The AgroMo base model produces the potential future crop yields and biomass under different climate scenarios. Hence, researchers may calculate the estimated costs of adaptation trajectories and develop accurate financial strategy plans to take control of climate change at individual level. The observed choices of farmers' managerial decisions, realized profits, and land values across the range of climate conditions allow us to assess the changes of future eco-systems at a given farm location and thus realize the essential developments in infrastructure, technology, and water supply management.

Though the current version of AgroMo is able to simulate the most important elements of the Hungarian agriculture (e.g., the effects of recurring heat stress and drought on crop yield, net primary production, and greenhouse gas balance, etc.), new developments are foreseen to extend the modeling possibilities in the future. Model self-initialization (or in other words spinup) is typically used to estimate initial conditions for the subsequent simulations. Due to the well-known

weaknesses of the self-initialization, efforts are in progress to improve the spinup process and harmonize its results with the observed soil organic matter pools of Hungarian soils (*Pásztor et al.,* 2013). Another exciting possibility in model development is the consideration of ozone damage in crop yield. As climate change is expected to increase the length of dry periods in Hungary that may be associated with high tropospheric ozone concentration, this effect may be important and cannot be neglected in the long term projections. Another feature that is currently missing from the AgroMo model is the quantification of the carbon cost of nitrogen acquisition via symbiotic mycorrhizal fungi, which is believed to consume a relatively large amount of primary production of plants (*Brzostek et al.,* 2014). Moreover, crop yield quality (e.g., gluten content) related simulation possibilities are also missing from AgroMo, so the model is planned to be improved with this feature as well.

Owing to its user friendly, flexible, and cross-platform interface as well as to the adjoined databases of climatic, soil, agromanagement, and experimental data, AgroMo will be able to effectively serve the stakeholders of the agricultural sector in their everyday work.

Acknowledgement*:* The research was funded by the Széchenyi 2020 programme, the European Regional Development Fund, the Hungarian Government (GINOP-2.3.2-15-2016-00028), and it was supported by the grant "Advanced research supporting the forestry and wood-processing sector´s adaptation to global change and the 4th industrial revolution", No. CZ.02.1.01/0.0/0.0/16_019/0000803 financed by OP RDE.

References

Ainsworth, E., Leakey, A., Ort, D.R., and *Long, S.P*., 2008: FACE-ing the facts. *New Phytologist 179*, 5–9. https://doi.org/10.1111/j.1469-8137.2008.02500.x

Ainsworth, E. and *Long, S*., 2005: What have we learned from 15 years of free-air CO2 enrichment (FACE)? A meta-analytic review of the responses of photosynthesis, canopy properties and plant production to rising CO2. *New Phytologist 165*, 351–372. https://doi.org/10.1111/j.1469-8137.2004.01224.x

Baldocchi, D.D., 2003: Assessing the eddy covariance technique for evaluating carbon dioxide exchange rates of ecosystems: past, present and future. *Glob. Change Biol. 9*, 479–492. https://doi.org/10.1046/j.1365-2486.2003.00629.x

Bartholy, J. and *Pongrácz, R*., 2005: Tendencies of extreme climate indices based on daily precipitation in the Carpathian Basin for the 20th century. *Időjárás 109*, 1–20.

Bindi, M., Palosuo, T., Trnka, M., and *Semenov, M*., 2015: Modelling climate change impacts on crop production for food security. *Climate Res. 65*, 3–5. https://doi.org/10.3354/cr01342

Brzostek, E.R., Fisher, J.B., Phillips, R.P., 2014: Modeling the carbon cost of plant nitrogen acquisition: Mycorrhizal trade-offs and multipath resistance uptake improve predictions of retranslocation. *J. Geophys. Res.: Biogeosci. 119*, 1684–1697. https://doi.org/10.1002/2014JG002660

Campbell, B.M., Vermeulen, S.J., Aggarwal, P.K., Corner-Dolloff, C., Girvetz, E., Loboguerrero, A.M., Ramirez-Villegas, J., Rosenstock, T., Sebastian, L., Thornton, P.K., and *Wollenberg, E*., 2016: Reducing risks to food security from climate change. *Glob. Food Secur. 11*, 34–43. https://doi.org/10.1016/j.gfs.2016.06.002

Csima, G., Horányi, A., 2008: Validation of the ALADIN-Climate regional climate model at the Hungarian Meteorological Service. *Időjárás 112*, 155–177.

Déqué, M., Marquet, P., and *Jones, R.G*., 1998: Simulation of climate change over Europe using a global variable resolution general circulation model. *Climate Dynamics 14*, 173–189. https://doi.org/10.1007/s003820050216

Dobor L, Barcza Z, Hlásny T, Havasi Á, Horváth F, Ittzés P, Bartholy J. 2015: Bridging the gap between climate models and impact studies: the FORESEE Database. *Geoscience Data Journal 2*:1-11. https://doi.org/10.1002/gdj3.22

Estes, L.D., Bradley, B.A., Beukes, H., Hole, D.G., Lau, M., Oppenheimer, M.G., Schulze, R., Tadross, M.A., Turner, W.R., 2013: Comparing mechanistic and empirical model projections of crop suitability and productivity: implications for ecological forecasting. *Glob. Ecol. Biogeogr. 22*, 1007–1018. https://doi.org/10.1111/geb.12034

EuropeanComission, 2018. Report from the Commission to the Council and the European Parliament on the implementation of Council Directive 91/676/EEC concerning the protection of waters against pollution caused by nitrates from agricultural sources based on Member State reports for the period 2012–2015. Report no. COM(2018) 257 final.

Ewert, F., Rötter, R.P., Bindi, M., Webber, H., Trnka, M., Kersebaum, K.C., Olesen, J.E., van Ittersum, M.K., Janssen, S., Rivington, M., Semenov, M.A., Wallach, D., Porter, J.R., Stewart, D., Verhagen, J., Gaiser, T., Palosuo, T., Tao, F., Nendel, C., Roggero, P.P., Bartosová, L., Asseng, S., 2015: Crop modelling for integrated assessment of risk to food production from climate change. *Environ. Model. Software 72*, 287–303. https://doi.org/10.1016/j.envsoft.2014.12.003

FAO, IFAD, UNICEF, WFP, WHO, 2017. Building Resilience for Peace and Food Security. Rome: FAO. Report no.

Farquhar, G.D., von Caemmerer, S., Berry, J.A., 1980: A biochemical model of photosynthetic CO2 assimilation in leaves of C3 species. *Planta 149*, 78–90. https://doi.org/10.1007/BF00386231

Fodor, N., Challinor, A., Droutsas, I., Ramirez-Villegas, J., Zabel, F., Koehler, A-K., Foyer, C., 2017: Integrating Plant Science and Crop Modeling: Assessment of the Impact of Climate Change on Soybean and Maize Production. *Plant Cell Physiol. 58*,1833–1847. https://doi.org/10.1093/pcp/pcx141

Fodor, N., Máthéné-Gáspár, G., Németh, T., 2012: Modeling the Nutrient Balance of the Soil-Plant System using the 4M Simulation Model. *Commun. Soil Sci. Plant Anal. 43*, 60–70. https://doi.org/10.1080/00103624.2012.631415

Fodor, N., Máthéné-Gáspár, G., Pokovai, K., and *Kovács, G*., 2003: 4M-software package for modelling cropping systems. *Eur. J. Agronomy 18*, 389–393. https://doi.org/10.1016/S1161-0301(02)00126-0

Hidy, D., Barcza, Z., Haszpra, L., Churkina, G., Pintér, K., and *Nagy, Z*., 2012: Development of the Biome-BGC model for simulation of managed herbaceous ecosystems. *Ecol. Model. 226*, 99–119. https://doi.org/10.1016/j.ecolmodel.2011.11.008

Hidy, D., Barcza, Z., Marjanovic, H., Ostrogovic Sever, M.Z,, Dobor, L., Gelybó, G., Fodor, N., Pintér, K., Churkina, G., Running, S., Thornton, P., Bellocchi, G., Haszpra, L., Horváth, F., Suyker, A., and *Nagy, Z*., 2016: Terrestrial ecosystem process model Biome-BGCMuSo v4.0: summary of improvements and new modeling possibilities. *Geosci. Model Dev.*, 4405–4437.

Jacob, D., Petersen, J., Eggert, B., Alias, A., Christensen, O.B., Bouwer, L.M., Braun, A., Colette, A., Déqué, M., Georgievski, G., Georgopoulou, E., Gobiet, A., Menut, L., Nikulin, G., Haensler, A., Hempelmann, N., Jones, C., Keuler, K., Kovats, S., Kröner, N., Kotlarski, S., Kriegsmann, A., Martin, E., van Meijgaard, E., Moseley, C., Pfeifer, S., Preuschmann, S., Radermacher, C., Radtke, K., Rechid, D., Rounsevell, M., Samuelsson, P., Somot, S., Soussana, J-F., Teichmann, C., Valentini, R., Vautard, R., Weber, B., and *Yiou, P*., 2014: EURO-CORDEX: new high-resolution climate change projections for European impact research. *Reg. Environ. Change 14*, 563–578. https://doi.org/10.1007/s10113-013-0499-2

Jarvis, A., Lau, C., Cook, S., Wollenberg, E.V.A., Hansen, J., Bonilla, O., and *Challinor, A*., 2011: An integrated adaptation and mitigation framework for developing agricultural research: Synergies and trade-offs. *Experiment. Agric. 47*, 185–203. https://doi.org/10.1017/S0014479711000123

Jones, J.W., Antle, J.M., Basso, B., Boote, K.J., Conant, R.T., Foster, I., Godfray, H.C.J., Herrero, M., Howitt. R.E., Janssen, S., Keating, B.A., Munoz-Carpena, R., Porter, C.H., Rosenzweig, C., and

Wheeler, T.R., 2017: Brief history of agricultural systems modeling. *Agric. Syst. 155*, 240–254. https://doi.org/10.1016/j.agsy.2016.05.014

Kern, A., Barcza, Z., Marjanović, H., Árendás, T., Fodor, N., Bónis, P., Bognár, P., Lichtenberger, J., 2018: Statistical modelling of crop yield in Central Europe using climate data and remote sensing vegetation indices. *Agric. Forest Meteorol. 260-261*, 300–320. https://doi.org/10.1016/j.agrformet.2018.06.009

Kis, A., Pongracz, R., and *Bartholy, J.*, 2017: Multi-model analysis of regional dry and wet conditions for the Carpathian Region. *Int. J. Climatol. 37*, 4543–4560. https://doi.org/10.1002/joc.5104

Knutti, R. and *Sedláček, J.*, 2012: Robustness and uncertainties in the new CMIP5 climate model projections. *Nat. Climate Change 3*, 369. https://doi.org/10.1038/nclimate1716

Lakatos, M. and *Bihari, Z.*, 2011. *A közelmúlt megfigyelt hőmérsékleti- és csapadéktendenciái.* In (eds. *Batholy, J., Bozó, L., Haszpra, L.)* Klímaváltozás – 2011: Klímaszcenáriók a Kárpátmedence térségére. Budapest, Magyar Tudományos Akadémia és Eötvös Loránd Tudományegyetem Meteorológiai Tanszék. 146–169. (In Hungarian)

Lakatos, M., Szentimrey, T., and *Bihari, Z.*, 2011: Application of gridded daily data series for calculation of extreme temperature and precipitation indices in Hungary. *Időjárás 115*, 99–109.

Leng, G. and *Huang, M.*, 2017: Crop yield response to climate change varies with crop spatial distribution pattern. *Scientific Rep. 7*, 1463. https://doi.org/10.1038/s41598-017-01599-2

Lobell, D.B. and *Burke, M.B.*, 2010: On the use of statistical models to predict crop yield responses to climate change. *Agric. Forest Meteorol. 150*, 1443–1452. https://doi.org/10.1016/j.agrformet.2010.07.008

Meehl, G.A., Covey, C., Delworth, T., Latif, M., McAvaney, B., Mitchell, J.F.B., Stouffer, R.J., and *Taylor, K.E.*, 2007: THE WCRP CMIP3 Multimodel Dataset: A New Era in Climate Change Research. *Bull. Amer. Meteorol. Soc. 88*, 1383–1394. https://doi.org/10.1175/BAMS-88-9-1383

Nakicenovic, N. and *Swart, R.*, 2000: Special report on emission scenarios. Cambridge University Press.

Olesen, J., Trnka, M., Kersebaum, K., Skjelvåg, A., Seguin, B., Peltonen-Sainio, P., Rossi, F., Jerzy, K., and *Micale, F.*, 2011: Impacts and adaptation of European crop production systems to climate change. *Eur. J. Agronomy 34*, 96–112. https://doi.org/10.1016/j.eja.2010.11.003

Pásztor, L., Szabó, J., Bakacsi, Z., and *Laborczi, A.*, 2013: Elaboration and applications of spatial soil information systems and digital soil mapping at Research Institute for Soil Science and Agricultural Chemistry of the Hungarian Academy of Sciences. *Geocarto International 28*, 13–27. https://doi.org/10.1080/10106049.2012.685895

Pieczka, I., Pongrácz, R., Bartholy, J., and *Szabóné André K.*, 2018: Future temperature projections for Hungary based on RegCM4.3 simulations using new Representative Concentration Pathways scenarios. *Int. J. Glob. Warming 15*, 277–292. https://doi.org/10.1504/Ijgw.2018.10014245

Pongrácz, R., Bartholy, J., and *Kis, A.*, 2014: Estimation of future precipitation conditions for Hungary with special focus on dry periods. *Időjárás 118*, 305–321.

Porter, J., Xie, L., Challinor, A., Cochrane, K., Howden, S., Iqbal, M., Lobell, D., and *Travasso, M.*, 2014. *Chapter 7: Food security and food production systems.*In: Climate Change 2014: Impacts, Adaptation, and Vulnerability. Part A: Global and Sectoral Aspects. Contribution of Working Group II to the Fifth Assessment Report of the Intergovernmental Panel on Climate Change, Cambridge University Press. 485–533.

Power, A.. 2010: Ecosystem services and agriculture: tradeoffs and synergies. *Phil.Transact. Roy. Soc. B: Biol. Sci. 365*, 2959–2971. https://doi.org/doi:10.1098/rstb.2010.0143

Roeckner, E., Brokopf, R., Esch, M., Giorgetta, M., Hagemann, S., Kornblueh, L., Manzini, E., Schlese. U., and *Schulzweida, U.*, 2006: Sensitivity of simulated climate to horizontal and vertical resolution in the ECHAM5 atmosphere model. *J. Climate 19*, 3771–3791. https://doi.org/10.1175/jcli3824.1

Rosenzweig, C., Jones, J.W., Hatfield, J.L., Ruane, A.C., Boote, K.J., Thorburn, P., Antle, J.M., Nelson, G.C., Porter, C., Janssen, S., Asseng, S., Basso, B., Ewert, F., Wallach, D., Baigorria, G., Winter, J.M., 2013: The Agricultural Model Intercomparison and Improvement Project (AgMIP): Protocols and pilot studies. *Agric. Forest Meteorol. 170*, 166–182. https://doi.org/10.1016/j.agrformet.2012.09.011

Running, S.W. and *Coughlan, J.C.*, 1988: A General Model of Forest Ecosystem Processes for Regional Applications I. Hydrologic Balance, Canopy GAS Exchange and Primary Production Processes. *Ecol. Model. 42*, 125–154. https://doi.org/10.1016/0304-3800(88)90112-3

Running, S.W. and *Gower, S.T.*, 1991: FOREST-BGC, A general model of forest ecosystem processes for regional applications. II. Dynamic carbon allocation and nitrogen budgets. *Tree physiol. 9*, 147–160.

Spinoni, J., Szalai, S., Szentimrey, T., Lakatos, M., Bihari, Z., Nagy, A., Németh, Á., Kovács, T., Mihic, D., Dacic, M., Petrovic, P., Kržič, A., Hiebl, J., Auer, I., Milkovic, J., Štepánek, P., Zahradnícek, P., Kilar, P., Limanowka, D., Pyrc, R., Cheval, S., Birsan, M-V., Dumitrescu, A., Deak, G., Matei, M., Antolovic, I., Nejedlík, P., Štastný, P., Kajaba, P., Bochnícek, O., Galo, D., Mikulová, K., Nabyvanets, Y., Skrynyk, O., Krakovska, S., Gnatiuk, N., Tolasz, R., Antofie, T., and *Vogt, J.*, 2015: Climate of the Carpathian Region in the period 1961–2010: climatologies and trends of 10 variables. *Int. J. Climatol. 35*, 1322–1341. https://doi.org/10.1002/joc.4059

SQLite. 2019. (http://www.sqlite.org.)

Stocker, T., Alexander, L., Allen, M., IPCC Working Group Science. 2013. Climate change 2013 the physical science basis Working Group I contribution to the fifth assessment report of the Intergovernmental Panel on Climate Change. IPCC.

Taylor, K.E., Stouffer, R.J., and *Meehl, G.A.*. 2011: An Overview of CMIP5 and the Experiment Design. *Bulletin of the American Meteorological Society 93*:485-498. https://doi.org/10.1175/BAMS-D-11-00094.1

Thornton, P.E., 2000: User's Guide for Biome-BGC, Version 4.1.1. ftp://daac.ornl.gov/data/model_archive/ BIOME_BGC/biome_bgc_4.1.1/ comp/bgc_users_guide_411.pdf)

Torma, C., Bartholy, J., Pongrácz, R., Barcza, Z., Coppola, E., and *Giorgi, F.*, 2008: Adaptation and validation of the RegCM3 climate model for the Carpathian Basin. *J. Climate 112*, 233-247.

Trusilova, K., Trembath, J., and *Churkina, G.*, 2009: 16: Parameters estimation and validation of the terrestrial ecosystem model BIOME-BGC using eddy-covariance flux measurements. https://doi.org/10.4126/98-004414248

Webber, H., Ewert, F., Olesen, J., Müller, C., Fronzek, S., Ruane, A., Bourgault, M., Martre, P., Ababaei, B., Bindi, M., Ferrise, R., Finger, R., Fodor, N., Gabaldón-Leal, C., Gaiser, T., Jabloun, M., Kersebaum, K., Lizaso, J., Lorite, I., and *Wallach, D.*, 2018: Diverging importance of drought stress for maize and winter wheat in Europe. *Nat. Commun. 9*, 4249. https://doi.org/10.1038/s41467-018-06525-2

Wheeler, T. and *von Braun, J.*, 2013: Climate Change Impacts on Global Food Security. *Science 341*, 508. https://doi.org/10.1126/science.1239402

DOI:10.28974/idojaras.2020.2.5

IDŐJÁRÁS

Quarterly Journal of the Hungarian Meteorological Service
Vol. 124, No. 2, April – June, 2020, pp. 227–251

Changing climatic sensitivity and effects of drought frequency on the radial growth of *Fagus sylvatica* at the xeric frontiers of Central Europe

Balázs Garamszegi *[,1], **Miklós Kázmér**[2], **László Kolozs**[3], and **Zoltán Kern**[4]

[1]*Forest Research Institute*
National Agricultural Research and Innovation Centre
Várkerület 30/A, 9600 Sárvár, Hungary

[2]*Department of Palaeontology and MTA-ELTE Geological*
Geophysical and Space Science Research Group
Eötvös Loránd University
Pázmány Péter sétány 1/C, 1117 Budapest, Hungary

[3]*Forestry Directorate*
National Food Chain Safety Office
Frankel Leó út 42-44, 1023 Budapest, Hungary

[4]*Institute for Geological and Geochemical Research*
Research Centre for Astronomy and Earth Sciences
MTA Centre for Excellence; Budaörsi út 45, 1112 Budapest, Hungary

**Corresponding Author e-mail: balazs.garamszegi@gmail.com*

(Manuscript received in final form July 26, 2019)

Abstract— The influence of climate on the vitality and growth of European beech (*Fagus sylvatica* L.) has become a focus of forest research over the last decade. Beech locally reaches its continental xeric limit in Hungary within its European distribution area, giving a unique opportunity to study the climatic sensitivity of the species, based on tree-ring analysis. A comparison of four geographically and climatically different sites is presented from Hungary, combining data collected on stand level with systematic forest inventory plots. Tree-ring width chronologies covering the past 90–100 years of the lifetime of mature and middle-aged trees and different climatic variables were used to evaluate the growth-climate relationships and recent growth trends of the selected beech stands by multivariate regression analysis. Strong relationships were found between annual radial growth and (mainly water availability related) meteorological variables of the vegetation season, exceeding previous results from elsewhere in Europe. A clear spatiotemporal variability of the growth sensitivity was also revealed, following a (climatic) gradient from the northern to the southwestern parts of the country. In the northern sites, climatic sensitivity was found to be more fluctuating, while southwestern sites facing more continuous effects of changing climatic conditions seem to show weakening correlation over time. Trends of relative basal area increments and climatic

sensitivity of growth over the past decades may be due to unfavorable climatic changes, though extreme and recurrent drought events superimposed on the long-term trends seem to have a decisive impact on growth patterns and associated resilience of beech.

Key-words: beech, climate change, drought index, tree-ring, basal area increment, xeric edge

1. Introduction

Among various other ecosystem services, forests play a decisive role in the regulation of their own environment and habitat factors, including climate on a scale ranging from stand to global (*Bonan*, 2008). Forests, therefore, are of key importance in the mitigation of and adaptation to climate change (e.g., *Smith et al.*, 2014), however, they are not static systems – similarly to the climate itself –, but undergo continuous change, closely interacting with their environment (e.g., *Meier et al.,* 2012). Changing environmental (climatic) conditions are currently posing a great challenge to forests, especially to those located at the margins of their distribution and/or with reduced ecological functionality (*Mátyás,* 2010). In the face of climate change induced xeric limit shifting, predicting distribution changes of beech (*Fagus sylvatica* L.) became a great interest to European forest science. Being a widely dominant tree species across the (intensively managed) forests of the continent (*Fig. 1*), a possible loss in competitiveness could raise significant ecological concerns (*Geßler et al.,* 2007; *Mátyás et al.*, 2010). Although decline had already been demonstrated at places from its southern edge of distribution (*Jump et al.*, 2006b; *Peñuelas et al.*, 2007), the topic gained further attention following severe droughts in the early 2000s affecting major parts of Europe (*Czajkowski et al.*, 2005; *van der Werf et al.*, 2007; *Fotelli et al.*, 2009; *Mátyás et al.*, 2010; *Jezík et al.*, 2011).

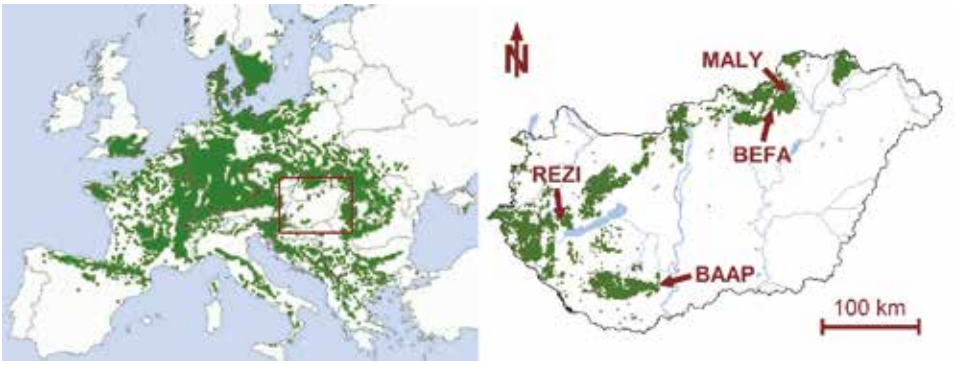

Fig. 1. Location of study sites within the range of distribution of beech (*Fagus sylvatica* L.) in Europe (left) and Hungary (right). The rectangle on the European distribution map marks the crop area corresponding to the country scale map. (Map sources: EUFORGEN 2009, NÉBIH 2015).

Different studies have reached different conclusions and opinions concerning the future and adaptability of beech, approaching the subject from various perspectives, including modeling, monitoring, and field experiments. Many of the modeling results predicted a widespread beech decline in Central and Southern Europe (e.g., *Czúcz et al.*, 2011; *Stojanović et al.*, 2013), while others suggested a more decisive resilience to climate change and adaptive capacity (e.g., *Jump et al.*, 2006a; *van der Maaten,* 2012; *Tegel et al.*, 2014). More complex models dealing with species migration and genetic adaptability gave more complex results, indicating a mosaic of habitats in the future at the continental xeric margins of distribution (e.g., *Kramer et al.*, 2010). Incorporating extreme climatic events (e.g., droughts) and their frequency in bioclimatic models can also lead to a better understanding of future beech persistence at its distribution limit (*Rasztovits et al.*, 2014). More recent studies showed the importance of stand characteristics, associated with different forest management techniques, such as effects of species composition on stand-level drought tolerance (*Mölder* and *Leuschner*, 2014; *Metz et al.*, 2016). Field experiments and monitoring studies, artificial drought experiments and provenance trials also provide important data to quantify the climatic adaptability of beech (e.g., *Mátyás et al.*, 2009; *Thiel et al.*, 2014).

Tree-ring analysis is also considered as a powerful research tool for tracking the effects of the changing habitat conditions on tree biomass production of temperate tree species. In the case of beech, these methods are particularly useful on account of the usually clear relationships between tree-ring widths and climatic factors (*Dittmar et al.*, 2003; *Lebourgeois et al.*, 2005). Climate sensitivity of beech has been studied on several scales in time and space also with conclusions referring to the issue of climate change and regional aspects (e.g., *Čufar et al.*, 2008; *van der Maaten*, 2012; *Weber et al.*, 2013; *Garamszegi* and *Kern*, 2014; *Tegel et al.*, 2014; *Cavin* and *Jump*, 2016; *Hacket-Pain et al.*, 2016; *Roibu et al.*, 2017). Besides interannual climatic impact on growth, longer term effects of ecological and climatic changes on radial growth were usually investigated (e.g., *Piovesan et al.*, 2008; *Gillner et al.*, 2013).

Contributing to the several on-going researches, the primary aims of our study were to evaluate, compare, and track any shift in growth-climate relationships over the last century and trends of growth associated with climatic changes and drought frequency in four Hungarian forest sites dominated by beech as a (mixing) tree species. Considering the special locations close to a local continental xeric edge within the European beech distribution area, an emphasized climatic sensitivity was supposed to find among the sample sites. Nevertheless, as documented changes in environmental conditions vary from site to site even within the relatively small and integrated geographical region represented by Hungary, we also searched for possible differences. We also tried to find relations to reported decisive

mortality events of beech prior to our study (*Lakatos* and *Molnár*, 2009; *Janik et al.*, 2016) and emerging trends of drought damages in Hungarian forests (*Hirka et al.*, 2018), including an outlook to climate indices defining the climatic needs of the species, as well.

2. Materials and methods

2.1. Study areas and climate data

Two submontane beech stands from northern Hungary (MALY, BEFA), and two sites at lower elevations in western and southern Hungary (REZI, BAAP) were selected as core study areas (*Fig. 1*). At all but one of the investigated stands, beech is dominant, and possible disturbances on growth due to other species are weak. At the southernmost BAAP site, the species was present only as a rare mixing species, though still in form of dominant individuals. Site characteristics, such as soil type and hydrological conditions were similar among all four sites (*Table 1*). Due to the modest water retention capacity of soils and limited water availability, each site depends on balanced intra-annual distribution of precipitation.

Table 1. Location of the investigated beech stands and comparison of selected site and stand characteristics

	MALY	**BEFA**	**REZI**	**BAAP**
coordinates	48.14°N 20.54°E	48.02°N 20.36°E	46.87°N 17.25°E	46.20°N 18.61°E
elevation a.s.l.	500 m	500 m	200 m	200 m
slope, aspect	5-20°, N	10-15°, NW	5-10°, NE	10-15°, SW
soil type	Cambisol/Luvisol	Cambisol	Cambisol	Cambisol/Luvisol
soil texture	loam	loam	sand	loam
soil depth	0.5-0.9 m	0.4-0.6 m	0.6-1.0 m	0.6-1.0 m
beech mixing ratio	85-100%	80%	70% (overstory)	<5%
main mixing species	*Quercus petraea*	*Quercus petraea, Carpinus betulus*	*Quercus cerris, Carpinus betulus*	*Tilia sp., Quercus cerris,*
stand age (2014)	93±15 yr	65±5 yr	86±10 yr	n.a.
avg. tree height	31 m	21 m	28 m	n.a.

Site climate was evaluated using gridded meteorological datasets, first of all, monthly precipitation and temperature data and 3-month standardized precipitation evaporation index (*SPEI*; *Vicente-Serrano et al.*, 2010) from the CARPATCLIM project (*Szalai et al.*, 2013). This dataset, with a spatial resolution of 0.1°x0.1°, is currently considered as the most representative gridded climate data source available for the region, but on the other hand, it covers only a relatively short, 50-year period from 1961 to 2010. For longer term investigations, the CRU TS4.01 temperature (*Harris et al.*, 2014) and the GPCC V8 analysis precipitation (*Schneider et al.*, 2018) datasets served with basic meteorological information for the period 1901–2016, though at a coarser (0.5°x0.5°) spatial resolution.

Besides the climatic variables above, two further types of drought indices were used to visualize long-term changes in stand climate, namely the Ellenberg quotient (*EQ*; *Ellenberg,* 1988) and the simplified forest aridity index (*FAI*; *Führer et al.*, 2011). Both indices were developed for evaluating the main climatic forest type distribution zones within Central Europe and Hungary, respectively. *EQ* is computed from the precipitation sum of the entire year and July mean temperature, while *FAI* combines monthly precipitation and temperature of the main vegetation season. Higher values of both indices represent more arid conditions. The associated climatic limit for beech is usually considered to be 30 by *EQ* (*Ellenberg*, 1988; *Standovár* and *Kenderes*, 2003) and 4.75 based on *FAI* (*Führer et al.*, 2011).

Climate diagrams of the study areas (including changes between 1961–1985 and 1986–2010) are presented in *Fig. 2* based on the CARPATCLIM data; alternatively, *EQ* and *FAI* moving average time series are shown in *Fig.3* comparing a climatically representative site from northern (BEFA) and western Hungary (REZI) from the beginning of the previous century (1901–2016) based on the joint CRU/GPCC data. The use of different climate datasets raises the question about representativeness and homogeneity of the results. High covariance and correlation between the two data sources (CARPATCLIM and joint CRU/GPCC; *Table 2)* allowed parallel use of them for well-defined purposes, though. Major differences between the mean values in the case of MALY site can be explained by bias originating in the mean elevation difference between the grid cells compared to the actual target site. Consequently, precipitation is very likely overestimated in CARPATCLIM and underestimated in GPCC for the MALY site, while temperature is, conversely, under- and overestimated by them.

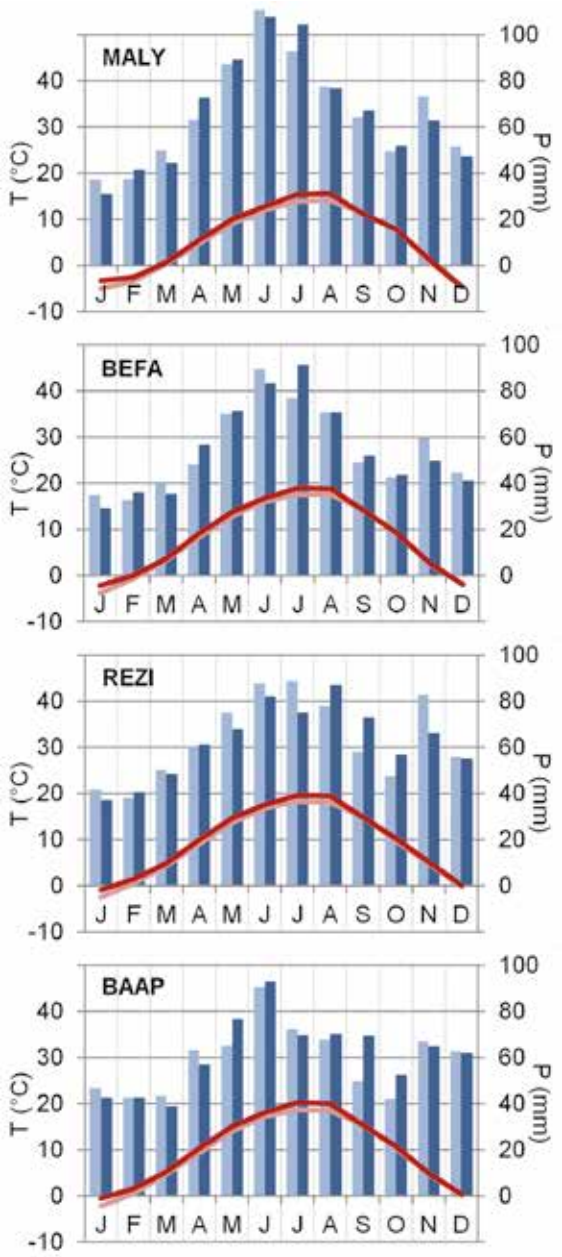

Fig. 2. Climate diagrams for the study sites, based on the CARPATCLIM dataset. Intra-annual patterns of changing climate can be tracked by comparison of the periods 1961-1985 (light colored bars and line) and 1986-2010 (darker colors). Minimum and maximum monthly mean temperature and annual precipitation sum during the second period 1986-2010 were -4.5 °C, 15.7 °C, 803 mm at MALY; -2.2 °C, 19.0 °C, 661 mm at BEFA; -0.8 °C, 19.7 °C, 751 mm at REZI, and -0.5 °C, 20.3 °C, 741 mm at BAAP.

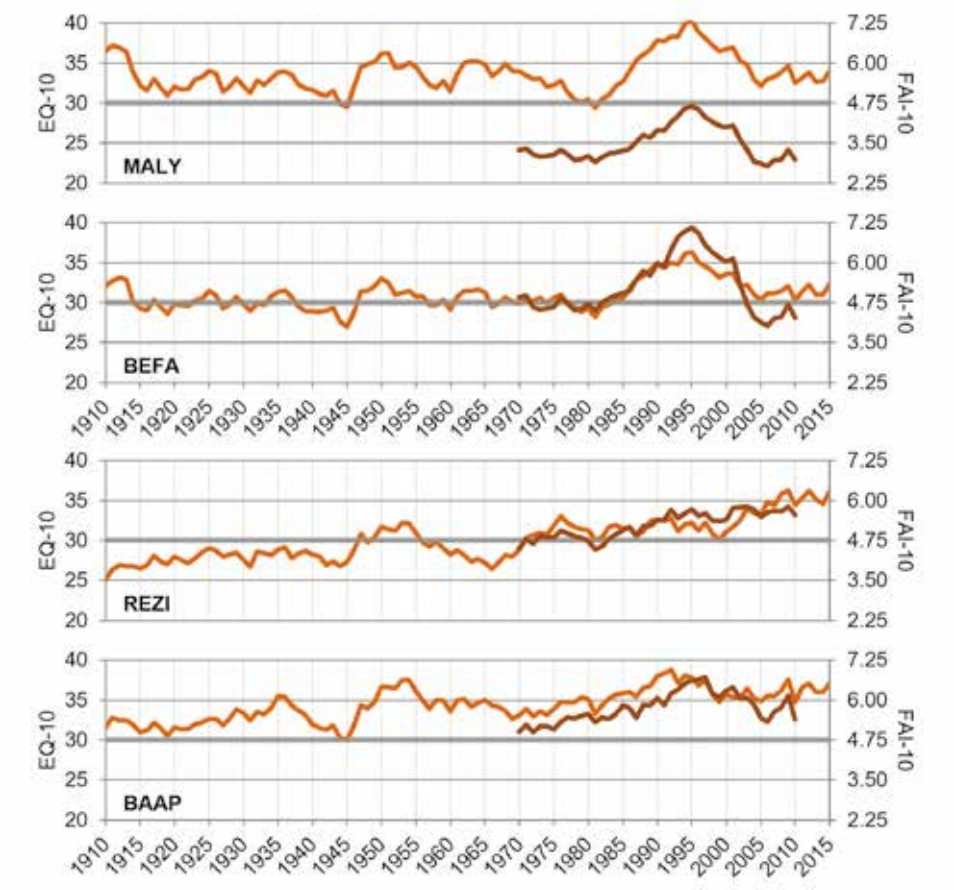

Fig. 3. Trends of *EQ* from the beginning of the last century (*Ellenberg,* 1988; CRU/GPCC) and of the *FAI* index for the shorter period of 1961–2010 (*Führer et al.* 2011; CARPATCLIM), both smoothed by 10-year moving averages. Shaded horizontal grey line represents the hypothetical xeric limit of beech habitats, associated with each index.

Table 2. Comparison of the CARPATCLIM (a) and CRU/GPCC (b) climate datasets for the four study sites during the period 1961-2010. Basic climate variables such as annual precipitation sum (P_{ann}; in mm) and mean temperature of July (T_{jul}; in °C) are compared with the use of the statistics of mean value (*mean*), (relative) difference between sub-periods 1961-1985 and 1986-2010 ($\delta m_{25\text{-}yr}$/$\Delta m_{25\text{-}yr}$), standard deviation (*sdev*), and the correlation (*correl*) between the datasets

		MALY		BEFA		REZI		BAAP	
		a	**b**	**a**	**b**	**a**	**b**	**a**	**b**
P_{ann}	*mean*	801	603	660	625	758	677	727	611
	$\delta m_{25\text{-}yr}$	+0.3%	-0.1%	+0.3%	+0.5%	-1.7%	-1.4%	+3.6%	+3.1%
	sdev	194	147	157	138	135	120	143	115
	correl		0.935		0.967		0.958		0.971
T_{jul}	*mean*	14.7	19.6	18.3	18.9	19.0	20.8	19.5	21.0
	$\Delta m_{25\text{-}yr}$	+1.50	+1.24	+1.45	+1.34	+1.36	+1.64	+1.49	+1.72
	sdev	1.53	1.36	1.48	1.41	1.31	1.45	1.38	1.48
	correl		0.990		0.992		0.976		0.989

2.2. Tree sampling, measurement, and data standardization

At BEFA, MALY, and REZI sites, 7–7 disc samples from freshly-cut logs and additional increment cores from 3–4 (co-)dominant trees were collected between 2010 and 2015 in multiple collection campaigns, while two disc samples and increment cores from ten dominant individuals (2 per tree) were collected at BAAP site, earlier, in 2002. Part of the REZI samples originated from a sanitary felling following drought damages, which effect will be discussed later. Extending the sample taken from the central study areas and also to further mitigate possible bias due to differences in tree age and other unknown local disturbances, some additional cores from (co-)dominant trees were also assorted from the regular fieldwork plots coinciding with beech dominated stands of the National Forest Inventory (NFI; NÉBIH, 2016). This extension was spatially adjusted to the grid cell size of the used climate data. The increment cores were extracted at breast height (~1.3 m above ground level), while the disk samples were collected from fallen tree trunks typically from part of the log representing the 0.5 to 1.5 m height segment above the original ground level.

Samples were processed following standard dendrochronological protocols (*Stokes* and *Smiley,* 1968) and ring-width measurements were made at a resolution of 0.01 mm along two radii per each sample tree, using LINTAB measuring table and TSAP-Win 4.67 software (*Rinn,* 2005). Ring-width series

were cross-dated, first by visual comparison and finally checked using the COFECHA program (*Holmes*, 1983). The measuring and cross-dating were largely performed using the facilities of the Budapest Tree-Ring Laboratory (*Kázmér* and *Grynaeus*, 2003). Parameters of sample trees and measured variables are shown in *Table 3*.

Table 3. Information on sample trees and derived tree-ring chronologies: sample depth (*n*); mean age (*age*; yrs) and breast-height stem diameter of sample trees (*DBH*; in cm) with their standard deviation; mean tree-ring width (*mTRW*; in mm) and standard deviation of tree-ring widths (*sdTRW*); first (*FDR*) and last (*LDR*) dated ring and first (*FAY*) and last (*LAY*) accepted years to final chronologies. *FAY* and *LAY* indicate the length of the used standard chronologies with the given mean interseries correlation (*Rbar*) and expressed population signal (*EPS*) and selected autoregression order (*ARord*)

	MALY	**BEFA**	**REZI**	**BAAP**
n	20	21	22	18
age	76±25	70±25	74±16	80±21
DBH	39±9	30±7	41±12	31±11
mTRW	2.11	1.89	2.52	1.90
sdTRW	1.23	1.03	1.33	1.07
FDR	1882	1882	1902	1892
LDR	2015	2015	2016	2015
FAY	1914	1930	1931	1921
LAY	2015	2015	2015	2013
Rbar	0.432	0.342	0.365	0.440
EPS	0.916	0.895	0.915	0.923
ARord	1	1	1	1

In order to remove age-related trend and growth disturbances due to forest dynamics, tree-ring width (*TRW*) measurements were detrended (*Cook et al.*, 1990). Based on earlier comparison of multiple detrending methods (*Garamszegi* and *Kern*, 2014), we chose a 30-year cubic smoothing spline to model the growth trend of the individual series (*Cook* and *Peters*, 1981). This flexible model of non-parametric regression retains any expected interannual-subdecadal variation of the radial increments. Detrending and index calculation were processed by ARSTAN software (*Cook* and *Krusic*, 2006), deriving

individual *TRW* indices as a ratio between the raw measurement and modeled growth. Pre-whitened, residual versions of the produced *TRW* chronologies were used, with the order of the autoregressive model being selected via the Akaike information criterion (*AIC*) (*Table 3*). Variance adjustment, adapting the running window approach was applied to the derived chronologies to minimize variance bias due to changing sample replication and effects of fluctuating interseries correlation (*Frank et al.*, 2007). The final chronologies were calculated as bi-weight robust mean of individual series. Mean basal area increments (*BAI*) were also derived from the raw *TRW* measurements, using the TSAP software. *BAI* was estimated for the core sites directly from tree-ring measurements along the two representative radii for stem diameter including the pith, and it was derived back from measured breast height diameter in case of *NFI* trees.

Signal strength of the *TRW* index chronologies was checked using the expressed population signal (*EPS*) statistics (*Wigley et al.*, 1984; *Buras*, 2017). Mean interseries correlation (*Rbar*) and *EPS* were calculated within 30-year running windows. The periods of further analysis were set between when a minimum replication of 5 sample trees occurs and where the running *EPS* statistics exceed the traditional 0.85 acceptance level (*Wigley et al.*, 1984). By these means, juvenile growing phrases were also coarsely excluded from the analysis. Signal-strength statistics of the accepted periods suggest a robust signal (*Table 3*). The significant cross-correlations found between the site chronologies also confirm this and reveal a macroclimatic connection even between the contrasting eco-regions (*Table 4*).

Table 4. Cross correlation between each site tree-ring index chronologies for the common period 1931-2013. Each correlation is at $p < 0.01$ significance level

	MALY	**BEFA**	**REZI**
BEFA	0.841		
REZI	0.672	0.625	
BAAP	0.528	0.581	0.666

2.3. Data processing and analysis

The evaluation of the site conditions and processing of climate indices and tree ring chronologies were followed by a preliminary Pearson correlation analysis between climatic variables of the more local CARPATCLIM dataset and *TRW* chronologies of core study areas. Here, monthly climate elements of the

preceding and the growing year were involved in the analysis, as suggested by previous studies (e.g., *Di Filippo et al.*, 2007), namely monthly precipitation sums, mean temperatures and *SPEI* values from the previous year's April to the growing year's September. Statistical significance of the relationships was tested by the bootstrap response method using the 'bootRes' package (*Zang* and *Biondi*, 2013) under the R statistical program environment (R Development Core Team, 2014).

To identify shifts in growth-climate relationships, multivariate linear regression analysis with 31-year windows and 10-year steps was done, modeling *TRW* indices of the entire growth series with monthly climate records from CRU/GPCC datasets. Potential monthly climatic determinants were selected via the preliminary correlation analysis, focusing also on hypothetical main growing months, besides checking statistical significance. Coefficient of determination (R^2) of the regression model was used for evaluation of decadal shifts in climate influence on growth, while (moving) partial correlation coefficients between climatic predictors and *TRW* indices served as indicators of intra-annual meteorological dependence of increment formation. By using the same climatic predictors for each site and periods, overparameterization of the regression models may have happened, however, this enabled a uniform handling of data and an easier direct comparison of the results. With the use of partial correlations, potential biases due to a notable degree of autocorrelation in the mean temperature of consecutive months and a frequently occurring negative correlation between temperature and precipitation during summer months were also tried to eliminate.

Finally, changing site climate and frequency of drought events were assessed using the *SPEI* indices (CARPATCLIM), in search of possible relations to the basal area growth in the studied four stands since 1981 and with a special focus on the REZI beech mortality case. Here, *BAI* chronologies were used instead of *TRW*, since those were found to be better approximators of total annual tree growth and so of the vitality and competitivity of trees (e.g., *Jump et al.*, 2006b; *Gillner et al.*, 2013). For a better comparison, relative *BAI* ratios were calculated for the period 1980–2010 with a reference period of 1971–1990 by each series and sites. Slopes of the individually fitted linear trends of each period were also compared.

3. Results

3.1. Changing stand climate

During the latter half of the 20th and first decade of the 21st century, mean annual temperatures rose by 0.6–0.8 °C at the study sites, with the highest rate in mid-summer (1.2–1.6 °C), comparing the periods 1961-1985 and 1986–2010. Meanwhile, annual precipitation stayed practically unchanged. Only the REZI

site faced a slight precipitation decrease of ~1.5% and the BAAP site an increase of ~3–3.5% (*Table 2*). More detailed intra-annual patterns of changing climate can be seen in the climate diagrams (*Fig. 2*). At the northern sites (BEFA, MALY), a notable increase was detected in the July precipitation, while in case of REZI, a clear shift to the late summer and autumn months was visible in the distribution of annual precipitation. At the southern BAAP site, autumn precipitation also increased, but without significant decrease or even slight increase in late spring and in the summer months.

These patterns also mark the differences between *EQ* and *FAI* climate indices (*Fig. 3*). The REZI site clearly faced the most monotonous trend of aridification, already beyond the hypothetical xeric distribution limit of beech during the latter decades, agreed by both indices and climate datasets. BAAP and BEFA sites were continuously over and near to these xeric limits, respectively. Taking the more site-specific CARPATCLIM based *FAI* time series into consideration, MALY was the most humid habitat, even though the larger scale climate data indicated this region controversially as more arid. However, as noted before, any values should be handled with caution for this area, due to the inconsistency of climate datasets. Both northern sites (MALY, BEFA) faced a peak of driest conditions during the early 1990s.

3.2. Climate influence on the radial growth

Regarding the basic climatic variables (precipitation and temperature), the strongest correlations were found with precipitation, particularly with the rainfall of late spring and early summer months (*Fig. 4*). Mean temperatures showed a slight non-significant negative influence on growth during the same period. Apparent correlations with weather conditions of the early previous autumn were also observed usually with similar sign as in the growing period. The four study sites showed similar patterns of monthly correlation coefficients, though some differences can be observed, as well (e.g., the lack of August precipitation's relationship with REZI and BAAP site's growth). Combining effects of temperature, evaporation and precipitation within *SPEI* in a 3-month window resulted in higher correlation with growth, increasing correlation coefficients up to 0.72 during July in case of MALY.

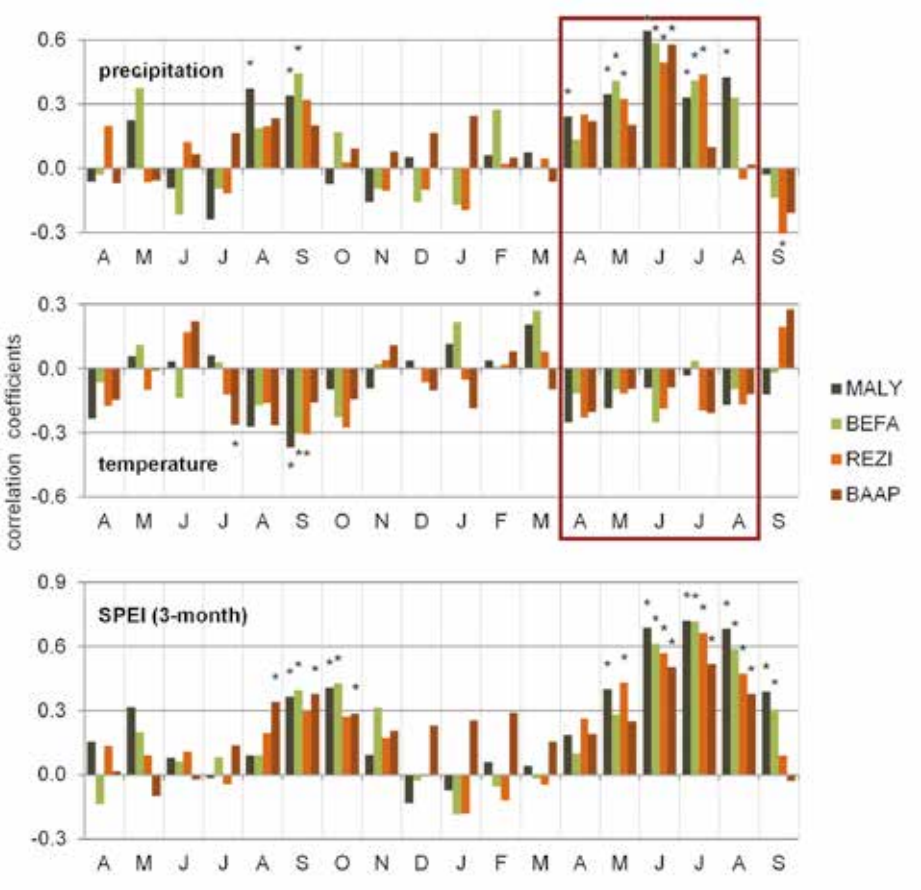

Fig. 4. Growth-climate correlations between CARPATCLIM monthly precipitation and temperature as well as 3-month standardized precipitation evaporation index (*SPEI*) data and TRW site chronologies for period 1961-2000. Months from the previous year's April to the growing year's September are employed in the correlation analysis. Precipitation and temperature of months April-August in the growing year were selected for further investigations; * marks significant relationships tested by the bootstrap method.

A group of growing months from April to August was selected for the more detailed multiple regression analysis with temperature and precipitation data (*Fig. 5*), even when mean temperature values did not show significant correlations with the growth during the entire period of 1961–2000. By the longer-term analysis, positive effects of precipitation were emphatically present, with the dominance of June rainfall highlighted. The limiting role of temperature was described as more influential by partial correlations. Negative relationships

were confirmed in general, with significant months of May and July at MALY and BEFA, and April at REZI and BAAP sites during several periods. In a single case at BEFA, a significant positive correlation with July temperature was also found during the earliest period of the previous century. The limiting role of late spring temperatures compared to effects of precipitation was most pronounced at the southernmost, climatically marginal BAAP site, although with the highest rate of unexplained variance. Relationships of the marginal months of the growing season (April and August) showed sometimes greater fluctuations and clearer trends, though varying to a great degree from site to site. Significance of temperature determination was changing much more remarkably, than those of precipitation.

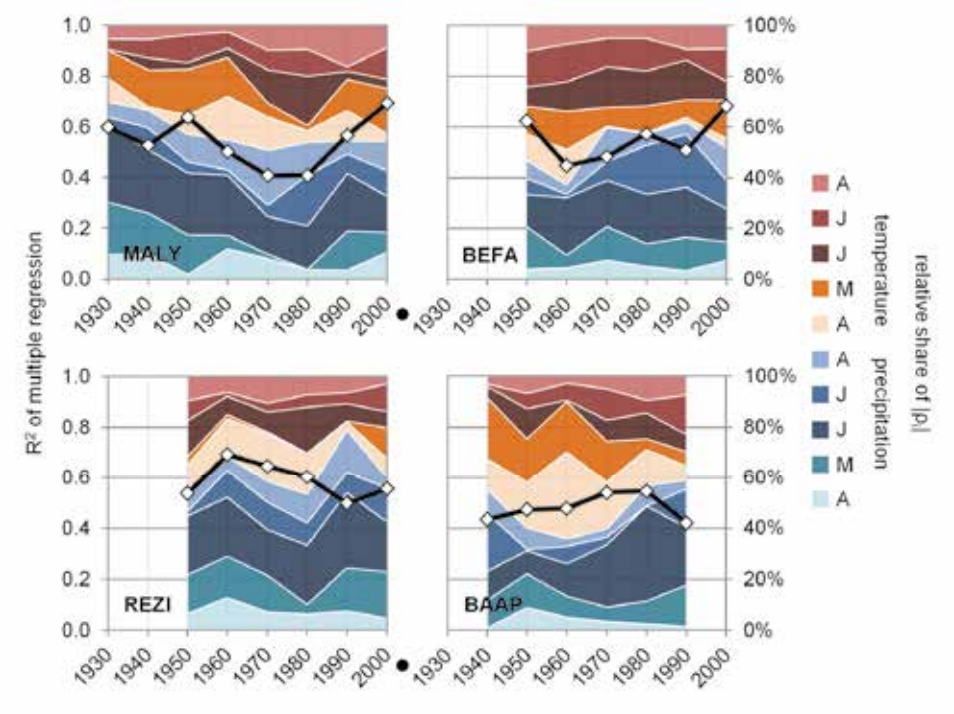

Fig. 5. Results of the multiple regression analysis of *TRW* site chronologies with April-August climate variables. R^2 value of regression strength represents changing climate influence (black curves with diamonds), while relative magnitudes of partial correlation coefficients (in absolute values; |ρi|) imply the distribution of the annual increment's formation in months of the main growing season in 31-year windows with 10-year overlap, using climate data of CRU/GPCC. Horizontal axis labeling indicates the mid-year of 31-year periods.

In case of the two northern sites (MALY, BEFA), an overall strengthening climatic determination of growth was visible over the last decades, involving also several monthly variables as significant determinants (*Table 5*), however, stronger relationships could be observed during the earlier periods of the last century, followed by an intermediate depression around the mid-20th century. In contrary, at the REZI and BAAP sites, the climatic influence was stronger around the mid-last century with a more recent slight fallback (*Fig. 5*). Despite this weakening in the total explained variance, many individual monthly variables were identified as significant in case of REZI, as well, for the period of 1985–2015 (*Table 5*). The overall climatic determination of growth was strongest in case of MALY ($R2$=0.69 during 1985–2015) and REZI ($R2$=0.69 during 1945–1975), but it was also similarly high in case of BEFA for the last period of analysis ($R2$=0.68 during 1985-2015). Regression coefficients, their significance and $R2$ statistics of the used multivariate linear models are summarized in *Table 5* for the latter mid-20th century (1945–1975) and the last available period for each site.

Table 5. Estimates of the regression coefficients for each monthly climatic variable (with indicating their $p<0.05$ significance) and R^2 and adjusted R^2 statistics of the used regression models for the period 1945–1975 (*a*) and the last available period for each site (*b*; 1975–2005 for BAAP and 1985–2015 for the other three sites)

	MALY		**BEFA**		**REZI**		**BAAP**	
	a	**b**	**a**	**b**	**a**	**b**	**a**	**b**
P(APR)	0.0016	**-0.0027***	0.0006	-0.0016	0.0014	0.0011	0.0007	0.0004
P(MAY)	0.0005	0.0012	0.0005	0.0010	**0.0016***	**0.0041***	0.0012	0.0037
P(JUN)	**0.0014***	**0.0025***	**0.0016***	**0.0026***	**0.0018***	**0.0037***	0.0012	**0.0037***
P(JUL)	-0.0002	0.0015	0.0001	**0.0016***	0.0007	**0.0029***	-0.0007	0.0023
P(AUG)	0.0010	**0.0020***	0.0003	**0.0021***	0.0004	-0.0008	0.0002	0.0007
T(APR)	-0.0307	-0.0111	-0.0292	-0.0134	-0.0282	0.0275	**-0.0766***	0.0196
T(MAY)	-0.0255	**-0.1132***	-0.0277	**-0.0823***	0.0036	**0.0654***	-0.0491	0.0223
T(JUN)	0.0078	-0.0225	-0.0268	-0.0438	-0.0178	-0.0288	-0.0017	0.0302
T(JUL)	0.0142	**-0.0684***	0.0369	**-0.0662***	-0.0046	0.0558	0.0250	-0.0584
T(AUG)	-0.0065	0.0498	-0.0215	0.0506	0.0177	0.0193	-0.0080	-0.0304
Intercept	1.0978	**3.2369***	1.5647	**2.9229***	0.8974	**-2.2116***	2.1191	1.0102
R^2	0.502	0.693	0.446	0.681	0.691	0.555	0.477	0.420
adj. R^2	0.252	0.540	0.170	0.522	0.536	0.332	0.215	0.130

3.3. Trends of basal area increments

Radial growth slowed down in the 1990s at the core sites, regardless of age and site conditions (relative *BAI*<1, *Fig. 6*). Note here that growth rates at drier habitats (BEFA, BAAP) having lower yield potential were initially lower (*Table 6*). Increments also became more unstable with age and higher *BAI* rates, both intra-series and between individual sample trees, with higher relative interannual variability and diverging quartiles of individual series (*Fig. 6, Table 6*). The mean increment curve of some REZI trees, those were affected by a drought induced mortality event beginning with the early 2000s, even turned into a strong decrease with some of them already stopping xylem formation 5–6 years prior to their sanitary harvesting in 2015. Most of the other trees from this site (both stand and NFI) also showed a clear growth decline for the corresponding years. The other three sites faced a slight growth release during the last years of the investigated period. Number of available *BAI* series generally represent almost full sample depth (MALY: *n*=20, BEFA: *n*=19, REZI: *n*=20, BAAP: *n*=17), however, in case of BAAP there was a fast reduction in available series after 2001 with only n=5 sample trees remaining in 2010, which could cause bias in possible conclusions for the last decade at this single site. The other study sites faced only a minor sample reduction in the very last year of 2010, with a decrease in available individual series by 4 and 2 samples at MALY and REZI, respectively.

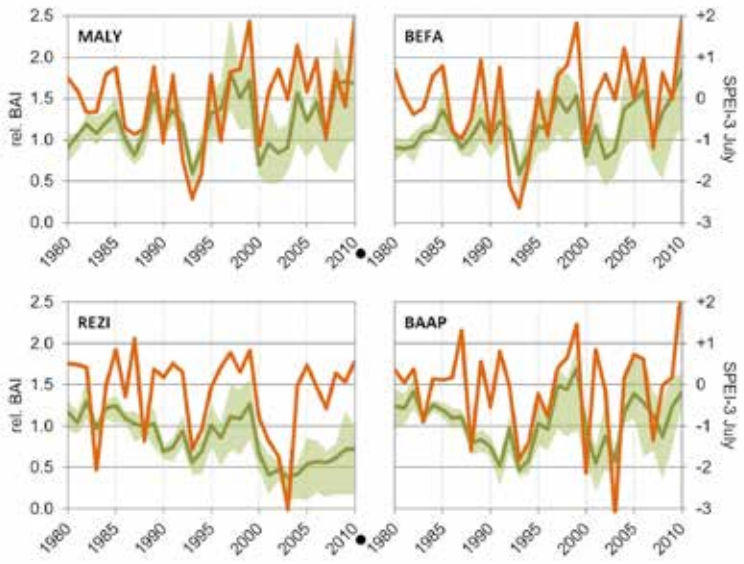

Fig. 6. Relative basal area increments (*rel. BAI*; shaded area indicates interquartile range) with the reference period of 1971–1990 and time series of the July 3-month standardized precipitation evaporation index (*SPEI-3 July*; CARPATCLIM) during the period 1980-2010. Sample depth at BAAP site reduces monotonously after 2001 to 5, while it is stable and represents almost the whole available sample size at the other three sites.

Table 6. Mean basal area increment (*BAI*) of the sample trees and mean slope of the linear trend (regression beta parameter; *BAI* trend) fitted on individual trees for the reference period of 1971–1990 (a) and the investigated decades of 1980–2010 (b); with interquartile range indicated in brackets

	mean BAI (mm^2)		BAI trend (mm^2/yr)	
	a	**b**	**a**	**b**
MALY	1972 (1053–2732)	2248 (1374–2971)	59.1 (17.2–72.6)	3.9 (-27.1–20.1)
BEFA	1226 (822–1532)	1260 (1054–1565)	6.1 (5.5–31.4)	9.9 (-11.6–18.2)
REZI	2856 (1874–3660)	2370 (1632–2547)	25.8 (-5.7–52.7)	-63.0 (-100.6–-33.9)
BAAP	1453 (708–1705)	1613 (1104–1958)	19.5 (-1.0–23.4)	27.1 (-19.3–44.6)

Looking behind the general trends of *BAI* curves, effects and severity of particular drought periods of the past decades can be also differentiated (*Fig. 6*). Major drought events were selected by the July values of the 3-month *SPEI* index (showing previously the closest relationship with growth variations) and checked also by pointer year analysis. Extreme droughts were associated to *SPEI* values lower than -1. A return periodicity of such events seemed to be usually 5–10 years. The severest country-scale summer droughts were identified during the years 1992–1994, affecting first of all the norther region (MALY, BEFA). Here, individual years of less extreme, but notable additional droughts were 1990, (1996), 2000, and 2007. At the southwestern sites, individual years with drier summers were already present (1983, 1988), and they were also affected by several extreme droughts beginning with 2000. In case of BAAP, however, these happened mostly in individual years with breaks in-between, while REZI faced continuous summer droughts between 2001–2003, meaning that altogether this site was affected by the most frequent and prolonged extreme drought periodicity.

The relative *BAI* values followed rather well the *SPEI* indices (*Fig. 6*). After the 1992–1994 droughts, growth at most sites recovered relatively fast, exceeding the 1971–1990 average *BAI* values with exception of the REZI trees, where a slower recovery of growth was noticeable. With the beginning of the new drought period in 2000 (severest at BAAP site in that year) increments at all sites dropped in the same year all over the country. After that, in the northern region, MALY and BEFA started to recover again, while in case of REZI, a clear and lasting growth decline started, affecting most of the sample trees.

4. Discussion and conclusion

Forest tree species, close or in a changing climate getting closer to their xeric (retreating) range edge, are generally facing increased sensitivity to climatic conditions (*Jump et al.*, 2010; *Mátyás et al.*, 2010). This phenomenon is generally revealed by our case study, in terms of regression analysis between climatic variables and radial growth traits and by the course of basal area increments compared to recurrent droughts. Higher sensitivity at the originally more mesic sites, compared to the drier ones can be evinced due to the naturally higher resistance of the more drought-adapted marginal populations (*Dittmar et al.*, 2003; *Weber et al.*, 2013; *Cavin* and *Jump*, 2016). This could be confirmed by the growth decline at the originally beech-favored REZI or probably also by the stronger correlations found at the most humid MALY site. The partial correlation analysis in 31-year windows, however, also showed that the expected strengthening impact of climate on growth was not uniform among trees from different sites and considering monthly climate elements, but a varying sensitivity to climatic factors over time can be also concluded for all sites (*Weber et al.*, 2013). Another study pointed out recent decreased climatic determination of Scots pine growth on the edge of its climatic tolerance in the vicinity of the REZI site (*Misi* and *Náfrádi*, 2017), that might be also applicable in case of REZI trees (and partially BAAP) during the last 31-year period, assuming the same climatic trends. This attribute of decreasing interannual growth-climate correlation does not necessarily contradict high climatic sensitivity in other terms though (cf., decreased drought resistance of REZI trees).

Similarly to a range of previous findings, strong correlation of radial growth was found with precipitation data, in particular with the rainfall of the late spring and early summer months (e.g., *Geßler et al.*, 2007; *van der Werf et al.*, 2007; *Hacket-Pain et al.*, 2016), sometimes also referred to as the main growing season (*Führer et al.*, 2011). Mean temperature in this same period also seemed to have a negative influence on radial growth, most probably as a consequence of the stimulation of transpirative water loss (*Čufar et al.*, 2008; *Führer et al.*, 2016; *Hacket-Pain et al.*, 2016). Therefore, the more complex climatic variable of the 3-month *SPEI*, showed the strongest relationships with growth, is widely used in other studies, as well (e.g., *Hacket-Pain et al.*, 2016). Concluding the results from each site, usually very high correlation coefficients were found with climatic variables (up to r=0.67 in case of June precipitation and r=0.72 in case of July *SPEI*), exceeding growth-climate correlations of most previous analyses from Europe (e.g., *Čufar et al.*, 2008; *van der Maaten*, 2012; *Tegel et al.*, 2014; *Cavin* and *Jump*, 2016; *Roibu et al.*, 2017; *Stojanović et al.*, 2018). Apparent and significant correlations with the meteorological conditions of previous autumn and late summer could be also observed (Fig. 4), reported by other studies (e.g., *Hacket-Pain et al.*, 2016; *Roibu et al.*, 2017), probably also

due to the connections to physiological processes of the storage period and with a possible relation to reproductive traits (*Drobyshev et al.*, 2010; *Hacket-Pain et al.*, 2015). Differences in climatic sensitivity between study sites may be also due to the natural genetic diversity and high phenological plasticity of beech (*Jump et al.*, 2006a; *Prislan et al.*, 2013; *Thiel et al.*, 2014), but differences in climatic conditions of the study sites might be seen as a principal driver combined with effects of other site factors (*Table 1; Figs. 2* and *3* and *6*). Climate change usually results in an earlier leaf unfolding and beginning of the vegetation season (*Čufar et al.*, 2012; *Prislan et al.*, 2013), but a possible elongation of the growing season on the other cutting edge with increment formation delayed to late summer months is widely reported, as well (*van der Werf et al.*, 2007; *Jezík et al.*, 2011; *Tegel et al.*, 2014; *Führer et al.*, 2016). Moving partial correlations of the multivariate analysis could reveal both tendencies at some extent by increasing importance of April-May, July-August in the total climatic determination of growth.

Multidecadal trends of basal area increments indicate more stagnating growth rates or even decline (REZI) for the investigated sites during the past 30-40 years (*Fig. 6*). This finding is similar to reports from Mediterranean countries (*Jump et al.*, 2006b; *Piovesan et al.*, 2008), but also from Southern Germany (*Dulamursen et al.*, 2017) and another site in western Hungary (*Führer et al.*, 2016). Under optimal conditions, basal area growth curves increase almost monotonously, but later asymptotically with age. Decreasing trend usually appears when approaching the end of the individual beech tree's lifetime, therefore, clearly reduced stem growth rates can be a (predictive) sign of a long-term decline (*Piovesan et al.*, 2008; *Gillner et al.*, 2013; *Delaporte et al.*, 2016). In comparison to other, especially to norther sites, some of the REZI trees underwent a drastic growth reduction, that could be interpreted as a predictive sign of vitality loss, which lead to drought-induced mortality event accounting also for the later sanitary interventions. This event was also well-linked to a reported mass mortality affecting widespread beech stands of western Hungary (*Lakatos* and *Molnár*, 2009). Beech decline in the region also raised the question of accurate projection of favorable beech habitats by time-averages of specific climate indices. The use of more complex indices may bring considerable benefits (*Führer et al.*, 2011; *Mellert et al.*, 2016), meanwhile, the common lack of knowledge of precise stand level climatic conditions should also be noted.

Drought is an important extreme climate phenomenon that can strongly affect physiology and growth of temperate tree species even on the longer term (*Bréda et al.*, 2006). In case of beech, these stress effects could be even more notable (*Scharnweber et al.*, 2011; *Rasztovits et al.*, 2014; *Roibu et al.*, 2017). Including extreme and more importantly recurrent drought events in the analysis improved the understanding of growth reduction and decline, also in our case. When talking about effects of drought on the vitality and growth of beech, most of the studies usually refer to the 2003 drought, that was widely reported and

investigated in many parts of Europe (e.g., *Czajkowski et al.*, 2005; *Bréda et al.*, 2006; *van der Werf et al.*, 2007). However, looking at the time series of the *SPEI* indices (*Fig. 6*), the impression is that the abiotic side of tree mortality events in/after 2003 was more like a denouement in a chain of recurrent drought events of different severity. This observation is in line with the coincidence between biotic damages and mortality of beech and droughts in Hungary (*Janik et al.*, 2016). Early-1990s droughts affected northern Hungary more strongly (represented by MALY and BEFA), while the early-2000s drought period was more expressed over western Hungary, causing significant damages there (*Lakatos* and *Molnár*, 2009; *Janik et al.*, 2016). It should be also noted that the (south)western sites (REZI and BAAP) seemed to face some years of severe droughts already during the 1980s. Timing, frequency, and severity of dry periods combined with soil properties seemed to play a key role in determining the resilience capacity of individual forest stands (e.g., *Móricz et al.*, 2018). The drought-induced tree decline phenomenon in the closer region of the REZI site was not limited to only beech trees either. After another severe drought later in 2012, extensive damages took also place among black pine stands in this region (*Móricz et al.*, 2018). In addition to the higher exposure to droughts, this site was the only one with sandy soil texture, thus, with lowest water retention capacity, amplifying further the effects of the discussed drought events. Small-scale mosaics of remaining standing trees in sanitary felling patches at REZI site showed regained vitality during a later field visit, despite of the disrupted stand structure leading to higher exposure. The marginal habitats of south Hungary interestingly avoided major abiotic and associated biotic damages, also due to the different climatic impact and the lack of the continuous multiannual drought period of 2000–2003 (*Fig. 6*). Management plans and reforestation activity at the BAAP site, however, neglected beech in the more recent regeneration periods.

Our findings altogether confirm the pronounced climate sensitivity of beech growth at the continental xeric limit, but also reveal its variability both in interannual patterns comparing the different sites and over the investigated periods. Recent trends of climate change and additional extreme events could be also tracked along the changing climatic sensitivity of growth and in basal area growth decline, however, some of the sites faced recently less remarkable effects, and periods of more pronounced climatic sensitivity can be found also in the earlier part of the 20th century. Since tree rings are unique indicators of growth in respect of both time frequency and spatial availability, their application to more precise and dynamic forest growth estimation and forest inventories could be also significant (*Rohner et al.*, 2016), in which context our results also gave evidence for a working and useful merge of regular NFI plot sampling with a more traditional dendrochonological sampling design. On the other hand, this combination of data revealed the relatively young average age of Hungarian beech forests, which may limit research attempts on long-term

beech dendroclimatology. Nevertheless, under the projected climate change, growth sensitivity assessments performed on a wider scale can also serve with useful information for future species and reproductive material selection for forest regeneration, including the search for potentially better adapted provenances from the xeric-marginal habitats (*Mátyás,* 2016).

Acknowledgements: We acknowledge the Eger, Mályinka, Keszthely, and Bátaszék State Forestry Offices and *Dr. László Palcsu* (Institute for Nuclear Research, MTA) for tree samples and site information. Special thanks to colleges of the National Food Chain Safety Office (NÉBIH) for contribution of core samples and the national beech distribution map along with the National Forest Inventory Program. We acknowledge the kind help of *Dr. István Gábor Hatvani* (Institute for Geological and Geochemical Research, MTA) in parts of the statistical analysis and the useful comments of *Dr. Ernő Führer* (Forest Research Institute, NARIC). The research was supported by the 'Lendület' program of the Hungarian Academy of Sciences (LP2012-27/2012). This is contribution No.64 of '2ka Palæoclimatology' Research Group and No.33 of Budapest Tree-Ring Laboratory.

References

Bonan, G.B., 2008: Forests and climate change: forcings, feedbacks, and the climate benefits of forests. *Science 320,* 1444–1449. https://doi.org/10.1126/science.1155121

Bréda, N, Huc, R., Granier, A., and *Dreyer E,* 2006: Temperate forest trees and stands under severe drought: a review of ecophysiological responses, adaptation processes and long-term consequences. *Ann For Sci 63,* 625–644. https://doi.org/10.1051/forest:2006042

Buras, A., 2017: A comment on the expressed population signal. *Dendrochronologia 44*, 130–132. https://doi.org/10.1016/j.dendro.2017.03.005

Cavin, L., and *Jump, A.S.,* 2017: Highest drought sensitivity and lowest resistance to growth suppression are found in the range core of the tree *Fagus sylvatica* L. not the equatorial range edge. *Glob Change Biol 23*, 362–379. https://doi.org/10.1111/gcb.13366

Cook, E.R., Briffa, K., Shiyatov, S., and *Mazepa, V.,* 1990: Tree-ring standardization and growth-trend estimation. In (eds: *Cook, E.,* and *Kairiukstis, L.*) Methods of Dendrochronology. Applications in the Environmental Sciences;. Kluwer Academic Publishers

Cook, E.R., and *Krusic, P.J.,* 2006: ARSTAN4.1b_XP. http://www.ldeo.columbia.edu

Cook, E.R., and *Peters K,* 1981: The smoothing spline: a new approach to standardizing forest interior tree-ring width series for dendroclimatic studies. *Tree Ring Bull 41*, 45–53.

Čufar, K., De Luis, M., Saz, M.A., Črepinšek, Z., and Kajfež-Bogataj, L., 2012: Temporal shifts in leaf phenology of beech (Fagus sylvatica) depend on elevation. Trees 26, 1091–1100. https://doi.org/10.1007/s00468-012-0686-7

Čufar, K., Prislan, P., de Luis, M., and *Gričar, J.,* 2008: Tree-ring variation, wood formation and phenology of beech (*Fagus sylvatica*) from a representative site in Slovenia, SE Central Europe. *Trees 22,* 749–758. https://doi.org/10.1007/s00468-008-0235-6

Czajkowski, T., Kühling, M., and *Bolte, A.,* 2005: Einfluss der Sommertrockenheit im Jahre 2003 auf das Wachstum von Naturverjüngungen der Buche (*Fagus sylvatica* L.) im nordöstlichen Mitteleuropa. *Allg Forst Jagdztg 176*, 133–143. (In German)

Czúcz, B., Gálhidy, L., and *Mátyás, C.,* 2011: Present and forecasted xeric climatic limits of beech and sessile oak distribution at low altitudes in Central Europe. *Ann For Sci 68*, 99–108. https://doi.org/10.1007/s13595-011-0011-4

Delaporte, A., Bazot, S., and *Damesin, C.,* 2016: Reduced stem growth, but no reserve depletion or hydraulic impairment in beech suffering from long-term decline. *Trees 30*, 265–279. https://doi.org/10.1007/s00468-015-1299-8

Di Filippo, A., Biondi, F., Čufar, K., De Luis, M., Grabner, M., Maugeri, M., Saba, E.P., Schirone, B., and Piovesan, G., 2007: Bioclimatology of beech (Fagus sylvatica L.) in the Eastern Alps:

spatial and altitudinal climatic signals identified through a tree-ring network. J Biogeogr 34, 1873–1892. https://doi.org/10.1111/j.1365-2699.2007.01747.x

Dittmar, C., Zech, W., and *Elling, W.*, 2003: Growth variations of common beech (*Fagus sylvatica* L.) under different climatic and environmental conditions in Europe – a dendroecological study. *For Ecol Manage 173*, 63–78. https://doi.org/10.1016/S0378-1127(01)00816-7

Drobyshev, I., Övergaard, R., Saygin, I., Niklasson, M., Hickler, T., Karlsson, M., and Sykes, M.T., 2010: Masting behaviour and dendrochronology of European beech (Fagus sylvatica L.) in southern Sweden. For Ecol Manage 259, 2160–2171. https://doi.org/10.1016/j.foreco.2010.01.037

Dulamsuren, C., Hauck, M., Kopp, G., Ruff, M., and *Leuschner, C.,* 2017: European beech responds to climate change with growth decline at lower, and growth increase at higher elevations in the center of its distribution range (SW Germany). *Trees 31*, 673–686. https://doi.org/10.1007/s00468-016-1499-x

Ellenberg H, 1988: Vegetation ecology of Central Europe. Cambridge University Press

EUFORGEN, 2009: Distribution map of Beech (*Fagus sylvatica*). www.euforgen.org

Fotelli, M.N., Nahm, M., Radoglou, K., Rennenberg, H., Halyvopoulos, G., and *Matzarakis, A.,* 2009: Seasonal and interannual ecophysiological responses of beech (*Fagus sylvatica*) at its south-eastern distribution limit in Europe. *For Ecol Manage 257*, 1157–1164. https://doi.org/10.1016/j.foreco.2008.11.026

Frank, D., Esper, J., and *Cook, E.R.*, 2007: Adjustment for proxy number and coherence in a large-scale temperature reconstruction. *Geophys Res Lett 34*, L16709. https://doi.org/10.1029/2007GL030571

Führer, E., Edelényi, M., Horváth, L., Jagodics, A., Jereb, L., Kern, Z., Móring, A., Szabados, I., and *Pödör, Z.,* 2016. Effect of weather conditions on annual and intra-annual basal area increments of a beech stand in Sopron Mountains in Hungary. *Időjárás 120*, 127–161.

Führer, E., Horváth, L., Jagodics, A., Machon, A., and *Szabados, I.,* 2011: Application of new aridity index in Hungarian forestry practice. *Időjárás 115*, 205–216.

Garamszegi, B., and *Kern, Z.,* 2014: Climate influence on radial growth of *Fagus sylvatica* growing near the edge of its distribution in Bükk Mts., Hungary. *Dendrobiology 72*, 93–102. https://doi.org/10.12657/denbio.072.008

Geßler, A., Keitel, C., Kreuzwieser, J., Matyssek, R., Seiler, W., and Rennenberg, H., 2007: Potential risks for European beech (Fagus sylvatica L.) in a changing climate. Trees 21, 1–11. https://doi.org/10.1007/s00468-006-0107-x

Gillner, S., Rüger, N., Roloff, A., and *Berger, U.,* 2013: Low relative growth rates predict future mortality of common beech (*Fagus sylvatica* L.). *For Ecol Manage 302*, 372–378. https://doi.org/10.1016/j.foreco.2013.03.032

Hacket-Pain, A.J., Cavin, L., Friend, A.D., and *Jump, A.S.,* 2016: Consistent limitation of growth by high temperature and low precipitation from range core to southern edge of European beech indicates widespread vulnerability to changing climate. *Eur J For Res 135*, 897–909. https://doi.org/10.1007/s10342-016-0982-7

Hacket-Pain, A.J., Friend, A.D., Lageard, J.G., and *Thomas, P.A.,* 2015: The influence of masting phenomenon on growth–climate relationships in trees: explaining the influence of previous summers' climate on ring width. *Tree Physiol 35*, 319–330.

Harris, I., Jones, P.D., Osborn, T.J., and *Lister, D.H.*, 2014: Updated high-resolution grids of monthly climatic observations–the CRU TS3. 10 Dataset. *Int J Climatol 34,* 623–642. https://doi.org/10.1002/joc.3711

Hirka, A., Pödör, Z., Garamszegi, B., and *Csóka, G.,* 2018: A magyarországi erdei aszálykárok fél évszázados trendjei (1962-2011). *Erdészettudományi Közlemények 8*, 11–25. (In Hungarian) https://doi.org/10.17164/EK.2018.001

Holmes, R.L., 1983: Computer-assisted quality control in tree-ring dating and measurement. *Tree Ring Bull 43*, 69–75.

Janik, G., Hirka, A., Koltay, A., Juhász, J., and Csóka, G., 2016. 50 év biotikus kárai a magyar bükkösökben. Erdészettudományi Közlemények 6, 45–60. (In Hungarian) https://doi.org/10.17164/EK.2016.005

Ježík, M., Blaženec, M., Střelcová, K., and *Ditmarová, Ľ.,* 2011: The impact of the 2003-2008 weather variability on intra-annual stem diameter changes of beech trees at a submontane site in central Slovakia. *Dendrochronologia 29*, 227–235. https://doi.org/10.1016/j.dendro.2011.01.009

Jump, A.S., Cavin, L., and *Hunter, P.D.,* 2010: Monitoring and managing responses to climate change at the retreating range edge of forest trees. *J Environ Monitor 12*, 1791–1798. https://doi.org/10.1039/b923773a

Jump, A.S., Hunt, J.M., Martínez-Izquierdo, J.A., and *Peñuelas, J.,* 2006a: Natural selection and climate change: temperature-linked spatial and temporal trends in gene frequency in *Fagus sylvatica*. *Mol Ecol 15*, 3469–3480. https://doi.org/10.1111/j.1365-294X.2006.03027.x

Jump, A.S., Hunt, J.M., and *Peñuelas, J.,* 2006b: Rapid climate change-related growth decline at the southern range edge of *Fagus sylvatica*. *Glob Change Biol 12*, 2163–2174. https://doi.org/10.1111/j.1365-2486.2006.01250.x

Kázmér, M., and *Grynaeus, A*., 2003. The Budapest Tree-Ring Laboratory. Association for Tree-Ring Research Newsletter 1, 5–6.

Kramer, K., Degen, B., Buschbom, J., Hickler, T., Thuiller, W., Sykes, MT., and *de Winter, W.,* 2010: Modelling exploration of the future of European beech (*Fagus sylvatica* L.) under climate change – Range, abundance, genetic diversity and adaptive response. *For Ecol Manage 259*, 2213–2222. https://doi.org/10.1016/j.foreco.2009.12.023

Lakatos, F., and *Molnár, M.,* 2009: Mass mortality of beech (*Fagus sylvatica* L.) in South-West Hungary. *Acta Silv Lign Hung 5*, 75–82.

Lebourgeois, F., Bréda, N., Ulrich, E., and *Granier, A.,* 2005: Climate-tree-growth relationships of European beech (*Fagus sylvatica* L.) in the French Permanent Plot Network (RENECOFOR). *Trees 19*, 385–401. https://doi.org/10.1007/s00468-004-0397-9

van der Maaten, E., 2012: Climate sensitivity of radial growth in European beech (*Fagus sylvatica* L.) at different aspects in southwestern Germany. *Trees 26*, 777–788. https://doi.org/10.1007/s00468-011-0645-8

Mátyás, C., 2010: Forecasts needed for retreating forests. *Nature 464*, 1271. https://doi.org/10.1038/4641271a

Mátyás, C., 2016. Guidelines for the choice of forest reproductive material in the face of climate change. FORGER Guidelines 2016, www.fp7-forger.eu

Mátyás, C., Berki, I., Czúcz, B., Gálos, B., Móricz, N., and *Rasztovits, E.*, 2010: Future of beech in Southeast Europe from the perspective of evolutionary ecology. *Acta Silv Lign Hung 6*, 91–110.

Mátyás, C., Božič, G., Gömöry, D., Ivanković, M., and *Rasztovits, E.*, 2009: Transfer analysis of provenance trials reveals macroclimatic adaptedness of European beech (*Fagus sylvatica* L.). *Acta Silv Lign Hung 5*, 47–62.

Meier, E.S., Lischke, H., Schmatz, D.R., and *Zimmermann, N.E.,* 2012: Climate, competition and connectivity affect future migration and ranges of European trees. *Global Ecol Biogeogr 21*, 164–178. https://doi.org/10.1111/j.1466-8238.2011.00669.x

Mellert, K.H., Ewald, J., Hornstein, D., Dorado-Liñán, I., Jantsch, M., Taeger, S., Zang, C., Menzel, A., and Kölling, C., 2016: Climatic marginality: a new metric for the susceptibility of tree species to warming exemplified by Fagus sylvatica (L.) and Ellenberg's quotient. Eur J For Res 135, 137–152. https://doi.org/10.1007/s10342-015-0924-9

Metz, J., Annighöfer, P., Schall, P., Zimmermann, J., Kahl, T., Schulze, ED., and *Ammer, C.*, 2016: Site-adapted admixed tree species reduce drought susceptibility of mature European beech. *Glob Change Biol 22*, 903–920. https://doi.org/10.1111/gcb.13113

Misi, D., and *Náfrádi, K.,* 2017: Growth response of Scots pine to changing climatic conditions over the last 100 years: a case study from Western Hungary. *Trees 31*, 919–928. https://doi.org/10.1007/s00468-016-1517-z

Mölder, I., and *Leuschner, C.,* 2014: European beech grows better and is less drought sensitive in mixed than in pure stands: tree neighbourhood effects on radial increment. *Trees 28*, 777–792. https://doi.org/10.1007/s00468-014-0991-4

Móricz, N., Garamszegi, B., Rasztovits, E., Bidló, A., Horváth, A., Jagicza, A., Illés, G., Vekerdy, Z., Somogyi, Z., and *Gálos, B*., 2018: Recent Drought-Induced Vitality Decline of Black Pine (Pinus nigra Arn.) in South-West Hungary – Is This Drought-Resistant Species under Threat by Climate Change? Forests 9, 414.

NÉBIH, 2015: Forest resources and forest management in Hungary, 2014. National Food Chain Safety Office, Directorate of Forestry, Budapest

NÉBIH, 2016: Forest Inventory 2010-2014. National Food Chain Safety Office, Directorate of Forestry, Budapest. portal.nebih.gov.hu/en/erdoleltar/

Peñuelas, J., Ogaya, R., Boada, M., and *Jump, A.S.,* 2007: Migration, invasion and decline: changes in recruitment and forest structure in a warming-linked shift of European beech forest in Catalonia (NE Spain). *Ecography 30*, 829–837. https://doi.org/10.1111/j.2007.0906-7590.05247.x

Piovesan, G., Biondi, F., Di Filippo, A., Alessandrini, A., and *Magueri, M.,* 2008: Drought-driven growth reduction in old beech (*Fagus sylvatica* L.) forests of the central Apennines, Italy. *Glob Change Biol 14*, 1265–1281. https://doi.org/10.1111/j.1365-2486.2008.01570.x

Prislan, P., Gričar, J., de Luis, M., Smith, K.T., and *Čufar, K.,* 2013: Phenological variation in xylem and phloem formation in *Fagus sylvatica* from two contrasting sites. *Agr Forest Meteorol 180*, 142–151. https://doi.org/10.1016/j.agrformet.2013.06.001

Rasztovits, E., Berki, I., Mátyás, C., Czimber, K., Pötzelsberger, E., and *Móricz, N.,* 2014: The incorporation of extreme drought events improves models for beech persistence at its distribution limit. *Ann For Sci 71*, 201–210. https://doi.org/10.1007/s13595-013-0346-0

R Development Core Team, 2014: R: A Language and Environment for Statistical Computing, R Foundation for Statistical Computing. Vienna, Austria

Rinn, F., 2005. TSAP reference manual. Heidelberg, Germany

Rohner, B., Weber, P., and *Thürig, E.,* 2016: Bridging tree rings and forest inventories: How climate effects on spruce and beech growth aggregate over time. *For Ecol Manage 360*, 159–169. https://doi.org/10.1016/j.foreco.2015.10.022

Roibu, C.C., Popa, I., Kirchhefer, A.J., and *Palaghianu, C.,* 2017: Growth responses to climate in a tree-ring network of European beech (*Fagus sylvatica* L.) from the eastern limit of its natural distribution area. *Dendrochronologia 42*, 104–116. https://doi.org/10.1016/j.dendro.2017.02.003

Scharnweber, T., Manthey, M., Criegee, C., Bauwe, A., Schröder, C., and *Wilmking, M.*, 2011: Drought matters – declining precipitation influences growth of Fagus sylvatica L. and Quercus robur L. in north-eastern Germany. For Ecol Manage 262, 947–961. https://doi.org/10.1016/j.foreco.2011.05.026

Schneider, U., Becker, A., Finger, P., Meyer-Christoffer, A., and *Ziese, M.,* 2018: *GPCC Full Data Monthly Product Version 2018 at 0.5°:* Monthly Land-Surface Precipitation from Rain-Gauges built on GTS-based and Historical Data. Global Precipitation Climatology Centre. http://gpcc.dwd.de/

Smith, P., Bustamante, M., Ahammad, H., Clark, H., Dong, H., Elsiddig, E.A., Haberl, H., Harper, R., House, J., Jafari, M., et al., 2014: Agriculture, Forestry and Other Land Use (AFOLU). In (eds: *Edenhofer, O., Pichs-Madruga, R., Sokona, Y., Farahani, E., Kadner, S., Seyboth, K., Adler, A., Baum, I., Brunner, S., Eickemeier, P., et al.*). Climate Change 2014: Mitigation of Climate Change. Contribution of Working Group III to the Fifth Assessment Report of the Intergovernmental Panel on Climate Change; Cambridge University Press

Standovár, T., and *Kenderes, K.,* 2003: A review on natural stand dynamics in beechwoods of East Central Europe. *Appl Ecol Environ Res 1*, 19–46. https://doi.org/10.15666/aeer/01019046

Stojanović, D.B., Kržič, A., Matović, B., Orlović, S., Duputié, A., Djurdjević, V., and *Stojnić, S.,* 2013: Prediction of the European beech (*Fagus sylvatica* L.) xeric limit using a regional climate model: An example from southeast Europe. *Agr Forest Meteorol 176*, 94–103. https://doi.org/10.1016/j.agrformet.2013.03.009

Stojanović, B.D., Levanič, T., Matović, B., Stjepanović, S., and *Orlović, S.,* 2018: Growth response of different tree species (oaks, beech and pine) from SE Europe to precipitation over time. *Dendrobiology 79*, 97–110. https://doi.org/10.12657/denbio.079.009

Stokes, M.A., and *Smiley, T.L.,* 1968: An introduction to tree-ring dating. The University of Chicago Press

Szalai, S., Auer, I., Hiebl, J., Milkovich, J., Radim, T., Stepanek, P., Zahradnicek, P., Bihari, Z., Lakatos, M., Szentimrey, T., et al., 2013: Climate of the Greater Carpathian Region. Final Technical Report. www.carpatclim-eu.org

Tegel, W., Seim, A., Hakelberg, D., Hoffmann, S., Panev, M., Westphal, T., and *Büntgen, U.,* 2014: A recent growth increase of European beech (*Fagus sylvatica* L.) at its Mediterranean distribution limit contradicts drought stress. *Eur J For Res 133*, 61–71. https://doi.org/10.1007/s10342-013-0737-7

Thiel, D., Kreyling, J., Backhaus, S., Beierkuhnlein, C., Buhk, C., Egen, K., Huber, G., Konnert, M., Nagy, L., and *Jentsch, A.*, 2014: Different reactions of central and marginal provenances of Fagus sylvatica to experimental drought. *Eur J For Res 133,* 247–260. https://doi.org/10.1007/s10342-013-0750-x

Vicente-Serrano, S.M., Beguería, S., and *López-Moreno, J.I.,* 2010: A multiscalar drought index sensitive to global warming: the standardized precipitation evapotranspiration index. *J Climate 23*, 1696–1718. https://doi.org/10.1175/2009JCLI2909.1

Weber, P., Bugmann, H., Pluess, A.R., Walthert, L., and *Rigling, A.,* 2013: Drought response and changing mean sensitivity of European beech close to the dry distribution limit. *Trees 27*, 171–181. https://doi.org/10.1007/s00468-012-0786-4

van der Werf, G.W., Sass-Klaassen, U.G., and *Mohren, G.M.J.,* 2007: The impact of the 2003 summer drought on the intra-annual growth pattern of beech (*Fagus sylvatica* L.) and oak (*Quercus robur* L.) on a dry site in the Netherlands. *Dendrochronologia 25*, 103–112. https://doi.org/10.1016/j.dendro.2007.03.004

Wigley, T.M.L., Briffa, K.R., and *Jones, P.D.*, 1984: On the average value of correlated time series, with applications in dendroclimatology and hydrometeorology. *J Clim Appl Meteorol 23*, 201–213. https://doi.org/10.1175/1520-0450(1984)023<0201:OTAVOC>2.0.CO;2

Zang, C., and *Biondi, F.,* 2013: Dendroclimatic calibration in R: the bootRes package for response and correlation function analysis. *Dendrochronologia, 31*, 68–74. https://doi.org/10.1016/j.dendro.2012.08.001

DOI:10.28974/idojaras.2020.2.6

IDŐJÁRÁS

Quarterly Journal of the Hungarian Meteorological Service
Vol. 124, No. 2, April – June, 2020, pp. 253–276

Hungarian regions and cities towards an adaptive future – analysis of climate change strategies on different spatial levels

Mária Szalmáné Csete * and **Attila Buzási**

Department of Environmental Economics
Budapest University of Technology and Economics
Magyar tudósok krt. 2., H-1117, Budapest, Hungary

**Corresponding Author e-mail: csete@eik.bme.hu*

(Manuscript received in final form January 23, 2020)

Abstract— Nowadays, urban areas are increasingly identified as strategic fields of climate change-related actions. Climate change is an increasingly complex challenge for these territories. Tackling climate change, moreover, in a sustainable way, is a priority in the European Union, which has set several ambitious short- and long-term mitigation, adaptation, and sustainability targets. It is a central issue of how society can respond to the climate emergency that is affected by and depends on the vertical and horizontal interrelations among different stakeholders, organizations, governance actors, etc., and their activities. Countries, regions, counties, and cities around the world react by developing climate strategies. The operationalization of the high-level political agreements and discourses is uncertain, and the policies in practice should also be evaluated on regional and city levels, just as the milestones of related strategic planning processes fostering local adaptive capacity. According to regional and urban governance, it is pivotal addressing not only mitigation but adaptation issues to be able to foster sustainable regional development, also considering the UN Sustainable Development Goals (SDGs) specified in the Agenda 2030. Adaptation to climate change is increasingly becoming a priority for policy action. It also has high relevance to find the synergic interrelations towards an adaptive future. This paper evaluates the recent changes in Hungarian regional and urban planning in relation to climate policy approach and reports a state of adaptation oriented spatial planning on NUTS-3 (Nomenclature of Territorial Units for Statistics) and LAU-1 (Local Administrative Units) levels. The results are based on the collection of all relevant climate change-related strategic documents on these levels in Hungary and on the analysis of specific information. There is a lack of knowledge related to the comprehensive adaptation policy and planning on regional and local levels in Hungary. The results of the evaluation show the state-of-art knowledge related to possible adaptation pathways and the various engagement level for climate policy approach on different spatial levels in Hungary. In the case of the examined research area, the development of more mitigation oriented planning documents and low level of adaptation measures and monitoring process management tools is seen as critical.

Key-words: climate strategies, SECAP-Sustainable Energy and Climate Action Plan, adaptation pathways, sustainable regional development, NUTS-3, LAU-1, Hungary

1. Introduction

Reducing adverse effects of climate change by taking into consideration both mitigation and adaption activities are at the forefront in current policies (*European Commission*, 2011; *UNFCCC*, 2015) and international scientific interests (*Sharifi* and *Yamagata*, 2016; *Mendizabal et al.*, 2018). Dated back to Agenda 21 proposals from the Rio Earth Summit in 1992, various spatial levels are urged by the UN at the end of the Climate Summit in 2019[1] to develop and to perform concrete actions and implementations in the field of climate change.

Hungary is facing numerous challenges regarding changing climatic patterns (*Bartholy et al.*, 2007, 2009; *Szépszó*, 2008; *Krüzselyi et al.*, 2011; *Torma et al.*, 2011; *Pongrácz et al.*, 2013, 2014; *Kis et al.*, 2017); therefore, it can be stated that climate change adaptation is a crucial part of the long-term sustainability in the center of the Carpathian Basin. Based on the review of the international literature, numerous studies regarding climate adaptation in a Hungarian context can be found concerning various relevant sectors, such as tourism (*Csete et al.*, 2013; *Kovács* and *Unger*, 2014; *Csete* and *Szécsi*, 2015; *Kovács et al.*, 2017); natural assets (*Malatinszky et al.*, 2013; *Mezösi et al.*, 2013; *Hlásny et al.*, 2014; *Mezősi et al.*, 2014; *Szabó et al.*, 2016); human health (*Páldy et al.*, 2005; *Páldy and Bobvos*, 2010; *Solymosi et al.*, 2010; *Törő et al.*, 2010; *Bobvos et al.*, 2015); agriculture (*Jolánkai and Birkás*, 2007; *Zemankovics*, 2012; *Gaál et al.*, 2014; *Li et al.*, 2017a, 2018); water management (*Werners et al.*, 2009; *Lóczy*, 2010; *Blanka et al.*, 2013; *Mezösi et al.*, 2013; *Rojas et al.*, 2013); energy supply and demand from different perspectives (*Bartholy et al.*, 2003; *Tánczos and Török*, 2007; *Szlávik* and *Csete*, 2012; *Hrabovszky-Horváth et al.*, 2013); transport (*Szendrő et al.*, 2014); or urban development issues (*Csete and Horváth*, 2012; *Czakó*, 2013; *Buzási*, 2014; *Csete and Buzási*, 2016; *Li et al.*, 2017b; *Kántor et al.*, 2018). Apart from the relative richness of literature with regards to adaptation issues, highly heterogeneous knowledge can be found if we try to analyze climate adaptation activities on a different spatial level. On NUTS-1 level (countries), among other things, *Berkhout et al.* (2015), *Heidrich et al.* (2016), and *Pietrapertosa et al.* (2018) aimed at comparing climate change policies and plans, however, the regional and local scale regarding analysis of climate change strategies and other related thematic development plans is almost completely lacking with an emphasis on adaptation issues in Hungary. It is worth mentioning that some studies have been dealing with a comparison of local climate plans across Europe (*Heidrich et al.*, 2013; *Reckien et al.*, 2014, 2015, 2018); however, the selection of analyzed Hungarian cities is based on their total population; therefore, a small pool of Hungarian settlements have been involved and evaluated. Cities or more precisely, local level play a crucial role in climate

[1] https://www.un.org/en/climatechange/un-climate-summit-2019.shtml

adaptation activities (*Rosenzweig et al.*, 2010; *Hunt* and *Watkiss*, 2011; *Millard-Ball*, 2013; *Wamsler et al.*, 2013; *Ürge-Vorsatz et al.*, 2018), but NUTS-3 level is often out of scope of analysis of climate change plans from both mitigation and adaptation point of view, while counties are highly important actors on climate adaptation issues in Hungary. During the previous years, numerous Hungarian cities and counties were engaged in developing their climate strategies to reduce GHG emissions and to be prepared concerning changing climatic patterns and the adverse of climate change. Based on previously stated reasons, the present study aims at analyzing climate strategies of Hungarian counties and county seats by paying particular attention to adaptation issues. Relationships between planning procedures and outcomes of the selected strategies are analyzed; therefore, all documents were evaluated by applying a detailed survey that can grasp the most important strengths and weaknesses of the planning processes. In the following chapters, firstly, the applied methodology is introduced, then the main results grouped by counties and cities are revealed; finally, conclusions and potential opportunities are highlighted.

2. Methodology

There is an increasing demand on both the science and policy sides to deliver some performance evaluation related to climate planning on different spatial levels. It is pivotal to be able to see the current status of climate oriented urban planning, especially when the focus is on adaptation. Spatial adaptation actions, interventions, and options can be examined through the systematic evaluation and detailed analysis of Hungarian counties and county seats. Considering county (NUTS-3) and county seat (LAU-1) level, there is a lack of climate planning assessment in Hungary. However, in this country, it is traditionally a well-functioning and effective territorial level. Thus, the engagement of the examined areas towards the climate planning approach and notable adaptation can play a pivotal role in further sustainable regional development perspectives.

Fig. 1 shows the territorial scope of the evaluation, namely the 19 Hungarian counties and county seats plus the capital. Budapest, as the capital of Hungary, compared to the 19 counties and county seats, has special rights according to law. Due to the significant contribution to GDP and the dominant percentage of the Hungarian population, it was examined together with the group of counties in this evaluation process.

Fig. 1. Examined area: The 19 Hungarian counties (including the capital) and county seats.

Urban areas are expected to become increasingly crucial actors both in mitigation and adaptation issues, which can be an especially revise assumption in Europe, where the 74%[2] of the population lives in these areas. The municipalities on different spatial levels are usually more engaged towards climate-friendly and sustainable ways of developments in those cases and places, where they have the possibility to receive financial and expert support from central governments (*Eckersley et al.*, 2018; *Bellinson* and *Chu*, 2019; *Kern*, 2019). Regarding the international scientific literature, several research results can be found mainly dealing with general aspects, EU (*Castán Broto*, 2017; *Mendizabal et al.*, 2018; *Reckien et al.*, 2018, 2019) or country-specific (*Berkhout et al.*, 2015; *Heidrich et al.*, 2016; *Pietrapertosa et al.*, 2018), territorial scope aiming attention at climate change in urban planning processes. According to the review of the above mentioned relevant research papers and methodologies, the main steps of recent evaluation is based on the following:

1. Identification of the existing types of climate change-related strategic and planning documents on the relevant spatial levels (counties and the capital, county seats);
2. Examination of the availability of relevant climate change-related strategic and planning documents;

[2] https://www.statista.com/statistics/270860/urbanuzation-by-continent/

3. Selection of the relevant climate change-related strategic and planning documents;
4. Adaptation oriented questionnaire development for the in-depth analysis considering the main research questions;
5. Online collecting form development and conduct the in-depth analysis;
6. Evaluation of the research results.

On county, capital and county seat level identified relevant climate strategies and other planning documents types belong to climate strategies or Sustainable Energy and Climate Action Plans (SECAPs). Related to county-level climate strategies, common methodology and guideline development were supported by the central government as well as the elaboration of the documents. All of the identified document was available online. In cases where both types of document are existing, the climate strategy was prioritized. The main research question emphasized the recent knowledge and the state of adaptation planning on different spatial levels in Hungary. The main examined topics according to adaptation oriented questionnaire have the following structure:

A) General information:
   - County/county seat name
   - Weblink of the document
   - Year of document development
   - Type of document
   - Existence of document history

B) Content related information:
   - Spatial characteristics
     - General climate related outlook (global, regional, local)
     - Area-specific impacts based on identified local characteristics
     - Vulnerable social groups
   - Adaptation aims related information
     - Sectors related to the adaptation aims
     - Impacts related to the adaptation aims
     - Number of adaptation aims
     - Types of adaptation oriented actions, interventions
   - Monitoring phase

- Existence of monitoring phase
- Features of existing monitoring phase

- Document development and general layout
  - Stakeholder involvement
  - Proportion of adaptation compared to mitigation

An online collecting form was developed and used for the feasibility of the in-depth analysis. The data collection was conducted from the beginning of September to the end of October 2019.

3. Results

In the present chapter, results regarding the detailed analysis of counties and county seats will be presented in that order. Budapest is involved in the group of counties, due to its specific rights, size, and importance with regards to both mitigation and adaptation issues. The structure of the visualization is almost the same for both groups; however, it can be seen that there are some differences between the presentation of the results since some questions are more relevant and provide more specific outcomes in the case of cities rather than counties.

The first question was focusing on the date of approval concerning climate change strategies of counties. Since the Hungarian government decided to support the development of climate change strategies on NUTS-3 level through the Environment and Energy Operational Programme in 2016, consequently majority of strategies was developed and approved in 2018 (16 of 20), only Heves County, Győr-Moson-Sopron County, Bács-Kiskun County, and Vas County released their documents in the year of 2017. All of the analyzed documents on the county level are stand-alone climate strategies in terms of their type; moreover, the vast majority of them are the first attempt due to the lack of climate strategies on the NUTS-3 level in Hungary. 18 of 20 strategies have a general outlook on climate change with regards to global or local impacts, risks, and other related issues. In the climate strategy of Békés and Fejér counties, this thematic outlook is completely lacking.

Similar to the previously presented results, highlights of local-specific impacts of climate change concerning different time-scales are a well-documented part of the selected strategies, since 17 of them defined observed changes from the past, 19 of 20 have dedicated chapter regarding present impacts, and 19 of them paid attention to future projections (see *Fig. 2*). By focusing on the existing differences across strategies, it is worth mentioning that in the strategy of Békés County had nothing to do with past and present impacts, Baranya County Climate Strategy is not detailing future risks; moreover, the analysis of observed changes lacks in case of both Jász-Nagykun-Szolnok and Komárom-Esztergom counties.

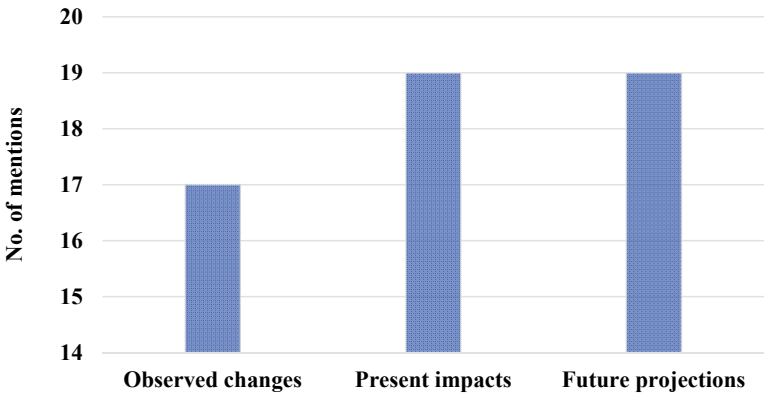

Fig. 2. Absolute number of mentions of local-specific impacts in climate strategies on county level.

Besides the collection of different impacts via a long time-scale, defined climate-related risks and actions were also revealed by analyzing the selected strategies. Based on the previously cited regional climate models, increasing temperature and changing precipitation patterns are the two significant impacts of climate change in the Carpathian Basin. Apart from them, it can be stated that other impacts can also be distinguished, such as waterlogging, flood, drought, extreme storms, etc., that affect counties and other spatial levels in a different way. *Fig. 3* represents the total number of mentions of different climate-related impacts in climate strategies of county level. Increasing temperature, drought, and storms were mentioned in every stand-alone document, while changing precipitation patterns have been defined in the case of 16 strategies. Risks regarding flood and waterlogging are less emphasized due to geographical differences of counties.

After collecting and analyzing climate-related impacts in selected climate strategies, detailed evaluation regarding distinguished actions has been performed to reveal potential lacks and opportunities to improve the quality of climate strategies by bridging the gap between defined impacts and related actions. *Table 1* shows this relationship as mentioned earlier between impacts and defined actions in the case of every county and by using a three-step approach. Green cells refer to the best scenario, where a given climate impact is distinguished in the analyzed document; moreover, at least one dedicated action (related to the impact) is also developed. The light yellow color means that actions can be found in the given strategy without a previously defined impact. Dark orange cells represent the worst case when a given impact is previously distinguished and marked as an important challenge for the county; however, there is no developed action related to that significant risk. Finally, N/D means

there is neither impact(s) nor action(s) in the analyzed strategy. It can be seen that increasing temperature and drought are the two impacts, where all county documents defined them and assigned related actions as well. In the case of storms, some strategies distinguished as associated climate impacts, but related actions have not been developed (Baranya, Csongrád, Győr-Moson-Sopron, and Jász-Nagykun-Szolnok counties). Flood and waterlogging are the two most heterogeneous impacts due to their strong local-specific and geographic-related features. In the climate strategy of Hajdú-Bihar County, Nógrád County, and Vas County, dark orange cells refer to the lack of actions besides the defined challenges regarding flood, while waterlogging is a relevant adverse effect of climate change in Hajdú-Bihar, Nógrád, Somogy, Szabolcs-Szatmár-Bereg, and Zala counties, related actions have not been found in their documents.

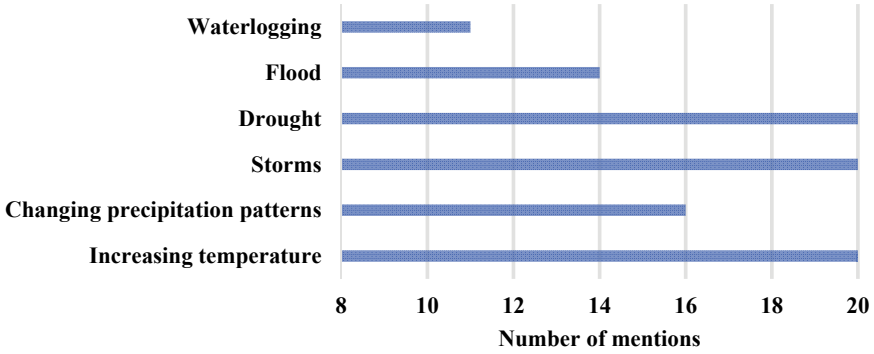

Fig. 3. Total number of mentions of climate-related impacts.

Considering adaptation issues through document analysis, distinguishing vulnerable social groups with regards to changing climate patterns and related weather extremes is a crucial component of effective climate strategies. For that purpose, *Fig. 4*. shows the total number of mentions of different vulnerable groups appearing in the selected and analyzed strategies on the county level. It can be stated that infants, elderly people, and people with cardiovascular disease are well involved in the documents as the most vulnerable social groups to heatwaves. People with disabilities have been mentioned in 8 of 20 documents; however, it is a much better inclusion compared to outdoor workers and poor people with only one mention. It cannot be found such a stand-alone document that took into consideration all of these vulnerable social groups: the majority of the strategies was focusing on the previously mentioned first three groups. Risks regarding outdoor workers appear in the climate strategy of Budapest, and poor

people were distinguished as a vulnerable societal dimension in the strategy of Tolna County. It is worth mentioning and emphasizing that the climate strategy of Vas County specified only one vulnerable social group (poor people) in the document.

Table 1. Pairs of climate-related impacts and dedicated actions

	Increasing temperature	Changing precip. patterns	Storms	Drought	Flood	Waterlogging
Bács-Kiskun County		N/D			N/D	
Baranya County					N/D	N/D
Békés County			N/D			N/D
Borsod-Abaúj-Zemplén County						
Budapest						N/D
Csongrád County						N/D
Fejér County					N/D	N/D
Győr-Moson-Sopron County						
Hajdú-Bihar County		N/D				
Heves County						
Jász-Nagykun-Szolnok County						
Komárom-Esztergom County						N/D
Nógrád County						
Pest County						
Somogy County						
Szabolcs-Szatmár-Bereg County						
Tolna County						
Vas County						N/D
Veszprém County					N/D	N/D
Zala County						

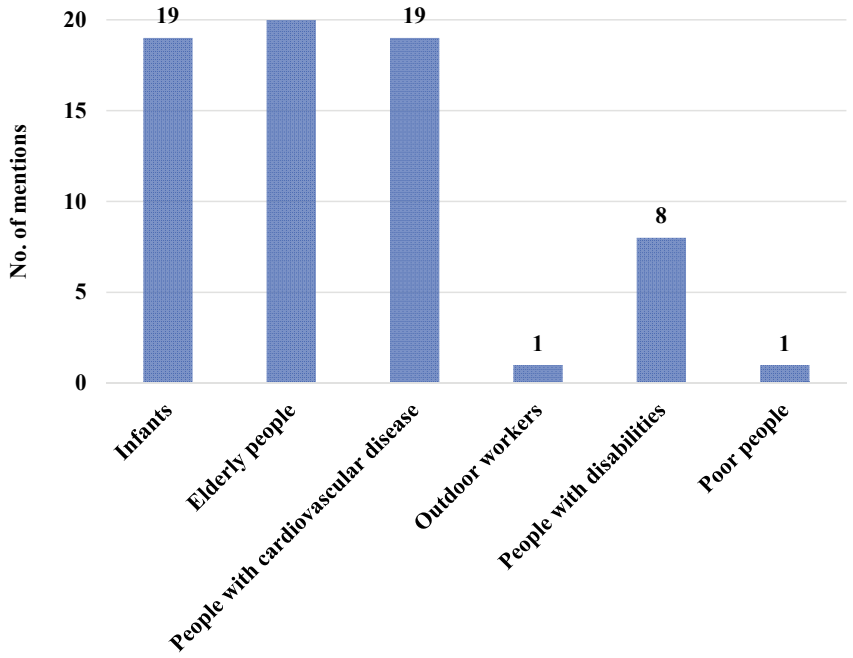

Fig. 4. Total number of mentions of vulnerable social groups.

Well-structured aims focusing on both existing and projected adverse effects of climate change are cornerstones of effective climate strategies. Based on this assumption, the following two sections are introducing the primary outcomes of our survey focusing on the aims regarding analyzed strategies. Firstly, *Fig. 5* represents the total number of mentions regarding whether a given sector is defined and distinguished through the adaptation aims in a given strategy or not. Based on the evaluation of the results, it can be stated that two main groups of sectors are appearing: in the first, pool, water management, agriculture, tourism, health, urban planning, and natural values are all well emphasized with between 17 and 20 mentions, respectively. However, forest fire, industry, transport, and energy supply are mentioned much less by the county-level climate strategies. It is worth emphasizing that the natural and social-based differences between counties entail different structures of aims and related sectors, but this gap, as mentioned earlier, between the two groups shall be emphasized.

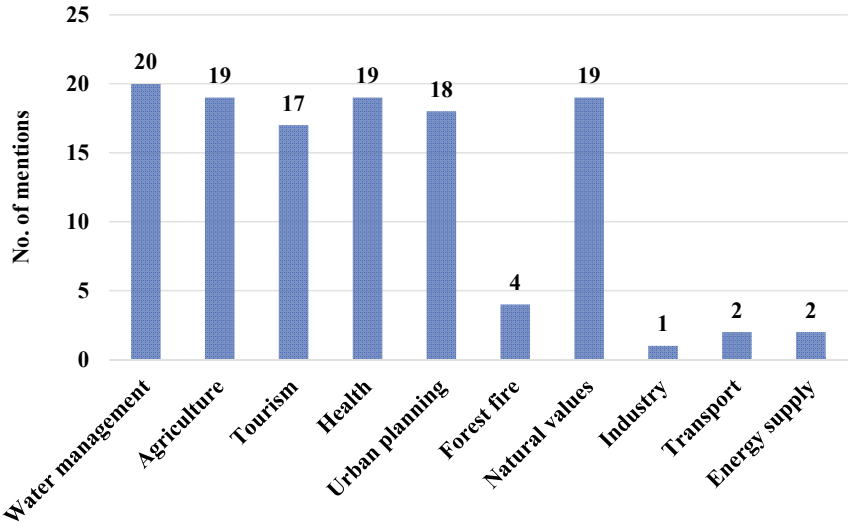

Fig. 5. Total number of mentions of sectors among the aims of climate strategies.

Developed and distinguished adaptation actions are crucial in the implementation phase and efficiently contribute to reducing the overall vulnerability of counties by covering as many critical issues as they can. Naturally, it cannot be declared that more adaptation actions entail less vulnerability in a linear relationship. However, complete with the previously introduced results, slightly more transparent conclusions can be made regarding the adaptation-oriented aim structure of the climate strategies of Hungarian counties. Therefore, *Fig. 6* aims at visualizing the total number of adaptation actions grouped by counties, respectively. Fejér and Komárom-Esztergom counties have the highest number of adaptation actions (with 25 and 19 actions), while the Baranya County Climate Strategy defined only five interventions. The average number of adaptation actions is approximately 11.

Besides the unquestionable importance of aims and their structure, evaluation of adaptation oriented interventions contributes to analyzing the county-level climate strategies more transparently. For that reason, our survey has a dedicated question about the main characteristics of interventions based on their types. The majority of climate strategies include technical solutions, policy tools, and awareness-raising projects, whit much less attention to education, financial tools, and research and development (R+D) actions. The presence of financial tools among adaptation actions is the least, only 5 of 20 climate strategies (Budapest, Nógrád County, Szabolcs-Szatmár-Bereg County, Veszprém County, and Zala County) have mentioned them as potential tools for improving adaptive capacity within the administrative borders.

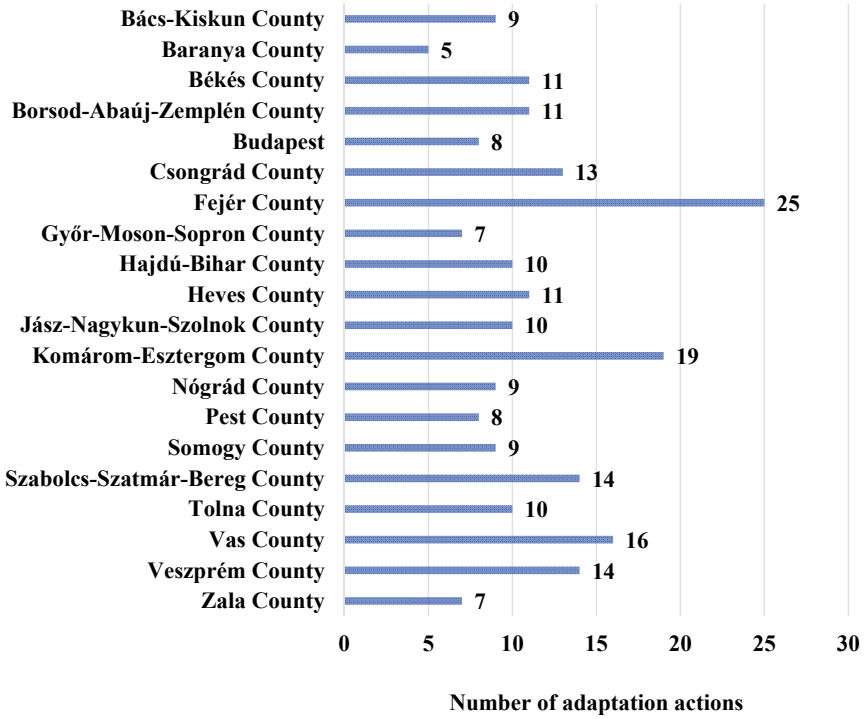

Fig. 6. Total number of adaptation actions in the analyzed climate strategies.

Monitoring phases in development strategies ensure the effectiveness of these documents by controlling and evaluating the processes which are needed to enhance climate adaptivity. In the case of Hungarian county-level climate change strategies, Jász-Nagykun-Szolnok and Vas counties' documents had nothing to do with the monitoring phase. On the opposite side, the vast majority of analyzed strategies have a comprehensive set of indicators, time frame, and budget allocation to enhance the effectiveness of their interventions. However, it shall be emphasized that preference order and responsibility issues have not been involved in the monitoring chapters at all. In a close context of the monitoring phase, the developed strategy-analysis survey has taken into consideration stakeholder inclusiveness during the preparation phase of the strategies. Only the Békés County Climate Strategy has not mentioned the list of involved stakeholders during the planning procedure, while the majority of climate strategies listed numerous NGOs, universities, public authorities, companies and other economic and social actors who were active contributors to the development of the county-level climate change strategies.

Finally, the last evaluated aspects regarding the strategies are the length of mitigation and adaptation-oriented pages. It is worth repeatedly emphasizing that the total length of adaptation-centered content is not closely related to its effectiveness, but an overview can be made by using this information about the strategies. *Fig. 7* summarizes the relative share of mitigation and adaptation-related contents in the face of the total length of the strategies in descending order. It means that the relatively lengthiest adaptation part of climate strategies can be found in the case of Vas County with 39%, while the shortest adaptation-oriented sections can be read in the Jász-Nagykun-Szolnok County Climate Change Strategy. It shall be emphasized that the majority of strategies have paid more attention to adaptation issues (except Szabolcs-Szatmár-Bereg County and Somogy County), which is related to a clear trend of shifting the main intervention points from mitigation actions to adaptation ones in the international policy-making processes. The role of industry, transport, and energy supply concerning improvement of adaptive capacity is clear, however, these sectors were barely specified in the county-level strategies.

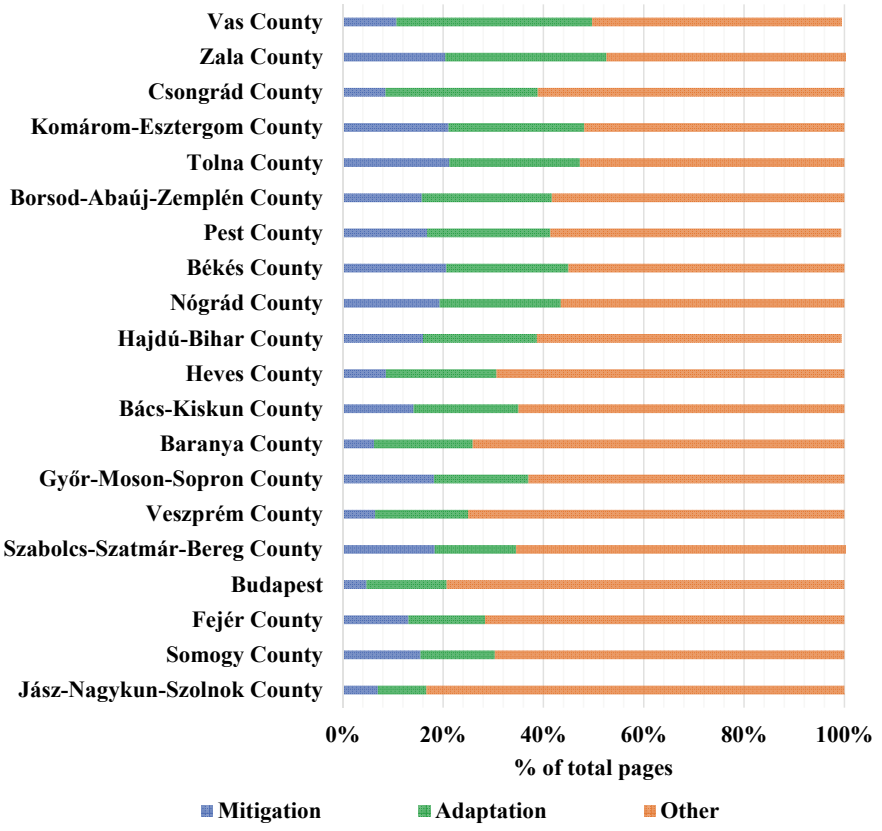

Fig. 7. Relative share of adaptation- and mitigation-oriented contents in the strategies.

There are 19 county seats on LAU-1 level in Hungary. Out of the 19 cities, 63% have accepted some type of climate-related strategic or planning document. These documents were involved into the in-depth evaluation process considering the same questionnaire as in case of the counties and the capital. Two main types of documents can be found on this level, one of them is urban climate strategy, the other one is Sustainable Energy and Climate Plan (SECAP). 62% of the county seats have SECAPs and the other 38% goes for the urban climate strategy. According to the year of the document developments it can be seen, that the oldest and still existing one was accepted in 2007, that is the urban climate strategy of Tatabánya. This county seat is a founding member city of the Climate-friendly Municipality Association and was among the first three cities in Hungary which worked out urban climate strategy. The latest climate strategy, that belongs to the county seat of Miskolc, was accepted in 2017. The 8 SECAPs has been developed between 2017 and 2019. Only 23% of the evaluated documents have some existing history in the form of a planning document that is related to climate approach. A bit more than half of the examined documents includes paragraphs or chapters that are dealing with some general climate-related outlook on global, regional, or local level. It puts the climate change approach into context and provides a good background for easier understanding for the reader.

The absolute numbers of area-specific impacts are shown in the *Fig. 8*. All of the three types so the observed changes, the present impacts and the future projections are well represented in the examined documents. The most popular were the projection for the future. These information can be descriptive enough for decision makers or local residents as well.

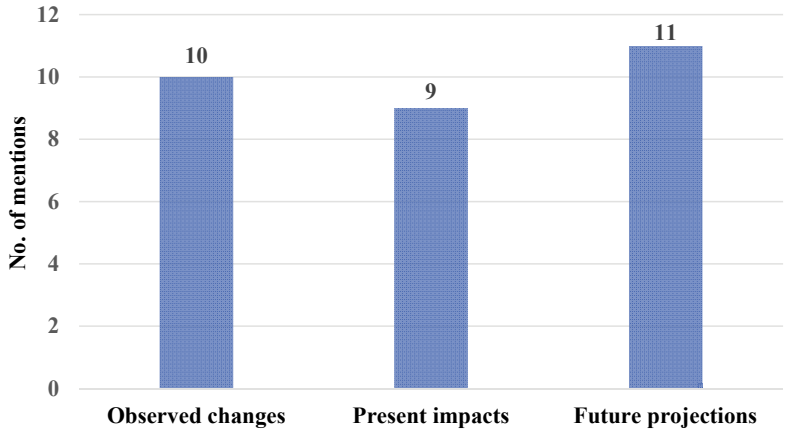

Fig. 8. Absolute number of mentions of area-specific impacts based on identified local characteristics (county seats).

There are mentioned a wide range of climate-related impacts in the evaluated county seat documents, as can be seen in *Fig. 9*. The three most significant impacts are the temperature increase, the changing of the precipitation patterns and floods. Droughts, floods, forest fires belong to the next group based on the number of mentions. On the county seat level, the emphasis of local features may justify this diversity.

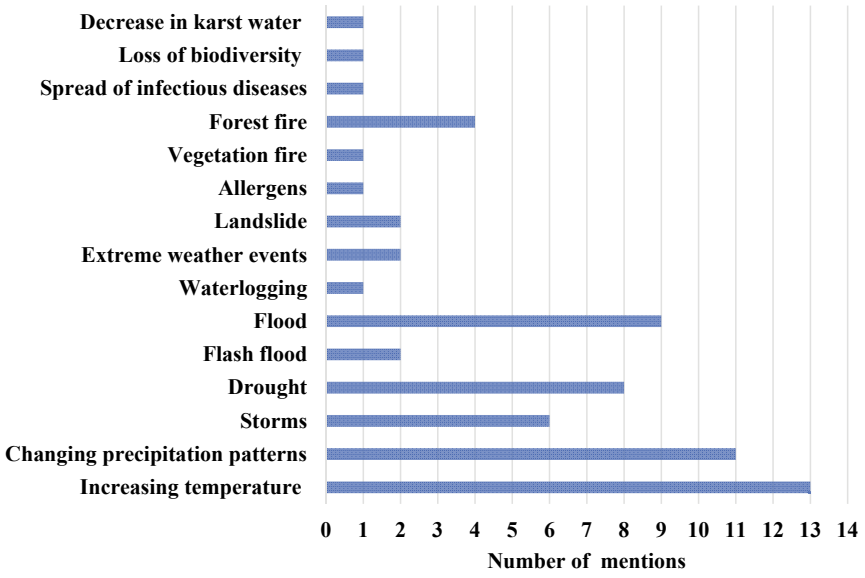

Fig. 9. Total number of mentions of climate-related impacts (county seats).

As was mentioned previously, according to the methodology, the next step is to check and analyze the consistency of the evaluated documents considering climate-related impacts and dedicated actions. *Table 2* shows the results of this evaluation in case of county seats with SECAPs. There is not any action without impact. The significant proportion of the non-defined category is apparent. The existence or the lack of adaptation aims is independent of the date of the document development or assessment. Due to the requirements of the Covenant of Mayors for SECAPs, it is necessary to deal with the strengths and weaknesses of a territory, develop risk and vulnerability assessments that can allow convenient adaptation strategy development that can be converted into SECAP's actions.

The latest climate strategy was accepted in 2017 by the representative body of the municipality of Miskolc. However, not that document shows the best interrelations concerning climate-related impacts and adaptation actions. The

best results, according to the consistency evaluation, can be seen related to the county seat of Eger that is shown in *Table 3*. This document was developed in 2012. The lack of knowledge transfer can be seen related to other cities.

Table 2. Climate-related impacts and dedicated actions in county seat SECAPs

	Debrecen	Dunaújváros	Kaposvár	Salgótarján	Szeged	Szolnok	Veszprém	Zalaegerszeg
Increasing temperature								
Changing precipitation patterns		N/D						
Storms	N/D		N/D	N/D				N/D
Drought				N/D				N/D
Flash flood	N/D	N/D			N/D	N/D	N/D	N/D
Flood								N/D
Waterlogging		N/D	N/D	N/D	N/D	N/D	N/D	N/D
Extreme weather events	N/D	N/D	N/D	N/D	N/D		N/D	N/D
Landslide	N/D		N/D	N/D	N/D	N/D		N/D
Allergens	N/D		N/D	N/D	N/D	N/D	N/D	N/D
Vegetation fire	N/D	N/D	N/D	N/D	N/D		N/D	N/D
Forest fire	N/D	N/D	N/D	N/D	N/D	N/D	N/D	N/D
Spread of infectious diseases	N/D		N/D	N/D	N/D	N/D	N/D	N/D
Loss of biodiversity	N/D	N/D	N/D	N/D	N/D	N/D	N/D	
Decrease in karst water	N/D	N/D	N/D	N/D	N/D	N/D	N/D	N/D

N/D	non-defined
	impact and action(s)
	action(s) without impact
	impact without action(s)

Table 3. Climate-related impacts and dedicated actions in county seat climate strategies

	Eger	Miskolc	Szekszárd	Szombathely	Tatabánya
Increasing temperature					
Changing precipitation patterns					
Storms		N/D		N/D	N/D
Drought			N/D		N/D
Flash flood	N/D	N/D	N/D	N/D	N/D
Flood			N/D		N/D
Waterlogging	N/D	N/D	N/D	N/D	N/D
Extreme weather events		N/D	N/D	N/D	N/D
Landslide	N/D	N/D	N/D	N/D	N/D
Allergens	N/D	N/D	N/D	N/D	N/D
Vegetation fire	N/D	N/D	N/D	N/D	N/D
Forest fire		N/D		N/D	
Spread of infectious diseases	N/D	N/D	N/D	N/D	N/D
Loss of biodiversity	N/D	N/D	N/D	N/D	N/D
Decrease in karst water	N/D		N/D	N/D	N/D

N/D	non-defined
	impact and action(s)
	action(s) without impact
	impact without action(s)

Altogether 3 examined document deals with the vulnerable social groups despite the importance of this aspect in adaptation planning and concerning adaptation pathways. These documents mention as vulnerable social groups, the infants and younger children, the elderly population, and people with chronic cardiovascular disease.

Almost half of the evaluated documents do not define any sector related to adaptation aims (see *Fig. 10*). The most emphasized sector among the adaptation aims is water management due to its unpredictability and importance according to living standards, quality of life, and sustainability. The same importance was given to the following four as agriculture, health, energy industry, and urban planning. These are followed by transport, tourism, nature conservation, and finally, waste and disaster management can be found in the chart.

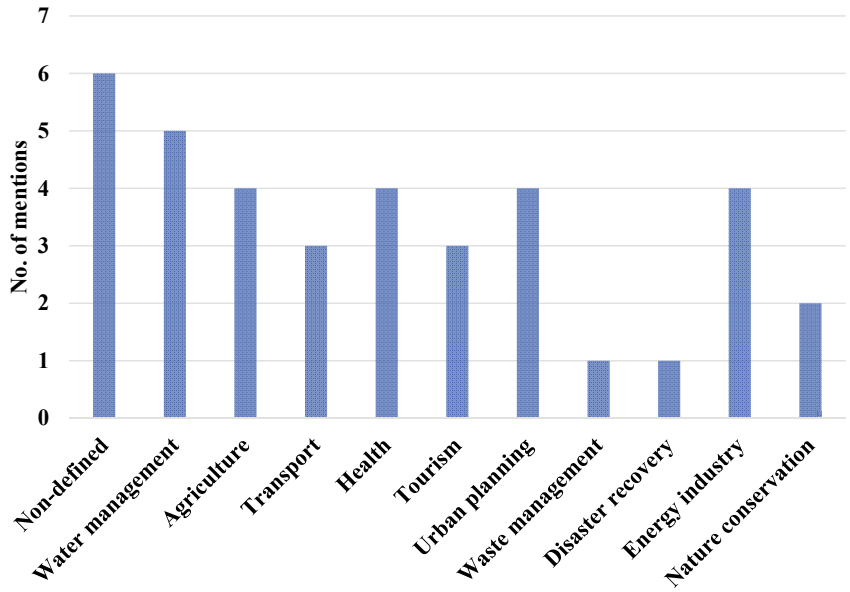

Fig. 10. Total number of mentions of sectors among the aims of examined county seat level documents.

Based on the evaluation of the 13 climate-related strategic documents on the county seat level, it can be seen that in the case of 69% of the examined documents, the overall lack of adaptation aims can be stated. Thus, only 31% of the documents discuss some details according to the adaptation aims.

Fig. 11 gives an overview of the adaptation actions and shows the high percentage of the non-defined category. The core actions belong to the technical solution or awareness-raising, followed by education and policy-related actions.

Only 31% of the evaluated documents gives at least a general overview, according to monitoring. In two cases, indicators and timeframe were also mentioned as necessary parts of the monitoring phase. None of the evaluated document mentions the importance and meaning of partnership. Only four cases deal with an open discussion about the planned document with different local actors and stakeholders.

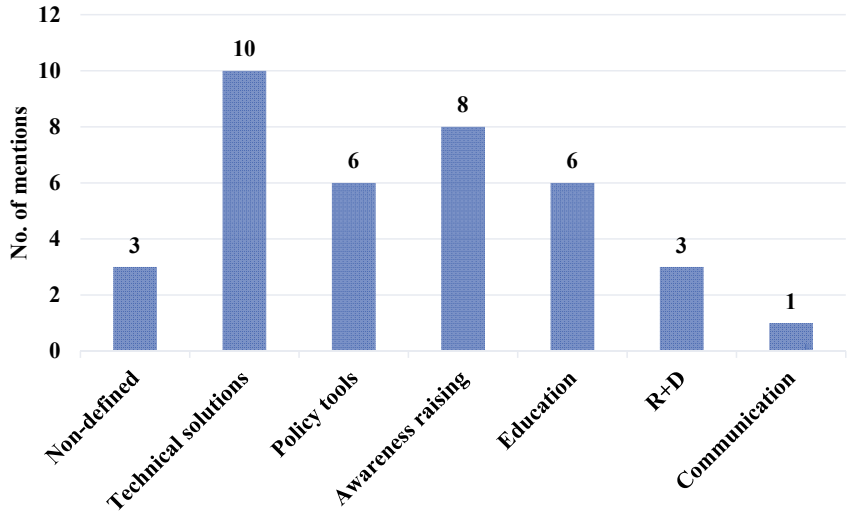

Fig. 11. Total number of mentions of adaptation actions among the aims of examined county seat level documents.

According to *Fig. 12* on the county seat level, the representation of the relative share of adaptation and mitigation-oriented content can be seen. Clearly, the least represented approach is an adaptation to climate change despite the importance of this kind of activities, interventions, and tools in order to support the transition towards sustainable regional development. The most adaptation-focused documents were formulated in Szeged and Dunaújváros, that is followed in the row by Tatabánya, Szekszárd, Eger, Salgótarján. There is a complete lack of adaptation content that can be found in the case of Debrecen.

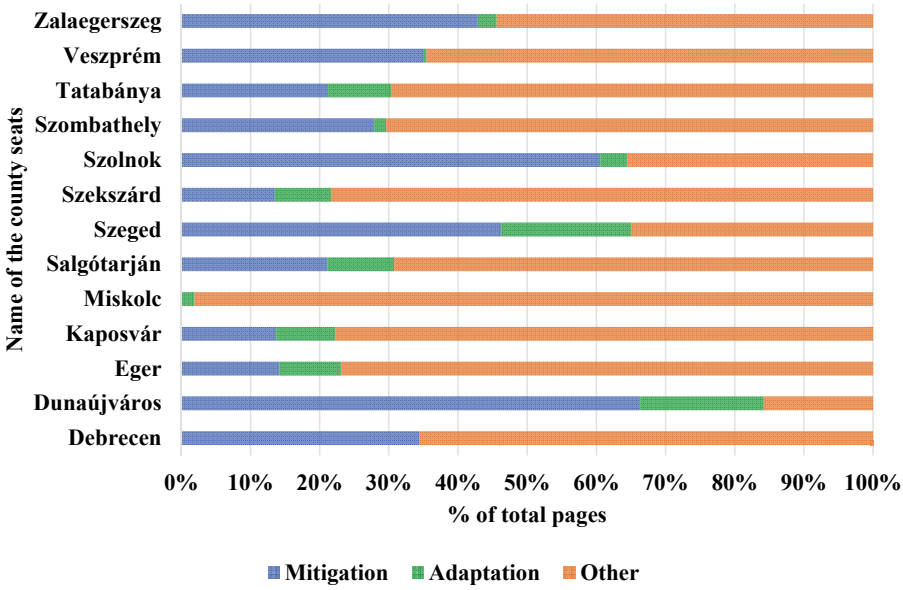

Fig. 12. Relative share of adaptation- and mitigation-oriented content in the examined documents.

4. Conclusion

The Hungarian counties made an unquestionably enormous effort by developing their climate change strategies during the past years. Content analysis of documents revealed their complexity and heterogeneity; however, a strict methodological guideline developed by the Alliance of Climate-friendly Settlements were available. The survey applied for identifying key strengths and weaknesses of climate change strategies on the county level was a crucial part of this process and entailed to define several further recommendations. Firstly, it shall be emphasized that county-level climate change strategies cover all of the relevant climate-related impacts regarding both the present and future. Nevertheless, after a detailed analysis of actions, it can be stated that best practices regarding the planning phase in terms of impacts-actions pairs are severely limited, since numerous climate strategies can be found in which relevant impacts were mentioned without any related actions or vice versa. Vulnerable social groups are also defined and introduced by the analyzed documents. However, it is worth mentioning that the inclusiveness of vulnerable people is weak: outdoor workers, people with disabilities, and poor people have not been taken into consideration in an emphasized way regardless of their vulnerability to changing climatic patterns.

A further weakness of strategy-making processes can be characterized by paying attention to the outcomes of content analysis regarding the number of mentions of different sectors through the adaptation-oriented goals. From the planning perspective, diversification of tools regarding the implementation of actions is crucial to enhance the effectiveness of a given strategy. The majority of climate strategies include technical solutions, policy tools, and awareness-raising projects, with much less attention to education, financial tools, and R+D actions. Besides the lack of given types of actions, some deficiencies concerning the monitoring phase have also been characterized: a complete lack of contents regarding priorities between aims and goals and of responsibilities during the implementation phase. Last but not least, the share of adaptation-related content varies significantly from 39% (Vas County) to 10% (Jász-Nagykun-Szolnok County) that represents a significant heterogeneity in terms of the relative importance of adaptation issues in a given strategy. It cannot be stated clearly that lengthy adaptation contents are related to an improved quality of strategies; however, it shall be declared that paying more attention to climate adaptation issues is in parallel with EU-level activities nowadays and the near future.

Considering climate planning documents on the county seat (LAU-1) level, more diverse and heterogeneous results can be seen compared to the county level. This heterogeneity of adaptation issues can be found both in the evaluated climate change-related strategies and SECAPs in the case of the Hungarian county seats. Based on our in-depth evaluation of this level, according to adaptation in several cases, the lack of the appropriate planning document is the most striking. This diversity visible, for example, in the case of climate-related impacts. On county seat level, the planned adaptation aims, related sectors, and actions are significantly underrepresented in the evaluated documents. The monitoring phase can also be seen as a crucial point in further developments for an adaptive future on different spatial levels.

Acknowledgements: The research reported in this paper was supported by the Higher Education Excellence Program of the Ministry of Human Capacities in the frame of the Water sciences & Disaster Prevention research area of the Budapest University of Technology and Economics (BME FIKP-VÍZ).

References

Bartholy, J., Radics, K., and Bohoczky, F., 2003: Present state of wind energy utilisation in Hungary: Policy, wind climate, and modelling studies. *Renew. Sustain. Energy Rev. 7*, 175–186. https://doi.org/10.1016/S1364-0321(03)00003-0

Bartholy, J., Pongrácz, R., and *Gelybó, G.Y.*, 2007: Regional climate change expected in Hungary for 2071-2100. *Appl. Ecol. Environ. Res. 5*, 1–17. https://doi.org/10.15666/aeer/0501_001017

Bartholy, J., Pongracz, R., Torma, C., Pieczka, I., Kardos, P., and *Hunyady, A.*, 2009: Analysis of regional climate change modelling experiments for the Carpathian Basin. *Int. J. Glob. Warming 1*, 238–252. https://doi.org/10.1504/IJGW.2009.027092

Bellinson, R. and *Chu, E.*, 2019: Learning pathways and the governance of innovations in urban climate change resilience and adaptation. *J. Environ. Policy Planning*, *21*, 76–89. https://doi.org/10.1080/1523908X.2018.1493916

Berkhout, F., Bouwer, L.M., Bayer, J., Bouzid, M., Cabeza, M., Hanger, S., Hof, A., Hunter, P., Meller, L., Patt, A., Pfluger, B., Rayner, T., Reichardt, K., and *van Teeffelen, A.*, 2015: European policy responses to climate change: progress on mainstreaming emissions reduction and adaptation. *Reg. Environ. Change 15*, 949–959. https://doi.org/10.1007/s10113-015-0801-6

Blanka, V., Mezosi, G., and *Meyer, B.*, 2013: Projected changes in the drought hazard in Hungary due to climate change. *Időjárás 117*, 219–237.

Bobvos, J., Fazekas, B., and *Páldy, A.*, 2015: Assessment of heat-related mortality in budapest from 2000 to 2010 by different indicators. *Időjárás*, *119*, 143–158.

Buzási, A., 2014: Will Budapest be a climate-resilient city? - Adaptation and mitigation challenges and opportunities in development plans of Budapest. *Eur. J.Sustain. Develop. 3*, 277–288. https://doi.org/10.14207/ejsd.2014.v3n4p277

Castán Broto, V., 2017: Urban Governance and the Politics of Climate change. *World Develop. 93*, 1–15. https://doi.org/10.1016/j.worlddev.2016.12.031

European Commission, 2011: A Roadmap for moving to a competitive low carbon economy in 2050.

Csete, M. and *Horváth, L.*, 2012: Sustainability and green development in urban policies and strategies. *Appl. Ecol. Environ. Res. 10*, 185–194. https://doi.org/10.15666/aeer/1002_185194

Csete, M., Pálvölgyi, T., and *Szendrő, G.*, 2013: Assessment of climate change vulnerability of tourism in Hungary. *Reg. Environ. Change 13*, 1043–1057. https://doi.org/10.1007/s10113-013-0417-7

Csete, M. and *Szécsi, N.*, 2015: The role of tourism management in adaptation to climate change – a study of a European inland area with a diversified tourism supply. *J. Sustain. Tourism 23*, 477–496. https://doi.org/10.1080/09669582.2014.969735

Csete, M. and *Buzási, A.*, 2016: Climate-oriented assessment of main street design and development in Budapest. *J. Environ. Engineer. Landscape Manage. 24*, 258–268. https://doi.org/10.3846/16486897.2016.1185431

Czakó, V., 2013: Drowning the suburb: settlement planning and climate change adaptation in a Hungarian metropolitan area. *Urban Res. Practice 6*, 95–109. https://doi.org/10.1080/17535069.2012.762221

Eckersley, P., England, K., and *Ferry, L.*, 2018: Sustainable development in cities: collaborating to improve urban climate resilience and develop the business case for adaptation. *Publ. Money Management*, *38*, 335–344. https://doi.org/10.1080/09540962.2018.1477642

Gaál, M., Quiroga, S., and *Fernandez-Haddad, Z.*, 2014: Potential impacts of climate change on agricultural land use suitability of the Hungarian counties. *Reg. Environ. Change 14*, 597–610. https://doi.org/10.1007/s10113-013-0518-3

Heidrich, O., Dawson, R.J., Reckien, D., and *Walsh, C.L.*, 2013: Assessment of the climate preparedness of 30 urban areas in the UK. *Climatic Change*, *120*, 771–784. https://doi.org/10.1007/s10584-013-0846-9

Heidrich, O., Reckien, D., Olazabal, M., Foley, A., Salvia, M., de Gregorio Hurtado, S., Orru, H., Flacke, J., Geneletti, D., Pietrapertosa, F., Hamann, J.J.P., Tiwary, A., Feliu, E., and *Dawson, R.J.*, 2016: National climate policies across Europe and their impacts on cities strategies. *J. Environ. Manage. 168*, 36–45. https://doi.org/10.1016/j.jenvman.2015.11.043

Hlásny, T., Mátyás, C., Seidl, R., Kulla, L., Merganičová, K., Trombik, J., Dobor, L., Barcza, Z., and *Konôpka, B.*, 2014: Climate change increases the drought risk in Central European forests: What are the options for adaptation? *Forestry J. 60*, 5–18. https://doi.org/10.2478/forj-2014-0001

Hrabovszky-Horváth, S., Pálvölgyi, T., Csoknyai, T., and *Talamon, A.*, 2013: Generalized residential building typology for urban climate change mitigation and adaptation strategies: The case of Hungary. *Energy and Build. 62*, 475–485. https://doi.org/10.1016/j.enbuild.2013.03.011

Hunt, A. and *Watkiss, P.*, 2011: Climate change impacts and adaptation in cities: A review of the literature. *Climatic Change 104*, 13–49. https://doi.org/10.1007/s10584-010-9975-6

Jolánkai, M. and *Birkás, M.*, 2007: Global climate change impacts on crop production in Hungary. *Agric. Conspectus Scientificus 72*, 17–20.

Kántor, N., Chen, L., and *Gál, C. V.*, 2018: Human-biometeorological significance of shading in urban public spaces—Summertime measurements in Pécs, Hungary. *Landscape Urban Plann. 170*, 241–255. https://doi.org/10.1016/j.landurbplan.2017.09.030

Kern, K., 2019: Cities as leaders in EU multilevel climate governance: embedded upscaling of local experiments in Europe. *Environ. Politics 28*, 125–145. https://doi.org/10.1080/09644016.2019.1521979

Kis, A., Pongrácz, R., and *Bartholy, J.*, 2017: Multi-model analysis of regional dry and wet conditions for the Carpathian Region. *Int. J Climatol 37*, 4543–4560. https://doi.org/10.1002/joc.5104

Kovács, A., and Unger, J., 2014: Analysis of the tourism climatic conditions in Hungary concerning the subjective thermal sensation characteristics of the south-hungarian resident, Acta Climatologics et chorologica *47–48*, 77–84.

Kovács, A., Németh, Á., Unger, J., and *Kántor, N.*, 2017: Tourism climatic conditions of Hungary – present situation and assessment of future changes Attila. *Időjárás 121*, 79–99.

Krüzselyi, I., Bartholy, J., Horányi, A., Pieczka, I., Pongrácz, R., Szabó, P., Szépszó, G., and *Torma, C.*, 2011: The future climate characteristics of the Carpathian Basin based on a regional climate model mini-ensemble. *Adv. Sci. Res. 6*, 69–73. https://doi.org/10.5194/asr-6-69-2011

Li, S., Juhász-Horváth, L., Harrison, P.A., Pintér, L., and *Rounsevell, M.D.A.*, 2017a: Relating farmer's perceptions of climate change risk to adaptation behaviour in Hungary. *J. Environ.Management*, *185*, 21–30. https://doi.org/10.1016/j.jenvman.2016.10.051

Li, S., Juhász-Horváth, L., Pedde, S., Pintér, L., Rounsevell, M.D.A., and *Harrison, P.A.*, 2017b: Integrated modelling of urban spatial development under uncertain climate futures: A case study in Hungary. *Environ. Model. Software 96*, 251–264. https://doi.org/10.1016/j.envsoft.2017.07.005

Li, S., Juhász-Horváth, L., Pintér, L., Rounsevell, M.D.A., and *Harrison, P.A.*, 2018: Modelling regional cropping patterns under scenarios of climate and socio-economic change in Hungary. *Sci. Total Environ. 622–623*, 1611–1620. https://doi.org/10.1016/j.scitotenv.2017.10.038

Lóczy, D., 2010: Flood hazard in Hungary: A re-assessment. *Centr. Eur. J. Geosci. 2*, 537–547. https://doi.org/10.2478/v10085-010-0029-0

Malatinszky, Á., Ádám, S., Falusi, E., Saláta, D., and *Penksza, K.*, 2013: Climate change related land use problems in protected wetlands: A study in a seriously affected Hungarian area. *Climatic Change 118*, 671–682. https://doi.org/10.1007/s10584-012-0689-9

Mendizabal, M., Heidrich, O., Feliu, E., García-Blanco, G., and *Mendizabal, A.*, 2018: Stimulating urban transition and transformation to achieve sustainable and resilient cities. *Renew. Sustain. Energy Rev. 94*, 410–418. https://doi.org/10.1016/j.rser.2018.06.003

Mezösi, G., Meyer, B.C., Loibl, W., Aubrecht, C., Csorba, P., and Bata, T., 2013: Assessment of regional climate change impacts on Hungarian landscapes. *Reg. Environ. Change 13*, 797–811. https://doi.org/10.1007/s10113-012-0326-1

Mezősi, G., Bata, T., Meyer, B.C., Blanka, V., and *Ladányi, Z.*, 2014: Climate Change Impacts on Environmental Hazards on the Great Hungarian Plain, Carpathian Basin. *Int. J. Disaster Risk Sci. 5*, 136–146. https://doi.org/10.1007/s13753-014-0016-3

Millard-Ball, A., 2013: The Limits to Planning: Causal Impacts of City Climate Action Plans. *J. Planning Educ. Res. 33*, 5–19. https://doi.org/10.1177/0739456X12449742

Páldy, A., Bobvos, J., Vámos, A., Kovats, R.S., and *Hajat, S.*, 2005: The Effect of Temperature and Heat Waves on Daily Mortality in Budapest, Hungary, 1970 - 2000, In: (eds. *Kirch, W., Bertollini, R.*, and *Menne, B*.) Extreme Weather Events and Public Health Responses. Springer Berlin Heidelberg, Berlin, Heidelberg, 99–107. https://doi.org/10.1007/3-540-28862-7_10

Páldy, A., and *Bobvos, J.*, 2010: Health Impacts of Heat Waves of 2007 in Hungary -- Background and Experiences, In: Global Warming: Engineering Solutions (eds. Dincer, I., Hepbasli, A., Midilli, A., and Karakoc, T.H.). Springer US, Boston, MA, 629–642. https://doi.org/10.1007/978-1-4419-1017-2_44

Pietrapertosa, F., Khokhlov, V., Salvia, M., and *Cosmi, C.*, 2018: Climate change adaptation policies and plans: A survey in 11 South East European countries. *Renew. Sustain. Energy Rev. 81*, 3041–3050. https://doi.org/10.1016/j.rser.2017.06.116

Pongrácz, R., Bartholy, J., and *Bartha, E.B.*, 2013: Analysis of projected changes in the occurrence of heat waves in Hungary. *Adv. Geosci. 35*, 115–122. https://doi.org/10.5194/adgeo-35-115-2013

Pongrácz, R., Bartholy, J., and *Kis, A.*, 2014: Estimation of future precipitation conditions for Hungary with special focus on dry periods. *Időjárás 118*, 305–321.

Reckien, D., Flacke, J., Dawson, R.J., Heidrich, O., Olazabal, M., Foley, A., Hamann, J.J.P., Orru, H., Salvia, M., de Gregorio Hurtado, S., Geneletti, D., and *Pietrapertosa, F.*, 2014: Climate change response in Europe: What's the reality? Analysis of adaptation and mitigation plans from 200 urban areas in 11 countries. *Climatic Change*, *122*, 331–340. https://doi.org/10.1007/s10584-013-0989-8

Reckien, D., Flacke, J., Olazabal, M., and *Heidrich, O.*, 2015: The influence of drivers and barriers on urban adaptation and mitigation plans-an empirical analysis of European Cities. *PLoS ONE 10*, 1–21. https://doi.org/10.1371/journal.pone.0135597

Reckien, D., Salvia, M., Heidrich, O., Church, J.M., Pietrapertosa, F., De Gregorio-Hurtado, S., D'Alonzo, V., Foley, A., Simoes, S.G., Krkoška Lorencová, E., Orru, H., Orru, K., Wejs, A., Flacke, J., Olazabal, M., Geneletti, D., Feliu, E., Vasilie, S., Nador, C., Krook-Riekkola, A., Matosović, M., Fokaides, P.A., Ioannou, B.I., Flamos, A., Spyridaki, N.A., Balzan, M. V., Fülöp, O., Paspaldzhiev, I., Grafakos, S., and *Dawson, R.*, 2018: How are cities planning to respond to climate change? Assessment of local climate plans from 885 cities in the EU-28. *J. Cleaner Product 191*, 207–219. https://doi.org/10.1016/j.jclepro.2018.03.220

Reckien, D., Salvia, M., Pietrapertosa, F., Simoes, S.G., Olazabal, M., De Gregorio Hurtado, S., Geneletti, D., Krkoška Lorencová, E., D'Alonzo, V., Krook-Riekkola, A., Fokaides, P.A., Ioannou, B.I., Foley, A., Orru, H., Orru, K., Wejs, A., Flacke, J., Church, J.M., Feliu, E., Vasilie, S., Nador, C., Matosović, M., Flamos, A., Spyridaki, N.A., Balzan, M. V., Fülöp, O., Grafakos, S., Paspaldzhiev, I., and *Heidrich, O.*, 2019: Dedicated versus mainstreaming approaches in local climate plans in Europe. *Renew. Sustain. Energy Rev. 112*, 948–959. https://doi.org/10.1016/j.rser.2019.05.014

Rojas, R., Feyen, L., and *Watkiss, P.*, 2013: Climate change and river floods in the European Union: Socio-economic consequences and the costs and benefits of adaptation. *Glob. Environ. Change*, *23*, 1737–1751. https://doi.org/10.1016/j.gloenvcha.2013.08.006

Rosenzweig, C., Solecki, W., Hammer, S.A., and *Mehrotra, S.*, 2010: Cities lead the way in climate-change action. *Nature 467*, 909–911. https://doi.org/10.1038/467909a

Sharifi, A. and *Yamagata, Y.*, 2016: Principles and criteria for assessing urban energy resilience: A literature review. *Renew. Sustain. Energy Rev. 60*, 1654–1677. https://doi.org/10.1016/j.rser.2016.03.028

Solymosi, N., Torma, C., Kern, A., Maróti-Agóts, Á., Barcza, Z., Könyves, L., Berke, O., and *Reiczigel, J.*, 2010: Changing climate in Hungary and trends in the annual number of heat stress days. *International J. Biometeorol. 54*, 423–431. https://doi.org/10.1007/s00484-009-0293-5

Szabó, B., Vincze, E., and *Czúcz, B.*, 2016: Flowering phenological changes in relation to climate change in Hungary. *Int. J. Biometeorol. 60*, 1347–1356. https://doi.org/10.1007/s00484-015-1128-1

Szendrő, G., Csete, M., and *Török, Á.*, 2014: The sectoral adaptive capacity index of Hungarian road transport. *Periodica Polytechnica Social Manage. Sci. 22*, 99–106. https://doi.org/10.3311/PPso.7377

Szépszó, G., 2008: Regional change of climate extremes over Hungary based on different regional climate models of the PRUDENCE project. *Időjárás 112*, 265–284.

Szlávik, J. and *Csete, M.*, 2012: Climate and energy policy in Hungary. *Energies 5*, 494–517. https://doi.org/10.3390/en5020494

Tánczos, K. and *Török, A.*, 2007: The linkage between climate change and energy consumption of hungary in the road transportation sector. *Transport 22*, 134–138. https://doi.org/10.3846/16484142.2007.9638111

Torma, C., Coppola, E., Giorgi, F., Bartholy, J., and *Pongrácz, R.*, 2011: Validation of a high-resolution version of the regional climate model RegCM3 over the Carpathian basin. *J.Hydrometeorol. 12*, 84–100. https://doi.org/10.1175/2010JHM1234.1

Törő, K., Bartholy, J., Pongrácz, R., Kis, Z., Keller, É., and *Dunay, G.*, 2010: Evaluation of meteorological factors on sudden cardiovascular death. *J. Forensic Legal Medic. 17*, 236–242. https://doi.org/10.1016/j.jflm.2010.02.008

UNFCCC, 2015: Adoption of the Paris agreement.

Ürge-Vorsatz, D., Rosenzweig, C., Dawson, R.J., Sanchez Rodriguez, R., Bai, X., Salisu Barau, A., Seto, K.C., and *Dhakal, S.*, 2018: Locking in positive climate responses in cities Adaptation-

mitigation interdependencies. *Nat. Climate Change 8*, 174–185. https://doi.org/10.1038/s41558-018-0100-6

Wamsler, C., Brink, E., and Rivera, C., 2013: Planning for climate change in urban areas: From theory to practice. *J. Cleaner Product. 50*, 68–81. https://doi.org/10.1016/j.jclepro.2012.12.008

Werners, S.E., Flachner, Z., Matczak, P., Falaleeva, M., and *Leemans, R.*, 2009: Exploring earth system governance: A case study of floodplain management along the Tisza river in Hungary. *Global Environmental Change*, *19*, 503–511. https://doi.org/10.1016/j.gloenvcha.2009.07.003

Zemankovics, M.H., 2012: Mitigation and adaptation to climate change in Hungary. *J. Central Eur. Agricult. 13*, 58–72. https://doi.org/10.5513/JCEA01/13.1.1015

DOI:10.28974/idojaras.2020.2.7

IDŐJÁRÁS

Quarterly Journal of the Hungarian Meteorological Service
Vol. 124, No. 2, April – June, 2020, pp. 277–297

Validating AquaCrop model for rainfed and irrigated maize and soybean production in eastern Croatia

Monika Marković[1*], **Marko Josipović**[2], **Milena Jančić Tovjanin**[3], **Vladimir Đurđević**[4], **Marija Ravlić**[1], and **Željko Barač**[1]

[1]*University of Josip Juraj Strossmayer in Osijek*
Faculty of Agrobiotechnical sciences Osijek
Vladimira Preloga 1, Osijek, Croatia

[2]*Agricultural Institute*
Južno predgrađe 17, Osijek, Croatia

[3]*University of Novi Sad*
Faculty of Agriculture
Novi Sad, Serbia

[4]*University of Belgrade*
Faculty of Physics
Institute of Meteorology
Dobracina 16, Beograd, Serbia

**Corresponding Author e-mail: monika.markovic@fazos.hr*

(Manuscript received in final form April 30, 2019)

Abstract— In this study, the AquaCrop model was used to quantify climate change impact on yield and net irrigation in maize and soybean production. Daily observed climate data (1961–1990) from Osijek weather station were used for past climate simulation, and output data from ECHAM model were dynamically downscaled under two IPCC SRES scenarios (A1B, A2) for two integration periods 2041–2070 and 2071–2100. The soil properties and crop data were presented from 6-year-long (2010–2015) field study of the Agricultural Institute in Osijek, Osijek-Baranja County. The climate results showed expected rise in air temperature up to 5 ºC and significantly lower precipitation up to 43.5%. According to results from the AquaCrop model, there is no change in maize yield in non-irrigated conditions, while in irrigated conditions there is a yield increase of 1.4 t ha^{-1} of dry matter (dm), with 80 mm higher net irrigation in comparison with the 1961–1990 period. As for soybean production, the increase in yield is expected in both non-irrigated and irrigated conditions. The yield increases up to 1.9 dm t ha^{-1} in irrigated conditions with 90 mm higher net irrigation in comparison with the 1961–1990 period. As for crop water indices, in non-irrigated conditions the water use efficiency (*WUE*) has a trend to decrease in the future, while in irrigated conditions it can slightly increase. Irrigation water use efficiency (*IWUE*) showed significantly higher increase in irrigated maize and soybean production.

Key-words: climate change, maize, soybean, yield, net irrigation, water efficiency

1. Introduction

Farms in Croatia can be characterized as considerably smaller than the EU average (14.4 ha) considering that the average farm size is 5.6 ha per holding, where one half of holdings are less than 2 ha (*Eurostat*, 2017). This fact is one of the most important specific restrictive effects on expansion of irrigation areas in Croatia. According to the recent published official data, in Croatia only 13,430 ha (1.4% of arable lands) is irrigated (*MEE*, 2014). In the Osijek-Baranja County, the study region, total equipped area for irrigation is 1,390 ha, whereby 512 ha with groundwater, while 878 ha with surface water (*Crostat*, 2006). Future expansion of irrigation areas in Croatia is encouraged by government and policy measures, so the goal is to provide infrastructure to implement irrigation on 65,000 ha of arable lands until the year 2020 (*Holjević et al.*, 2008). In Croatia, irrigation is manly used on supplementary basis to improve production of summer crops. Above 56% of agricultural areas in Croatia are categorized as arable lands, while in Osijek-Baranja County nearly 95% (200892 ha). Total agricultural land in Osijek-Baranja County is 212,095 ha, whereby 200,892 ha is arable land. In average 60.8% of arable lands are sown with maize, while 14.6% with soybean. The considerable yield variation of summer crops is mainly caused by unfavorable weather conditions. Not only because of the lack of rainfall but because of the dry periods which prolonged for fifteen years, local authorities proclaimed natural disaster of drought (2000, 2003, 2007, 2011, 2012, 2013, and 2015). According to *Perčec Tadić et al*. (2014) among all natural hazards in Croatia, drought causes the largest economic losses (39%). A more detailed analysis of drought phenomena in the Republic of Croatia have been done by *Cindrić et al.* (2016). Authors claim that the examined 2011/2012 drought in Osijek-Baranja County was characterized by extremely long duration with the highest magnitudes since the beginning of the twentieth century. *Branković et al*. (2009) have stated that during the twentieth century, the decline in annual amounts of precipitation in Osijek area is –4.1% in spring and –3% in autumn. As a result, in dry growing seasons, the yields of main summer crops grown in farm conditions are reduced as follows (*CBS*, 2018): maize yield was reduced by 39.7% (2010), 38.3% (2003), 28% (2007), 1.2% (2011), 22.1% (2012), 4.5% (2013), and 4.2% (2015), while soybean yields were reduced by 41.7% (2010), 29.3% (2003), 20.8% (2007), 25% (2013), and 8.3% (2015). Therefore, the importance of irrigation practice in this region is unquestionable. Furthermore, the yields of summer crops in several field studies are considerably increased by compensating the lack of rainfall with irrigation water. Some previously published results have evaluated the effect of irrigation treatments on maize yield in the study region. For example, in full irrigated plots, which was set to achieve soil water content of 80 to 100% of field capacity (FC), maize yield was by 25% (2011) and by 40% (2012) higher compared to control (dryland) plots (*Marković et al.*, 2015). As for soybean, in full irrigated plots

yields were by 9.4% (2007), 12.2% (2009), 46% (2012), and 18.8% (2013) higher compared to control plots (*Josipović et al.*, 2011, 2013). The irrigation efficiency (IE) is usually interpreted as the yield increase or reduction in irrigated agriculture. According to *Irmak et al.* (2011), irrigation efficiency (IE) is generally defined from three points of view: (1) the irrigation system performance, (2) the uniformity of water application, and (3) the response of the crop to irrigation. Some DSSAT crop simulations were done in term of climate changes and influence on maize production, and it was shown that in the future Croatia would belong to the area of decreased maize yields (*Vučetić*, 2008). The maize yield was simulated in non-irrigated conditions. This research emphasizes the importance of adaptation for summer crop production in terms of implementation of irrigation practice. The AquaCrop model was chosen in this paper to simulate the non-irrigated and irrigated production as the adequate and ideal crop model for irrigation evaluation, developed by Food and Agriculture Organisation of United Nation (FAO). According to *Farahani et al*. (2009), the FAO AquaCrop model provides a theoretical framework to investigate crop yield response to environmental stress, especially water and salinity. It simulates soil water balance and crop growth processes, based on input parameters and data, as a function of climate, soil, and plant interaction (*Foster et al*., 2017). The model precisely simulates the crop production, as it operates on a daily input data. In literature, AquaCrop model is well known in research community and successfully validated through many regions and various crops for field production: wheat (*Rezaverdinejad et al.*, 2014), maize (*Ahmadi et al*., 2015; *Paredes et al*., 2014; *Stricevic et al*., 2011), sugar beet (*Stričević et al*., 2014), and sunflower (*Todorovic et al*., 2009) crop production. The aim of this paper was to validate the AquaCrop model in non-irrigated and irrigated maize and soybean production for climate and soil conditions of Osijek-Baranja County (eastern Croatia). In the next step, the AquaCrop model was used to simulate maize and soybean production for future climate conditions for the 2041–2070 and 2071–2100 periods. Further results are presented: (a) the relative change in yield of maize and soybean in non-irrigated and irrigated conditions; (b) the change in net irrigation, water use efficiency (*WUE*), and irrigation water use efficiency (*IWUE*).

2. Materials and methods

2.1. Location

The field study was conducted at the research site of the Agricultural Institute in Osijek (45º32'N and 18º44'E). The area of Osijek (Osijek-Baranja County, eastern Croatia) has an altitude of 90 m. According to the Köppen climate classification system, the climate of Osijek is classified as moderately continental climate (Cfwbx) with an average annual precipitation of 650 mm, an

average air temperature of 10 ºC, and an annual sunshine of 1649 h. Mentioned climate data are expressed as an average for the 1961–1990 period. The soil is classified as gleysol (hydro-meliorated) WRB with its main characteristics presented in *Tables 1* and *2*. The soil analyses included mechanical, chemical, and soil water characteristics, sampled in two to four profile depth.

Table 1. Mechanical and hydrological characteristics of the soil at the research site

Profile (cm)	Clay (%)	Silt (%)	Sand (%)	BD (g/cm^3)	PWP (vol.%)	FC (vol.%)	SAT (vol.%)	TAW (mm)
0–32	32.5	64.7	2.8	2.58	23.65	36.57	39.52	129
32–50	31.3	66.4	2.3	2.65	24.52	35.59	40.88	110
50–70	25.5	68.2	6.3	-	-	-	-	200
70–105	21.6	71.8	6.6	-	-	-	-	200

BD = bulk density; PWP = permanent wilting point; FC = field capacity; SAT = saturation; TAW = total available water

Table 2. Chemical characteristics of soil at the research site

Profile (cm)	Organic carbon (%)	Nitrogen (%)
0–40	0.91	0.13
40–95	0.77	0.13

2.2. Past and future climate data

The past climate (1961–1990) presents daily weather data, observed at the weather station Osijek (45º32'N and 18º44'E) located nearby the experimental field. The data set includes maximum and minimum air temperature (ºC), insolation (h), precipitation (mm), vapor pressure (mbar), and wind speed (m/s). The reference evapotranspiration was calculated applying the FAO Penman-Monteith method (*Allen et al*., 1998). For the future climate conditions, the data were assumed from the integrated coupled model ECHAM, developed at the Max Planck Institute for Meteorology (*Roeckner et al*., 2003). The modeled data

were dynamically downscaled for two periods: from 2041 to 2070 and from 2071 to 2100. All simulations were done under the A1B and A2 (*IPCC*, 2001) scenarios for greenhouse gas (GHG) emissions for two the integration periods mentioned above, considering CO_2 effect. The average CO_2 concentration was 333.4 ppm for the 1961–1990 period, 545.7 mm (A1B scenario) and 551.0 ppm (A2 scenario) for the 2041–2070 period, and 662.4 ppm (A1B scenario) and 731.1 ppm (A2 scenario) for the 2071–2100 period.

2.3. Field study and crop management

Maize and soybean yield data, presented in this paper, were observed from a long-term field experiment for the 2010–2015 period. For the purpose of this study, yield data are presented for maize hybrids FAO 500 and 600, and soybean varieties 0–1 group. The region and field plots as well as the crop management were previously presented by *Josipović et al.* (2013) and *Marković et al.* (2017). Planting date, density, as well as observed phenology (sowing, emergence, flowering, and maturity) are presented in *Table 3*. The size of the maize hybrid plot was 19.6 m^2. Each year, maize hybrids were planted at 0.7 m row spacing, 0.25 m inter-row spacing, and depth of approximately 5 cm. The size of the soybean variety plot was 30 m^2. Seeding density for soybean crop was 550 seeds/m^2. Grain yield for both crops was measured after harvesting of each experimental plot, adjusted to 14% grain moisture and expressed as kg ha^{-1}.

Since the maize and soybean yield data for this study are expressed for irrigation treatment, here follows a more detailed description of the irrigation scheduling. Studied irrigation treatments included dryland (I_0-control) in both crop production, while the irrigated plot was designed to irrigate at 60–80% field water capacity (FWC) for maize (I_1) (*Hoogenboom et al*., 2012) and 80–100% FWC (I_2) for soybean, which is more vulnerable on the deficit in soil moisture. The size of irrigation plots for maize crop was 78.4 m^2, while for soybean it was 120 m^2. Irrigation was scheduled with the use of Watermark soil moisture sensors (model 200SS). The sensors were set up at two depths (15–20 cm and 25–30 cm) after the maize and soybean sowing, and were kept in soil until the harvest time. The Watermark sensors were calibrated for the soil on a trial site by comparing gravimetric measurements and sensor readings (*Marković*, 2013). The calibration curve is presented in *Fig. 1*. The maize and soybean were irrigated by use of traveling sprinkler system, which performed at the average speed of 15 m h^{-1} and provided 35 mm of irrigation water (1.5 l min^{-1}). Total amounts of water added in each growing season and irrigation treatments are presented in *Table 3*. Water for the system was pumped from 37 m deep well at a 5 to 7 l s^{-1} flow rate using an electric pump (5.5 kW). The analysis of chemical quality of irrigation water showed that the composition and concentrations of salts do not induce toxicity problems. The analysis was

interpreted according to FAO standards (*Ayers* and *Westcot*, 1985). The irrigation water use efficiency (*IWUE*) was determined as

$$IWUE = \frac{(Y_d - Y_i)}{I}, \quad (1)$$

where *IWUE* is the irrigation water use efficiency (kg m^{-3}), *Yd* is the yield (kg) on dry plots, *Yi* is the yield (kg) on irrigated plots, and *I* (m^3) is the net irrigation water (*Nakayama et al*., 1979). The water use efficiency (*WUE*) was determined as

$$WUE = Y \,/\, ET_0 \,, \quad (2)$$

where *WUE* is the water use efficiency (kg m^{-3}), *Y* is the economic yield (kg m^{-3}) for irrigation level, and ET_0 (m^3) is the reference crop evapotranspiration (*Kang et al*., 2000). The reference crop evapotranspiration (ET_0) was calculated according to the Penman-Montheith method by using the AquaCrop model.

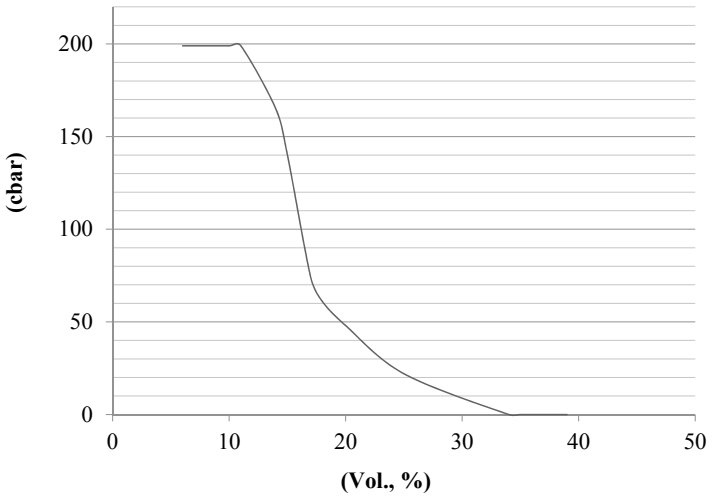

Fig. 1. Calibration curve of the Watermark sensors for the soil type at the study site. (*Marković*, 2013)

Table 3. Planting date, density, and observed phenology for maize and soybean crops

Year	Plant density (plant/m^2)	Sowing (date)	Emergence (date)	Flowering (date)	Harvest (date)	Precipitation (mm)	Irrigation (mm)
				Maize			I_1
2010	5.84-5.31	May 6	May 16	July 26	Oct 5	605.1	35
2011	5.98-5.87	May 3	May 15	July 14	Sep 25	210.7	105
2012	5.89-5.36	Apr 28	May 6	July 29	Sep 15	247.2	175
2013	5.92-5.38	Apr 30	May 12	July 21	Oct 2	388.3	105
2014	5.71-6.42	May 6	May 18	July 25	Oct 4	395.0	140
2015	6.02-6.45	Apr 30	May 11	July 27	Sep 20	292.2	140
				Soybean			I_2
2010	59-61	Apr 28	May 5	June 24	Sep 20	522.7	105
2011	60-64	Apr 20	May 2	June 8	Sep 8	216.4	245
2012	59-64	Apr 27	May 3	June 16	Sep 6	215.4	245
2013	60-62	Apr 25	May 5	June 20	Sep 12	252.1	210
2014	59-62	May 6	May 18	June 19	Sep 20	457.7	175
2015	58-62	Apr 21	May 5	June 12	Sep 10	280.7	210

2.4. Data analyses

Two statistical methods were used to analyze, evaluate, and compare observed yield data from field experiments and simulation yield results, to measure the AquaCrop model goodness of fit in our environmental conditions. First the relative deviation (*Törnvist et al*., 1985) was calculated between the simulated and observed dry matter yields for each year. The method was chosen to show how the model works and its sensitivity to various climate conditions each year under the same or similar crop management activity:

$$r = \frac{(S-M)}{(M \text{ x } 100)}, \tag{3}$$

where r is the relative deviation (%), M is the observed yield (dm t ha^{-1}), and S is the simulated yield (dm t ha^{-1}). The crop model fits when r is less than 15% (*Tsuji et al*., 1998). The second method selected for quantitative summary of goodness of fit was the root mean square error (*RMSE*):

$$RMSE = \sqrt{\left(\frac{1}{\text{n}}\right)\sum_{i=1}^{n}(y_i - \hat{y}_i)^2}, \tag{4}$$

where *RMSE* is the root mean square error (dm t ha^{-1}), y_i is measured value, $\hat{y}_i$ is the corresponding simulated value, and n is the number of measurements (*Wallach et al*., 2018). The *RMSE* has the same unit as the measured value y.

2.5. AquaCrop model, input data, calibration, and validation

The AquaCrop model is developed by FAO to simulate the crop response on the environmental stress. It is described by *Steduto et al.* (2009) in details. The model calculates daily biomass based on daily transpiration data, using reference evapotranspiration (ET_0), and normalized water productivity. The simulated yield is calculated as the product of daily biomass using the harvest index (HI). As the water is of the main importance in the AquaCrop model, it also simulates the changes in the soil water content during the growing season by means of a soil water balance. The soil water balance consists of the incoming water (rainfall, irrigation, and capillary rise), and outgoing water (runoff, evapotranspiration, and deep percolation) contained in different profiles of soil root zone depth. The moment for irrigation is possible to be calculated in the model, as the fixed amount of water retained and depleted in the root zone at any moment of the season. That possibility gives an opportunity to simulate irrigation efficiency on crop productivity (*Greaves* and *Wang*, 2017). To safely use simulation results by the AquaCrop model, it is necessary to do local calibration and validation for the chosen crop. The model requires a relatively small number of input data which describes the soil–crop–weather environment in which the crop develops (*Stricevic et al*., 2011). Using input data, observed daily weather data, soil characteristics, field management data, and crop parameters, the AquaCrop model was calibrated for maize and soybean production. For maize production, the model version 5.0 provides files with parameters suitable for the simulation of maize production, but with default values. These values were chosen only as a starting point, then the final key parameters were modified to fit the local crop management. All crop parameters were calibrated for the FAO 500–600 type maize hybrids, so that the crop model may simulate and present the real crop production in our local conditions. In *Table 4* final parameters are given, which are used for AquaCrop model calibration for maize and soybean production. Initial canopy cover was 0.37% with maximum canopy cover 96% in maize production (*Table 4*). The base air temperature was set to 8 ºC and the upper temperature to 30 ºC. Water productivity was 33 g m^2 and harvest index was 44% (*Table 4*). The crop management was standard for our agro-ecological conditions for maize and soybean growing. Soil fertility was considered as sufficient to achieve an ideal yield genetic potential, thus we could estimate only the effects climate change conditions. Net irrigation for maize and soybean is presented in *Table 3*. The AquaCrop model was calibrated for maize production for year 2010, results are and shown in *Table 5*. The relative deviation between the non-irrigated observed

and simulated dry matter yields was 3%, and it was 3.9% between the irrigated observed and simulated yields. The absolute change for net irrigation was 20.7 mm.

Table 4. Default and final parameters for the Aquacrop model calibration for maize and soybean production

Description	**Maize default**	**Maize final** (value)	**Soybean default**	**Soybean final** (value)	**Units/meaning**
Base temperature	8	8	5	8	ºC
Cut-off temperature	30	30	30	30	ºC
Initial canopy cover (CC_o)	0.49	0.37	1.65	2.95	%
Canopy expansion (CGC)	16.3	23.1	1.6	9.6	% / day
Maximum canopy cover (CCx)	96	96	98	98	%
Canopy decline coefficient (CDC) at senescence	11.7	11.7	2.9	2.9	% / day
Water productivity. (WP*)	33.7	33	16	16	as fraction of TAW (%)
Reference harvest index (HI_o)	48	44	40	30	common for good conditions (%)

Table 5. Calibration (2010) and validation of maize grain yield (dm t ha^{-1}) for the 2010–2015 period

	Non irrigated			**Irrigated**		
Year	**Observed yield (dm t ha^{-1})**	**Simulated yield (dm t ha^{-1})**	**Relative deviation (%)**	**Observed yield (dm t ha^{-1})**	**Simulated yield (dm t ha^{-1})**	**Relative deviation (%)**
2010	7.9	7.7	-2.5	7.9	7.6	-3.9
2011	6.4	7.0	9.4	7.6	7.7	1.8
2012	6.4	5.7	-10.9	7.7	7.8	0.8
2013	7.4	6.9	-6.8	7.2	7.5	3.8
2014	10.5	7.8	-25.7	11.9	7.8	-34.2
2015	7.4	6.8	-8.1	9.3	7.8	-16.5

The validation was done for a six-year period from 2010 to 2015, at the same location (*Table 5*). The relative deviation between simulated and observed dry matter yields was calculated for each year according to *Törnvist et al.* (1985) indicating how model fits in various climate conditions under the same crop management. The relative deviation between non-irrigated simulated and observed yields varied from 3 to 11%, while in irrigated conditions from 0.8 to 16.5%, except in year 2014. The absolute change in net irrigation varied from 2.3 to 38.8 mm, except for 2014. The highest deviation in yield as well as the absolute change in net irrigation (93.9 mm) occurred in 2014. In that year, the number of rainy days was above the long-term average, with very significant higher precipitation at the end of the growing season.

This significant difference between simulated and observed yield values is a consequence of the model inability to simulate the plant reaction to stress in extreme conditions, such as high variations in daily air temperature and precipitation sum in short time intervals (*Lalic et al*., 2011). The second method selected for quantitative summary of goodness-of-fit was the RMSE method (*Wallach et al.*, 2018). For the 5-year-long period (without the extreme weather year, 2014), it was 0.3 dm t ha^{-1} under non-irrigated maize production and 0.4 dm t ha^{-1} under irrigated maize production. The *RMSE* value was below 0.5 dm t ha^{-1} and showed that the model fits under our environmental conditions. The AquaCrop model was also calibrated for soybean 0 to 1 maturity group variety for year 2011 (*Table 6*). The relative deviation between non-irrigated simulated and observed dry matter yields was 1% and 3.8% in irrigated conditions. Absolute change for net irrigation was 3.2 mm. The model was validated for the 6-year-long experiment at the same experimental field (*Table 6*). The relative deviation between simulated and observed yields varied from 0 to 9% in non-irrigated conditions and from 0.4 to 5.1% in irrigated conditions, except in year 2010, when the relative deviation was 22 and 25.2%, due to heavy precipitation. The absolute change for net irrigation varied from 1.6 to 30 mm, except in year 2014, when the precipitation was considerably higher than the long-term average at the end of the growing season. The *RMSE* for 6-year-long period was 0.07 dm t ha^{-1} under non-irrigated conditions and 0.09 dm t ha^{-1} under irrigated conditions, which improves the model validation under our environmental conditions.

To estimate the climate change impact on yield, net irrigation, and *WUE* in future conditions, it is necessary to keep same crop management operations and crop parameters in model as in the period of 2010–2015. The crop parameters and phenology stages, which were kept the same for the 1961–1990 period and future conditions are presented in *Table 7*. In the model, sowing and phenology were set at the average sowing date, emergence, maximum canopy cover, flower appearance and maturity date (*Table 7*). Additionally, under irrigated conditions, the readily available water was set to 80%, below which the soil water content in the root zone may not drop. This irrigation method in the model, including defined and set local soil hydrological characteristics, gave similar net irrigation quantities to measured net irrigation from field experiments.

Table 6. Calibration (2011) and validation of I group maturity soybean grain yield (dm t/ha) for the 2010 to 2015 period

Year	Non irrigated			Irrigated		
	Observed yield (dm t ha^{-1})	Simulated yield (dm t ha^{-1})	Relative deviation (%)	Observed yield (dm t ha^{-1})	Simulated yield (dm t ha^{-1})	Relative deviation (%)
2010	2.9	3.5	22	2.8	3.5	25.2
2011	3.0	3.0	-1	3.9	3.7	-3.8
2012	2.4	2.5	5	3.7	3.7	-0.4
2013	2.9	2.9	0	3.8	3.7	-4.2
2014	3.1	3.3	7	3.5	3.7	5.1
2015	2.7	2.9	9	3.8	3.8	-1.4

Table 7. Calendar days of maize and soybean by phenological phases for crop simulations for the 1961–1990 period and expected climate conditions

Phenological phase	Maize (calendar days)	Soybean (calendar days)
To emergence	9	10
Maximum canopy cover	44	73
Maximum rooting depth	85	93
Start of canopy senescence	104	104
Maturity	152	137
Start of flowering	82	56
Length building up HI	70	82
Duration of flowering	20	46

3. Results

3.1. Past and future climate conditions

In the 1961–1990 period, the observed data were analyzed: air temperature and precipitation in the growing season AS (from April to September) and the drought period JJA (from June to August) (*Table 8*). The temperature was 19.1 °C in the AS period and 20.3 ºC in the JJA period, while the precipitation

was 290.7 mm for the growing season and 211.2 mm for JJA period (*Table 8*). For future conditions, the absolute change in temperature and relative change in precipitation was calculated for the 2041–2070 and 2071–2100 periods under two scenarios (A1B, A2) in compare to 1961–1990 (*Table 9*). In future conditions, rise in temperature in both periods under two scenarios is expected. There was no significant difference between the two scenarios from 0.3 to 0.5 ºC. In the AS period, the expected increase in temperature for the 2041–2070 period is 2.8 ºC (A1B) and for 2071–2100 is 4.6 ºC (A2). In the JJA drought period, the expected increase in temperature is 2.9 ºC (A1B) in 2041–2070 and 5.0 °C (A2) in 2071– 2100 (Table 9). The analyzed precipitation amount showed a significant decrease in future conditions compared to the past climate data of the period 1961–1990. In a comparison of the two scenarios, the A1B scenario showed lower precipitation for future conditions, especially for the 2041–2070. In AS period, for 2041–2070, lower precipitation by 28.2% (A1B) and 16.5% (A2) is expected. In the 2071–2100 period, more decrease in precipitation is expected, by 34.8% (A1B) and 33.7% (A2) in AS compared to 1961–1990. During JJA summer months, a considerable decrease in precipitation is expected as well. In the 2041–2070 period, the expected reduction in precipitation is 35.2% (A1B) and 25.8% (A2). Furthermore, for the 2071–2100 period, 43.55% (A1B) and 43.4% (A2) reduction is expected compared to the 1961–1990 period (*Table 9*).

Table 8. Climate conditions for the 1961–1990 period at Osijek location (t - temperature; p - precipitation)

	April-September		**June-July-August**	
	t (ºC)	**p (mm)**	**t (ºC)**	**p (mm)**
1961–1990	19.1	290.7	20.3	211.2

Table 9. Absolute change in temperature (°C) and relative change in precipitation (%) for 2041–2070 and 2071–2100 using ECHAM model under A1B and A2 scenarios (t - temperature; p - precipitation)

	A1B				**A2**			
	April- September		**June-July-August**		**April- September**		**June-July-August**	
	t (°C)	**p (%)**	**t (°C)**	**p (%)**	**t (°C)**	**p (%)**	**t (°C)**	**p (%)**
2041–2070	2.8	-28.2	2.9	-35.2	2.3	-16.5	2.4	-25.8
2071–2100	4.3	-34.8	4.5	-43.5	4.6	-33.7	5.0	-43.4

3.2. Climate change impact on maize and soybean yields, net irrigation, WUE, and IWUE

In past climate conditions (1961–1990), the simulated maize yield in non-irrigated conditions was as usual in real conditions, about 7.3 dm t ha^{-1}, and 7.1 dm t ha^{-1} in irrigated conditions (*Tables 10* and *11*). For the same period of time, the *WUE* ranged from 1.32 kg m^3 in non-irrigated to 1.28 kg m^3 in irrigated conditions. As for *IWUE*, net irrigation (40 mm) reduced the maize yield for 3.53 kg mm^{-1}. According to the analyzed yield results, in future conditions it is expected a little lower or the same yield in non-irrigated maize production, and higher yield values when the maize is under irrigated conditions (*Tables 10* and *11*). In the 2041–2070 period, in non-irrigated conditions, the maize should have 0.4 dm t ha^{-1} lower (A1B) or 0.2 dm t ha^{-1} (A2) higher yield. During the same period, the *WUE* for non-irrigated conditions for A1B scenario is 1.14 kg m^3 and 1.28 kg m^3 for A2 scenario. In the further period, till 2100, it is expected that the yield slightly decrease from 0.6% (A1B) to 0.3% (A2) compared to the 1961–1990 period. Furthermore, the *WUE* for this period is 1.07 kg m^3 for A1B and 1.11 kg m^3 for A2 scenario (*Table 10*). In irrigated conditions, maize production showed an increase in yield from 1.0 dm t ha^{-1} in 2041–2070 and 1.4 dm t ha^{-1} in 2071–2100. There were no significant differences between the results of the two scenarios. In irrigated conditions, it is important to mention that the net irrigation is expected to increase in both periods. In 2041–2070, the absolute change in net irrigation was 74.8 mm (A1B) and 38.3 mm (A2). For 2041–2070, the *WUE* is 1.34 kg m^3 and *IWUE* is 11.8 kg mm for A1B scenario while for the A2 scenario *WUE* is 1.37 kg m^3 and *IWUE* is 7.64 kg m^3 (*Table 11*). In 2071–2100, further increase in net irrigation up to 80.7 mm under A2 scenario is expected. For this period, *WUE* is 1.33 kg m^3 for both scenarios, while *IWUE* is 14.01 kg mm for A1B and 12.16 kg mm for A2 scenario. In soybean production, the crop simulations for the 1961–1990 period showed, that soybean yield was similar to real yield produced in Croatia, 2.9 dm t ha^{-1} in non-irrigated conditions and 3.2 dm t ha^{-1} in irrigated conditions (*Tables 12* and *13*). As for *WUE*, it ranges from 0.56 kg m^3 in non-irrigated to 0.60 kg m^3 in irrigated soybean production, while the *IWUE* was 1.9 kg mm. In future conditions, in both periods yield increase is expected. In 2041–2070, in non-irrigated production, the expected increase is from 0.7 (A1B) to 0.9 dm t ha^{-1} (A2) in soybean yield, while the larger increase is expected in the period 2071–2100, for 0.9 dm t ha^{-1} under A1B scenario and 1.1 dm t ha^{-1} under A2 scenario. The *WUE*, for the mentioned period, ranged from 0.61 to 0.68 kg m^3 for A1B and A2 scenarios for 2041–2070, and from 0.63 to 0.66 kg m^3 in 2071–2100 (*Table 12*). The rise in soybean yield in irrigated conditions is also noticeable, 1.3 (A1B) and 1.8 dm t ha^{-1} (A2) in the 2041–2070 period and 1.3 (A1B) to 1.9 dm t ha^{-1} (A2) in the 2071–2100 period. There was no significant difference between the scenario results. In irrigated soybean production for that period

WUE is 0.6 kg m^3, while *IWUE* is 1.9 kg mm (*Table 13*). In irrigated production, the net irrigation was significantly higher in both periods, than in the 1961–1990 period. The absolute change in net irrigation is expected to be 82.9 (A1B) and 46.3 mm (A2) in the 2041–2070 period and 103.5 (A1B) 93.3 mm (A2) in the 2071– 2100 period. The *WUE* for the 2041–2070 period ranges from 0.78 to 0.80 kg m^3 for A1B and A2 scenarios. Furthermore, for the 2071– 2100 period it ranges from 0.82 to 0.85 kg m^3. As for *IWUE* for the 2041–2070 period, it ranges from 4.89 to 4.27 kg mm for A1B and A2 scenarios, while for the 2071–2100 period it ranges from 5.39 to 5.56 kg mm for A1B and A2 scenarios (*Table 13*).

Table 10. Average yield (dm t/ha) and water use efficiency (*WUE*, kg/m^3) for non-irrigated maize crop in 1961–1990 and future conditions under A1B and A2 SRES scenarios

Period		Yield (dmt/ha)	Precipitation (mm)	ETo (mm)	WUE (kg/m^3)
1961–1990		7.3	313	551	1.32
2041–2070	A1B	6.9	220	607	1.14
	A2	7.5	205	629	1.28
2071–2100	A1B	6.7	260	591	1.07
	A2	7.0	206	637	1.11

A1B; A2 = scenarios, *WUE* = water use efficiency

Table 11. Average yield (dm t/ha), water use efficiency (*WUE*, kg/m^3) and irrigation water use efficiency (*IWUE*, kg/mm) for irrigated maize crop in 1961-1990 and future conditions under A1B and A2 SRES scenarios

		Yield (dmt/ha)	Net irrigation (mm)	Precipitation (mm)	ETo (mm)	WUE (kg/m^3)	IWUE (kg/mm)
1961–1990		7.1	40	313	554	1.28	-3.53
2041–2070	A1B	8.2	110	220	609	1.34	11.8
	A2	8.1	75	262	594	1.37	7.64
2071–2100	A1B	8.4	120	205	631	1.33	14.01
	A2	8.5	120	206	640	1.33	12.16

A1B; A2 = scenarios; *WUE* = water use efficiency; *IWUE* = irrigation water use efficiency

Table 12. Average yield (dm t ha^{-1}) and water use efficiency (WUE, kg m^3) for non-irrigated soybean crop in 1961–1990 and future conditions under A1B and A2 SRES scenarios

Period		Yield (dmt/ha)	Precipitation (mm)	ETo (mm)	WUE (kg/m^3)
1961–1990		2.9	291	524	0.56
2041–2070	A1B	3.6	209	580	0.61
	A2	3.8	243	564	0.68
2071–2100	A1B	3.8	190	602	0.63
	A2	4.0	193	608	0.66

A1B; A2 = scenarios, *WUE* = water use efficiency

Table 13. Average yield (dm t/ha) and water use efficiency (*WUE*, kg/m^3) and irrigation water use efficiency (*IWUE*, kg/mm) for irrigated soybean crop in 1961–1990 and future conditions under A1B and A2 SRES scenarios

		Yield (t/ha)	Net irrigation (mm)	Precipitation (mm)	ETo (mm)	WUE (kg/m^3)	IWUE (kg/mm)
1961–1990		3.2	110	291	524	0.60	1.90
2041–2070	A1B	4.5	190	209	580	0.78	4.89
	A2	4.5	155	243	564	0.80	4.24
2071–2100	A1B	5.0	210	190	602	0.82	5.39
	A2	5.1	200	193	608	0.85	5.56

A1B; A2 = scenarios; WUE = water use efficiency; IWUE = irrigation water use efficiency

4. Discussion

4.1. Climate and production of maize and soybean in the1961–1990 period

The climate data from the 30-year-long period of 1961–1990 were observed and two main agro climatic indices, temperature and precipitation were analyzed. The mean temperature was 19.1 ºC for the growing season and 20.3 ºC for the drought sensitive period. That were optimal conditions for maize and soybean vegetative and generative growths (*Miladinović et al*., 2008). The agro-climatic index, which mostly affects crop growth in interaction with air temperature and has direct impact on yield is precipitation. The observed precipitation for the

growing season was 290.7 mm. In the medium season, maize and soybean 0 to 1 variety, in our moderate continental climate under gleysol conditions has a water demand of 250–300 and 520–1000 mm for the growing season (*Komljenović* and *Todorović*, 1998; *Miladinović et al*., 2008). In the drought sensitive period (JJA), when the temperature is the highest during the season, the optimal soil moisture is necessary for field crops. The observed precipitation in this period was 211.2 mm. The lack or excessive amount of rainfall (2010 and 2014) accompanied with high temperatures have negative impact on crop growth and yield. In such years, the irrigation is necessary, as an adaptation measure. The observed climate data for the 1961–1990 period was described as moderate continental climate, under hypogley soil type, gave an optimal condition for maize and soybean growth and yield.

4.2. Climate change impact on yield for the 2041–2070 and 2071–2100 periods

In future conditions, higher air temperature from 2.3 ºC in 2041–2070 and up to 4.6 ºC in 2071–2100 is expected for the growing season. The reduction in precipitation was also noted during the growing season from 16.5 to 34.8%, and lower values are expected during the summer months (JJA) from 25.8 to 43.5%. Such changes in climate were also predicted for this region by *Vučetić* (2011) and for Eastern Europe by CECILIA (2006). As for Eastern Europe conditions, *Rolbiecki et al.* (2017) have stated that for the region of northern Poland during the 2021–2050 period, the increase of water needs of the forest nurseries from 12 to 15% is expected. Authors have compared the mentioned period to the reference years of 1981–2010 and stated, that the water needs of nurseries in future climate conditions will rise in the growing period (April-September) from 427 to 489 mm on clay and from 498 to 560 mm on sandy soil. Higher air temperatures, accompanied with lower precipitation and lack of soil moisture mainly causes crop yield decrease (*Prasad* and *Staggenborg*, 2008). In the paper, in non-irrigated maize production slightly lower yield is expected under the A1B scenario and no change in yield under the A2 scenario. The yield predictions in maize production for Eastern Europe showed yield decrease from 10 to 24% on chernozem and cambisol soils under climate change. In irrigated maize production in this paper, analyses showed the possible increase in yield under climate change in both climate periods and scenarios. The higher yield is expected due to an adequate irrigation sprinkler method with higher net irrigation of 80 mm, or as two additional irrigation treatments (40 mm) than in 1961–1990. Under climate change, in non-irrigated soybean production rise in yield from 0.7 to 1.1 dm t ha^{-1} is expected, and in irrigated conditions, the expected rise is from 1.3 to 1.9 dm t ha^{-1}. This increase in yield together with a very reasonable increase in CO_2 concentration are also expected in the Eastern Europe predictions (CECILIA, 2006). Soybean is a C3 crop with high potential in yield increase under higher level of CO_2 concertation (*Southworth et al*., 2002; *Wittwer*, 1995). The primary

reason is that increased concentration of atmospheric CO_2 will reduce photorespiratory losses of carbon in the C3 plant, thereby enhancing plant growth and productivity (*Allen et al*., 1988). It has been reported that soybean yield will rise by 30% under the predicted 555 ppm CO_2 concentration in Illinois, assuming that soybean is well-watered and not facing nutrient stress (*Southworth et al*., 2002). In irrigated conditions, a rise in net irrigation up to 100 mm to 2100 is expected, which means that three-times more than in 1961–1990.

4.3. Climate change impact on WUE and IWUE for the 2041–2070 and 2071–2100 periods

In average, the *WUE* for maize crop in non-irrigated conditions was the highest in the 1961–1990 period and has a trend to decrease in the future climate scenarios. This is in accordance with the results of *Kang et al.* (2015). Authors have stated that water use indices of maize under non-irrigated conditions will decrease, while the evapotranspiration efficiency, crop water use efficiency, and total water use efficiency will be larger in future conditions. In our study, the highest *WUE* is in periods with the lowest precipitation amount. In scenarios and period comparison, there are no considerable differences in the *WUE* value in the study. As for *IWUE*, it is noticeable that irrigation reduced maize yield during the 1961–1990 period. During the 2041–2070 period, considerably higher *IWUE* is expected in the A1B scenario, the scenario with a lower amount of precipitation, compared to the A2 scenario. In further period, there is no considerable differences between the *IWUE* values. The overall *WUE* in non-irrigated maize production, under climate change, is expected to decrease compared to the 1961–1990 period. On the other hand, in irrigated conditions, under climate change, higher *WUE* and *IWUE* values are expected as well, which is in accordance with a previous research of *Kang et al.* (2015). The lowest *WUE* in non-irrigated soybean production is in the 1961–1990 period, when the lowest precipitation was observed, compared to the future climate conditions. As the precipitation is expected to decrease, especially after year 2041 and further, the *WUE* will be increased under both scenarios and periods. In a comparison of two scenarios, higher *WUE* is noticed under the A2 scenario. For the 2041–2070 period, the higher *IWUE* is in scenario A1B, with lower rainfall amount and higher net irrigation. In future climate conditions, in both periods and scenarios, increase in *WUE* and *IWUE* is expected. Generally, according to the results of our study, the higher I*WUE* in future climate scenarios could be a result of the yield increase. *Deihimfard et al.* (2018) also claim, that besides the yield increase, in future climate conditions the improved *WUE* is the result of the decreased evapotranspiration, yet in our study this is not the case. According to the results of our study, in the future climate, the ET_0 increase is noticeable as well.

5. Conclusions

Detailed analyses of climate and model results showed that

- Possible higher air temperature up to 5 ºC, accompanied with significantly lower precipitation up to 43.5% are expected, especially during summer months in future conditions.
- In maize production, in non-irrigated conditions, slightly lower or no change in yield, while in irrigated conditions higher yield up to 1.4 dm t ha^{-1} with 80 mm higher net irrigation, or two extra irrigation treatments per growing season are expected.
- In non-irrigated maize production, *WUE* is expected to decrease while no change in irrigated production will occure.
- The I*WUE* results showed very significant increase trend in the future climate.
- In non-irrigated soybean production, higher yield up to 1.1 dm t ha^{-1}, while in irrigated conditions 1.9 dm t ha^{-1} increase in yield are expected in the future conditions. In irrigated conditions, net irrigation is expected to be 90 mm higher, or three extra irrigation treatments will be needed compared to the 1961–1990 period.
- In soybean production, a slight increase in *WUE* under both non-irrigated and irrigated conditions is expected.
- In irrigated conditions, the I*WUE* results showed very significant increase in the future conditions.

Based on the analyses, a possible benefit for both crops is observed under climate change in non-irrigated and irrigated conditions as well. In maize production, the benefit is expected only under irrigated conditions, due to crop efficiency in irrigation and very significant increase in *IWUE*, while the increase in soybean yield is expected in both non-irrigated and irrigated conditions. The simulated higher yield is due to the expected increase in the CO_2 concentration in the future climate. Soybean is a C3 plant, which is more sensitive to higher CO_2 concentrations than C4 plants (maize, sorghum, millet), which can greatly benefit productivity. The increase in *WUE,* and especially *IWUE,* in soybean production is due to the expected increase in yield. The analyzed yield, net irrigation, and *IWUE* results showed potential prosperity in irrigated conditions under climate change. This could classify Osijek-Baranja County as priority area for further irrigation action plans. Some small-scale irrigation programs introduced by the government could assist the sustainable crop production in the study area.

Acknowledgement: The research described here was funded by the Serbian Ministry of Science and Technology under project No. III 43007 “Research of climate changes and their impact on environment. Monitoring of the impact, adaptation and moderation” for 2011–2018.

References

Allen R.G., Pereira L.S., Raes D., and *Smith M.,* 1988: Crop evapotranspiration-guidelines for computing crop water requirements. FAO Irrigation and drainage paper 56. Food and Agriculture Organization, Rome.

Ahmadi, S.H., Mosallaeepour, E., Kamgar-Haghighi, A.A., and *Sepaskhah, A.A.,* 2015: Modeling Maize Yield and Soil Water Content with AquaCrop Under Full and Deficit Irrigation Managements. *Water Res. Manage. 29,* 2837–2853. https://doi.org/10.1007/s11269-015-0973-3

Ayres, R.S. and *Westcot, D.W.,* 1985*:* Water Quality for Agriculture. FAO Irrigation and Drainage Paper 29. Rome.

Branković, Č., Cindrić, K., Gajić-Čapka, M., Göttler, I., Patarčić, M., Srnec, L., Vučetić, V., and *Zaninović, K.,* 2009: Fifth National Communication of the Republic of Croatia under the United Nation Framework Convention on the Climate Change (UNFCCC). Republic of Croatia.

CBS (Croatian Bureau of Statistics), 2018: Crop production. First release.

CECILIA (Central and Eastern Europe Climate Change Impact and Vulnerability Assessment), 2006: Climate change impacts in central-eastern Europe: Project No. 037005, Report: D6.1: Crop yield and forest tree growth changes influenced by climate change effects, regional conditions and management systems. National Forest Center, Forest Research Institute Zvolen.

Cindrić, K., Telišman Prtenjak, M., Herceg-Bulić, I., Mihajlović, D., and *Pasarić, Z.,* 2016: Analysis of the extraordinary 2011/2012 drought in Croatia. *Theor. Appl. Climatol. 123*, 503–522. https://doi.org/10.1007/s00704-014-1368-8
https://www.dzs.hr/Hrv_Eng/publication/2018/01-01-14_01_2018.htm. Accessed 27 June 2018.

Crostat, Croatian Bureau of Statistic, 2006: Agricultural census 2003. https://www.dzs.hr/eng/DBHomepages/Agricultural%20Census%202003/Agricultural%20Census%202003.htm. Accessed 02 August 2018.

Eurostat, 2017: Key figures on Europe. https://ec.europa.eu/eurostat/documents/3217494/8309812/KS-EI-17-001-EN-N.pdf/b7df53f5-4faf-48a6-aca1-c650d40c9239. Accessed 02 May 2018.

Deihimfard, R., Eyni-Nargeseh H., and *Mokhtassi-Bidgoli A.,* 2018: Effect of Future Climate Change on Wheat Yield and Water Use Efficiency Under Semi-arid Conditions as Predicted by APSIM-Wheat Model. *Int. J. Plant Product. 12*, 115–125. https://doi.org/10.1007/s42106-018-0012-4

Farahani, H.J., Izzi, G., and *Oweis, T.Y.,* 2009: Parameterization and evaluation of the AquaCrop model for full and deficit irrigated cotton. *Agronomy J. 101*, 469–476. doi:10.2134/agronj2008.0182s

Foster G.L., *Royer D.L.,* and *Lunt D.J.* 2017: Future climate forcing potentially without precedent in the last 420 million years. *Nat. Commun. 8*, 1–8.

Greaves G.E. and *Wang Y.M.,* 2017: Identifying Irrigation Strategies for Improved Agricultural Water Productivity in Irrigated Maize Production through Crop Simulation Modelling. *Sustainability 9*, 630.

Holjević D., Marušić J., and *Romić D.,* 2008: Implementation of the National Irrigation Plan in the Republic of Croatia // XXIV Conference of the Danubian countries on the hydrological forecasting and hydrological bases of water, 146–146.

Hoogenboom G., Jones J.S., Sibiry P.C., Traore K., and *Boote J.* 2012: Experiments and Data for Model Evaluation and Application. n book: Improving Soil Fertility Recommendations in Africa using the Decision Support System for Agrotechnology Transfer (DSSAT).

Irmak, S., Odhiambo, Lameck O. Kranz, William L., Eisenhauer, and *Dean E.,* 2011: Irrigation Efficiency and Uniformity, and Crop Water Use Efficiency. *Biol. Syst. Engineer. Pap. Pub.* https://digitalcommons.unl.edu/biosysengfacpub/451. Accessed 02 April 2018.

IPPC, 2001: Availabe at: https://www.ipcc.ch/sr15/

Josipović, M., Sudarić, A., Kovačević, V., Marković, M., Plavšić, H., and *Liović, I.,* 2011: Irrigation and nitrogen fertilization influences on soybean variety (*Glycine max (L.) Merr.*) properties. *Poljoprivreda 1*, 9–15.

Josipović, M, Sudarić, A., Rezica, S., Plavšić, H., Marković, M., Jug, D., and *Stojić, B.* 2013: Influence of irrigation and variety on the soybean grain yield and quality in the no nitrogen fertilization condition. Proceedings & Abstract 2nd International Scientific Conference. Soil and Crop Management: Adaptation and Mitigation of Climate Change. 26-28 September, 2013, Osijek, Croatia.

Kang, S.Z., Shi, P., Pan, Y.H., Liang, Z.S., Hu, X.T., and *Zhang, J.* 2000: Soil water distribution, uniformity and water-use efficiency under alternate furrow irrigation in arid areas. *Irrigation Sci. 19*,181–190. https://doi.org/10.1007/s002710000019

Kang, Y., Khan S., and *Ma X.,* 2015: Analysing Climate Change Impacts on Water Productivity of Cropping Systems in the Murray Darling Basin, Australia. *Irrigat. draingae 64*, 443–453. https://doi.org/10.1002/ird.1914

Komljenović, I. and *Todorović, J.,* 1998: Opšte ratarstvo. Banja Luka: Univerzitet u Banja Luci. (In Serbian)

Lalic B., Mihailovic D., and *Podrascanin Z.* 2011: Future state of climate in Vojvodina and expected effects on crop production. *Field Veg. Crop Res.,* 48, 403–418

Marković, M., 2013: Utjecaj navodnjavanja i gnojidbe dušikom na prinos i kavlitetu zrna hibrida kukuruza *(Zea mays L.)*. Doktorska disertacija. Poljoprivredni fakultetu, Sveučilište Josipa Jurja Strossmayera u Osijeku, Osijek, Croatia. (In Croatian)

Marković, M., Tadić, V., Josipović, M., Zebec, V., and *Filipović, V.* 2015: Efficiency of maize irrigation scheduling in climate variability and extreme weather events in eastern Croatia. *J. Water.Climate Change 6*, 586–595. DOI: 10.2166/wcc.2015.042

Marković, M., Josipović, M., Šoštarić, J., Jambrović, A., and *Brkić, A.* 2017: Response of Maize (*Zea mays* L.) Grain Yield and Yield Components to Irrigation and Nitrogen Fertilization. *J. Centr. Eur. Agricult. 18*, 55–72. DOI: 10.5513/JCEA01/18.1.1867

MEE (Ministry of Environment and Energy), 2014: Sixth national communication and first biennial report of the republic of Croatia under the United Nations framework convention on climate change. https://unfccc.int/files/national_reports/annex_i_natcom_/application/pdf/eu_nc6.pdf. Accessed 01 October 2018.

Miladinović, J., Hrustić, M. and *Vidić, M.,* 2008: *Soja*. Bečej: Institut za ratarstvo i povrtarstvo. Srbija.

Nakayama, F.S., Bucks, D.A., Clemmens, A.J., 1979: *Assess. Trickle Emitter Appl. Unif.* American Society of Agricultural Engineers (Trans. ASAE 1979) *22*, 816–821.

Paredes, P., de Melo - Abreu, J.P., Alves, I., and *Pereira, L.S.,* 2014: Assessing the performance of the FAO AquaCrop model to estimate maize yields and water use under full and deficit irrigation with focus on model parameterization. *Agric. Water Manage. 144*, 81–97. https://doi.org/10.1016/j.agwat.2014.06.002

Perčec Tadić, M., Gajić-Čapka, M., Zaninović, K., and *Cindrić, K.* 2014: Drought vulnerability in Croatia. *Agriculturae Conspectus Scientificus 79*, 31–39.

Prasad, P.V.V. and *Staggenborg, S.A.,* 2008: Impacts of drought and/or heat stress on physiological, developmental, growth, and yield processes of crop plants. In: Response of Crops to Limited Water: Understanding and Modeling Water Stress Effects on Plant Growth Processes. Madison, WI, USA: American Society of Agronomy/ Crop Science Society of America/Soil Science Society of America.

Rezaverdinejad, V., *Khorsand*, A., and *Shahidi*, *A.*, 2014. Evaluation and comparison of AquaCrop and FAO models for yield prediction of winter wheat under environmental stresses. *J. Biodiv. Environ.Sci. 4,* 438–449.

Roeckner E., Bäuml G., Bonaventura L., Brokopf R., Esch M., Giorgetta M., Hagemann S., Kirchner I., Kornblueh L., Manzini E., Rhodin A., Schlese U., Schulzweida U., and *Tompkins A.,* 2003: The atmosheric general circulation model ECHAM5. Report No. 349. Max Planck Institute for Meteorlogy.

Rolbiecki, S., Kokoszewski, M., Gribauskiene, V., Rolbiecki, R., Jagosz, B., Ptach, W., and *Langowski, A.* 2017: Effect of expected climate changes on the water needs of forest nursery in the region of central Poland. Proceedings of the 8th International Scientific Conference Rural Development, 23-24 November 2017, Kaunash, Lithuania.

Southworth, J., Pfeifer, R.A., Habeck, M., Randolph, J.C., Doering, O.C., Johnston, J.J., and *Rao, D.G.* 2002: Changes in soybean yields in the Midwestern United States bas result of future change in climate variability, and CO_2. *Climatic Change 53*, 447–475.

Steduto P., Hsiao T.C., Raes D., and *Fereres E.* 2009. AquaCrop – the FAO crop model to simulate yield response to water: I. Concepts and underlying principles. *Agronomy J. 101*, 426–437.

Stricevic, R., Cosic, M., Djurovic, N., Pejic, B., and *Maksimovic, L.* 2011: Assessment of the FAO AquaCrop model in the simulation of rainfed and supplementally irrigated maize, sugar beet and sunflower. *Agric. Water Manage. 98*, 1615–1621. https://doi.org/10.1016/j.agwat.2011.05.011

Stričević, R., Đurović, N., Vuković, A., Vujadinović, M., Ćosić, M., and *Pejić, B.* 2014: Procena prinosa i potrebe šećerne repe za vodom u uslovima klimatskih promena na području Republike Srbije primenom AquaCrop modela. *J. Agricult. Sci.(Belgrade) 59*, 301–317. (In Serbian)

Todorovic, M., Albrizio, R., Zivotic, L., Abi Saab, M.-T., Stöckle, and *Steduto, P.,* 2009: Asssesement of AcuaCrop, CropSyst, and WOFOST models in the simulation of Sunflower growth under different water regimes. *Agronomy J.* 101, 509–521.

Törnvist, L., Vartia, P., and *Vartia, A.,* 1985: How Should Relative Changes Be Measured? *Amer. Statistic. 39,* 43–46.

Tsuji, G.Y., Hoogenboom G., and *Thornton P.K..,* 1998: Understanding Options for Agricultural Production. Springer.

Vučetić, V., 2008: Modeling of maize production in Croatia: present and future climate. *J. Agric. Sci. 149*, 145–157.

Wallach, D., Makowski, D., Jones, J.W., and *Brun, F.,* 2018: Working with Dynamic Crop Models. Methods, Tools and Examples for Agriculture and Environment. Elsevier Science, Oxford, UK.

Wittwer, S.H., 1995: Food, Climate, and Carbon Dioxide – The Global Environment and World Food Production. Boca Raton, FL: Lewis Publishers. An imprint of CRC Press.

DOI:10.28974/idojaras.2020.2.8

IDŐJÁRÁS

Quarterly Journal of the Hungarian Meteorological Service
Vol. 124, No. 2, April – June, 2020, pp. 299–309

Short Contribution

On the reliability of CALPUFF and AUSTAL 2000 modeling systems regarding smoke and vapor plume mergence

Pedram Jafari Shalkouhi [1], **Farideh Atabi** [1], **Faramarz Moattar** [1*], and **Hossein Yousefi** [2]

[1]*Department of Environmental Engineering*
Faculty of Natural Resources and Environment
Science and Research Branch, Islamic Azad University
Tehran, Iran

[2]*Department of Renewable Energies and Environmental Engineering*
Faculty of New Sciences and Technologies
University of Tehran
Tehran, Iran

**Corresponding author E-mail: pedram121212@yahoo.com*

(Manuscript received in final form January 9, 2020)

Abstract— Observations at power plants have shown that smoke plumes from stacks frequently merge with vapor plumes from cooling towers. Wind speed and direction play a key role in merging vapor and smoke plume. Mergence of stack and cooling tower plume leads to formation of undesirable substances such as sulfuric acid aerosols, acid mist, and acid fly ash. The present study shows that smoke and vapor plume mergence is a common phenomenon in Mátra power plant in Hungary; however more studies must be conducted in the future to reveal the type and number of plume mergence in the mentioned plant. The present work also indicates that the CALPUFF and AUSTAL 2000 modeling systems cannot provide enough information with regard to vapor and smoke plume mergence.

Key-words: smoke, vapor, wind, Mátra plant, CALPUFF, AUSTAL 2000

1. Introduction

Cooling towers eliminate heat from condenser cooling water by evaporation and reject this heat to the air in the form of a hot and humid plume. Cooling tower plumes consist of water vapor saturated air and liquid water in the form of suspended droplets. The emissions from stacks of fossil-fueled plants are primarily sulfur oxides and nitrogen oxides in addition to the usual constituents CO_2, N_2, O_2, and particulates such as fly ash and trace elements. Vapor plumes from the cooling tower of a power plant are similar in most respects to smoke plumes from the stack; however, the size difference is very great (*USEPA,* 1979).

2. Discussion

The potential effects of cooling tower and stack plume mergence include enhanced sulfate production and the ensuing production of undesirable substances such as sulfuric acid aerosols, acid mist, and acid fly ash. These interaction products may be generated from reactions involving sulfur dioxide and fly ash in stack plume with water vapor or water droplets contained in cooling tower plume. It should be pointed out that aerosols which are mentioned above refer to the dispersion of solid or liquid particles of microscopic size in gaseous media such as dust, smoke, or mist (*Rao* and *Rao,* 1989).

The results of smoke and vapor plume mergence could manifest itself in three ways as follows (*Knudson,* 1979):

1. Mist carried to the ground (subsequent to mergence with smoke plume) could have a lower pH due to dissolved acid sulfates.
2. Evaporation of mist (subsequent to plume mergence) could release dissolved sulfate aerosols resulting in the enhancement of plume sulfate levels.
3. Smoke plume sulfate levels could be enhanced due to the presence of water (vapor and droplets) associated with cooling tower plume.

Wind speed and direction play a key role in merging cooling tower and stack plumes. Therefore, wind rose at plant location should be used in determining the relative location of cooling tower with respect to stack when establishing plant arrangement and layout (*USEPA,* 1979).

Shalkouhi et al. (2017) reported that most of the studies with regard to stack and cooling tower plume mergence are dated back to the 70s and 80s. For example, *Kramer et al.* (1976), *Knudson* (1979), and *Haman* and *Malinowski* (1989) found that stack plumes frequently merge with cooling tower plumes in power plants.

There are multiple methods for determination of stack and/or cooling tower plume properties. One of these methods is uding a dispersion model like the *CALPUFF modeling system* (2011). Before 2011, the CALPUFF modeling system has been widely used for prediction of smoke plume properties only. For example, *Protonotariou et al.* (2005) reported that the overall performance of the CALPUFF modeling system was satisfactory. It must be pointed out that model evaluation studies involve selecting appropriate metrics or diagnostics (parameters summarizing key aspects of the behavior of a model) showing that the model can predict the metrics with appropriate accuracy compared with observations (*Fisher et al.,* 2015). In 2011, U.S.EPA included the ability of calculation of vapor plume in version 6 of the CALPUFF modeling system. Nevertheless, the CALPUFF modeling system cannot provide enough information about smoke and vapor plume mergence, considering the following argument:

As can be seen in *Fig. 1 Sarma* (1973) classified stack and cooling tower plume mergence into three different types. In the first type, the cooling tower plume mixes with the stack plume. In the second type, the stack plume mixes with the cooling tower plume. In the third type, both plumes spread more or less in parallel and merge at some distance away from their sources. For example, *Knudson* (1979) reported the first and second type, while *Dittenhoefer* and *de Pena* (1978), *Haman* and *Malinowski* (1989), and *Kramer et al.* (1976) revealed the third type (see *Table 1*).

Table1: Studies on different types of smoke and vapor plume mergences

Author/Authors	**First type**	**Second type**	**Third type**
Haman and *Malinowski* (1989)			√
Knudson (1979)	√	√	
Dittenhoefer and *Pena* (1978)			√
Kramer et al. (1976)			√

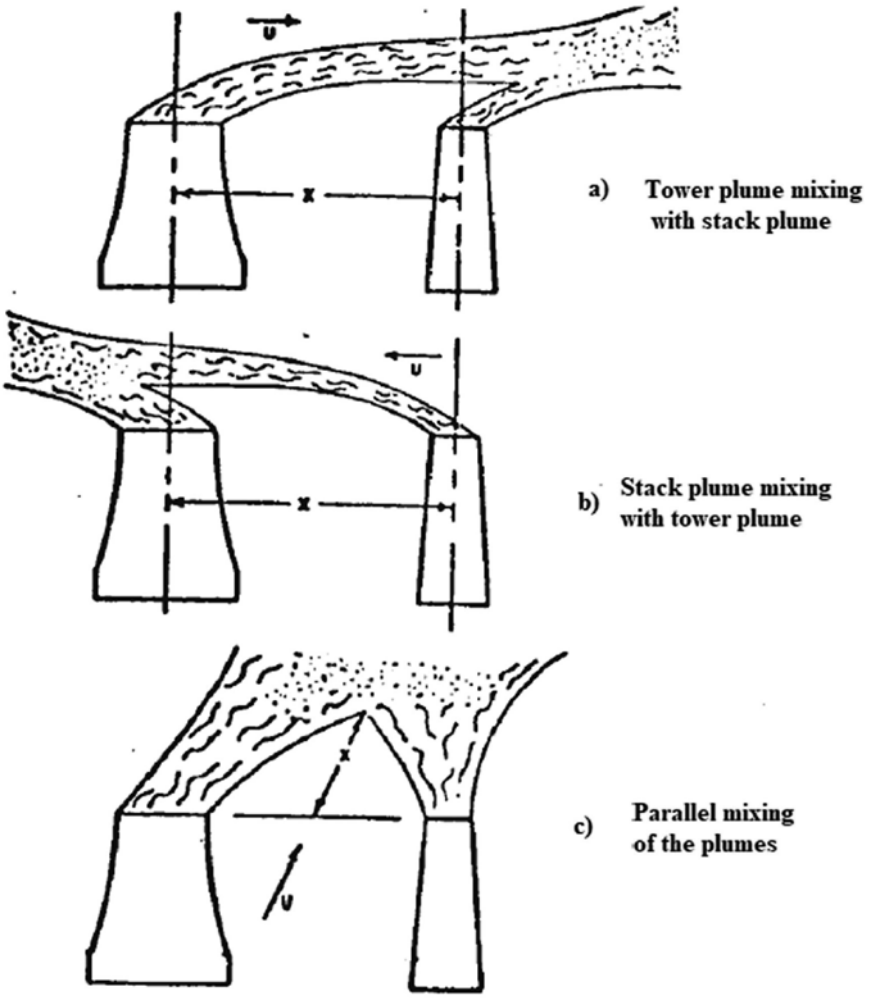

Fig.1. Different types of smoke and vapor plume mergence (*Sarma,* 1973).

In the first and second type, the plume height and length play an important role in merging the two plumes; while in the third type, the plume radius plays a key role in merging the two plumes (see *Fig. 2*).

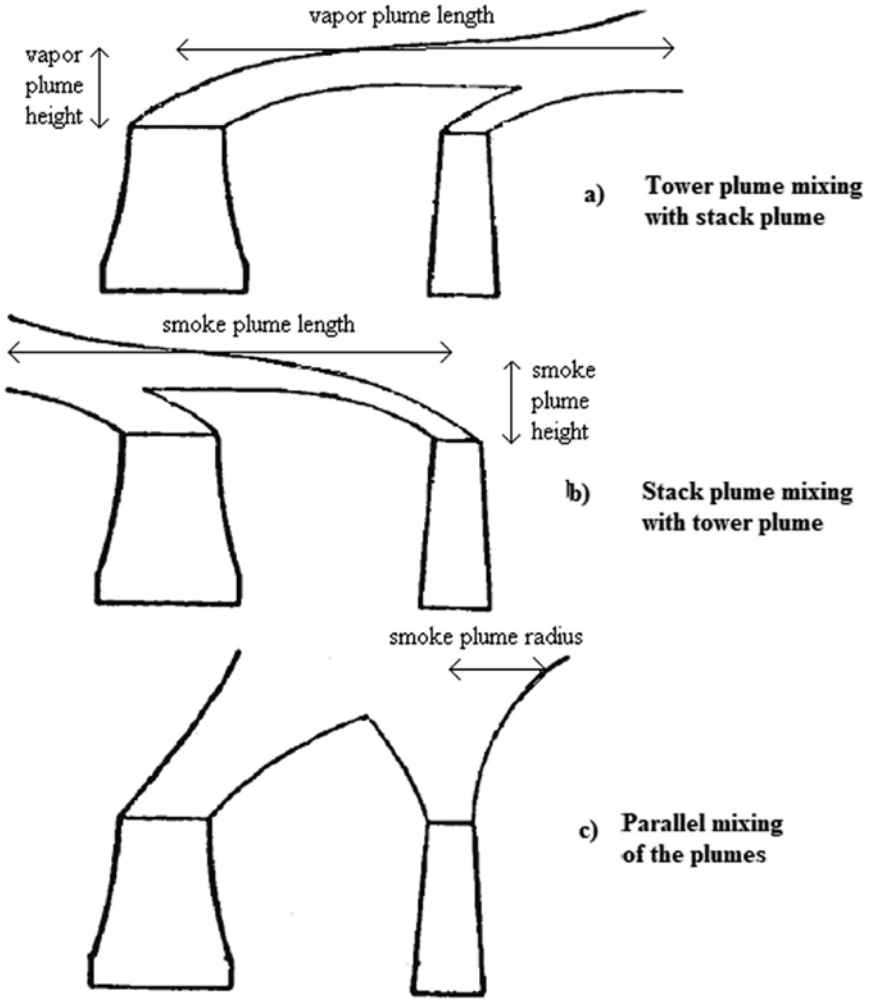

Fig. 2. Length, height, and radius of smoke and vapor plumes.

Moreover, in the CALPUFF modeling system, the momentum and buoyancy are treated according to the plume rise equations of Briggs (*Code of Federal Regulations,* 2009). These equations can be written as follows (*U.S. Materials Management Service,* 1985).

For unstable or neutral atmospheric conditions, the downwind distance of final plume rise is

$$xf = 3.5x^*, \tag{1}$$

where

$$x^* = 14F^{\frac{5}{8}}, \text{ when } F < 55 \ m^4 s^{-3},$$
$$x^* = 34F^{\frac{2}{5}}, \text{ when } F \geq 55 \ m^4 s^{-3}. \tag{2}$$

The final plume rise under these conditions is

$$\Delta h = 1.6F^{\frac{1}{3}}\left(3.5x^*\right)^{\frac{2}{3}}u^{-1}. \tag{3}$$

For stable atmospheric conditions, the downwind distance of final plume rise is

$$xf = \pi \ u \ s^{\frac{-1}{2}}, \tag{4}$$

where

$$s = g\frac{\partial\theta}{\partial z}T^{-1}. \tag{5}$$

The plume rise is

$$\Delta h = 2.6\left[F/\left(u \ s\right)\right]^{\frac{1}{3}}, \text{ for windy conditions,} \tag{6}$$

$$\Delta h = 5F^{\frac{1}{4}}s^{\frac{-3}{8}}, \text{ for near-calm conditions.} \tag{7}$$

In the above equations, g is the gravitational acceleration (ms^{-2}), d is the stack inside diameter at the top (m), F is the buoyancy flax parameter $\left[g \ v_s\left(\frac{d}{2}\right)^2\left(\frac{T_s - T}{T_s}\right)\right]$ (m^4s^{-3}), x^* is the distance at which atmospheric turbulence begins to dominate the entrainment (m), Δh is the plume rise above the stack top (m), x is the downwind distance from the source (m), T is the ambient air temperature (°k), Ts is the stack gas temperature (°k), u is the mean wind speed from the stack top to the plume top (ms^{-1}), v_s is the stack gas exit velocity (ms^{-1}),

$\partial\theta/\partial z$ is the vertical potential temperature gradient from the stack top to the plume top (°k m^{-1}), and *s* is the restoring acceleration per unit vertical displacement for adiabatic motion in the atmosphere, a stability parameter (s^{-2}).

The above equations do not include "smoke plume radius" as a predictor variable. On the other hand, in the CALPUFF modeling system, the vapor plume dimension is calculated by a processor named CTEMISS. There is no information in the literature which equation (e.g., *Hanna* (1976) or the other ones) is included in the CTEMISS. Among the vapor plume dimensions (height, length, and radius) only the height and length are computed by this processor; therefore, it can be stated that the CALPUFF modeling system is only valid for the first and second types of smoke and vapor plume mergences (see *Table 2*). Moreover, the radius of the plumes can also change change from time to time.

Table 2: The CALPUFF and AUSTAL 2000 modeling systems with regard to different types of smoke and vapor plume mergences

Model/Software	First type	Second type	Third type
CALPUFF	Valid	Valid	Invalid
AUSTAL 2000	Valid	Valid	Invalid

Another method for determination of smoke and/or vapor plume properties is using the *AUSTAL 2000* (2009) modeling system. Plume rise in connection with the discharge of exhaust by stacks is parametrically calculated according to the VDI 3782 Standard for Gaussian plume models. Also, plume rise of exhaust released by cooling towers is parametrically calculated according to VDI 3784 Standards for dispersions of natural-draft wet cooling emissions. There is no information in the literature which equations are included in the mentioned guidelines. Whereas among the smoke and vapor plume dimensions (height, length, and radius) only the height and length of smoke and vapor plumes are computed by the model, it can be stated that the AUSTAL 2000 is valid only for the first and second types of plume mergences, too.

Therefore, as indicated in *Table 3*, in order to investigate the third type of plume mergence, it is recommended to use other methods (e.g., satellite, airplane, and so on) instead of the CALPUFF and AUSTAL 2000 modeling systems. For example, *Dittenhoefer* and *de Pena* (1978) observed the third type

of smoke and vapor plume mergences from an airplane. Also, *Staylor* (1978) determined smoke plume radius from satellite imagery. *Pettyjohn* and *Mckeon* (1976) reported that satellite imagery provides a convenient and inexpensive means for monitoring smoke plumes.

Table 3: The ability of the CALPUFF and AUSTAL 2000 models and some other methods with regard to smoke and vapor plume dimension

Model/Method	**Plume height**	**Plume length**	**Plume radius**
CALPUFF	Valid	Valid	Invalid
AUSTAL 2000	Valid	Valid	Invalid
Satellite, airplane, etc	Valid	Valid	Valid

Overall, it can be stated that to cover all types of smoke and vapor plume mergences, plume radius as a predictor variable must be included in the CALPUFF and/or AUSTAL 2000 modeling systems.

2.1. Study area

In this section, smoke and vapor plume mergences are investigated in a real environment. *Fig. 3* shows the first type of smoke and vapor plume mergence pictured over the Mátra Power Plant, Hungary. As can be seen in the figure, the wind direction of WSW (west-southwest) causes this type of plume mergence. *Fig. 4* indicates the second type of vapor and smoke plume mergence in the mentioned plant. As shown in the figure, the wind direction of ENE (east-northeast) causes this type of plume mergence. It must be stated that other wind directions can cause the third type of plume mergence the Mátra plant.

Fig.3. First type of plume mergence in the Mátra Power Plant, Hungary.

Fig. 4. Second type of plume mergence in the Mátra Power Plant, Hungary.

In addition to wind speed and direction, a little distance between the stack and cooling towers in the Mátra plant plays an important role in merging smoke and vapor plumes. This distance is only about 370 meters (see *Fig. 4*). In contrast, *Knudson'*s (1979) results revealed that smoke and vapor plume mergence is a common phenomenon in a power plant in U.S.A., where the distance between stacks and cooling towers was about 1000 meters.

According to *Fig. 5*, the distance between the Mátra plant and the surrounding cities varies from 3–15 kilometers. Whereas up to 50 kilometers from emission sources is considered as near field in air pollution, the first type of plume mergence can affect Visonta city, the second type of plume mergence can affect Vécs city, and the third type of plume mergence can affect the other cities.

Therefore, for investigating the number of the first and second types of plume mergences in the Mátra plant in the future, it is recommended to use the CALPUFF and/or AUSTAL 2000 modeling systems. Also, for investigating the third type of plume mergences in the mentioned plant in the future, it is recommended to use satellite, airplane, etc observations.

Fig.5. The Mátra Power Plant and the surrounding cities.

3. Conclusions

The results of the present study showed that smoke and vapor plume mergence is a common phenomenon in the Mátra Power Plant in Hungary; however, more studies must be conducted in the future to reveal the type and number of plume mergences in the mentioned plant. The results also showed that the CALPUFF and AUSTAL 2000 modeling systems cannot provide enough information with regard to vapor and smoke plume mergences.

References

AUSTAL 2000. 2009: Version 2.4, Federal Environmental Agency (UBA), Berlin.

CALPUFF modeling system. 2011: Version 6, U.S. Environmental Protection Agency.

Code of Federal Regulations. 2009: Protection of Environment. U.S. General Services Administration, National Archives and Records Service, Office of the Federal Register.

Dittenhoefer, A. C. and *de Pena, R.G.,* 1978: A study of production and growth of sulfate particles in plumes from a coal-fired power plant. *Atmos. Environ. 12,* 297–306. https://doi.org/10.1016/B978-0-08-022932-4.50033-1

Fisher, B.E.A., Chemel, C., Sokhi, R.S., Francis, X.V., Vincent, K. J., Dore, A.J., Griffiths, S., Sutton, P., and *Wright, R.D.,* 2015: Regional air quality models and the regulation of atmospheric emissions. *Időjárás 119,* 355–378.

Haman, K.E., Malinowski, S.P., 1989: Observations of cooling tower and stack plumes and their comparison with plume model "ALINA"'. *Atmos. Environ. 23*, 1223–1234. https://doi.org/10.1016/0004-6981(89)90149-2

Hanna, S.R., 1976: Predicted and observed cooling tower plume rise and visible plume Length at the John E. Amos power plant. *Atmos. Environ. 10*, 1043–1052. https://doi.org/10.1016/0004-6981(76)90112-8

Knudson, D.A., 1979: Cooling Tower and Steam Plant Plume Mergence at the Watts Bar Site. Tennessee Valley Authority, Air quality Branch, TVA/AQB-I79/13, 49 pp.

Kramer, M.L., Smith, M.E., Butler, M.J., and *Seymour, D.E.,* 1976: Cooling towers and the environment. *J. Air Pollut. Cont. Assoc. 26,* 582–584. https://doi.org/10.1080/00022470.1976.10470287

Pettyjohn, W.A. and *Mckeon, J.B.,* 1976: Proceedings of the first international symposium on acid precipitation and the forest ecosystem; Gen. Tech. Rep. NE-23. Upper Darby, PA: U.S. Department of Agriculture, Forest Service, Northeastern Forest Experiment Station, 337–347.

Protonotariou, A., Bossioli, E., Athanasopoulou, E., Dandou, A., Tombrou, M., Flocas, H., Helmis, C., and *Assimakopoulos, V.,* 2005: Evaluation of CALPUFF modeling system performance: an application over the Greater Athens Area, Greece. *Int. J. Environ. Pollut. 24,* 22–35. https://doi.org/10.1504/IJEP.2005.007382

Rao, M.N. and *Rao, H.V.N.,* 1989: Air pollution. Tata McGraw-Hill Education, New Delhi.

Sarma, K.R.H., 1973: A Method of Calculation of Ground Level Concentration of Particulates due to Interaction of Cooling Tower Plumes with Stack Plumes of Large Power Plants. Paper presented at the Environmental and Geophysical Heat Transfer Conference, ASME HTD, Vol.4, 26–30.

Shalkouhi, P.J., Atabi, F., Moattar, F., and *Yousefi, H.,* 2017: Smoke and vapor plume mergence. *Croatian Meteorol. J. 52,* 51–57.

Staylor, W.F., 1978: Determination of stack plume properties from satellite imagery. *J. Spacecraft Rockets 15,* 92–99. https://doi.org/10.2514/3.57291

U.S. Materials Management Service. 1985: Union Oil Project/Exxon Project Shamrock and Central Santa Maria Basin Area Study: Environmental Impact Statement, Volume 2.

USEPA (U.S. Environmental Protection Agency). 1979: Nonwater Quality Impacts of Closed-Cycle Cooling Systems and the Interaction of Stack Gas and Cooling Tower Plume. EPA-600/7-79-090, 215 pp.

INSTRUCTIONS TO AUTHORS OF *IDŐJÁRÁS*

The purpose of the journal is to publish papers in any field of meteorology and atmosphere related scientific areas. These may be

- research papers on new results of scientific investigations,
- critical review articles summarizing the current state of art of a certain topic,
- short contributions dealing with a particular question.

Some issues contain "News" and "Book review", therefore, such contributions are also welcome. The papers must be in American English and should be checked by a native speaker if necessary.

Authors are requested to send their manuscripts to

Editor-in Chief of IDŐJÁRÁS
P.O. Box 38, H-1525 Budapest, Hungary
E-mail: journal.idojaras@met.hu

including all illustrations. MS Word format is preferred in electronic submission. Papers will then be reviewed normally by two independent referees, who remain unidentified for the author(s). The Editor-in-Chief will inform the author(s) whether or not the paper is acceptable for publication, and what modifications, if any, are necessary.

Please, follow the order given below when typing manuscripts.

Title page should consist of the title, the name(s) of the author(s), their affiliation(s) including full postal and e-mail address(es). In case of more than one author, the corresponding author must be identified.

Abstract: should contain the purpose, the applied data and methods as well as the basic conclusion(s) of the paper.

Key-words: must be included (from 5 to 10) to help to classify the topic.

Text: has to be typed in single spacing on an A4 size paper using 14 pt Times New Roman font if possible. Use of S.I. units are expected, and the use of negative exponent is preferred to fractional sign. Mathematical formulae are expected to be as simple as possible and numbered in parentheses at the right margin.

All publications cited in the text should be presented in the *list of references*, arranged in alphabetical order. For an article: name(s) of author(s) in Italics, year, title of article, name of journal, volume, number (the latter two in Italics) and pages. E.g., *Nathan, K.K.,* 1986: A note on the relationship between photosynthetically active radiation and cloud amount. *Időjárás 90,* 10–13. For a book: name(s) of author(s), year, title of the book (all in Italics except the year), publisher and place of publication. E.g., *Junge, C.E.,* 1963: *Air Chemistry and Radioactivity.* Academic Press, New York and London. Reference in the text should contain the name(s) of the author(s) in Italics and year of publication. E.g., in the case of one author: *Miller* (1989); in the case of two authors: *Gamov* and *Cleveland* (1973); and if there are more than two authors: *Smith et al.* (1990). If the name of the author cannot be fitted into the text: *(Miller,* 1989); etc. When referring papers published in the same year by the same author, letters a, b, c, etc. should follow the year of publication. DOI numbers of references should be provided if applicable.

Tables should be marked by Arabic numbers and printed in separate sheets with their numbers and legends given below them. Avoid too lengthy or complicated tables, or tables duplicating results given in other form in the manuscript (e.g., graphs). *Figures* should also be marked with Arabic numbers and printed in black and white or color (under special arrangement) in separate sheets with their numbers and captions given below them. JPG, TIF, GIF, BMP or PNG formats should be used for electronic artwork submission.

More information for authors is available: journal.idojaras@met.hu

Published by the Hungarian Meteorological Service

Budapest, Hungary

ISSN 0324-6329 (Print)

ISSN 2677-187X (Online)